Novel Approaches for the Lipid Modification of Carbohydrates-Syntheses, Surface-Active Properties and Supramolecular Self-Assemblies

Dissertation

zur Erlangung des Grades

Doktor der Naturwissenschaften (Dr. rer. nat.)

vorgelegt der

Bergische Universität Wuppertal

Fachbereich C – Mathematik und Naturwissenschaften

von

Sukhendu Nandi

Aus Kalkutta, Indien

2012

“Education is the manifestation of perfection present already in man” Swami Vivekananda

Eingereicht am: 03.01.2012
Tag der mündlichen Prüfung 25.01.2012

Die Dissertation kann wie folgt zitiert werden:

urn:nbn:de:hbz:468-20120705-103153-3
[http://nbn-resolving.de/urn/resolver.pl?urn=urn%3Anbn%3Ade%3Ahbz%3A468-20120705-103153-3]

Referent: Prof. Dr. H.-J. Altenbach
Koreferent: Prof. Dr. Manfred. P. Schneider

Table of Contents

Dedication

This thesis is dedicated to my parents
for their love, endless support
and encouragement

Acknowledgements

My deepest and profound gratitude goes first and foremost to my research supervisor Prof. Dr. Hans-Josef Altenbach and co-supervisor Prof. M. P. Schneider. They have been an amazing driving force and a true inspiration, constantly offering fresh input and ideas, and moral encouragement, notwithstanding their busy schedules. Without their tenacity I would have not been able to finish this thesis.

I sincerely express my gratitude to Dr. Karsten Lange and Dr. Bernd Jakob for their valuable scientific and constant inspiration during the course of my project. It has been a great pleasure to work with them. Their insightful comments and constructive criticisms at different stages of my research were thought-provoking and they helped me focus my ideas. I am grateful to them for holding me to a high research standard and enforcing strict validations for each research result, and thus teaching me how to do research.

I owe my deepest gratitude and gratefully acknowledge the enormous helps of Mr. Andre Mayer, Dr. Ralf Heiderhoff, Mr. Si Wang for SEM measurements and Dr. Jane Hübner for DSC analysis. Without their help I could not have obtained such relevant data to accomplish my work.

This scientific path would not be completed if not for the Bergische Universität Wuppertal. The university has provided me all the sophisticated, modern, necessary facilities and equipment. No words can fully express my appreciation for the prompt technical assistance rendered by former and current staff at the Bergische Universität Wuppertal, for their various forms of support during my study. They are Mr. Andreas Siebert, Mr. Boris Ihmenkamp, Mrs. Ilka Polanz and Miss Melanie Dausend.

I would also like to thank several fellow students, Mr. Engin Aydin, Mr. Ümit Gün, Mr. Gongkun Tang, Dr. Rachid Ihizane and Dr. Jochen Sturhan for being good friends during my time at Bergische Universität Wuppertal. I enjoyed their company during my tenure in Wuppertal. They helped me to stay sane through these difficult years. Their support and care helped me to overcome setbacks and to stay focused on my research. I greatly value their friendship and I deeply appreciate their belief in me.

And last but certainly not the least, I would like to express my deepest gratitude to my parents and Sagorica Nandi for their great love, care and support all thought these decades. Most importantly, none of this would have been possible without the love and patience of my family. My immediate family, to whom this dissertation is dedicated to, has been a constant source of love, concern, support and strength all these years. My extended family has aided

and encouraged me throughout this endeavour. I warmly appreciate the generosity and understanding of my extended family.

Abstract

Nature, and in this context agriculture, is providing a wealth of renewable and highly useful raw materials like fats and oils, plant proteins and carbohydrates. By selective combination of their molecular constituents (*e.g.* fatty acids, glycerol, amino acids, carbohydrates) a wide variety of surface active materials can be prepared. All of them, due to their molecular constitution being potentially highly biodegradable, continue to evoke considerable interest and are emerging as an important classes of bio-based materials on account of their potential applications in the fields of cosmetics, food processing and as emulsifiers and supramolecular gelators.

Environmental problems caused by human activities, such as the consumption of fossils raw materials and the emissions of greenhouse gases are well-recognised and calls have been made for immediate measures to develop a more sustainable society worldwide. Attention has also been made to the quest for sustainability within the field of chemistry. The concept of green chemistry based on renewable resources is being introduced into the production of chemicals in order to reduce the impact on the environment by replacing petroleum-based resources with renewable feedstock and by making chemical processes more efficient.

Thus in this thesis we describe the syntheses of surfactants, emulsifiers and self-assembled supramolecular gelators based on renewable raw materials and studies of their physico-chemical properties. Key reaction thereby is the conversion of naturally occurring hydroxycarboxylic acids (malic and tartaric acid) with fatty acid chlorides into the corresponding *O*-acylated hydroxycarboxylic acid anhydrides. These molecules are excellent electrophiles and hence undergo ring opening reaction with a wide variety of readily available nucleophiles (*e.g.* mono- and disaccharides, sugar alcohols and ascorbic acid) to generate a library of combination products with an enormous diversity in properties. The described combination products can be obtained in just two steps and in view of their amphiphile nature they may prove to be useful as surfactants for the preparation of oil in water emulsions in *e.g.* food industry and cosmetics.

1 Introduction

1.1 Renewable resources

The term renewable resources can be used for the substances which are derived from plants, animals or other organisms. Unlike fossil resources such as oil, natural gas or coal, they are constantly reproduced in reasonable periods of time. The use of oil for chemicals and as fuels since the beginning of the last century contributed significantly to economic growth in developed countries. With raising a demand of energy and since the price for fuel is increasing, there is a need to look for alternative sources of energy and basic chemicals. The concept of renewable resources has been introduced at the beginning of the 1980s and drawn considerable attention as they are environmental friendly, biodegradable and non-toxic. Raw materials or feedstock based on renewable resources are carbohydrates, fats, oils, starch and protein (Table 1). Each year in Germany 2.8 million tons of biomass has been used in the chemical industry (chemical pharmaceutical industry, paper and natural fiber processing industry). Compared to 1991, the industrial use of renewable raw materials has been increased significantly in Germany. Current estimation for renewable resources as feedstock in chemical industry in the year of 2009 are fats and oils (1.5 million tonnes) and carbohydrates (0.7 million tonnes) as major raw materials for technical applications.

raw meterials	1991	1998	2005	2007	2008 (preliminary estimate)	2009 (preliminary estimate)
fats and oils	900	1.150	1.150	1.450	1.450	1.500
carbohydrates	478	411	620	722	708	700
others	323	425	356	605	549	600
overall	1.701	1.986	2.126	2.777	2.707	2.800

Table 1: Consumption of renewable raw materials (excluding wood) in the chemical industry in Germany[1] in the years 1991 to 2009; in thousands of tons.

1.1.1 Carbohydrates and their potential as renewable resource

1.1.1.1 Carbohydrates as renewable resources

Carbohydrates are very important as renewable resources in terms of volume produced as they represent roughly 95% of the annually produced renewable biomass of about 200 billion tons; of these only 3% are used by man; the rest decays and recycles along natural pathways.[2]

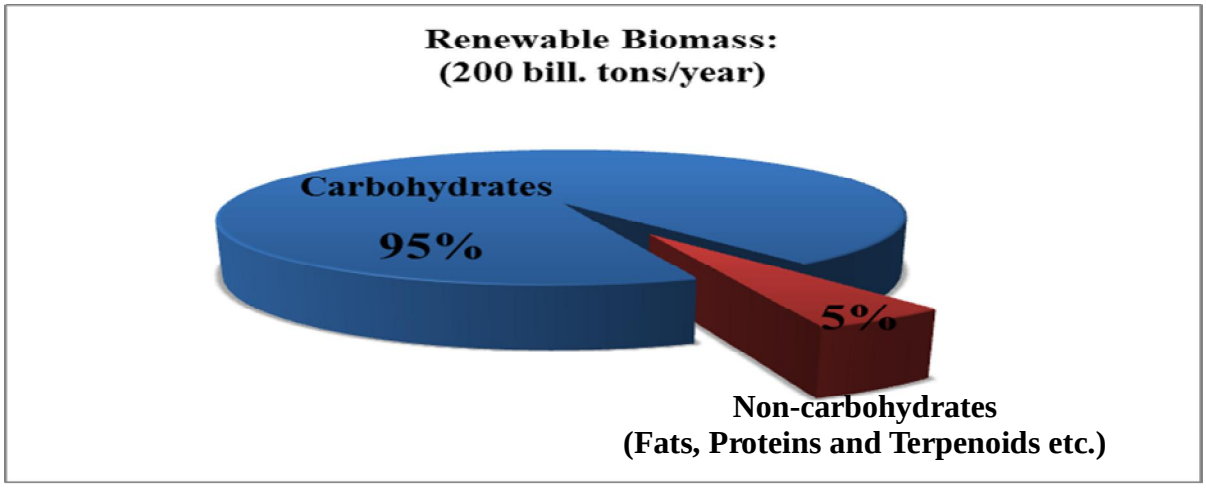

Irrespective of the enormous abundance of some carbohydrates and their vast potential as organic raw materials for the chemical industry, their chemistry and application has not yet been fully exploited.[3] The concept of "green chemistry"[4] based on renewable resources is being introduced into the production of chemicals/surface active compounds in order to reduce the impact on the environment through replacing petroleum-based resources with renewable feedstock and by making chemical processes more efficient. However, as our fossil raw materials are irrevocably decreasing, the end of cheap oil is realistically prognosticated[5] for 2040 at the latest and as the pressure on our environment is building up, the progressive changeover of chemical industry to renewable feedstock emerges as an inevitable necessity.[6] Due to the reduced supply of fossil raw materials the price for petrochemical products such as ethylene oxide, a precursor of the hydrophilic head of the conventional non-ionic surfactants will also rise.[7] In view of the impact of surfactants on the environment *raw materials as feedstock should be renewable rather than depleting wherever technically and economically practicable*.[8] The challenge posed by the necessity to increasingly replace fossil raw materials by those annually re-growing is obvious and systematic basic and applied research is developed for opening up new, non-food application fields based on carbohydrates in general and for mono- and disaccharides in particular, the latter being well suited for straightforward chemical transformations.[9] This rising demand requires that chemists transform inexpensive, bulk-scale accessible mono-and disaccharides–most notably glucose, fructose, sucrose, and *iso*maltulose into products with potential industrial applications (Figure 1).

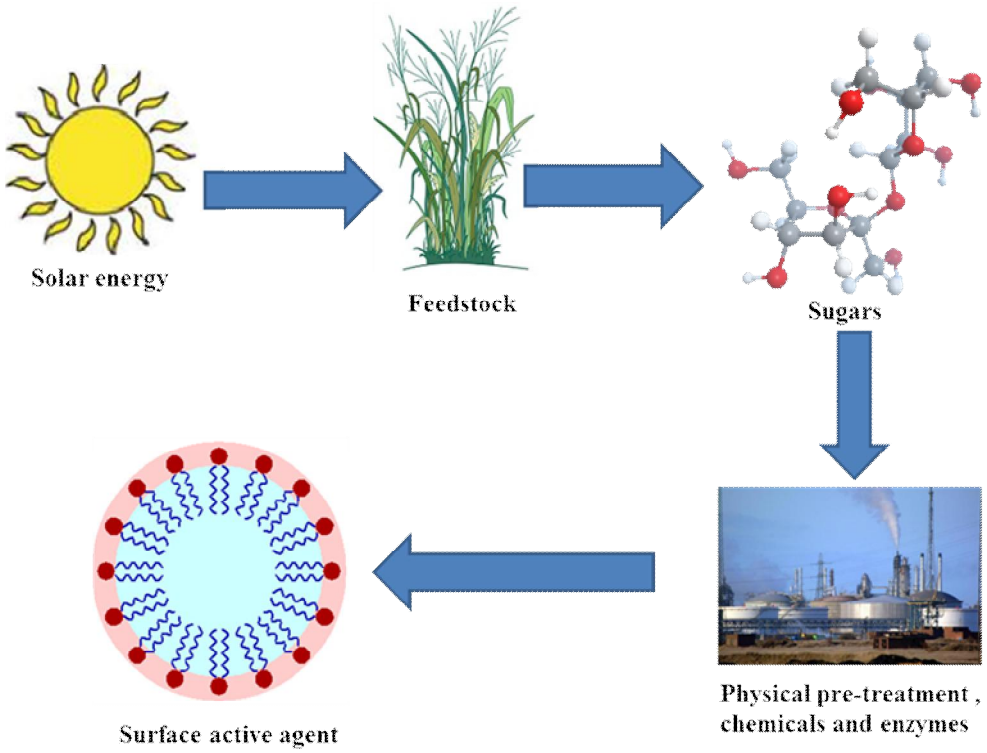

Figure 1: Biology of bioconversion of solar energy into bio-surfactants.[10]

The methods for such conversions should be simple, using cheap reagents or simple protection groups (if absolutely needed) and should aim for stable compounds with useful overall yields.

1.1.1.2 Natural abundance of carbohydrates as renewable feedstock and their potential as a felicitous alternative to petroleum based surfactants

The terrestrial biomass, which *Nature* provides us on an annual basis, is considerably more complex than fossil raw materials, constituting a multifaceted accumulation of low and high molecular weight products, exemplified by sugars, hydroxy and amino acids, lipids, and biopolymers such as cellulose, hemicelluloses, chitin, starch, lignin, and proteins. So far the most abundant of these organic materials, in fact, about 95% of the annually renewable biomass, are *carbohydrates*, a single class of natural products that, aside from their traditional uses for food, paper, and heat, are the major bio-feedstock to develop industrially and economically viable organic chemicals that are to replace those derived from petrochemical sources.[9]

The bulk of the annually renewable carbohydrate biomasses are polysaccharides, yet their non-food utilization is confined to textile, paper, and coating industries, either as such or in the form of simple esters and ethers. Organic commodity chemicals, however, are low molecular weight products; hence, they are more expediently acquired from low molecular

weight carbohydrates than from poly-saccharides. Accordingly, the constituent repeating units of these polysaccharides glucose (cellulose, starch), fructose (inulin), xylose (xylan), etc., or disaccharide versions thereof are the actual carbohydrate raw materials for organic chemicals with tailor-made industrial applications: they are inexpensive, ton-scale accessible, and provide an ensuing chemistry, better worked out and more variable than that of their polymers.[11]

		World production (metric t/year)	Price(Euro/kg)
sugars	sucrose	130 000 000	0.30
	D-glucose	5 000 000	0.60
	lactose	295 000	0.60
	D-fructose	60 000	1.00
	isomaltulose	50 000	2.00
	maltose	3 000	3.00
	D-xylose	25 000	4.50
	L-sorbose	60 000	7.50
sugar alcohols	*D*-sorbitol	650 000	1.80
	D-xylotol	30 000	5.00
	D-mannitol	30 000	8.00
sugar derived acids	*D*-gluconic acid	60 000	1.40
	L-lactic acid	>100 000	1.75
	citric acid	500 000	2.50
	L-tartaric acid	35 000	6.00
amino acids	*L*-lysine	40 000	5.50
	L-glutamic acid	500 000	7.00
basic chemicals	aniline	1300 000	0.95
	acetaldehyde	900 000	1.15
	adipic acid	1500 000	1.70
solvents	methanol	25 000 000	0.15
	toluene	6 500 000	0.25
	acetone	3 200 000	0.55

Table 2: Annual production volume and prices of simple sugars and sugar-derived alcohols and acids as compared to some petrochemicals derived basic chemicals and solvents.[a]

[a] Taken from F. W. Lichtenthaler, *Acc. Chem. Res*, **2002**, 35, 728–737.

Table 2 lists the availability and bulk-quantity prices of the eight least expensive sugars–all well below 10€/Kg–as compared to some sugar-derived naturally occurring compounds and also some basic chemicals from petrochemical sources. The results are surprising, since the five cheapest sugars, some sugar alcohols, and sugar-derived acids are not only cheaper than any other enantiopure product, such as hydroxy or amino acids, but are also comparable with basic organic bulk chemicals such as acetaldehyde or aniline. The basic prices of sucrose, glucose, and lactose are comparable to the price range of some standard organic solvents.

1.1.1.3 Commercially produced carbohydrate-derived surfactants and their advantages[12]

Recently considerable attention has been devoted to the replacement of polyoxyethylene chains as hydrophilic head groups contained in traditional surface active compounds by carbohydrates. Carbohydrate-derived surface active compounds (Scheme 1) are of advantage on account of their bio-compatibility and bio-degradability and also the fact that they are non-toxic, skin friendly and display synergistic effects in combination with other surfactants.[13] The applications are growing in the area of foods, pharmaceuticals, cosmetics and detergents.

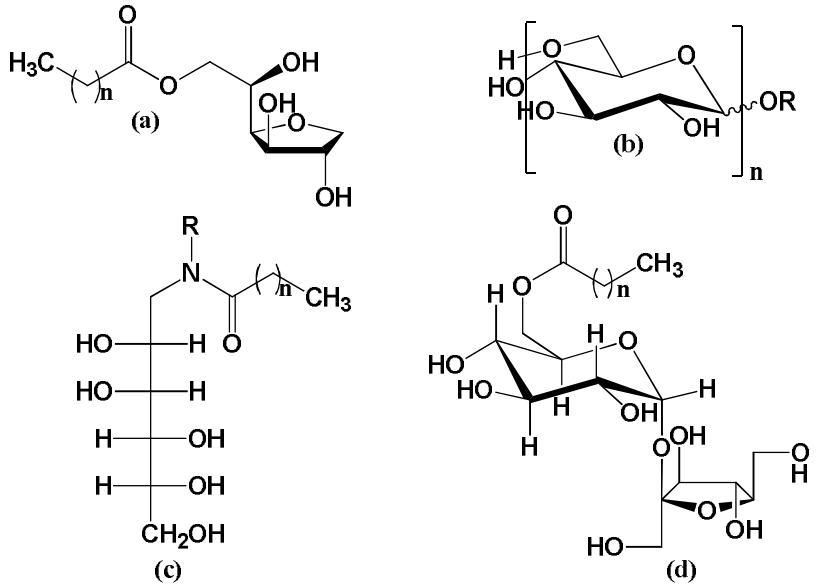

Scheme 1: Commercially produced carbohydrate derived surfactants; (**a**) sorbitan fatty acid esters (**b**) alkyl poly glucoside; (**c**) fatty acid glucamide; (**d**) fatty acid esters based on sucrose.

Carbohydrate based surfactants on an industrial scale are ethoxylated sorbitans, sucrose fatty acid esters, fatty acid glucamides and alkyl polyglucosides. The use of glucosides and amides rather than esters is of advantage since they are less readily hydrolysed and hence sustained for a longer time in alkaline media than esters.

1.1.1.4 The advantages of alkyl poly glucosides (APGs) [14]

Alkyl poly glucosides (APGs) are the simplest carbohydrate-derived surfactants. Their potential as alternative to the petrochemical based feedstock was revealed and their properties were investigated. They are the most important ingredients of the sugar-based surfactants with the largest worldwide production capacity.[14] Alkyl poly glucosides with different chain lengths and head groups have been synthesised and they can be commonly abbreviated as $\mathbf{C_nG_m}$, where n represents the number of carbons in the hydrocarbon chain and m corresponds to the number of glucose moieties in the structure.[15,16]

The industrial synthesis of alkyl poly glucosides is based on the *Fischer* glycosilation, basically an acid catalysed acetalisation that can be accomplished *via* a direct route or a two-step synthetic pathway involving a transglycosidation as shown in Scheme 2.

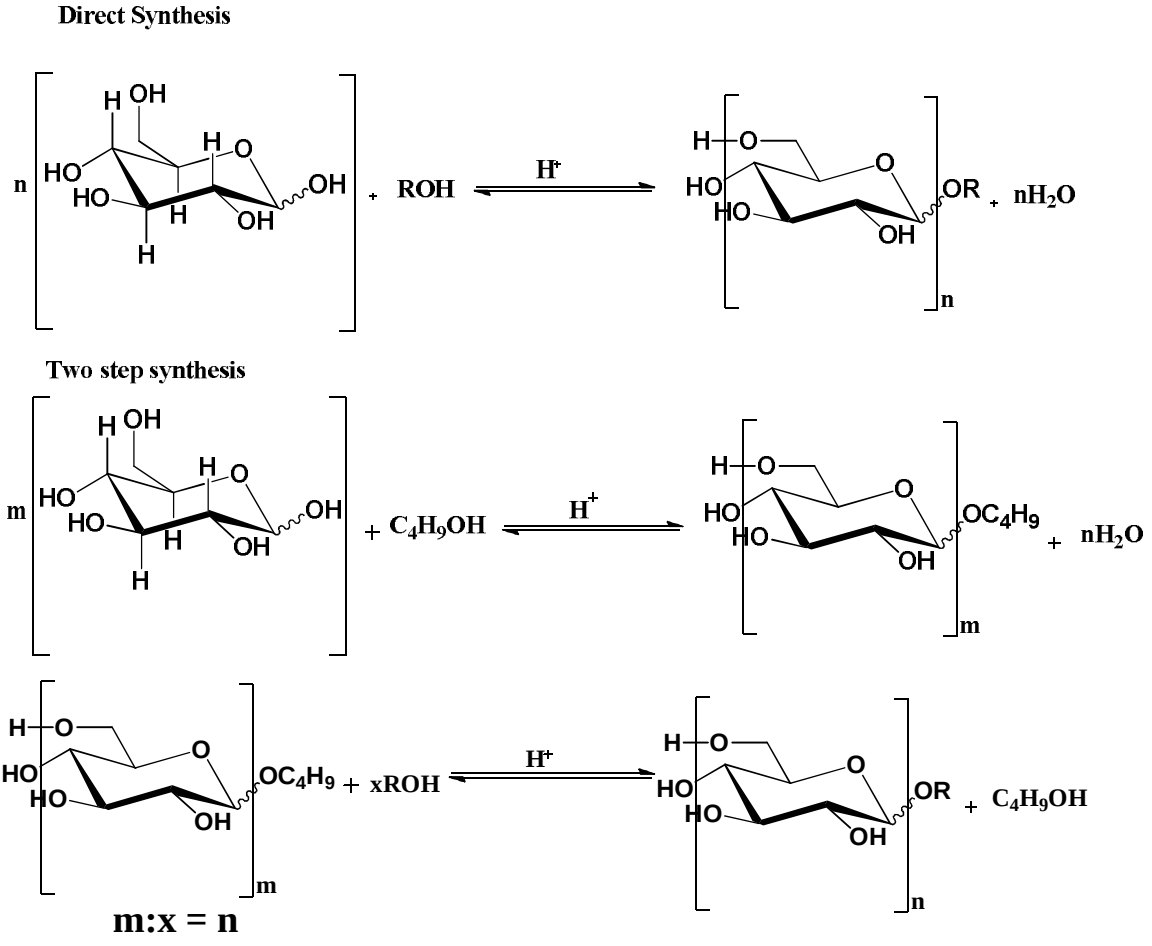

Scheme 2: Direct and two step synthesis of poly glucosides.[12]

Advantageous properties of APGs are skin friendliness, high synergism with anionic surfactants, and foam-stabilizing properties. This makes them particularly beneficial for the use as manual dishwashing detergents. Furthermore, they have a low toxicity and are completely biodegradable.

So far APGs have found only limited applications in laundry detergent compositions due to their relatively high price as compared to linear alkylbenzene sulfonates (ionic) and non-ionic alcohols.

1.1.2 Hydroxycarboxylic acids as renewable resources

Hydroxycarboxylic acids are a class of organic compounds which contain one or more carboxyl groups along with at least one hydroxy group. Some of them are produced by fermentation such as lactic acid. *L*-tartaric acid, malic acid and (with some exception) citric acid can be isolated from other natural sources and hence they belong to the class of renewable resources.

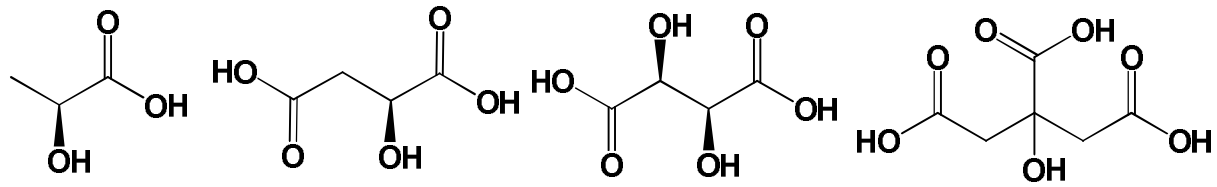

***L*-Lactic acid** ***L*-Malic acid** ***L*-Tartaric acid** **Citric acid**

1.1.2.1 Lactic acid

In mammals including men, *L*-lactate is constantly produced from pyruvate *via* the enzyme lactate dehydrogenase (LDH) in a process of fermentation during normal metabolism and exercise. Microorganisms can produce *D*-, *L*- or *DL*-lactic acid. Pure lactic acid is required for industrial purposes and as a food additive. It is obtained by fermentation of milk or whey with *Lactobacillus casei* and *Lactobacillus bulgaricus.* Lactic acid is known as milk acid in the food and beverage industry applications. It serves as a resource for cosmetic preparation. Citric acid is synthesized on industrial scale by fermentation.

1.1.2.2 *L*-Tartaric acid

Tartaric acid occurs in three stereoisomeric forms: the *(R,R)*-(+)-form (natural), the *(S,S)*-(−)-form and the (*R*,*S*)-*meso*-form. (*R*,*R*)-Tartaric acid is found in many plants and fruits both in free form and as potassium, calcium or magnesium salts. For example grape juice contains partly tartaric acid, and partly potassium tartrate. (*S*,*S*)-Tartaric acid is unnatural, very rare in nature, being found *e.g.* in the leaves of the West Africans tree *Bauhinia reticulata*. The (*S*,*S*)-tartaric acid has a spicy taste like citric acid. It is used as a buffer substance and frequently included in cosmetic formulations. It also serves as a complexing agent and hence produces chelate complexes with different metal ions.

1.1.2.3 Malic acid

S-(-)-Malic acid is found in apples, quinces, gooseberries, grapes and loganberries. Malic acid occurs in the human organism as an intermediate in the citric acid cycle and during gluconeogenesis. Optically active malic acid is produced as metabolite of fungi and bacteria. The peculiar, typical taste of malic acid allows its use for the flavoring of various pharmaceutical preparations. The malic acid is also used as an acidifier and acidity regulator in the confectionery industry and can act synergistically with antioxidants (E 296).

1.1.2.4 Citric acid

Citric acid can be found to 6-8% in lemons, in smaller amounts in berries and is also available from milk. Technically, citric acid with more than 90% purity can be obtained by fermentation. Worldwide about 550 000 tons of citric acid are produced annually.[17] Citric acid is by far the most commonly used food acid in the food industry (E 330). It is used as acidity regulator (for pH adjustment) for flavouring, as a complexing agent and synergist with antioxidants. Some triesters of citric acid are used as plasticizer in the manufacture of plastics.

1.2 Fats and oils as renewable resources

Fats and oils are triesters of glycerol containing mostly even-numbered and long chain un-branched fatty acids. Exceptions are fatty acid esters of long chain alcohols, so-called wax esters which occur in *e.g.* jojoba oil and spermaceti. The various fats and oils differ in their fatty acid composition (Table 3). According to the composition of fats and oils, they can be divided into the following groups: (i) saturated medium chain fatty acids such as lauric and myristic acid (ii) long chain saturated fatty acids such as palmitic and stearic acid and (iii) unsaturated fatty acids such as oleic, linoleic and linolenic acid. The fatty acid composition of various fats and oils is critical for their applications. Saturated medium chain fatty acids are useful in detergents and cleaning agents while long-chain unsaturated fatty acids because of the presence of double bonds in the core of the structure can be derivatized by relatively simple chemical processes and hence they are mostly used in the food industry or as polymerized resin.

common name	carbon atoms:double bonds	Coconut oil	Palm kernel oil	Palm oil	Cottonseed oil	Lard	Tallow	Olive oil	Corn oil	Peanut oil	Sunflower oil	Soya oil	Rapeseed oil(eruca poor)	Rapeseed oil(eruca rich)
caprylic	8:0	8.0	4.0	-	-	-	-	-	-	-	-	-	-	-
capric Acid	10:0	6.5	3.9	-	-	-	0.1	-	-	-	-	-	-	-
lauric Acid	12:0	47.	50.	-	0.1	0.1	0.2	-	0.1	0.1	0.1	0.1	-	-
myristic	14:0	17.	17.	2.5	1.0	1.4	2.5	0.7	0.5	0.1	0.3	0.4	1.1	-
palmitic	16:0	8.5	7.9	40.	23.	26.	22.	10.	11.	13.	5.9	10.	5.3	2.7
stearic Acid	18: 0	2.7	2.3	3.6	2.3	12.	17.	2.3	2.2	3.0	4.7	2.4	1.8	0.6
	>	0.2	0.5	-	0.9	0.6	0.1	0.4	1.0	5.3	1.5	0.8	0.7	3.6
oleic Acid	18:1	11.	45.	17.	45.	45.	78.	26.	39.	26.	23.	54.	9.6	
linoleic Acid	18:2	2.1	7.9	54.	9.2	1.7	7.2	58.	36.	61.	51.	24.	12.	
α-linolenic	18:3	-	-	-	0.6	1.1	0.2	0.6	0.8	0.5	0.4	8.5	10.	7.3
erucic acid	22:1	-	-	-	0.3	-	-	-	-	0.1	-	-	2.6	59.

Table 3: Concentration of various fatty acids in fats and oils.

1.3 Surfactants

1.3.1 History of surfactants

Surfactants or surface-active agents are one of the most abundant groups of chemicals used in everyday life.[18] In household goods synthetic surfactants are used as ingredients and also in pharmaceuticals, detergents and cosmetics.[18] Surfactants in industry are used in pulp and paper manufacturing, oil recovery, flotation where different minerals are separated from each other and a host of other applications.[18]

The use of surfactants is well known since ancient times. The oldest record of surfactant production was found in clay cylinders originating from ancient Babylon, dating back to about 2800 B.C.[18] A soap-like material was found in the cylinders and the inscriptions said that fats were boiled with ashes, a known soap-making method, although the purpose of the soap was not revealed.

In the 1950's, synthetic textiles became increasingly popular and the demand for surfactants other than simple soaps increased dramatically. This provoked chemists to design and synthesize novel synthetic surfactants.[18] The first series of synthetic surfactants were anionic

detergents with a branched hydrocarbon chain, which were not readily bio-degradable. Subsequently, foam accumulated on many lakes and rivers. Therefore, straight-chain surfactants which are better bio-degradable were introduced and the foaming problem was reduced.[18]

A further problem arose from the blend of surfactants with phosphates and polyphosphates, which form ion complexes and thus soften the water and disperse the pigments. However, due to their activities as fertilisers when they were discharged into the waste water they caused excessive growth of algae in downstream waters. Subsequent death of the algal blooms can lead to oxygen depletion (since so much oxygen is used in their biodegradation) followed by widespread death of fish and other aquatic organism. The uses of detergents containing phosphates are today restricted. The use of other surfactants that might harm the environment, for example phenol-containing surfactants, are also highly restricted today due to environmental concerns.

The demand of environmental friendly surfactants (non-toxic and readily biodegradable) has led to the developments of new types of surfactants.

1.3.2 Chemical definition

Surfactants are amphiphilic molecules which contain a polar head group and a non-polar hydrocarbon tail.[19] The non-polar tail of a surfactant molecule usually consists of straight or branched hydrocarbon or fluorocarbon chains containing 8-18 carbon atoms. The hydrophilic head of a surfactant can be non-ionic, ionic, zwitterionic and accompanied by a counter ion in the last two cases. The ionic or polar head group of a surfactant is actually the “water loving group” which interacts strongly with water *via* dipole or ion-dipole interactions[19] whereas the hydrophobic tail (water rejecting group) interacts weakly with water molecules. The strong interactions between the polar heads and the water molecules actually render the surfactants to dissolve in water. However, surfactants also tend to self-assemble or aggregate when dissolved in either polar or non-polar environments. The so-called hydrophobic effect is the driving force for this aggregation in water caused by the hydrophobic tail to avoid contact with the water molecules. A single surfactant molecule is called a monomer. When the monomers self-assemble into aggregates there is a gain in entropy from the release of structured water molecules surrounding the monomer. This is referred to as hydrophobic hydration.[18] On the other hand this aggregation in water causes strong repulsions between the polar head groups. This repulsion originates from the hydrophobic force trying to minimize the unfavourable water/hydrocarbon contact area and thus bringing the head groups into close proximity with each other at the aggregate/water interface. The strength of the head group

repulsion depends on the nature of the surfactant. In case of nonionic surfactants the head group repulsion is mainly due to steric hindrance whereas for ionic surfactants the repulsion is of an electrostatic character. The electrostatic repulsion between head groups can be reduced by the addition of an electrolyte, *i.e.* a salt, which can reduce the electrostatic repulsion.[18]

1.3.3 Classification of surfactants

1.3.3.1 Classification of surfactants based on the nature of the hydrophilic head group

1.3.3.1.1 Anionic surfactants

When the polar head group of a surfactant is negatively charged it can be classified as anionic surfactant. Anionic surfactants are the most widely used for laundry, dishwashing liquids and shampoos because of their excellent cleaning properties and high wetting potential. They are particularly good at keeping the dirt away from fabrics, and removing residues of fabric softener from fabrics. Anionic surfactants are particularly effective at oily soil cleaning and oil/clay soil suspension. Still, they can react in the wash water with the positively charged water hardness ions (calcium and magnesium), which can lead to partial deactivation. The more calcium and magnesium ions are in the water, the more the anionic surfactant suffers from deactivation. To prevent this, the anionic surfactants need help from other ingredients such as builders (Ca/Mg sequestrates) and more detergent should be dosed in hard water. The most commonly used anionic surfactants are alkyl sulphates, alkyl ethoxylate sulphates and soaps (Figure 2).[20]

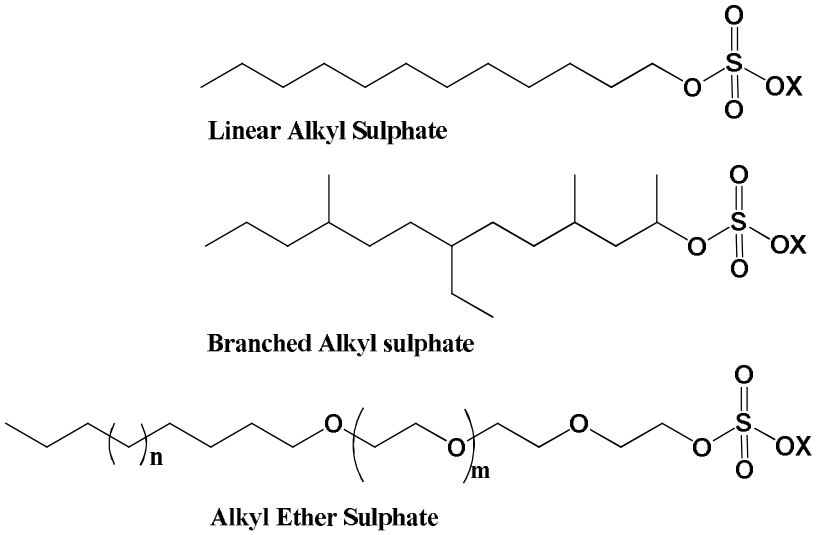

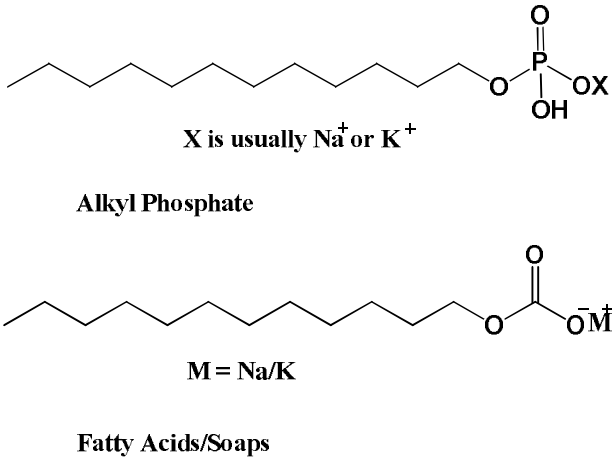

Figure 2: Examples for different types of anionic surfactants.

1.3.3.1.2 Cationic surfactants[19]

When the polar head group of a surfactant is positively charged it is classified as cationic surfactant. The most commonly used cationic surfactants are quaternary ammonium salts with general chemical formula R R′ R″ R‴ N^+ X^-, where R represents alkyl groups and X is mostly chloride. Among the quaternary ammonium salts the most widely used salts are alkyl trimethyl ammonium chloride or in some cases dialkyl dimethyl ammonium chloride where the length of the alkyl chains can vary from 8-18 carbon atoms. In general, dialkyl surfactants are less soluble in water than mono alkyl surfactants. Another most frequently used cationic surfactant is alkyl dimethyl benzyl ammonium chloride. They are compatible with inorganic metal ions and also hard water, but incompatible with protein-like materials and also anionic surfactants. They are also stable to pH change both in alkaline and acid media. They are widely used as co-surfactants.

1.3.3.1.3 Nonionic surfactants[19]

Nonionic surfactants are generally consisting of alkyl or alkyl aryl units as hydrophobic tail and polyoxyethylene or alditol units as polar head groups. The most common nonionic surfactants are based on ethylene oxide and are known as ethoxilated surfactants. Examples of ethoxilated surfactants are alcohol ethoxylates, alkyl phenol ethoxylates, fatty acid ethoxylates, monoalkaolamide ethoxylates, sorbitan ester ethoxylates, fatty amine ethoxylates and ethyleneoxide–propylene oxide copolymers (Table 4).

Another important class of nonionic surfactants are polyhydroxy products such as glycol esters, glycerol and poly glycerol esters, glucosides and sucrose esters.

hydrophobic tail	polar head groups	class of surfactants
alkyloxy-, alkylaryloxy	-$(CH_2$-$CH_2O)_n$-H	ethoxylated surfactants
alkylamino-		
acyloxy-		
acylamino-		
acylamino-		
acyl-	sugar units	sugar esters surfactants
alkyl		

Table 4: Some typical examples of non-ionic surfactants.

1.3.3.2 Surfactants based on renewable resources

In recent years several research groups and also industry have made enormous contributions to the synthesis of bio-based surfactants such as mono- and di-glycerides,[21,22,23] *N*-acylated amino acid and protein,[24,25,26,27] sugar esters[28,29,30] and their potential applications[31] have been well investigated (Scheme 3).

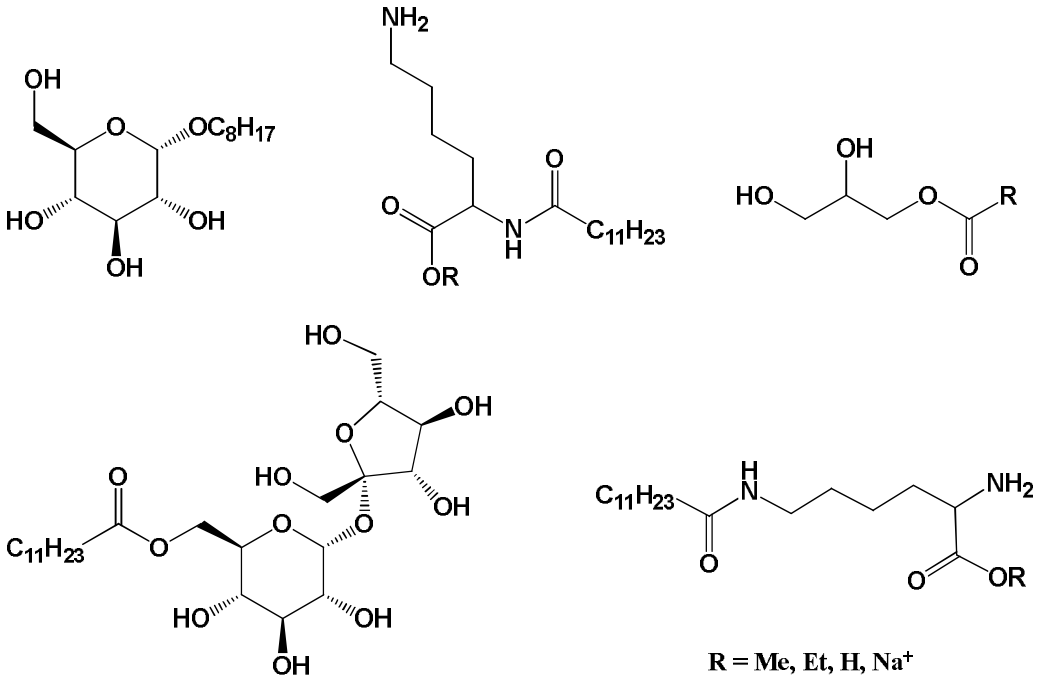

Scheme 3: Chemical structures of some biocompatible surfactants based on renewable resources.

1.3.3.3 Commercially produced surfactants

The best known, widely used and industrially produced surfactants are fatty alcohol polyglycol ethers,[32,33] fatty alcohol sulphates,[34] α-methyl esters sulfonates[35] and some synthetic methods for their preparation are shown below (Scheme 4).[36,37,38]

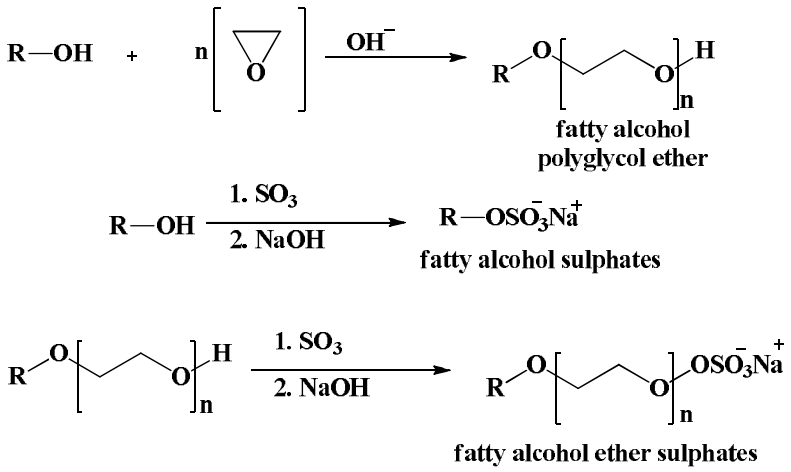

Scheme 4: Typical examples of commercially produced surfactants

1.3.4 Gemini surfactants

A gemini surfactant[39,40,41,42,43] (GS) consists of two conventional surfactant molecules chemically connected *via* a spacer unit. The two terminal hydrocarbon tails can be short or long; the two polar head groups can be cationic, anionic or nonionic; the spacer can be short or long, flexible or rigid.[43]

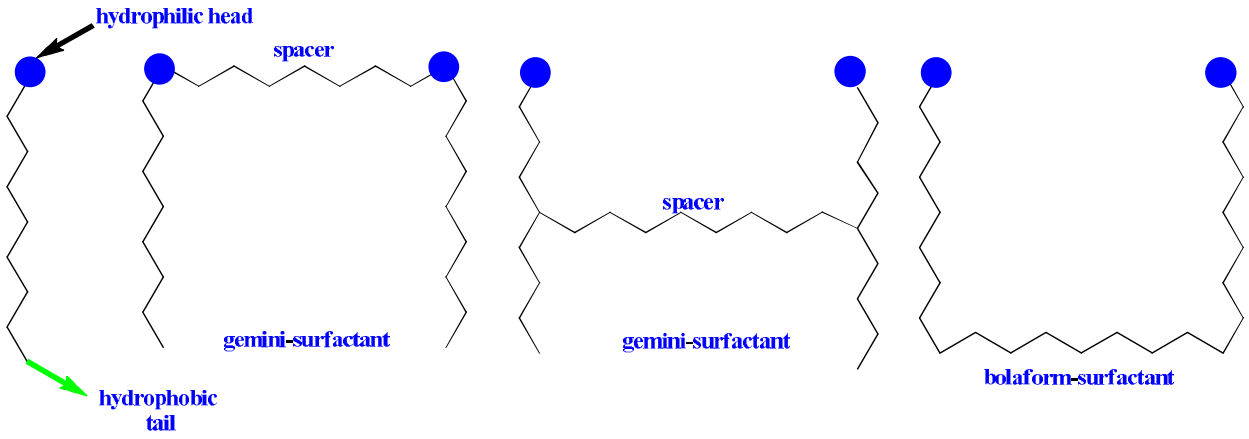

Figure 3: Structures of classical, gemini and bola type surfactants.

The spacer can be attached directly to the identical ionic head groups, each of which is in turn bound to an identical hydrocarbon tail. Alternatively, the two identical amphiphiles can be joined relatively close to the head groups (Figure 3).

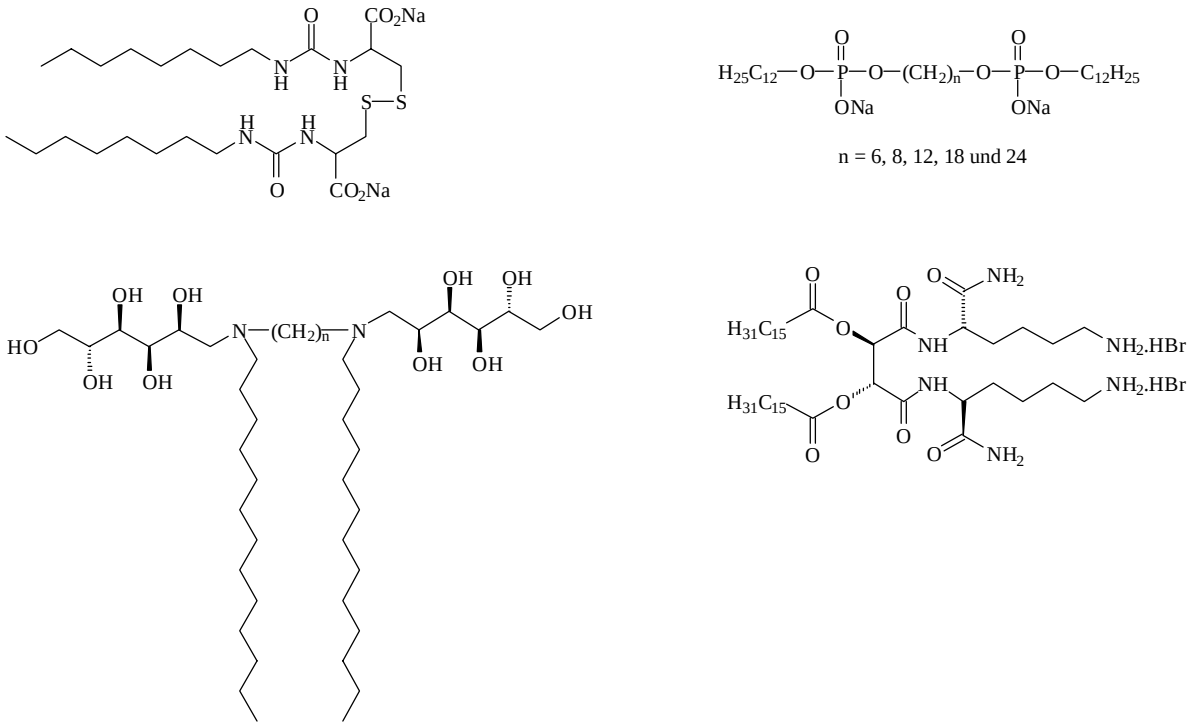

Figure 4: Some typical examples of gemini surfactants.[36]

The GSs need not be symmetrical about the centre of the spacer. GSs can self-assemble at much lower concentrations (CMCs) and therefore are superior in surface activity as compared to conventional surfactants. GSs are very attractive for catalysis and adsorption applications, new synthetic vectors for gene transfection, analytical separations, solubilisation processes, nanoscale technology, biotechnology, enhanced oil recovery and as paint additives.[43] On the other hand the surface properties of gemini surfactants are strictly related to their structure. It has been revealed that there is a loss in their surface properties when the point of attachment is too far away from the head group, such surfactants are called bolaform surfactants (Figure 3). Typical examples for geminal surfactants are shown in Figure 4.

1.3.4.1.1 *O-O′*-di-acylated tartaric acid as an example for a gemini surfactant

O-O′-di-acylated tartaric acid can be obtained by hydrolysis of *O-O′*-di-acylated hydroxycarboxylic acid anhydride and is a typical example for a gemini surfactant. The behaviour as gemini surfactant can be rationalised simply by assuming that the *O-O′*-di-acylated hydroxycarboxylic acid is actually a dimer *O*-acyl glycolic acid linked with a spacer unit of a bond length as shown in Figure 5. In order to compare the variation of the surface properties with the hydrocarbon chains a library of such amphiphiles can be synthesised.

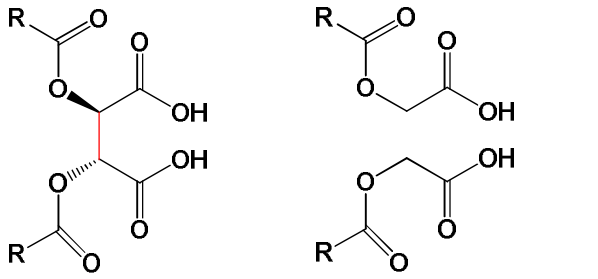

Figure 5: Structure of *O-O′*-di-acylated tartaric acid.

1.3.5 Surface tension and its reduction by a surfactant[b]

Surface tension is a property of the surface of a liquid that allows it to resist an external force. The cohesive forces among the liquid molecules are responsible for this phenomenon of surface tension. In the bulk of the liquid, each molecule is pulled equally in every direction by the surrounding molecules and they are particularly in a uniform field of force (Figure 6). The molecules at the surface do not have other molecules on all sides of them and therefore are pulled inwards. This creates some internal pressure and forces on liquid surfaces to contract to minimise surface energy. Surface tension is responsible for the shape of liquid droplets. Although easily deformed, droplets of water tend to be pulled into a spherical shape by the cohesive forces of the surface layer. In the absence of other forces, including gravity, drops of virtually all liquids would be perfectly spherical. The spherical shape minimizes the necessary "wall tension" of the surface layer according to Laplace's law.

[b] Taken from Wikipedia.

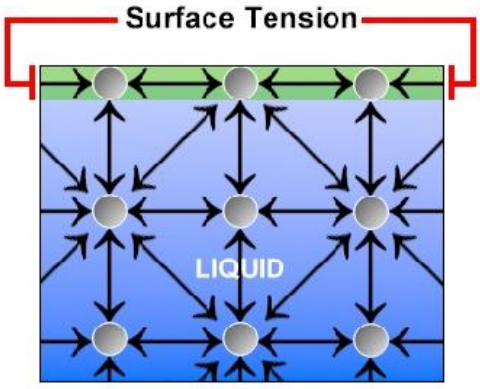

Figure 6: The forces acting on a liquid causing surface tension (taken from Wikipedia).

Since the surface of a liquid is in a state of tension, an attempt to penetrate along any line in the surface will require an additional force to hold the separate portions of the surface together. This force is called surface tension. It is expressed as perpendicular force acting on the unit length of the surface of a liquid. It can be also defined as energy per unit area on the surface of a liquid.

1.3.6 Formation of micelles and critical micelle concentration (CMC)

Upon introduction of surfactants (or any surface active materials) into the system, they will initially partition into the interface, reducing the system free energy by: (a) lowering the energy of the interface, and (b) removing the hydrophobic parts of the surfactant from contact with water.

Subsequently, when the surface coverage by the surfactants increases and the surface free energy (surface tension) decreases and the surfactants start aggregating into micelles, thus again decreasing the system's free energy by decreasing the contact area of hydrophobic parts of the surfactant with water (Figure 7).

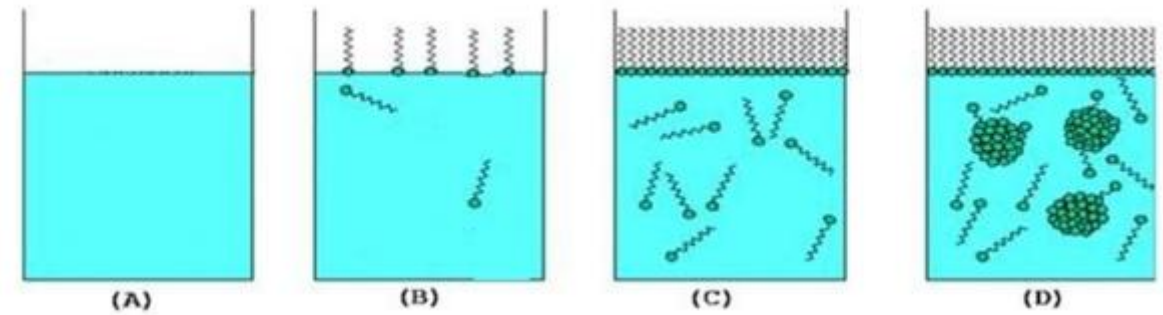

Figure 7: Solution of a surfactant in water.

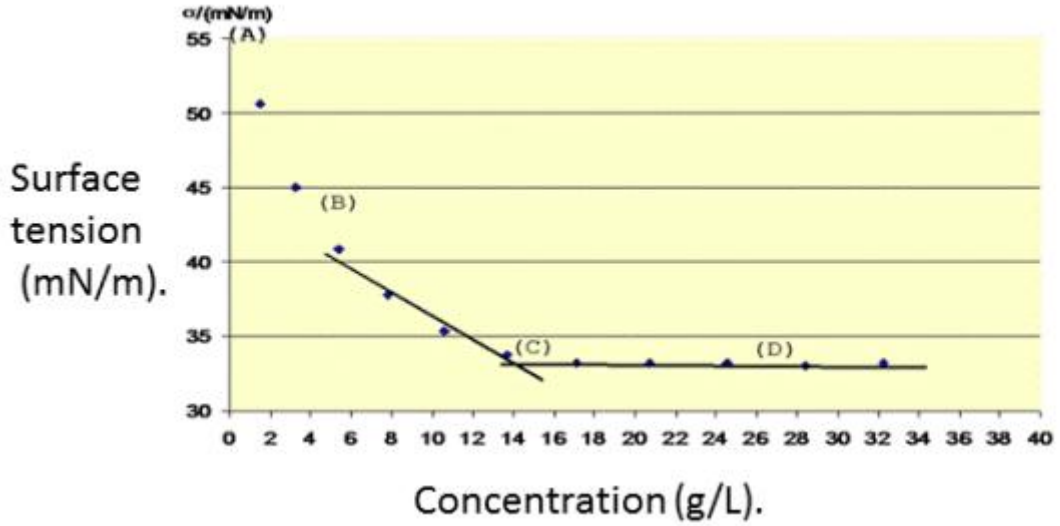

Figure 8: Variation of the surface tension of water with increasing surfactant concentrations.

The surfactant concentration at which micelle formation begins is known as the critical micelle concentration (CMC). As soon as the system reaches the CMC there is no more reduction of the surface tension with the surfactant concentration. The CMC values of surfactants can be determined using various methods based on surface tension, conductivity, light scattering, osmotic pressure or density measurements. In a micelle, the lipophilic tails of the surfactant molecules remain in the interior of the aggregates due to unfavourable interactions with the water molecules, whereas, due to favourable interactions with the water molecules the polar heads of the micelle form a hydrophilic outer layer to expose themselves towards the water and to protect the hydrophobic core of the micelle from water.

1.4 Low molecular weight gelators

1.4.1 Introduction

Discovery and design of low molecular weight compounds, that are capable of gelling water as well as a wide variety of organic solvents, *is a rapidly expanding area in research.*[44] Low-molecular weight gelators[45](LMWGs) represent one important class of materials which have attracted considerable interest in recent years on account of their unique features and potential applications for new soft organic materials,[46] template synthesis,[47] drug delivery,[48] cosmetics,[49] food processing, tissue engineering,[50] medical implants[51] to name just a few. On the other hand, LMWGS have several privileges[52] over polymer gels as they are mostly biodegradable and show a rapid response to external stimuli[53] like change[54] in pH or temperature[55] by which they can rapidly undergo gel to solution phase transition. Such sensitive response to external stimuli is not possible in conventional polymer systems. Most

supramolecular gels are composed of long nano-fibers which are self-assembled through supramolecular interactions such as hydrogen bonding, van der Waals, hydrophobic, π–π stacking, coordinating, donor-acceptor and or charge–transfer interactions. The one-dimensional (1-D) self-assembly of these gelling agents with fiber like structures eventually entangles to form a three-dimensional (3-D) network followed by entrapment and immobilization of the solvent molecules inside the interstice of the 3-D network by surface tension[56] and/or capillary forces[57] inducing gelation in that particular solvent.

1.5 Physical and chemical gelators: molecular interactions in the formation of the gelation network

Based on the interactions which are responsible for the formation of such highly ordered self-assembled gel network, gelators can be categorized into two classes, namely physical and chemical gelators.[58] A chemical gelator can be defined as a type of molecule in which the aggregation is mainly influenced and driven by covalent cross-linking between the compounds. Such aggregation will lead to the formation of a thermally irreversible gelation network. Examples of these systems include cross-linked polymeric systems,[59] which can be used for triggered drug release[60] or inorganic oxides[61] and also various inorganic gels like silica.

In a physical gel the types of interaction responsible for the aggregation are completely different and contrary to the interactions responsible for the construction of a gel network in a chemical gelator. Only non-covalent interactions are involved in the formation of gel fibers in a physical gelator and hence the solvent plays an important role in the gel formation. A lucid explanation from recent publications[62] reveals that not H-bonding but the hydrophobic interactions act as crucial key parameters to control gelation in water. However such interactions are either absent or considered not to be of major importance for gelation in organic solvents.[63] This means that, in order for aggregation of small organic molecules to occur in organic media, other types of interactions must be dominant. These interactions can be very different, ranging from hydrogen bonding, aromatic π–π interactions,[64] van der Waals force of attraction, and even gelation on the basis of London dispersion interactions alone have been reported (*vide infra*).[65] Of course, solvophobic and entropic contributions also play a major role. Unlike many chemical gels, such as cross-linked polymers (see above) most physical gels of LMOGs are thermally reversible. The forces responsible for the formation of their immobilizing network can be London dispersion interactions, hydrogen bonding, aromatic (π-π) interactions, ionic or organometallic coordination bonding, or (almost always)

a combination of these. The interconversion between gel and solution phase depend only on the disassembly and assembly of the constituent molecules at moderate temperatures, which makes these types of gelators excellent candidates for studies in supramolecular chemistry; since in both the highly viscous gel and the solution state the chemical composition is unchanged unless disassembly is concurrent with a form of chemical equilibrium, as in the case of coordination bonding.

1.5.1 Understanding the structure of the gel network

In order to understand the basic mechanism which is involved in the gelation process and also to learn about the way of formation of fibers during the gelation process, a gel can be broken down into primary, secondary and tertiary structures, similar to a protein (Figure 9).[66,67]

1.5.1.1 Primary structure of a gel

The primary structure (Ångström to nanometer scale) is determined by the recognition events on a molecular level which promote anisotropic aggregation in one or two dimensions of the gelator molecules. Assembly of small organic molecules in aqueous solvents into fibrous structures poses interesting challenges in the fields of molecular recognition and self-assembly. Hydrogen bonds, a common driving force for the aggregation in organogelators, lose their strength in water unless many are combined in a cooperative manner and protected from the solvent.[68] Instead, hydrophobic forces, which lack the precise directing ability of hydrogen bonds, become mostly important in aqueous environments.[69] Thus, a key factor for the design of organic hydrogelators is to control these hydrophobic interactions.

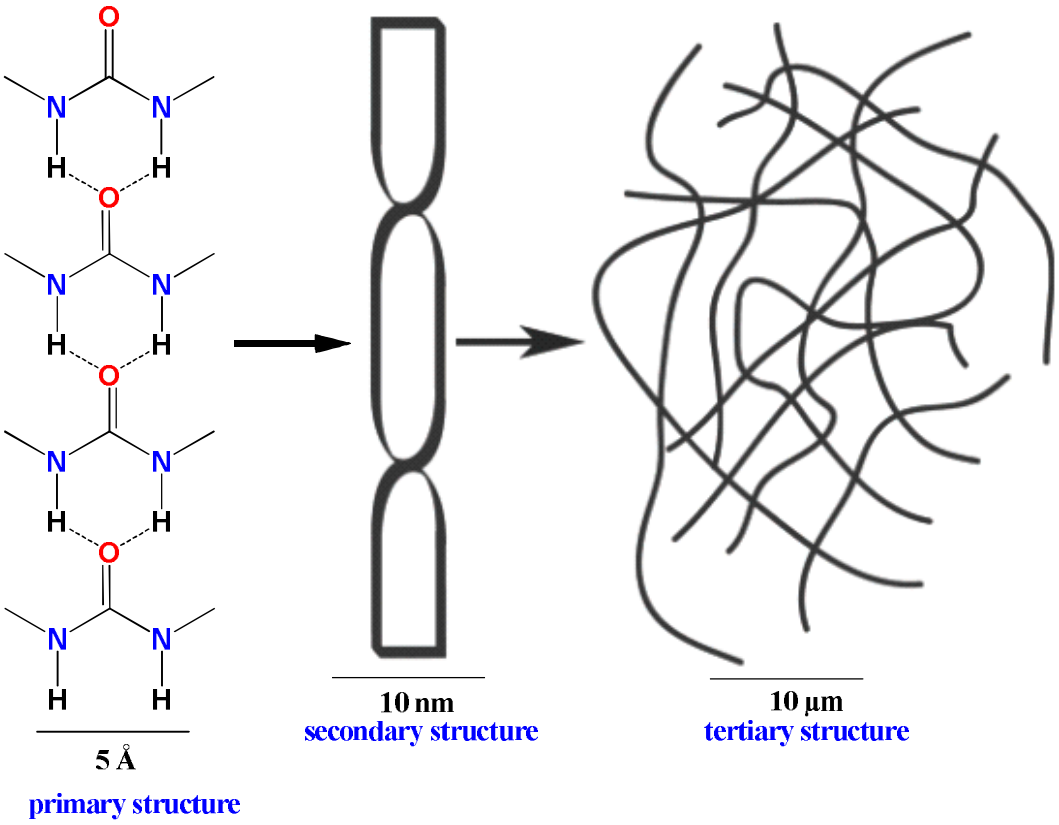

Figure 9: Primary, secondary and tertiary structure of a gel.[44]

1.5.1.2 Secondary structure of a gel

The secondary structure (nano- to micrometer scale) is defined as the morphology of the aggregates such as micelles, vesicles, fibers, ribbons or sheets. This secondary structure is directly influenced by the molecular structure.

1.5.1.3 Tertiary structure of a gel

The tertiary structure of a gel (micro- to millimeter scale) involves the interaction of individual aggregates and ultimately determines whether a gel is formed or instead fibers (or other aggregates) which precipitate from solution rather than being trapped inside.[44] The aggregation of gelator molecules occurs through both branched and entangled fibers. The long and thin flexible fibers are better able to trap solvent molecules than shorter fibers, thus leading to gelation.[66,70]

1.5.2 Gelation: an optional way of molecular aggregation

Gels derived from low molecular weight gelators are usually prepared by heating the corresponding compounds at elevated temperature in an appropriate solvent in order to dissolve the gelator molecules completely. During the course of heating one is actually supplying additional heat, a form of energy that is required to overcome the driving force for

aggregation due to strong intermolecular interactions between the molecules. When the solution is cooled down the molecules start to condense and they will have to choose between one of three possibilities which will depend on the mode of aggregation and also the choice of solvent: (a) highly ordered aggregation of the molecules giving rise to crystalline precipitation in solution, (b) a random aggregation leading to amorphous precipitation and (c) an aggregation process intermediate between those two leading to the formation of a gel (Figure 10).

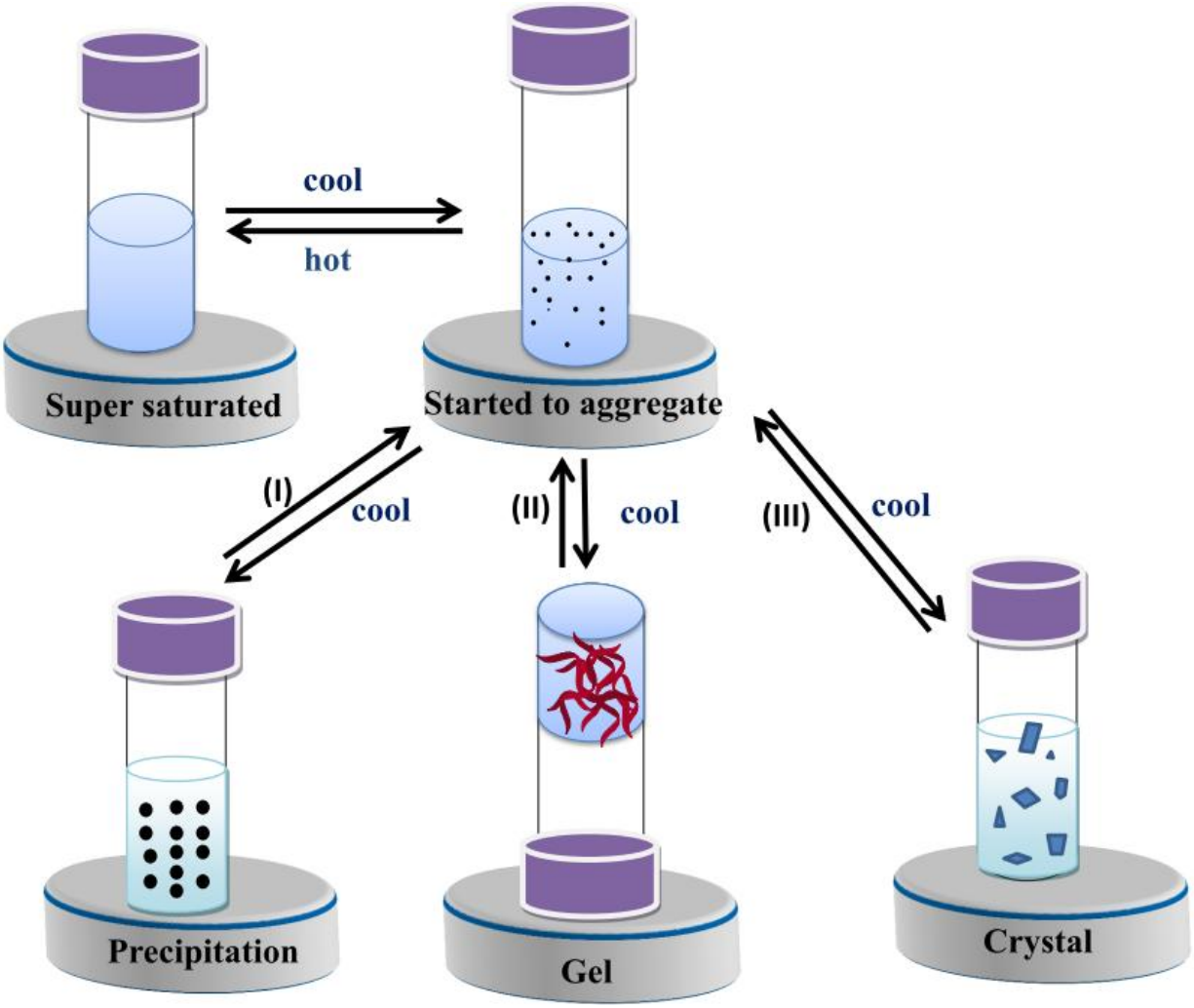

Figure 10: Schematic representation of different aggregation modes.

1.5.3 Understanding the formation of fibers during gelation

A good understanding of the details during the gelation processes is necessary to reveal and elucidate the possible structural requirement for the formation of a gel in a particular solvent. This knowledge facilitates the design of a specific gelator for a defined liquid with selected

properties as well as the preparation of gels suitable for various others applications;[71] rather than getting those by serendipity.

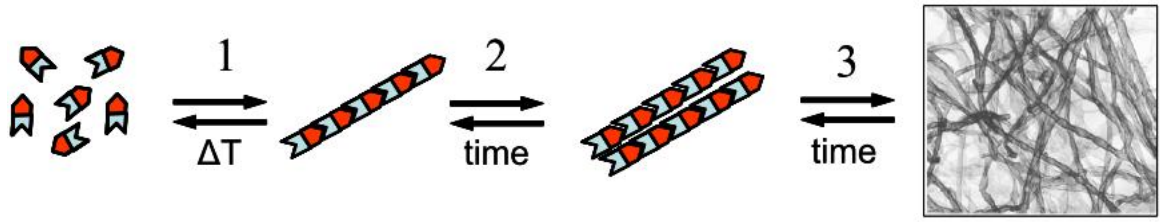

Figure 11: Schematic representation of the formation of a 3-D network starting from dissolved gelator molecules.[58]

Figure 11 represents the general steps which are involved during the gelation process. Upon cooling a supersaturated solution of a gelator in a particular solvent leads to intermolecular interactions between the gelator molecules and provides the driving force for the molecules to self-assemble. Due to the anisotropy of these interactions, self-assembly is favoured in one dimension and is leading to the formation of thin fibers. Along these fibers new fibers can grow or assemble, thereby creating bundles consisting of several thin fibers which minimize the large surface free energy of the single fibers. Over time these bundles grow and can occasionally split leading ultimately to the formation of a 3-D network. This is recognised at the macroscopic level in the formation of a gel. It has been revealed that anisotropy in intermolecular interaction leading to self-assembly of the gelator molecules is necessary for the formation of a gel fiber.[58] Intermolecular interactions between gelator molecules can include London dispersion forces, ionic-ionic, dipole-dipole, hydrogen bonding, van der Waals and π-π stacking interactions and in the majority of gel systems the combination of these forces are responsible for gelation. It has also been demonstrated that there is a delicate balance between gelator structure, intermolecular interactions and gelation properties. Even a small change in the molecular structure of the gelator can change the molecule from a gelator into a non-gelator.[72] On the other hand the molecules may still aggregate but the result can be crystallisation instead of gelation,[73] or the aggregation can be completely absent and the compound therefore is soluble.[74]

Gels are formed under kinetic control. Due to the presence of long fibers there is a large surface free energy which makes the gel state a meta-stable state.[75] The thermodynamically stable state is the crystalline state and it is apparent from studies that there must be an anisotropic driving force in the aggregation that inhibits crystallisation and leads to the formation of a gel. It was found that flexible or branched alkyl chains can prevent crystallisation, although it remains difficult to prevent crystallisation altogether.[76]

1.5.4 Measurement of gel to solution phase transition and gelation temperature

1.5.4.1 Differential scanning calorimetry

Gel-to-solution phase transition can be interpreted on the basic of the assumption that this transition represents actually the dissolution of the crystals in an ideal solution and therefore the van't Hoff equation is applicable for such gel-to-solution transitions in order to determine the melting enthalpy of a gel according to the equation below:

$$\frac{d \ln (C)}{d (1/T_{gs})} = - \frac{\Delta H_g}{R}$$

C = concentration of the gel

ΔH_g = enthalpy of the intermolecular interactions in the gel

T_{gs} = temperature at which the gel network breaks down

R = gas constant

Differential scanning calorimetry (DSC) is a thermo-analytical technique, in which the difference between the amount of heat required to increase the temperature of a sample and the reference is measured as a function of temperature. Both the sample and the reference are maintained at nearly the same temperature throughout the experiment. The physical or chemical changes like melting, crystallisation cross linking, sample decomposition and existence of polymorphic forms of the substance are leading to a change in enthalpy with respect to the reference. The DSC technique actually measures the change in enthalpy of the substance owing to physical or chemical change with respect to the reference. The corresponding signal attributing to that change is observed in the DSC thermogram. In practice the sample is normally placed in a heating block and the temperature of the sample is gradually increased at a constant rate and the same procedure is also repeated to the reference so that both the sample and the reference will have a constant temperature. But when the sample undergoes a physical or chemical change then the temperature of the sample will deviate from the reference due to release or gain in transition enthalpy. The colder block is allowed to heat again to compensate the difference in temperature between the sample probe and the reference. In the DSC scan the value of dH/dT is plotted against the sample temperature. For a supramolecular gel sample when the gel undergoes a reversible phase transition from highly viscous gel state to solution state an exothermic peak attributing to that change can be observed. The energy required for dissolution of gel fibers is measured and ΔH_g can be determined directly. If the endothermic peak in the DSC thermogram is absent or too weak to detect then this implies that formation of gel fibers is largely caused by hydrogen bonding. Consequently the system needs less energy to break such hydrogen bonds as well as

the gel network[77] and therefore the area under the peak in DSC thermogram is too small to be detected.

1.5.5 Morphology of a gel

When the formation of a gel is confirmed and properly mapped it is always recommended to make further investigations regarding the nature of the fibers in the gel network. The best morphological investigation can be done by simple and direct visualisation of the gel sample using optical microscopy. However in most cases, because of the smaller size and very low contrast it becomes difficult to analyse precisely the morphology and size of the fibers. Some contrast improvement techniques help to make the visualisation possible in certain cases. Electron microscopy is a powerful tool to visualise the delicate gel structures and intensive care must be taken to prepare appropriate gel sample for such measurement. In TEM and SEM experiments a highly diluted gel sample (to avoid overlayer of aggregate structures)[78] is prepared using the spin coating technique to prepare a very thin layer, followed by evaporation of the solvent by freeze-drying to induce minimum strain and stress on the gel sample during evaporation. Then the dried sample is coated with a heavy element (gold or platinum) by the sputter coating technique to enhance the contrast. After that, the samples are placed in an ultra-high vacuum chamber and imaged with an electron beam. Using these methods the gel fibers are not imaged in their native state and artefacts may arise upon drying and staining as these might induce stress on the gel fibers. Even when the macroscopic gel collapses during preparation for visualisation, the resolution is such case may still observe by electron microscopy and actually the fine structure of the collapsed structural elements.[78,156]

1.5.6 Driving forces leading to gel formation

The arrangement of the fibers in the self-assembled gel network of hydro- and organogelators is completely different and therefore the driving forces which have primary and/or major contributions for the gelation in water or an organic solvent are different. In hydrogelators the hydrophobic moieties are facing towards the inside of the assembly and the hydrophilic head groups are exposed to the water for interaction. In the case of organogelators the polar head groups are tilted inside and the hydrophobic parts are more likely to stay outside[79] in order to interact with the solvent.

As the arrangements of the fibers in the gel network of organo- and hydrogelators are different and depend upon the environment it is quite obvious and revealed recently that primarily it is not the hydrogen bonding but rather the hydrophobic interaction which is the key parameter controlling the gelation efficacies in water of the LMWGs.[80,81,82]A minute

structural change of the hydrophobic part tunes the supramolecular aggregation of the respective hydrogelator and cause a dramatic change in its gelation efficacy in water. In case of organogelators hydrogen bonding contributes mostly to the formation of self-assembled gel network and therefore the polar head group plays a very decisive role on the gelation efficacy in organic solvents.[83]

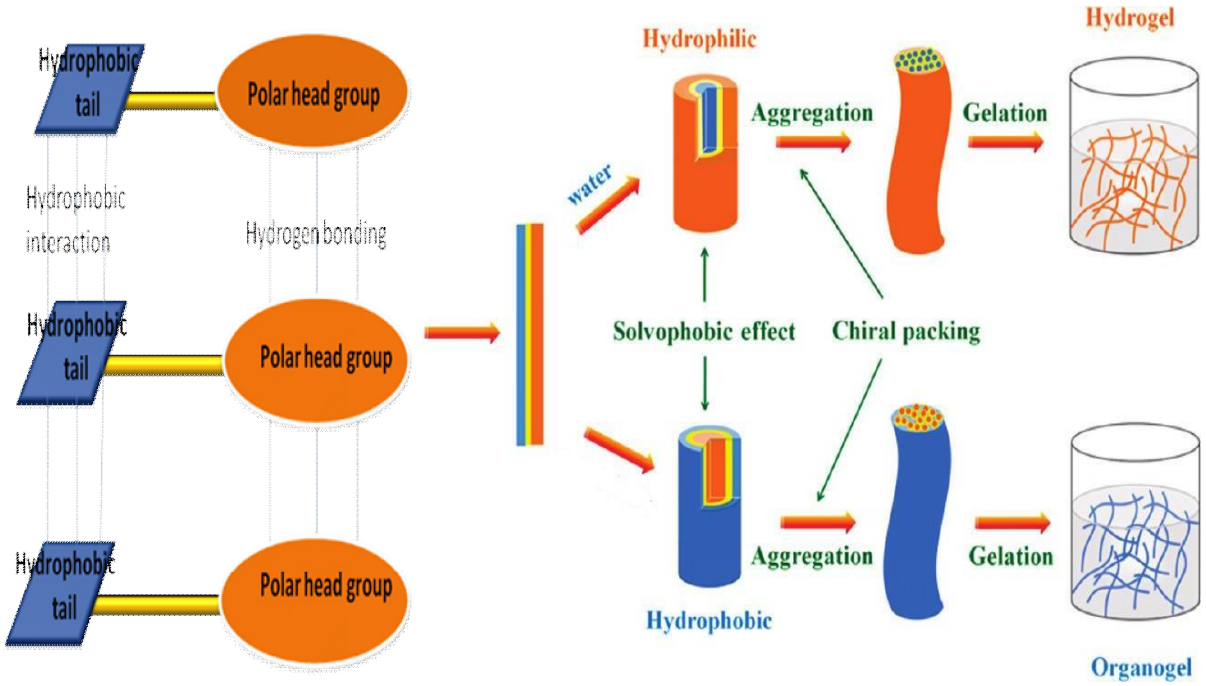

Figure 12: Effect of solvents on the arrangement of the fibers towards the formation of a gel-network.[83]

1.5.6.1 Investigation of driving forces leading to gel formation

Various spectroscopic techniques can be used to study gels. Since NMR, IR, UV/vis, CD, and fluorescence are temperature sensitive, they can be used to measure the temperature at which the gel forms. This is an alternative to DSC.[84] However, due to hysteresis effects, the temperature at which the gel forms and melts differs irrespective of the method used. The T_1 and T_2 relaxation times of NMR can be used to identify the parts of the LMWGs that have restricted conformational and translational motions.[85,86,87] Solid-state NMR can also be used for gel samples for the identification of the self-assembly and aggregations. The syntheses of LMWGs with covalently linked fluorescent probes and/or UV active groups have been used in probing hydrophobic pockets[88,89,90] especially in aqueous environments, and the aromatic groups of fluorescent probes also promote aggregation, both of which can be observed by small to moderate shifts in the emission spectrum. In addition to NMR, IR spectroscopy can be used to observe hydrogen bonding (O-H, N-H, and C=O vibrations) and it can also be used to determine whether a carboxylic acid is protonated.[91] Using IR one can also investigate the contribution of different kinds of physical interactions that are responsible for the formation

of a self-assembled gel network. By FT-IR spectroscopy information on the organisation of the fibers in the gel network can be obtained indirectly. By comparison of gelator molecules in solution with gelators in the gel state, the specific intermolecular interactions leading to gel formation can be deduced. A significant advantage of these techniques is that these can be applied to the native state of the gel.

1.5.7 Carbohydrates based low molecular weight gelators

Carbohydrates provide a large library of water soluble, chiral building blocks that have been used successfully to design organo- and hydrogelators. In addition to their ambidextrous and robust gelation abilities in a wide variety of organic solvents as well as in water, carbohydrate based LMWGs (C-LMWGs) also offer considerable advantages due to their large abundance and in being renewable resources. Due to the presence of multiple hydroxy groups embedded into the structural core, simple carbohydrates can be utilized as hydrogen bond donors or functionalized readily to give rise to gelators with dramatic changes in their properties. Sugars by the virtue of being biocompatible make them attractive candidates for hydrogels in biological applications.[92] Most importantly, from a medicinal standpoint, carbohydrates, like amino acids, are natural compounds so that simply derived C-LMWGs could be used in the human body potentially without harmful side effects. The numerous hydroxy groups are responsible for the solubility of carbohydrates in water and they have been used primarily to synthesize LMHGs.

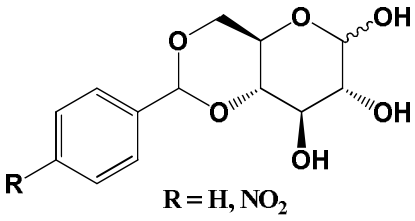

I

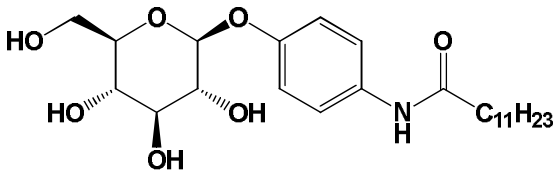

II

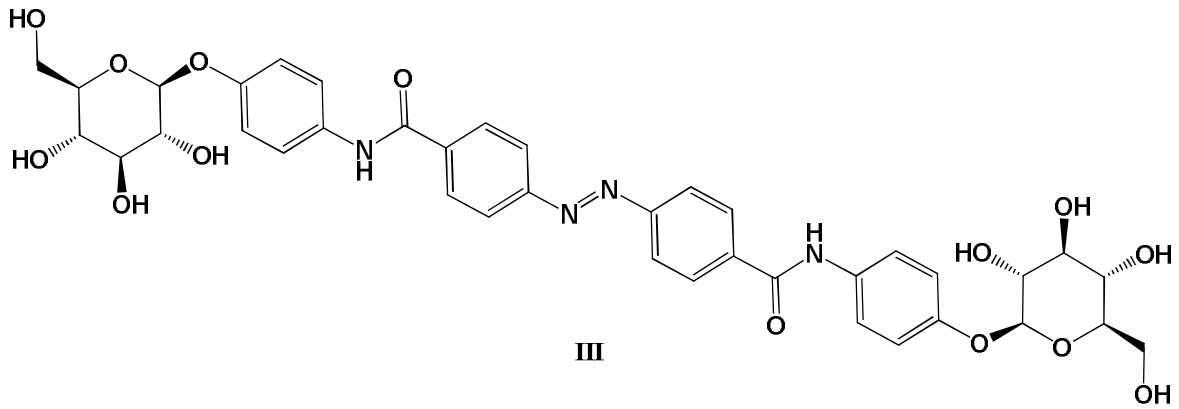

III

Compounds **I-III** are the typical examples of the C-LMWGs where the sugar units promote their solubility in water and because of the presence of aromatic units the molecules are enjoying π- π stacking in water which is mainly responsible for the formation of self-

assembled gel network. Some of these C-LMWGs are ambidextrous gelators and hence have abilities to gelatinise water as well as some organic solvents.

Thus Fuhrhop *et al.* have synthesized and studied the self-assembly properties of the first carbohydrate based gelators.[93] Any of the four aldoses (*D*-glucose, *D*-mannose, *D*-gulose, and *L*-mannose) was reacted individually with any of two amines (octyl and octadecyl) to generate a library of 8 potential C-LMHGs (**IV**-**VII**).

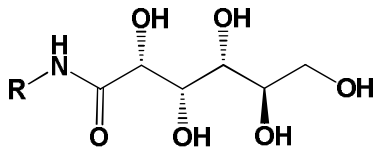

IV

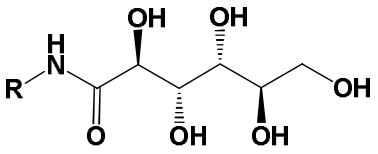

V

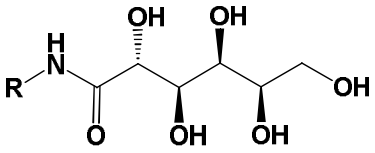

VI

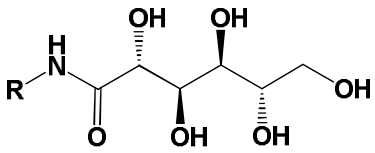

VII

R = C_8H_{17} , $C_{18}H_{37}$

V was found to produce long micellar fibers of only 4 nm in width with a minimum gelation concentration of 0.85 % (w/v). The *D*-mannonamide and *D*-gulonamide gave similar results with minimum gelation concentrations of 0.93 and 0.80%, respectively.

The groups of Shinkai, Hamachi, Shimizu have made enormous contributions and achieved a considerable advancement in the area of C-LMWGs. Shinkai *et al.* have reported the syntheses of some amphiphiles (**VIII**-**IX**) and bolaamphiphiles (**X**-**XI**) based on *D*-glucose. The long alkyl chains in gelators **VIII**-**XI** not only enhanced their solubilities in organic solvents, but also promoted the association among the fibers through van der Waals forces of attraction leading to eventual gel formation.[94]

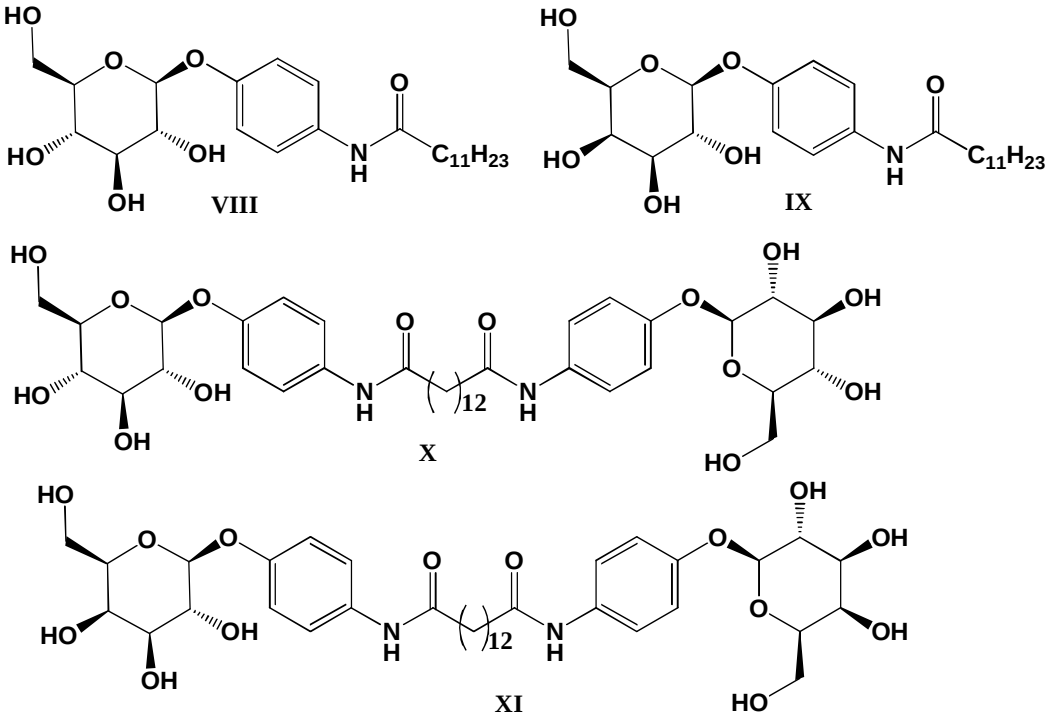

VIII and **IX** induced gelation in a wide range of organic solvents as well as in water in the presence of small amounts of alcoholic co-solvents, whereas **X**-**XI** can induce gelation in water without any co-solvent simply because of the presence of a sugar moiety at both ends of the bolaamphiphiles, thus increasing their solubility in water. The aqueous transparent hydrogels of **X** and **XI** consist of film like lamellar structures with 50 ± 100 nm thicknesses at extremely low concentration (0.05%). **VIII**-**XI** are typical examples of C-LMWGs which demonstrate that it is most likely that an aldopyranose moiety, an aminophenyl group and a long alkyl chain group of an amphiphile can enjoy intermolecular hydrogen-bonding, π-π stacking and interdigitated interactions and, therefore, should produce highly ordered, layered structures. The possible gelation of water and organic solvents by aldopyranoside-based compounds will thus strengthen the concept of unidirectional interaction as a prerequisite for gelation.

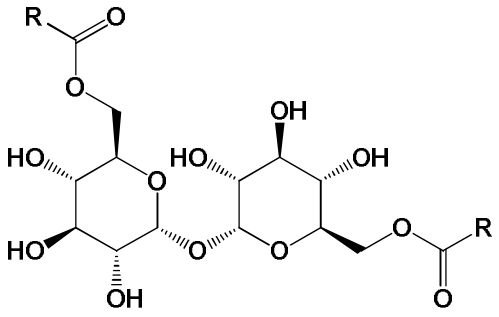

Figure 13: Symmetrical 6,6′-di-esters of trehalose that act as a gelator in organic solvents.

John George and his group have made also excellent contributions in the field of C-LMWGs. George *at al.* have reported the enzymatic syntheses of 6,6′-di-esters of trehalose (Figure 13) and their robust gelation abilities in a broad range of organic solvents, especially ethyl acetate and acetonitrile. The unique symmetry of these products play a key role in their gelation abilities.[95] The SEM image of the xerogel obtained from ethyl acetate revealed that they consist of 3-D entangled fiber-like aggregates with diameters of 10–500 nm and lengths in the micrometer scale. The high aspect ratios of the gel fibers clearly indicate that the intergelator interactions are highly anisotropic. Variation of minimum gelator concentrations of each gelator in a particular solvent with length of the hydrocarbon chains also have been described in a systematic way.[95]

2 Aims of the Thesis

The main goal and aim of this work was the regioselective lipid modification of mono-, disaccharides, polyols (sorbitol and mannitol) and vitamin C with *O*-acylated hydroxycarboxylic acid (malic and tartaric acid) anhydrides. These anhydrides are excellent electrophiles and hence can undergo ring opening reaction with a wide variety of nucleophiles based on renewable resources. This allows the generating of vast libraries of combination products with multifunctional properties such as surfactants, emulsifiers, gelators, antioxidants.

The further aim of this work was the investigations of the surface active-(foaming and emulsifying and CMCs) and gelation properties (gelation efficacies, minimum gelation concentrations and thermal stabilities of the gels) of the combination products by systematically altering the polar head groups and/or the hydrophobic tails of the *O*-acylated hydroxycarboxylic acid anhydrides. Thus a programme was developed to synthesise libraries of such amphiphiles with different polar head groups (*D*-glucose, *D*-glucosamine, *D*-galactose, *α*-methyl-*D*-glucose, sucrose, *D*-sorbitol and *D*-mannitol, *L*-ascorbic acid) and different hydrophobic tails by systematic variation of the fatty acid chains of the anhydrides (Figure 14). The combination products with *L*-ascorbic acid are expected to be soluble in native oils and–provided the antioxidant properties of such derivatives are maintained–could be useful for the stabilisation of native oils. Yet another aim of the present study was also to provide reaction conditions under which these combination products can be synthesized on a large (industrial) scale from renewable resources.

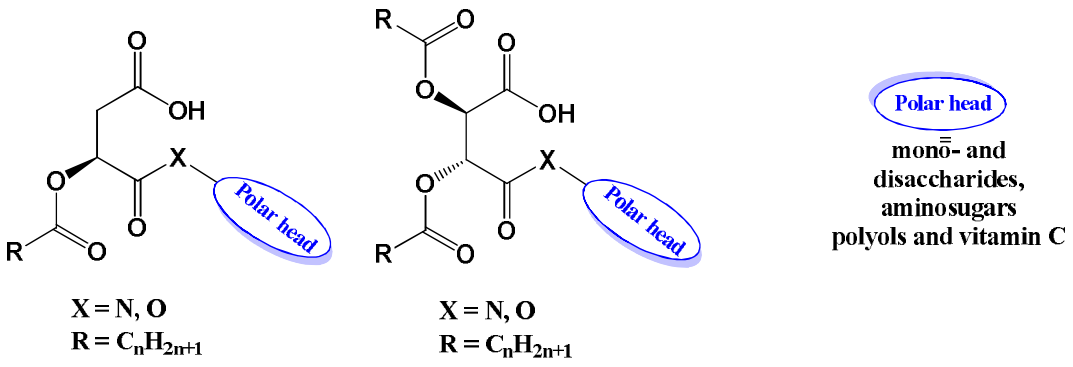

Figure 14: Combination products based on *O*-acylated hydroxycarboxylic acid anhydrides and nucleophiles derived from renewable resources.

3 Results and Discussion

3.1 Hydroxycarboxylic acid anhydrides: design strategy and syntheses

3.1.1 Syntheses of *O*-acylated hydroxy carboxylic acid anhydrides and their reactivity

In 2000 the research group of M. P. Schneider *et al.* discovered[96] by serendipity the almost quantitative conversion of citric acid by reaction with lauric acid chloride into the corresponding *O*-acylated citric acid anhydride (Scheme 5). The crystal structure of *O*-lauroyl citric acid anhydride has confirmed the formation of the anhydride instead of the originally expected *O*-lauroyl citric acid.

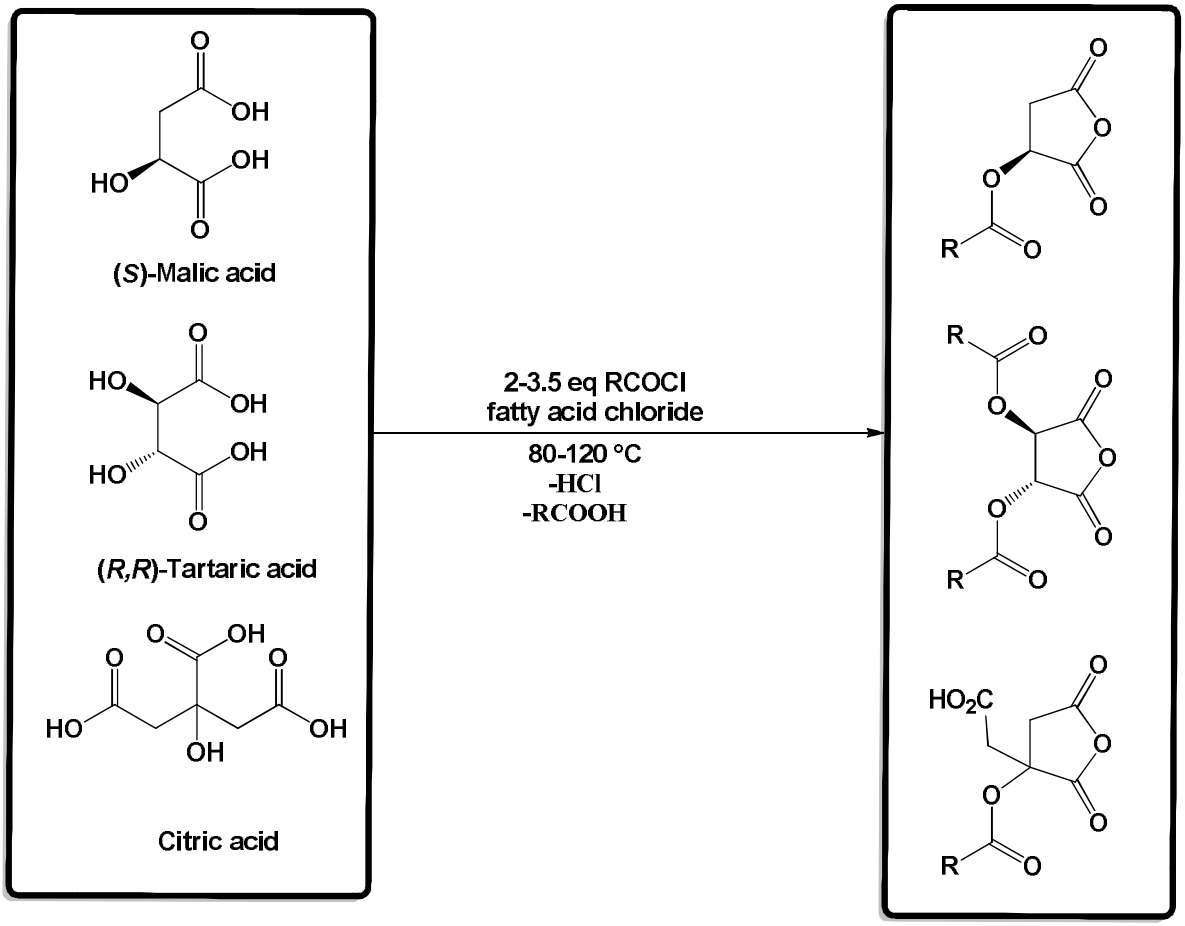

Scheme 5: Syntheses of *O*-acylated hydroxy carboxylic acid anhydrides.

Further investigations revealed that the above synthetic methodology is applicable also to other hydroxycarboxylic acids such as malic and tartaric acid leading to a library of these molecules by systematic alteration of the employed fatty acid chlorides.[97,98] These *O*-acylated

hydroxycarboxylic acid anhydrides are reactive electrophiles and hence can undergo ring opening reaction with suitable nucleophiles like alcohols, amines and polyols (*e.g.* sorbitol and mannitol) including glycerol, amino acids, carbohydrates and *L*-ascorbic acid to generate a wide variety of combination products with an enormous diversity in properties.

3.1.1.1 Syntheses of *O*-acylated malic acid anhydrides 1-6

3.1.1.1.1 General procedure

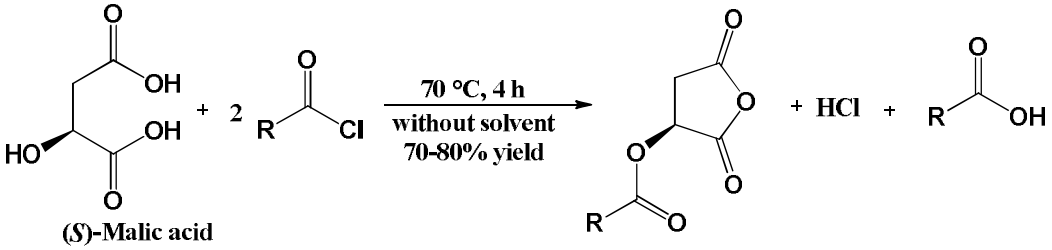

1 R = C_7H_{15}; 42%
2 R = C_9H_{19}; 70%
3 R = $C_{11}H_{23}$; 90%
4 R = $C_{13}H_{27}$; 78%
5 R = $C_{15}H_{31}$; 76%
6 R = $C_{17}H_{35}$; 82%

Scheme 6: Syntheses of *O*-acylated malic acid anhydrides **1-6**.

The general procedure for the syntheses of *O*-acylated malic acid anhydrides is as follows. One equivalent of (*S*)-malic acid is mixed with at least 2 eq fatty acid chloride and heated to 70-90 °C for several hours leading to formation of the corresponding *O*-acylated malic acid anhydrides. No solvent is used. The reactions are practically completed after 4 h. The products can be isolated usually by recrystallization from *n*-hexane.

3.1.1.2 Characterization of 1-6

In Figure 15 the ^{1}H NMR spectrum of **3** is shown, exemplifying this group of compounds**.** The ^{1}H NMR spectrum revealed that the proton having a chemical shift at δ = 5.52 (dd, *J* = 9.6, 6.1 Hz, 1H) ppm corresponds to the H-2 proton of **3**; the protons at C-2′ position are chemically different and appear as two separate dd at 3.38 (*J* = 18.9, 9.6 Hz, 1H), 2.97 (*J* = 18.9, 6.1 Hz, 1H) ppm, respectively. The signals for the lauroyl residue are clearly distinct from the rest of the molecule and are appearing between 2.48 to 0.87 ppm.

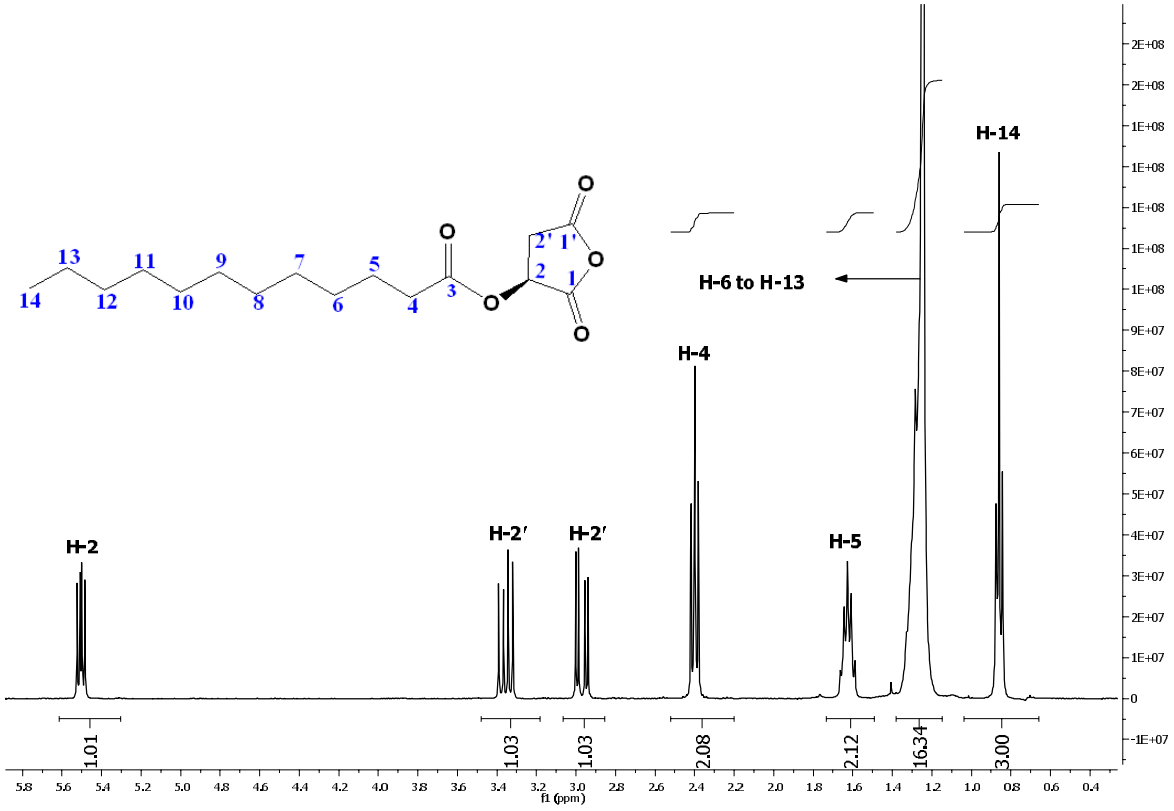

Figure 15: ^{1}H NMR spectrum of *O*-lauroyl malic acid anhydride (**3)** in $CDCl_3$.

The proton signals with chemical shift of δ = 2.48 – 2.36 (m, 2H), 1.73 – 1.55 (m, 2H), 1.38 – 1.08 (m, 16H), 0.87 (t, *J* = 7.1 Hz, 3H) ppm are the characteristic signals of the lauroyl residue and the assignments of all proton signals of the fatty acid residue are shown in Figure 15.

In Figure 16 the ^{13}C NMR spectrum of **3** is shown, exemplifying this group of compounds**.** The ^{13}C NMR spectrum shows the characteristic carbonyl carbon signals at C-1′, C-1, C-3 with chemical shifts of δ = 172.59, 167.97, 166.61 ppm respectively. Figure 16 also exhibits the characteristic CH and CH_2 signals of the malic acid unit which appear at δ = 67.46 and 35.05 ppm, respectively. The carbons with chemical shifts in the range of 35.05-13.98 ppm are the characteristic signals of the fatty acid chain and assignments of all signals are summarised in Figure 16.

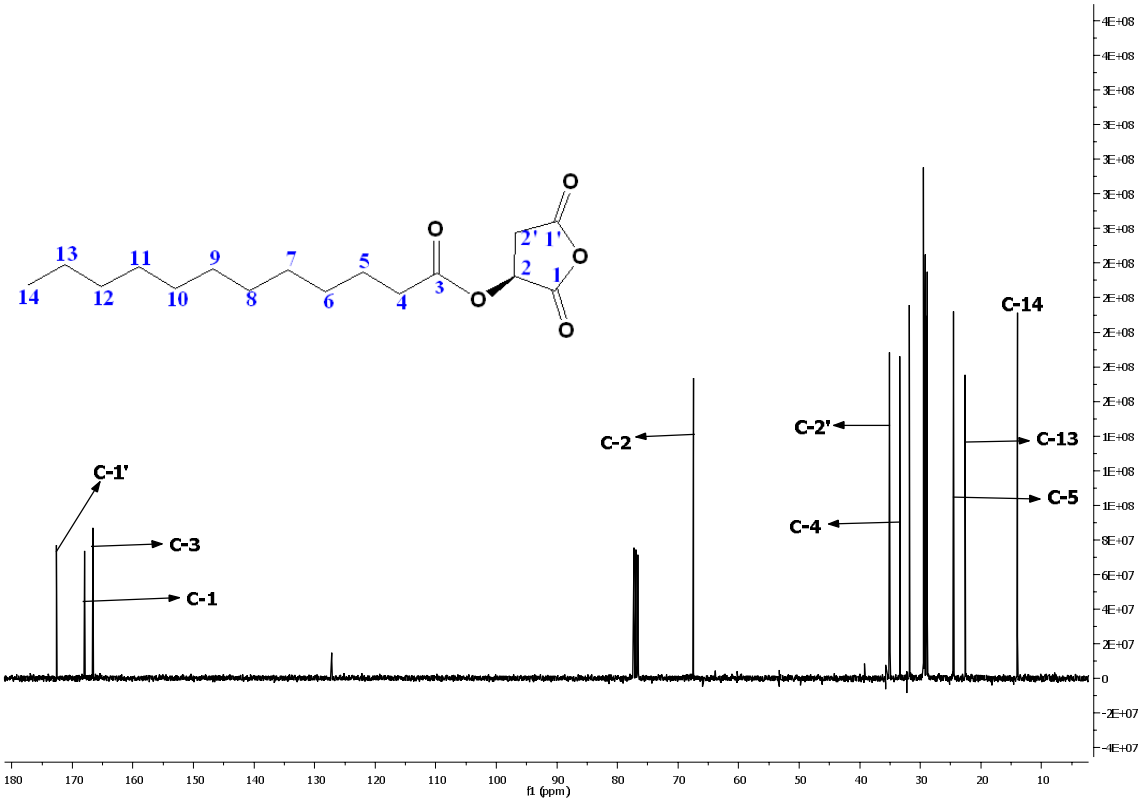

Figure 16: ^{13}C NMR spectrum of *O*-lauroyl malic acid anhydride (**3)** in $CDCl_3$.

3.1.1.3 Syntheses and characterisation of *O*-*O'*-di-acylated tartaric acid anhydrides (7-12)

3.1.1.3.1 General procedure

The syntheses of **7-12** were achieved in a similar way as described above for the syntheses of *O*-acylated malic acid anhydrides (section 3.1.1.1.1).

The general procedure for the syntheses of *O*-*O*-di-acylated tartaric acid anhydrides is as follows. 1 eq amount of (*R*,*R*)-tartaric acid is mixed with at least 3 eq amount of the corresponding fatty acid chloride and the mixture is heated to 90 °C for 24 h. No solvent is used. The reaction is practically completed after 24 h. The products can be isolated by recrystallization from *n*-hexane (Scheme 7).

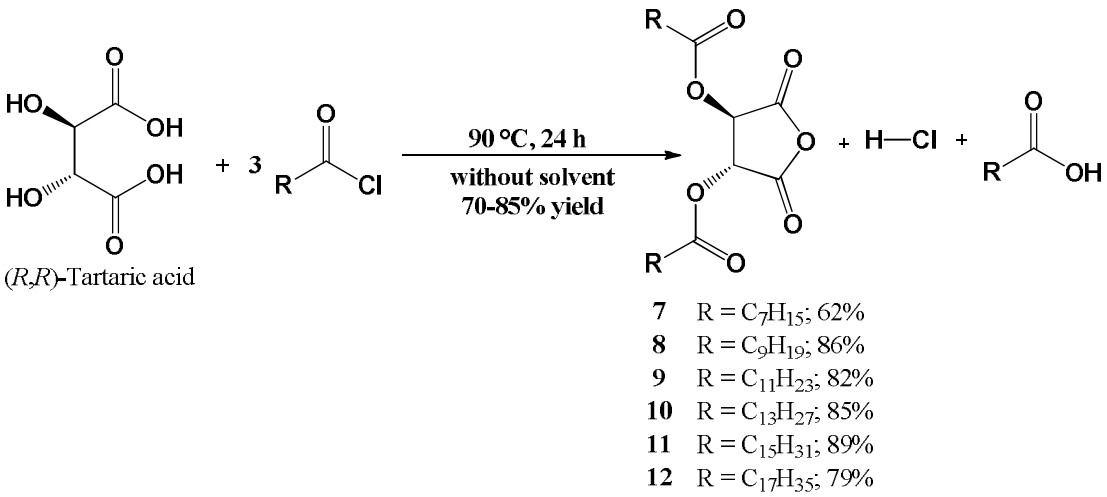

Scheme 7: Syntheses of *O-O′*-di-acylated tartaric acid anhydrides (**7-12)**.

3.1.1.3.2 Characterisation of 7-12

In Figure 17 the ^{1}H NMR spectrum of **9** is shown, exemplifying this group of compounds**.**

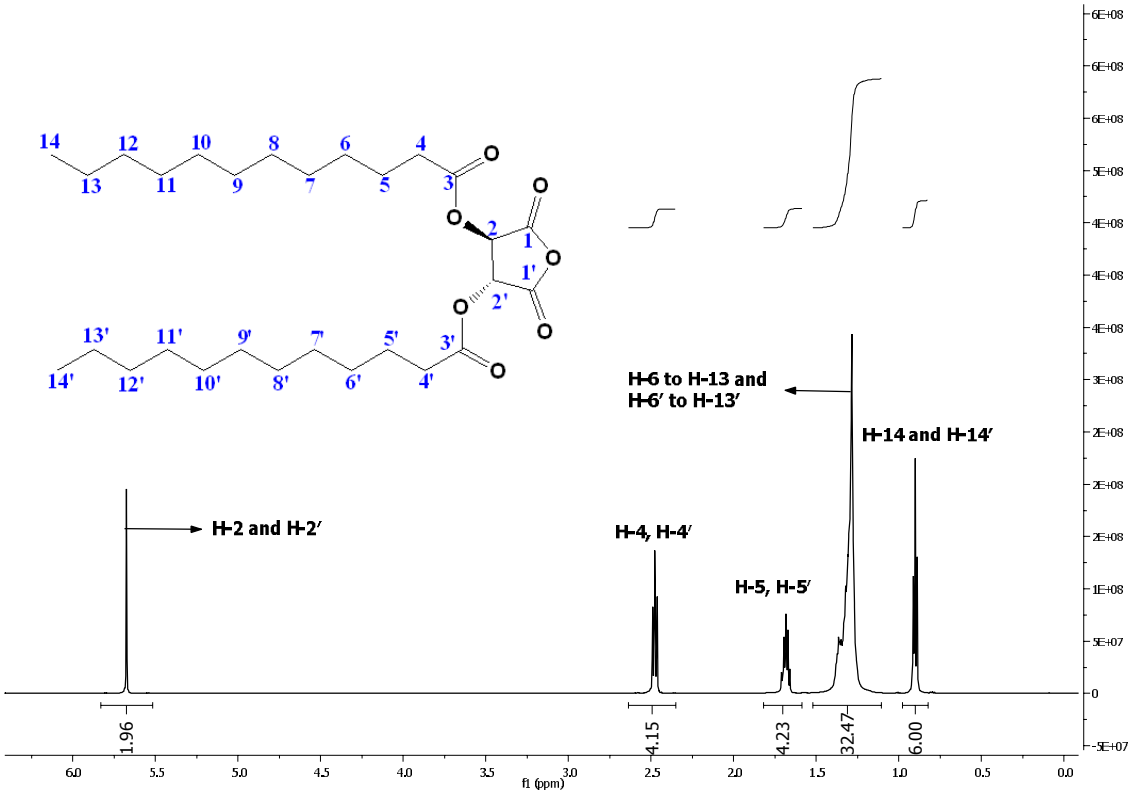

Figure 17: ^{1}H NMR spectrum of *O-O′*-di-lauroyl-tartaric acid anhydride (**9)** in $CDCl_3$.

In the ^{1}H NMR spectrum revealed that the protons with the chemical shift of δ = 5.67 (s, 2H) ppm correspond to the H-2 and H-2′ protons of **9** ; the signals of the fatty acid residue are clearly distinct from the rest of the molecule and are appearing in the range of 2.48 to 0.90 ppm. Signals with chemical shifts of δ = 2.48 (t, *J* = 7.5 Hz, 4H), 1.82 – 1.59 (m, 4H), 1.52 –

1.10 (m, 32H), 0.90 (t, *J* = 7.1 Hz, 6H) ppm are characteristic signals of the lauroyl residue and the complete assignments of all proton signals for the fatty acid residue are shown in Figure 17.

Figure 18 the ^{13}C NMR spectrum of **9** is shown, exemplifying this group of compounds**.**

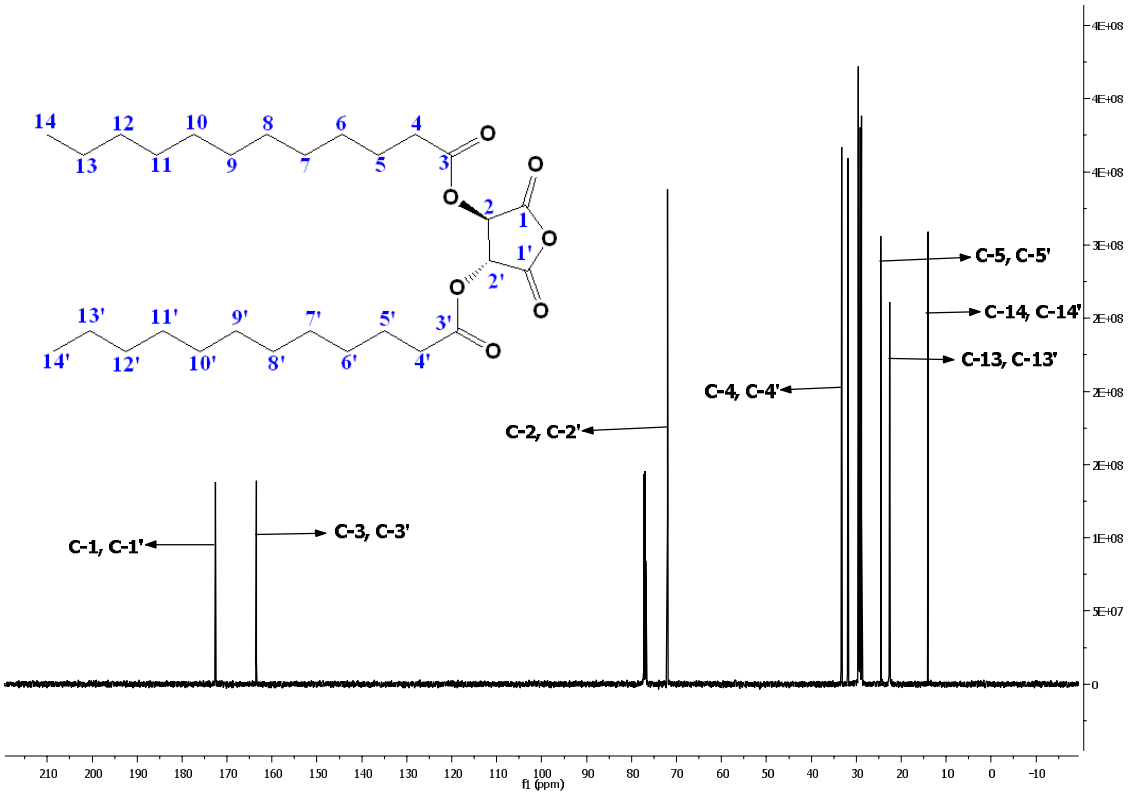

Figure 18: ^{13}C NMR spectrum of *O*-*O*′-di-lauroyl-tartaric acid anhydride (**9)** in $CDCl_3$.

The ^{13}C NMR spectrum shows the characteristic signals of the carbonyl groups at C-1, C-1′, C-3, C-3′ with chemical shifts of δ = 172.56, 163.48 ppm, respectively. Figure 18 also shows the characteristic CH signals of the tartaric acid unit at δ = 72.05 ppm. Carbons with chemical shifts between 33.29-14.15 ppm are characteristic for the fatty acid residue and the assignments of all the fatty acid carbon signals are summarized in Figure 18.

3.1.2 Conclusion

A series of *O*-acylated hydroxycarboxylic acid anhydrides have been synthesised in almost quantitative yield by the solvent free treatment of hydroxycarboxylic acids with fatty acid chlorides. In most of the cases the corresponding anhydrides were isolated from the crude mixture simply by recrystallization from *n*-hexane.

3.2 Lipid modification of *D*-glucose: synthesis and properties

3.2.1 Selective esterification of *D*-glucose with *O*-acylated hydroxycarboxylic acid anhydrides

The major goal of the current study was to achieve the selective esterification of one hydroxy group of *D*-glucose by using either protected glucose (where only one hydroxy group is free and hence available to react) or simply native *D*-glucose as starting material. The unsuccessful attempts for the selective acylation of *D*-glucose based on protection-deprotection strategies are described in sections 3.2.1.1.1 and 3.2.1.1.2. Acylation of the hydroxy group at the C-6 position of *D*-glucose was finally achieved by taking native *D*-glucose without any protection as described in section 3.2.1.2.

3.2.1.1 Earlier attempts

3.2.1.1.1 Attempt to prepare 6-*O*-acylated fatty acid esters of *D*-glucose

The first attempts for a selective acylation of *D*-glucose were based on a protection-deprotection strategy. For this, C-6 hydroxy group of *D*-glucose was selectively protected using trityl chloride[99] in the presence of triethylamine and pyridine at room temperature leading to the formation of 6-*O*-trityl-*D*-glucose (**10**) (Scheme 8). In the next step **10** was treated with acetic anhydride in the presence of pyridine to obtain 1,2,3,4-tetra-*O*-acetyl-6-*O*-triphenylmethyl-*β*-*D*-glucose[100] (**11**) in 41% yield. Deprotection of **11** was accomplished with 33% HBr in acetic acid to liberate the hydroxy group at C-6 position leading to the formation of 1,2,3,4-tetra-*O*-acetyl-*β*-*D*-glucose (**12**). **12** was then treated in chloroform with the *O*-acylated hydroxycarboxylic acid anhydride **3** in the presence of pyridine leading to 1,2,3,4-tetra-*O*-acetyl-6-*O*-acyl-*β*-*D*-glucose (**13**) in practically quantitative yield. Deprotection of the acetyl groups in **13** was attempted in the presence of NaOMe/MeOH in order to obtain 6-*O*-acyl-*D*-glucose. But in the presence of NaOMe also deacylation of the ester bonds took place.

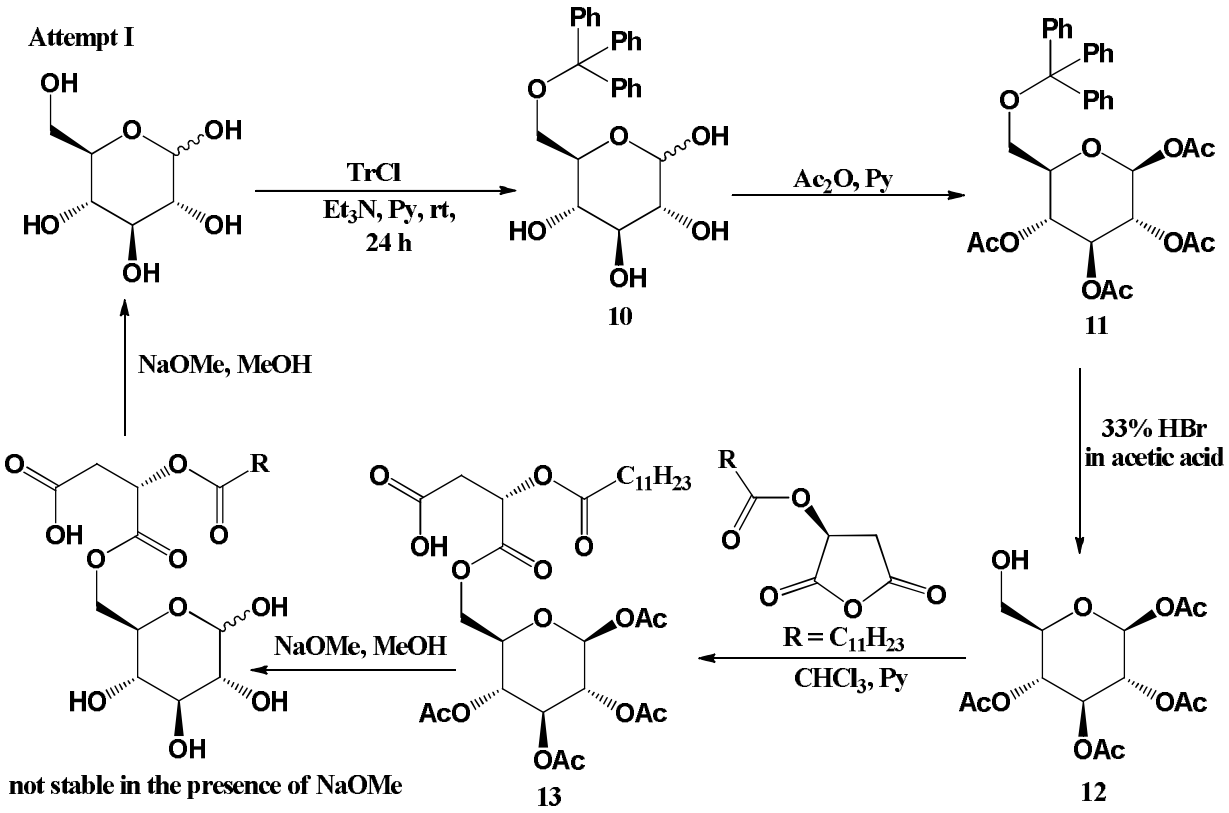

Scheme 8: Attempt for the syntheses of 6-*O*-acylated fatty acid esters of *D*-glucose.

3.2.1.1.2 Attempt to prepare 3-*O*-acylated fatty acid esters of *D*-glucose

In order to prepare selectively 3-*O*-acylated fatty acid esters of *D*-glucose a synthetic strategy was employed as represented in Scheme 9. First *D*-glucose was treated with acetone and sulphuric acid leading to 1,2:5,6-di-*O*-isopropylidine-*α*-*D*-glucofuranose (**14**) in 51% yield.[101] **14** was then acylated on the free hydroxy group at C-3 position by *O*-acylated malic acid anhydride **3** in chloroform in the presence of Py/DMAP in practically quantitative yield. Isolation of the product and its characterisation by HPLC-MS and ^{1}H- /^{13}C NMR, revealed that the product consisted of a mixture of two unidentified mono-acylated diastereomers. Deprotection of the isomeric 3-*O*-acylated 1,2:5,6-di-*O*-isopropylidine-*α*-*D*-glucofuranose (**15**) did not work even under very drastic reaction conditions such as treatment with aqueous trifluoroacetic acid or hydrochloric acid and reflux overnight.

Attempt II

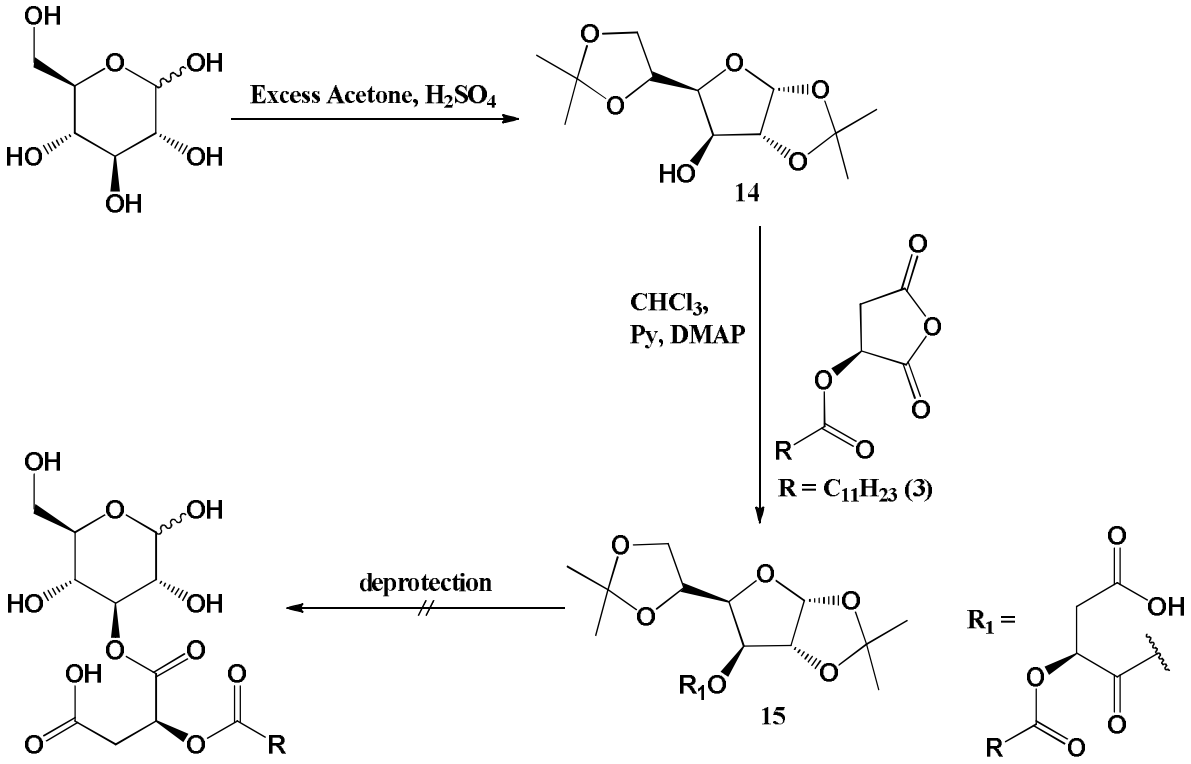

Scheme 9: Attempt for the syntheses of 3-*O*-acylated fatty acid esters of *D*-glucose.

3.2.1.2 Pyridine catalysed Lipid modification of *D*-glucose

After these unsuccessful attempts based on protection-deprotection strategies it was finally possible to obtain the desired products using a pyridine catalysed[102] opening of the anhydride in the presence of DMF as solvent (Scheme 10).

For this, *D*-glucose (5 eq) was dissolved in anhydrous DMF and then treated with the corresponding *O*-acylated hydroxycarboxylic acid anhydrides (1 eq). The reaction mixture was cooled to 0 °C followed by addition of dry pyridine (1 eq) at 0 °C under stirring under an argon atmosphere. Controlling the reaction temperature during the addition of pyridine is very crucial for the success of this reaction. At higher temperatures *β*-elimination of the *O*-acylated hydroxycarboxylic acid anhydride occurs as a competing reaction (Figure 19).[103]

After addition of pyridine the reaction was allowed to continue for 12 h (for malic acid anhydrides) and 3 d (for tartaric acid anhydrides). The crude product contains a mixture of mono-esterified diastereomers of glucose as confirmed by HPLC-MS. However the corresponding 6-*O*-acylated-*D*-glucose was selectively precipitated by dissolving the crude product in acetone.

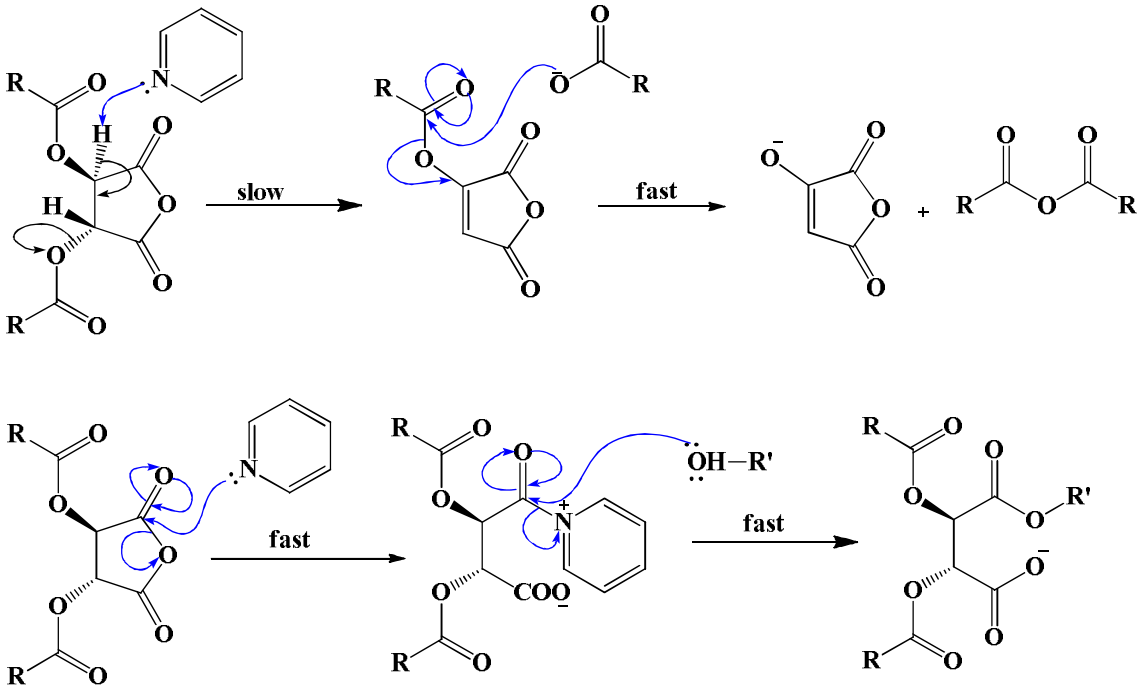

Figure 19: Mechanism of pyridine catalysed esterification and *β*-elimination of *O*-acylated hydroxycarboxylic acid anhydride.

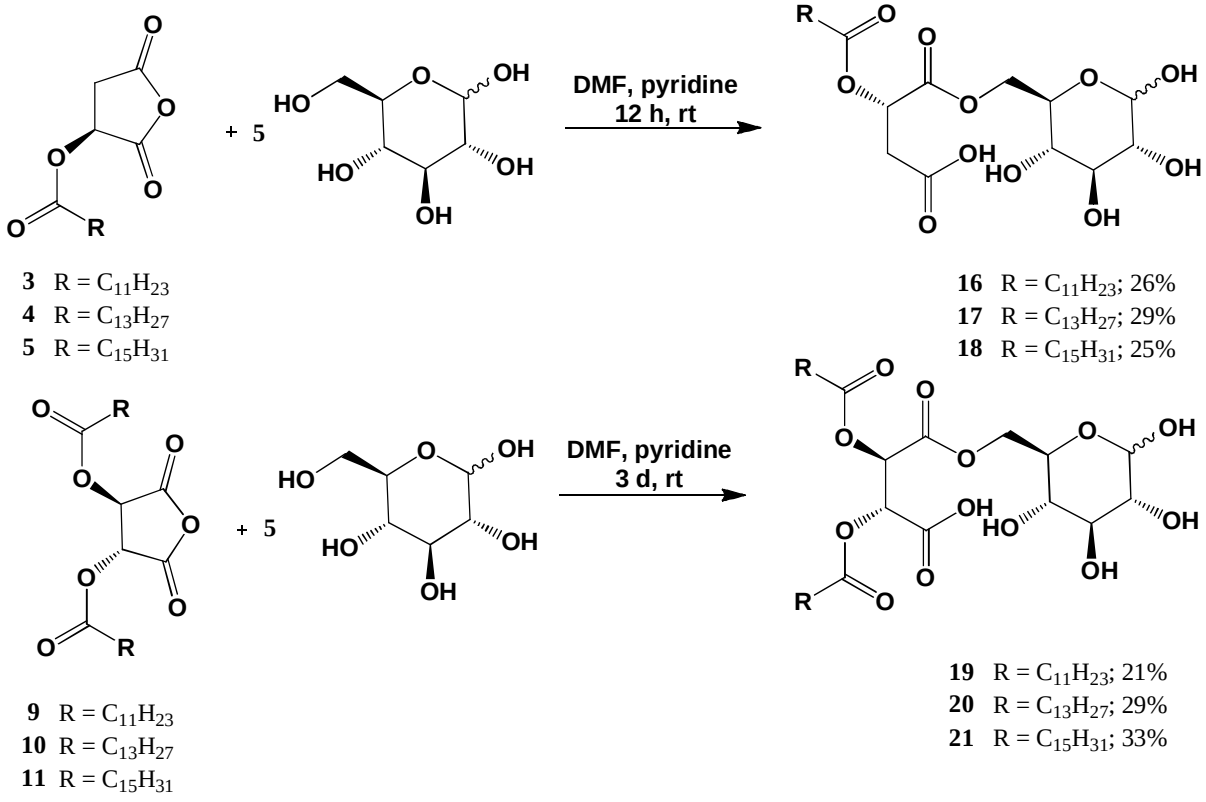

3 R = $C_{11}H_{23}$
4 R = $C_{13}H_{27}$
5 R = $C_{15}H_{31}$

16 R = $C_{11}H_{23}$; 26%
17 R = $C_{13}H_{27}$; 29%
18 R = $C_{15}H_{31}$; 25%

9 R = $C_{11}H_{23}$
10 R = $C_{13}H_{27}$
11 R = $C_{15}H_{31}$

19 R = $C_{11}H_{23}$; 21%
20 R = $C_{13}H_{27}$; 29%
21 R = $C_{15}H_{31}$; 33%

Scheme 10: Syntheses of 6-*O*-acylated fatty acid esters of glucose **16**-**21**.

After addition of pyridine the reaction was allowed to continue for 12 h (for malic acid anhydrides) or 3 d (for tartaric acid anhydrides). The crude product contains a mixture of

mono-esterified diastereomers of glucose as confirmed by HPLC-MS. However the corresponding 6-*O*-acylated-*D*-glucose derivatives were selectively re-precipitated from the crude mixture by dissolving the crude mixture in acetone.

3.2.1.2.1 Characterisation of 16-21

In Figure 20 the ^{1}H NMR spectrum of **19** is shown, exemplifying this group of compounds**.** The ^{1}H NMR shows the characteristic signals of the lauroyl residue at δ = 2.42 (m), 1.65 (m), 1.42 – 1.18 (m), 0.90 (t) ppm. Signals with chemical shifts between 5.11 –3.31 ppm are the characteristic signals of the ring protons of the *D*-glucose moiety and the assignments of all proton signals are shown in Figure 20.

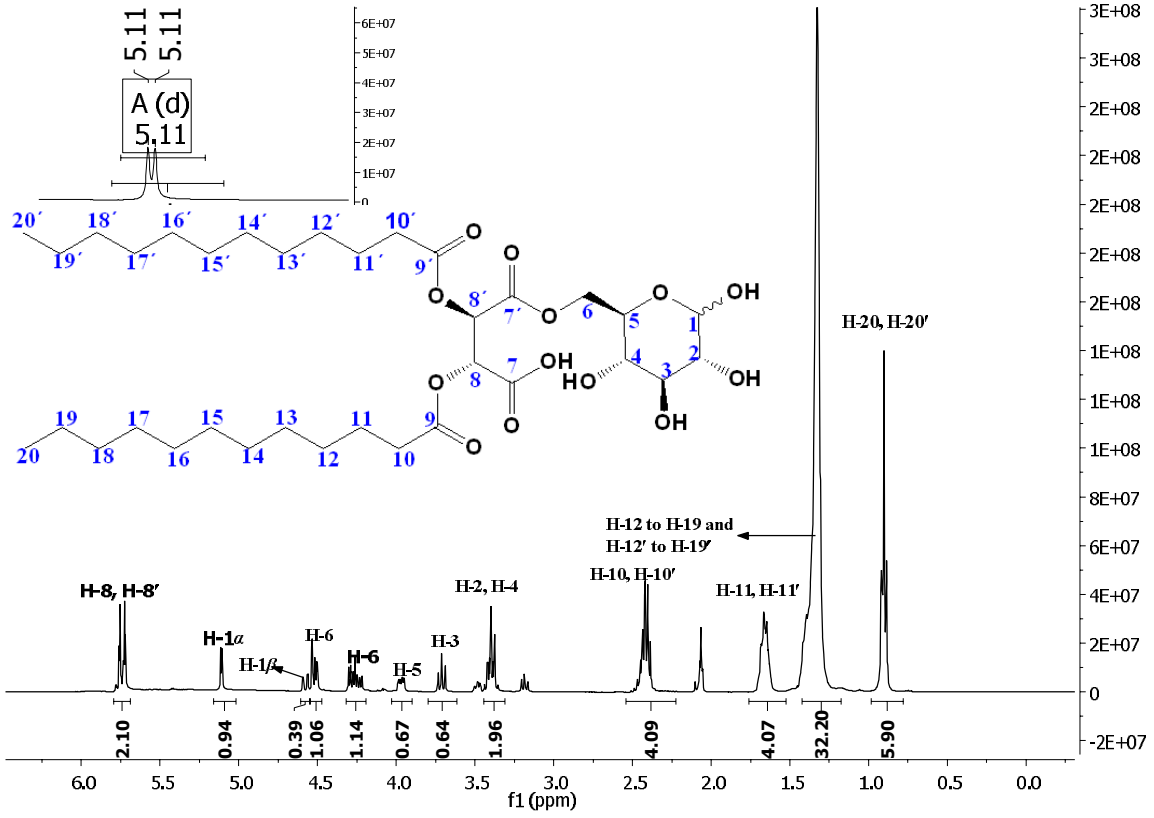

Figure 20: ^{1}H NMR spectrum of **19** in acetone-d_6.

19 consists of a diastereomeric mixture of *α* and *β* anomers and the proportion was determined by integration of the anomeric protons signals for *α* and *β* anomers. The proportion of *α* and *β* anomers depend on the fatty acid chains length of the *O*-acylated hydroxycarboxylic acid anhydrides. In *D*-glucose the protons at the C-6 position display chemical shifts at 3.86 (dd, *J* = 11.8, 2.0 Hz, 1H) and 3.81 (d, *J* = 4.0 Hz, 1H) ppm whereas in **19** the protons at the C-6 position are shifted downfield to 4.64 (dd, *J* = 8.1, 4.9 Hz, 1H, H-6), 4.46 – 4.32 (m, 1H, H-6′) ppm, clearly demonstrating that the esterification took place on the hydroxy group of the C-6 position. The protons with the chemical shifts δ = 5.88 (d, *J* = 2.8

Hz, 1H), 5.85 (d, *J* = 2.6 Hz, 1H) ppm are the H-8 and H-8′ protons of the tartaric acid moiety of **19**.

In Figure 21 the ^{13}C NMR spectrum of **19** is shown, exemplifying this group of compounds**.** The ^{13}C NMR spectrum shows the characteristic signals of the carbonyl carbon at C-9, C-9′, C-7 and C-7′ with chemical shifts of δ = 173.61, 173.38, 168.12, 167.33 ppm, respectively (Figure 21).

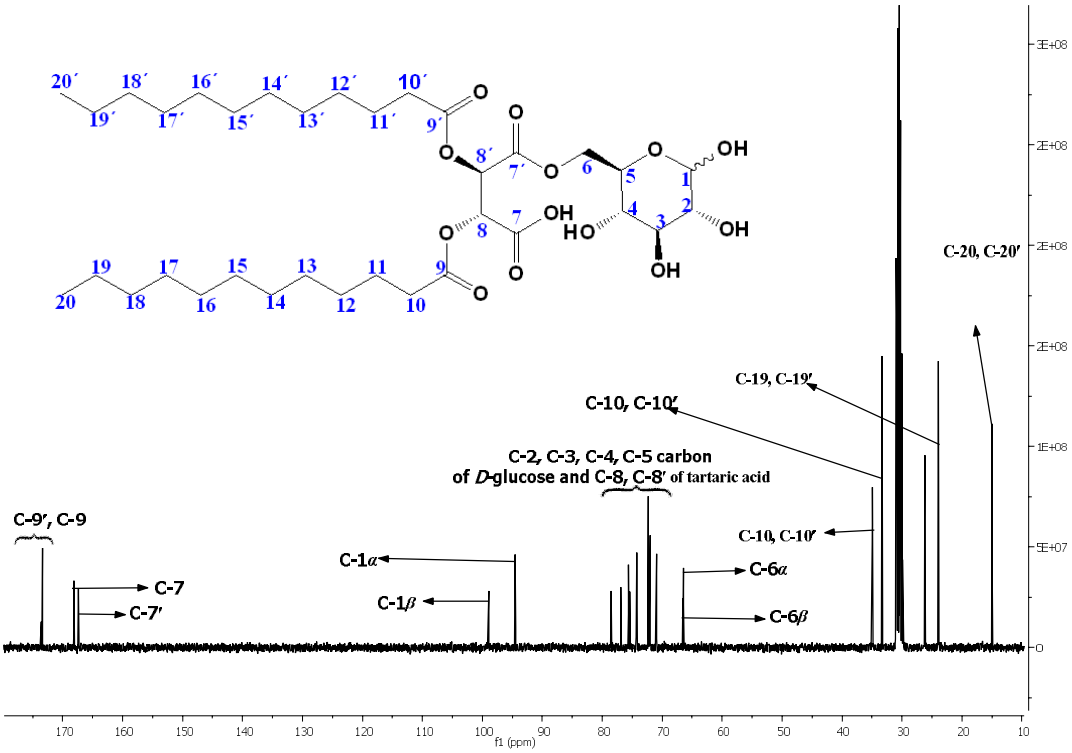

Figure 21: ^{13}C NMR spectrum of **19** in acetone-d_6.

Figure 21 also shows the characteristic CH signals of the tartaric acid unit at δ = 72.31, 72.08 ppm. The assignments of all ring carbons (C-1 to C-6) of the *D*-glucose unit of **19** were achieved based on 2-D NMR (^{1}H-^{1}H COSY, ^{1}H-^{13}C HSQC) and are summarized in Table 5.

compound	C-1	C-2	C-3	C-4	C-5	C-6
19*α*-anomer	94.49	74.28	75.63	72.31	70.96	66.41
α-*D*-glucose	94.19	74.15	75.19	72.12	73.18	63.22
19*β*-anomer	98.95	76.92	78.54	72.08	78.54	66.59
β-*D*-glucose	98.46	76.61	78.18	72.30	78.40	63.15

Table 5: Assignments of all ring carbons in ^{13}C NMR spectra of *D*-glucose and **19** (*α* and *β*).

The NMR spectra of **19** were compared with those of the published *D*-glucose based amphiphile 6-*O*-octanoyl-*D*-glucopyranose and the values are in perfect agreement as reported by I. Redmann *et. al.*[104] Esterification reaction clearly took place on the OH group of the C-6 position which was also confirmed by the downfield shift of the C-6 carbon by approximately 3 ppm as compared to pure *D*-glucose (Figure 22).

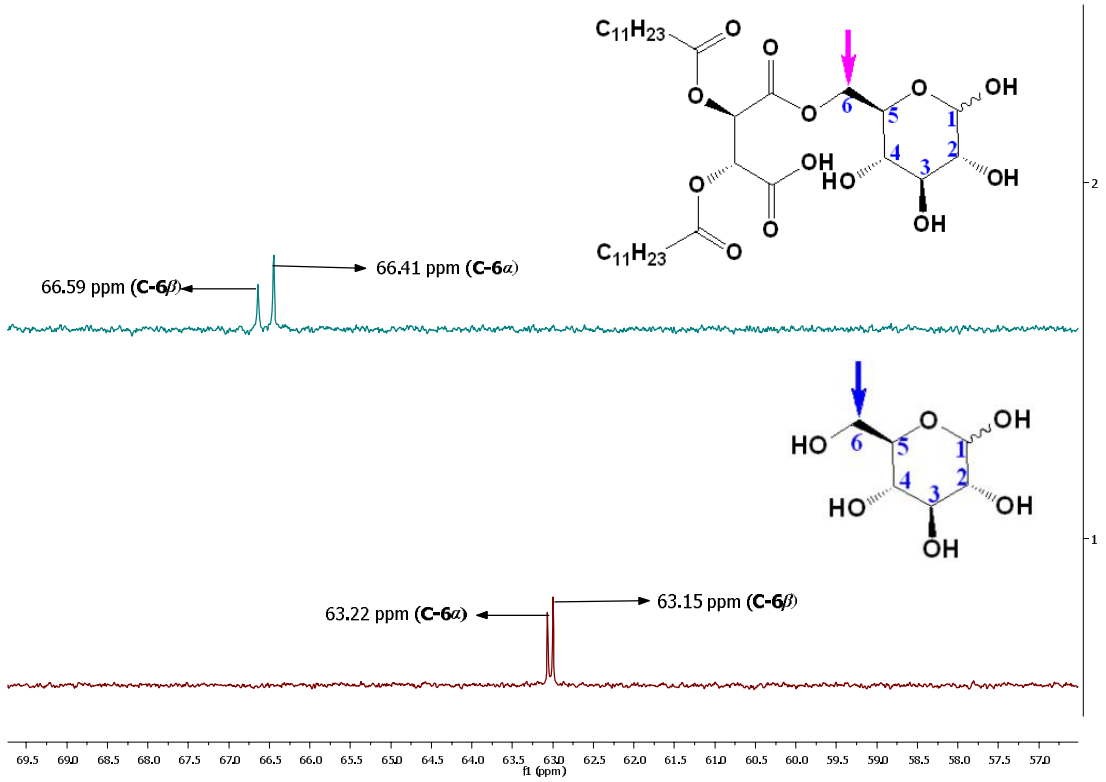

Figure 22: Expanded region of superimposed ^{13}C NMR spectra of *D*-glucose and **19** to demonstrate the downfield shift of C-6 carbon in **19**.

3.2.2 Gelation abilities of 16-21

16-21 exhibited gelation properties. The gelation abilities of **16**-**21** in different solvents were determined by the simple method[105] of being "stable to inversion" of the container and the results are shown in Table 6. For this a weighed amount of the corresponding amphiphiles (25 mg) and the solvent (500 µL) were placed in a septum-capped test tube and heated slowly in an oil bath until the solid was completely dissolved. The resultant mixture was allowed to cool to room temperature. Gelation is considered to have occurred if the solid aggregate was stable to inversion when the sample test tube was turned upside down.

compound	**16**	**17**	**18**	**19**	**20**	**21**
Water	S	TG	PTG	G	G	G
DMF	S	S	S	S	S	S
DMSO	S	S	S	S	S	S
ACN	S[a]	P	P	P	P	P
Methanol	S	S	S	S	S	S
$CHCl_3$	S	S	S	PG	P	P
CCl_4	G[b]	PG[b]	S	G	P	P
Benzene	S	S	S	G	P	P
Toluene	S	S	S	PG	P	P
Hexane	I	I	I	S	P	G
Acetone	S	S	S	S	S	S

G: gel; S: soluble; PG: partially gel; TG: transparent gel; AS: amorphous solid; I: insoluble even at the boiling point of the corresponding solvent; PTG: partially transparent and partially opaque gel; P: precipitation.
[a] But insoluble at + 4 °C.
[b] Not gel at room temperature, only able to make gelation at + 5 °C.

Table 6: Gelation abilities of *D*-glucose based amphiphiles **16**-**21** in different solvents.

The gel-to-solution phase transition temperature (T_{gel}) was determined by using DSC. DSC thermograms were recorded for all hydrogels (10%, w/v) in the temperature range of 10 °C to 90 °C with a heating rate of 2 °K/min. DSC thermogram (Figure 23) shows an endothermic peak corresponding to the phase transition from gel to solution. Hydrogels based on tartaric acid, most notably **20** and **21** show more than one endothermic maxima in the DSC thermograms clearly indicating that these hydrogels possess more than one mesomorphic[106] state in the gel state at room temperature. However with a gradual increase in temperature the gel molecules undergo a phase transition from one mesomorphic state to other. At a specific temperature which corresponds to the endothermic maxima in the DSC thermogram all the self-assembled gel molecules undergo a phase transition from a highly viscous gel to solution.

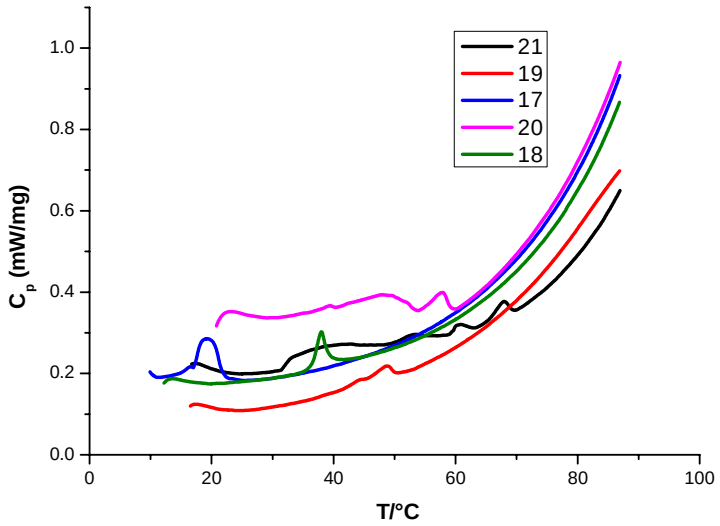

Figure 23: DSC thermograms of hydrogels derived from **17**-**21** (10%, w/v) in the temperature range between 10−90 °C (**16** does not form a gel).

The minimum gelation concentrations (MGCs) of each hydrogel were determined by adding additional 100µL portions of water until the concentration was insufficient to form a stable gel, all results are shown in Table 7.

All these gels are thermo-reversible as they melt when heated above the gelation temperature and revert to gel again through supramolecular interactions upon cooling. Among the above series of tartaric and malic acid based amphiphiles **19** can gelatinise some nonpolar solvents as well as water, whereas **16**, **17**, **18**, **20** and **21** can gelatinise only a few among the tested solvents besides water. This implies that a balance participation[107] of H-bonding and van der Waals interactions are very crucial to induce gelation in water as well as in organic solvents and this can be largely regulated by systematic alteration of the H-bonding unit or tuning the hydrocarbon chains. Ambidextrous gelation (gelling in water as well as in nonpolar organic solvents) properties of these amphiphiles might be useful for the development of hybrid materials in a variety of solvent as well as in water.[108]

3.2.2.1 Thermal stabilities of the hydrogels–relation to the hydrocarbon chains

Robustness and embodiment of gelation abilities of these amphiphiles in water can be illustrated by considering three parameters: (i) minimum gelation concentration, (ii) thermal stability of the hydrogel and (iii) number of water molecules entrapped by one gelator molecule (Table 7).

compound	MGC[a] (minimum gelation concentration, w/v).	T_{gel}	Number of water molecules entrapped[b]
16	non-gelator	–	–
17	2.8%	20 °C	~1000
18	3.1%	38 °C	~ 950
19	7.3%	50 °C	~500
20	4.6%	59 °C	~900
21	2.5%	67 °C	~1750

[a] For **17** determined at + 5 °C.
[b] For **17** determined at + 5 °C.

Table 7: Thermal stabilities and minimum gelation concentrations of *D*-glucose based hydrogel **16-21**.

These three parameters are clearly influenced by the length of hydrocarbon chain in the lipophilic part of the molecule. In case of both the tartaric and malic acid based amphiphiles the thermal stabilities of the hydrogels for the longer hydrocarbon chains length (C_{16} and C_{14}) are higher than for the corresponding compounds with shorter chains. Thus malic acid based amphiphile **18** with a longer hydrocarbon chain (C_{16}) produces very stable hydrogels at room temperature with a minimum gelators concentration of 3.1%, w/v (~950 water molecules are entrapped by one gelator molecule) whereas the corresponding amphiphile **17** with a shorter hydrocarbon chains (C_{14}) produces a stable hydrogel only at low temperatures, while **16** with a C_{12} hydrocarbon chain is not leading to a gel at all (Figure 24). Similar phenomena regarding the alkyl chain length dependence of MGCs and T_{gel}s have also been observed in the case of the tartaric acid based amphiphiles. This implies that one can regulate the structure and thermal stability of the hydrogel by tuning the length of the hydrocarbon chain attached to the *D*-glucose embedded hydrophilic core for desired and specific applications.[109] The high and low melting points of the hydrogels might be attributed to structural differences in the self-complementary assembly indicating more significant and adequate crystalline packing[110] for both tartaric and malic acid amphiphiles with long fatty acid chains as compared to shorter ones. Increasing the chain length for both tartaric and malic acid amphiphiles promotes more association among the fibers through van der Waals force of attraction and drives the molecules to arrange in highly ordered layered structures which eventually attributes to the higher thermal stabilities of the hydrogels.

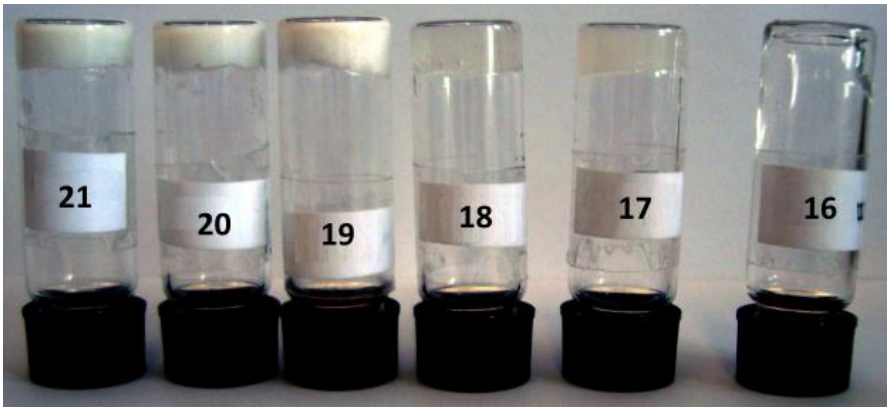

Figure 24 : Images of the hydrogels derived from **16**-**21**.

3.2.2.2 Morphology of the hydrogels 16-21: optical and scanning electron microscopy studies

In order to get deeper and more precise visualization of the morphology of the hydrogel, optical and scanning electron microscopic measurements have been performed by taking xerogel obtained from 1.04% (w/v) hydrogel of **21**. The optical electron microscopic image revealed that the 3-D network structure of the hydrogel consists of numerous fibrillar networks with pores inside (Figure 25).

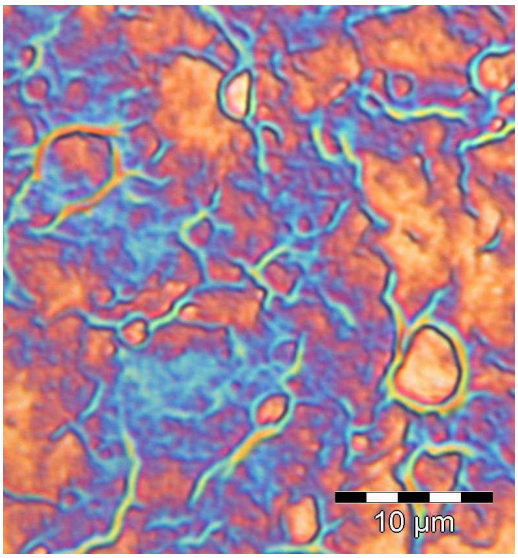

Figure 25: Optical image of 1.04% (w/v) xerogel of **21** obtained from water.

The fibers inside the gelation network are several micrometers (8-12 µm) in length and 500-700 nm in diameter which are entangled with each other to produce 3-D network which eventually induces gelation. SEM images have confirmed the size distribution of the fibers and morphology of the hydrogel of **21**(Figure 26).

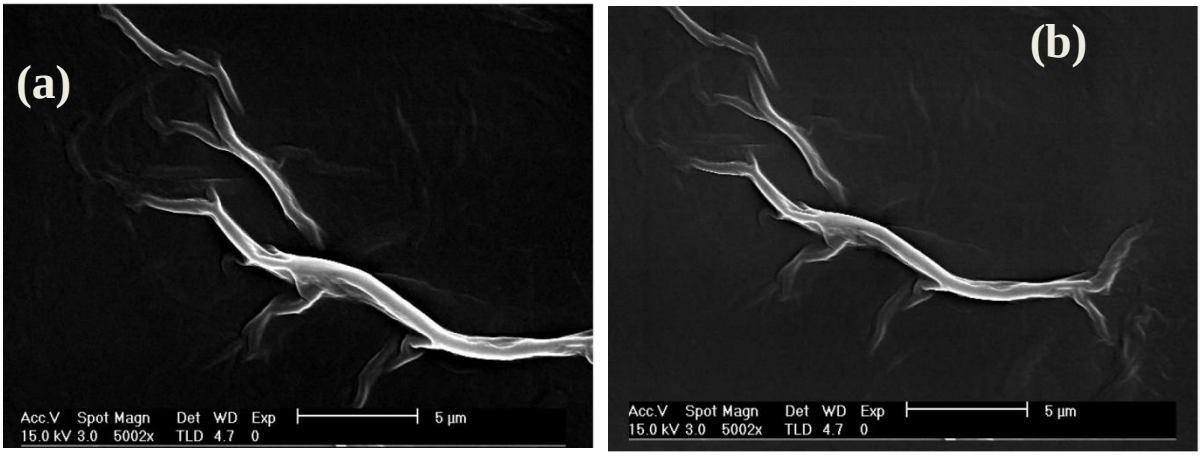

Figure 26: SEM images of 1.04% (w/v) xerogel of **21** obtained from water with slight changes in contrast between (**a**) and (**b**).

3.2.2.3 Driving forces leading to the formation of the hydrogels

3.2.2.3.1 Gelation abilities of 21 in DMSO/water solvent mixtures

In order to obtain a better and precise understanding of the kind of interactions between the molecules during the gelation process in water, gelation experiments were carried out using 500 µL of 10% (w/v) of **21**, a representative gelator, in DMSO/water solvent mixtures (Figure 27 and Table 8).

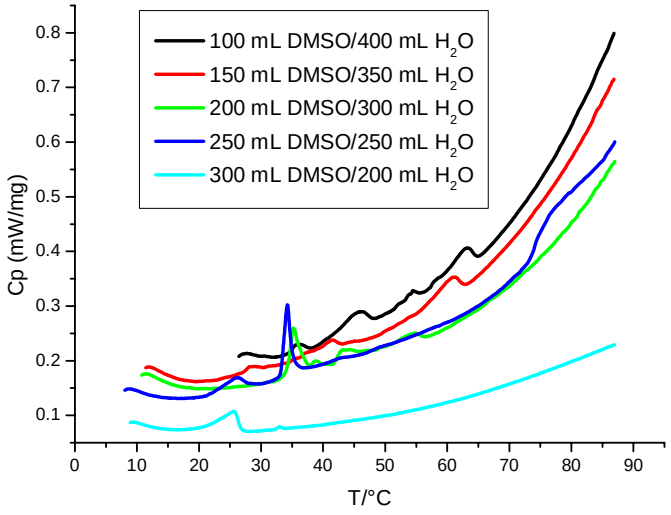

Figure 27: DSC thermograms of the gels obtained from **21** (10%, w/v) in DMSO/water solvent mixture.

Although gelation occurs equally well for all systems containing between 0 µL/500 µL and 300 µL/200 µL (v/v) DMSO/water solvent mixtures, the values of the T_{gel} decrease considerably with an increasing DMSO content in the gel sample, with a maximum value of T_{gel} for the gel sample containing only water.

The results clearly imply that the hydrogel of **21** is destabilized in the presence of DMSO. Since DMSO in the presence of water can contribute to hydrogen bonding[111,112] within the gel network which destabilize the gel network in water with sufficient DMSO concentration. This signifies that van der Waals forces of attraction across the hydrocarbon chains are probably the principle driving force for the gelation of **21** in water. Beside this evidence, the increase in the thermal stabilities of the hydrogels with increase of the hydrocarbon chain length implies that van der Waals forces of attraction across the hydrocarbon chain become very crucial and play a decisive role to control gelation in water.

DMSO:H_2O (µL/µL)	**21**	T_{gel}
0:500	G	67 °C
100:400	G	63 °C
150:350	G	61 °C
200:300	G	54 °C
250:250	TG	33 °C
300:200	G	26 °C
400:100	S[a]	-
500:0	S	-

S: soluble; TG: transparent gel; S: soluble.
[a] But became very transparent gel after one month.

Table 8: Thermal stabilities of the gels obtained from **21** in DMSO/water solvent mixtures.

3.2.2.3.2 IR spectroscopic studies

In addition to the van der Waals forces of attraction across the hydrocarbon chains synergetic and significant contributions of intermolecular hydrogen bonding during the gelation process was confirmed by ATR-IR spectra of the xerogel (10%, w/v) of **21** obtained from D_2O and DMSO solutions (Figure 28).

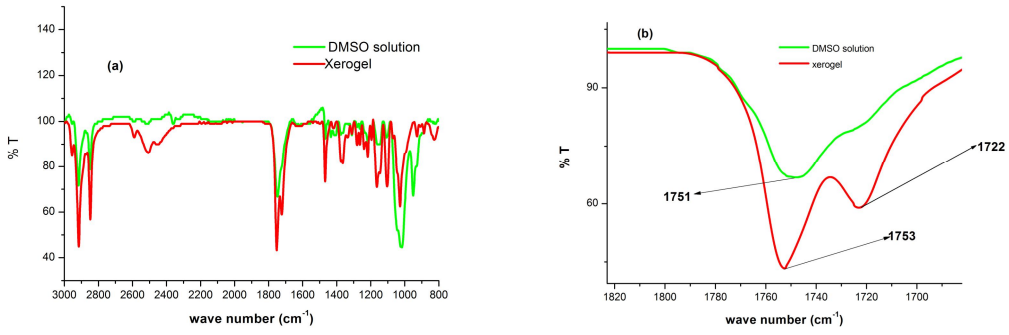

Figure 28: (**a**) Superimposed FT-IR spectra of **21** (10%, w/v) in DMSO solution and the xerogel obtained from D_2O; (**b**) expanded region of the superimposed FT-IR spectra of **21** in DMSO solution and the xerogel obtained from D_2O.

The IR spectra of **21** reveal that in DMSO solution the band appearing at 1753 cm^{-1} can be assigned to the stretching vibration of the carbonyl group of all esters and non-hydrogen bonded carboxylic acid group whereas in the xerogel obtained from D_2O the stretching vibrations of a set of carbonyl groups are shifted to 1722 cm^{-1}. This observation strongly supports the existence of hydrogen bonding between the carbonyl groups in the gel phase.

3.2.2.3.3 NMR spectroscopic studies

In order to obtain even more precise and deeper insights into the orientation of the molecules with respect to each other in the self-assembled state and the contribution of the different groups through selective supramolecular interactions within the gel network, temperature-dependent ^1H NMR spectroscopic measurements have been carried out using 7.2% (w/v) of **21**, a representative gelator, in D_2O/DMSO-d_6 solvent mixture (1:1.8, v/v) (Figure 29). In D_2O, the gel molecules are self-assembled into a highly organized rigid network and consequently their signals are quite broadened and unresolved even at 95 °C due to long correlation times.[113] Therefore, another gel sample was prepared in a D_2O/DMSO-d_6 solvent mixture in order to obtain a relatively less rigid gel network.[114] With gradual increase in temperature from 30 to 90 °C the signals for the fatty acid protons were found to be slightly shifted downfield[115] and became sharper as compared to the signals at 30 °C (Figure 30).

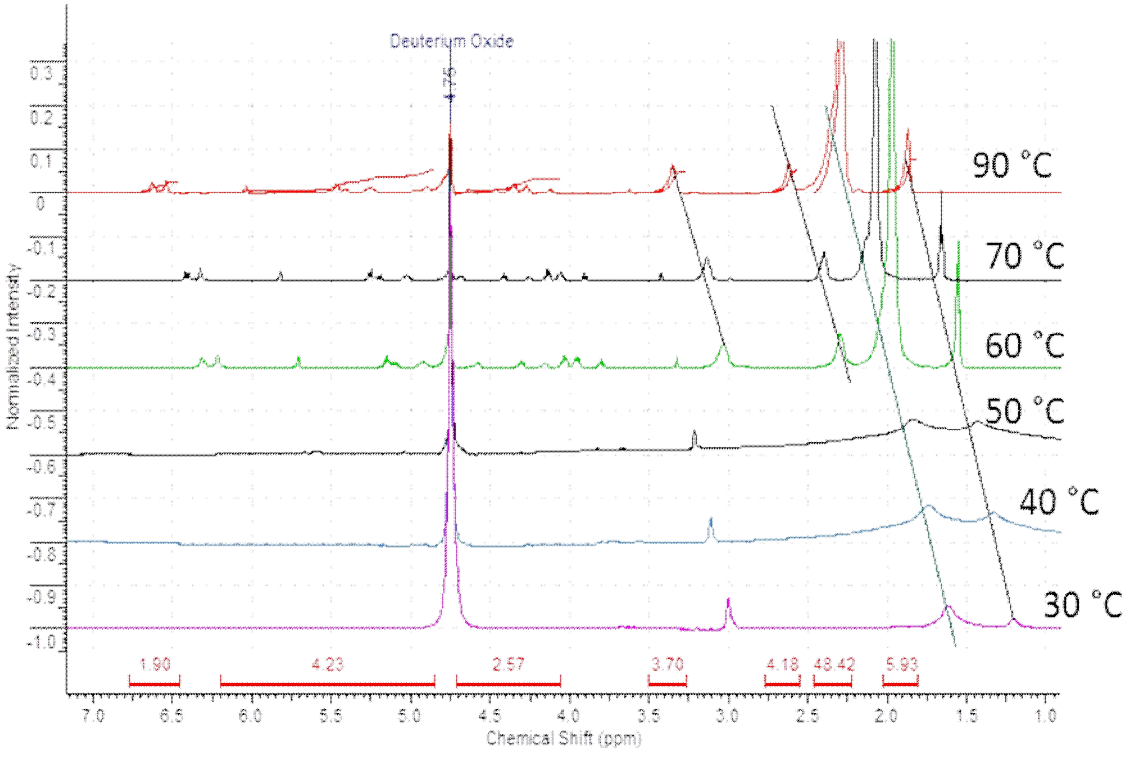

Figure 29: Variable temperature ^1H NMR spectra of **21** (7.2%, w/v) in D_2O/DMSO-d_6 solvent mixture (1:1.8, v/v).

This indicates that a gradual increase in temperature is leading to a disordering of the self-assembled, highly ordered gel network into its isotopic form. In addition to that, broadening of the fatty acid proton signals in the gel phase suggests the existence of van der Waals forces between the hydrocarbon chains inside the gel network. These results afford noticeable evidence for the stabilization of self-assembled structure by the synergetic contributions of both hydrogen bonding and van der Waals force of attraction between the hydrocarbon chains in the gel phase.

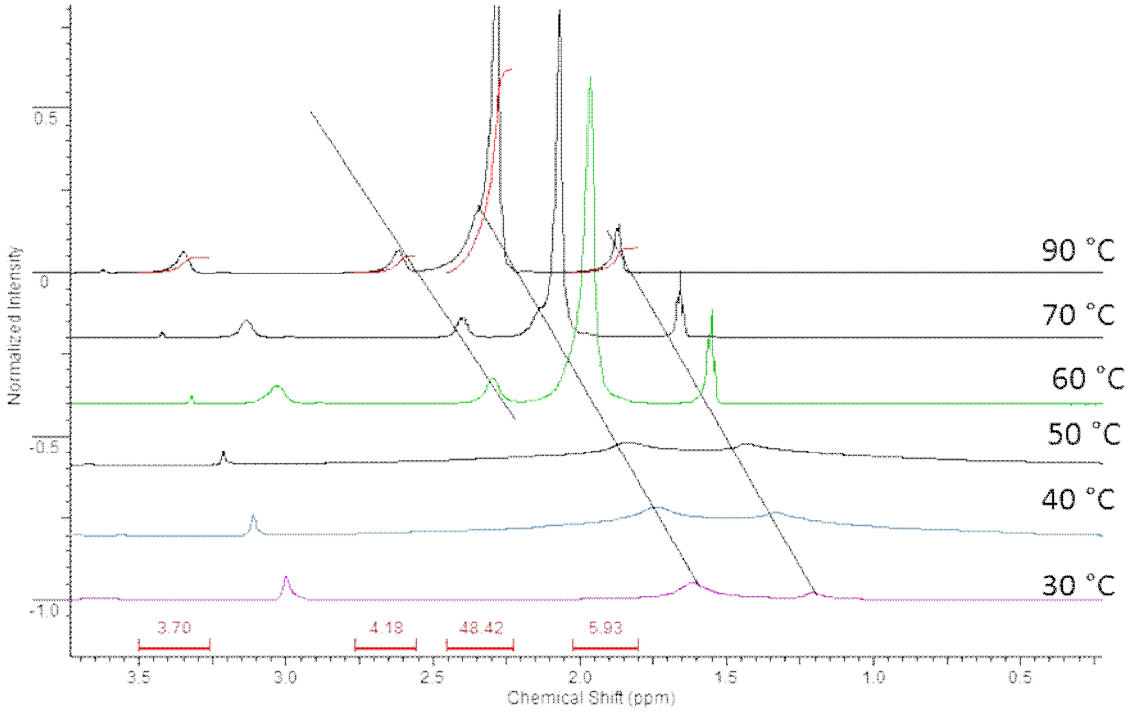

Figure 30: Expanded region of variable temperature ^{1}H NMR spectra of **21** (7.2%, w/v) in D_2O/DMSO-d_6 solvent mixture (1:1.8, v/v).

3.2.2.3.4 CD spectroscopic studies

In order to obtain some information about supramolecular chirality induced by the gel network (rather than the inherent chirality of the individual gelator molecule), CD spectroscopic measurements were conducted by using self-assembled **21** in water as shown in Figure 31. The CD spectrum of self-assembled **21** in water exhibits a negative cotton effect,[116,117] thus implying that the dipole moments orientate in an anticlockwise direction in the aggregate of the gel in water. In spite of having chiral *D*-glucose and (*R*,*R*) tartaric acid moieties in the core of the structure, **21** does not exhibit any CD cotton effect in methanol[94,117,118,119] solution which implies that there is an intimate and intrinsic relationship between the chiral expression ability and the growth and stability of the three dimensional gel network. This chiral expressing ability of the self-assembled structure is strongly related to the noncovalent supramolecular association within the self-aggregated structure.

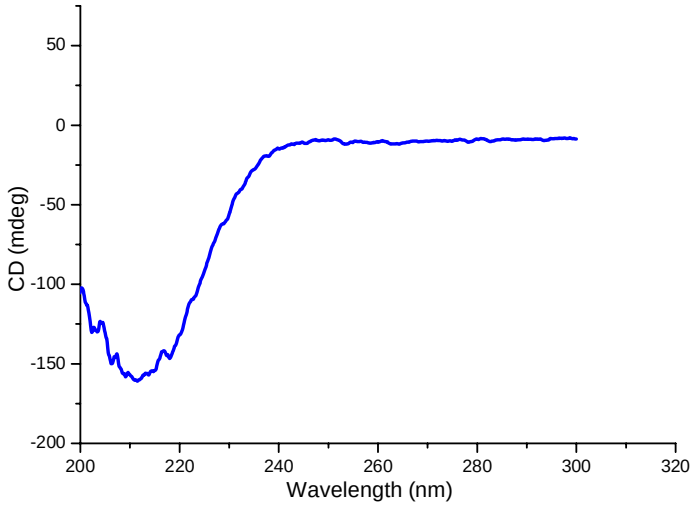

Figure 31: CD spectrum of self-assembled **21** in water (0.12%, (w/v).

3.2.3 Surface and interface properties

3.2.3.1 Foaming and emulsifying properties of 16-21

Amphiphiles **16-21** are surface active agents which display good foaming and emulsifying abilities as shown in Table 9.

compound[a]	foaming ability (mL) of 0.1% solution	foam stability (mL) of 0.1% solution	HLB values
16	682	675	>18
17	449	445	9
18	140	130	7
19	245	242	10
20	51	42	9
21	43	40	<3
SDS	765	720	-

[a] For foaming properties triethanolamine salts have been used.

Table 9: Foaming and emulsifying properties of *D*-glucose based amphiphiles **16-21** in water.

In case of both the tartaric and malic acid based amphiphiles the foaming ability is much higher for the shorter hydrocarbon chain length compounds than in those with longer carbon chains. For a given hydrocarbon chain length the foaming abilities of the malic acid based amphiphiles is much higher than for the corresponding tartaric acid based amphiphiles (Table 9).This could be attributed also to the difference in solubility of the surfactants[120] in water as

the solubility of both the malic and tartaric acid surfactants is highly influenced by the hydrocarbon chains length. Among the series of amphiphiles, **16** displays excellent foaming ability which is comparable to sodium dodecyl sulphate (SDS). Thus this compound might be a useful alternative to SDS which causes untoward side effects.[121] **17** and **19** display foaming abilities in the moderate range whereas **18**, **20** and **21** are not foaming at all. The foaming abilities of these amphiphiles are reflected in their HLB values.

Owing to their strong hydrophilic or lipophilic in nature respectively, amphiphiles **16** and **21** do not have any HLB values (Table 9) whereas compounds **17-20** show HLB values in the range of 7-10 and hence they might be useful for the preparation of oil in water emulsions, *e.g.* for food and cosmetic applications.

3.2.3.2 CMC values of 16-21

The CMC values of the amphiphiles **16-21** have been determined by the ring method[122] based on surface tension measurements (Figure 32).

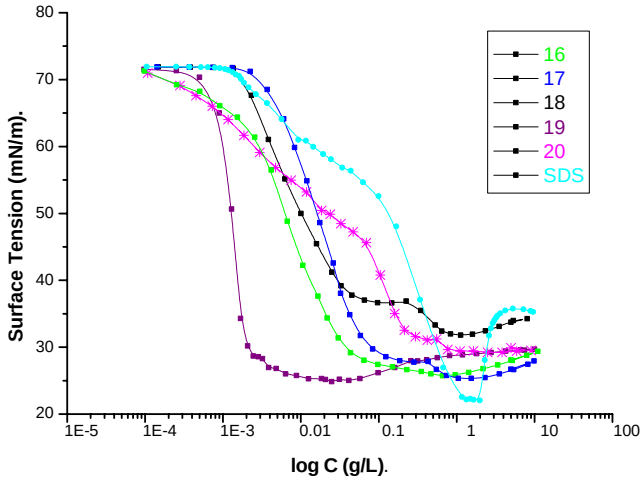

Figure 32: Plot of surface tensions *vs.* logarithm of concentrations (log C, g/L) for **16-21** in water at 25 °C.

Both the CMC values and γ_{CMC} (surface tension at CMC) of the amphiphiles **16-21** can be obtained from a plot of the surface tensions γ (mN/m) against log C (g/L) and the results are summarised in Table 10. In the case of the malic acid based amphiphiles **16-18** there is a slight increase in CMC with the hydrocarbon chain length while in case of **16-17** a very low value of γ_{CMC} is found. This essentially implies that these amphiphiles have an inherent tendency to adsorb strongly at the air/water interface and orient themselves thereby causing a reduction of the tension on the air/water interface. The CMC value of tartaric acid based **19** is much lower than that for malic acid based amphiphiles which essentially implies that tartaric acid based **19** is a *quasi* gemini surfactant; in the core of the molecules two hydrocarbon

chains are connected by a spacer and hence facilitate the surfactant molecules to pack closely at air/water interface due to the interactions between the hydrocarbon chains.[123] Thus **19** displays a CMC value which is 3 orders of magnitude lower than that of the commercially available surfactant SDS and hence might be useful alternative to this surfactant.

compound[a]	CMC (mol/L)	γ_{CMC} (mN/m)
16	8.76×10^{-5}	21.5
17	1.54×10^{-4}	21.6
18	1.43×10^{-4}	26.6
19	2.42×10^{-6}	20.5
20	9.36×10^{-4}	29.6
21	-	-
SDS	8.0×10^{-3}	22.1

[a] For the measurement of CMC values triethanolamine salts have been used.

Table 10: CMCs and γ_{CMC} s (mN/m) of the *D*-glucose based amphiphiles **16-21** in water.

3.2.4 Antimicrobial activities of 16-21

Frequently, for numerous applications, it is highly desirable to develop so-called functional surfactants, *i.e.*, surface-active compounds which show additional benefits. In this context the antimicrobial properties are highly useful for applications in the cosmetic field, consumer products, cleaning liquids for medical instruments, as well as for the stabilization of industrial emulsions against deterioration by bacteria and fungi.[171] Hence, the above synthesized surfactants were tested regarding their activities against a series of bacteria (Gram negative: *Pseudomonas putida mt2*, *Escherichia coli*, *Enterobacter aeruginosa*; Gram positive: *Staphylococcus aureus*; *Micrococcus luteus*, and eukaryotic species such as fungi (*Aspergillus niger*, *Candida albicans*). Most of the synthesized surfactants showed activity against a variety of the above microorganisms, particularly against *S. aureus*, *M. luteus*, and *Candida albicans*.

Especially the malic and tartaric acid based amphiphiles **16** and **19,** both with C_{12} hydrocarbon chains exhibited high activities against almost all the investigated microorganisms (Table 11).

substance	*Ps. Putida mt2*	*E. coli*	*Enterobacter aer.*	*S. aureus*	*M. luteus*	*Asp. niger*	*Ca. albicans*
16	-	++	+++	+++	+++	(+)	++
17	++	-	(+)	+++	+++	-	+++
18	(+)	-	-	-	++	-	+
19	++	(+)	(+)	+++	+++	-	++
20	++	-	+	+++	-	(+)	++
21	(+)	-	-	(+)	(+)	-	+

- = No spot; (+) = overgrown spot; + = spot with colonies; ++ = spot with only a few colonies; +++ = clear spot without colonies.

Table 11: Antimicrobial properties of **16-21** (inhibition zones).

3.2.5 Conclusion

On the basis of the above results, the structural requirement for the self-assembly of the above carbohydrate based amphiphiles to form highly organized nano-fibers has begun to be elucidated. Thus in general carbohydrates in combination with fatty acids might be appropriate candidates to induce gelation in water as well as in some other non-polar solvents. Both the hydrogen bonds and van der Waals interactions are indispensable for the formation of highly organised self-assembled structures in water. One can also conclude that in the case of *D*-glucose based amphiphiles the length of the hydrocarbon chains attached to the hydrophilic head group have a crucial impact on the self-assembling process as well as on the rigidity of the gel network in water, which eventually regulates the thermal stabilities of the hydrogels. A systematic investigation was carried out in order to draw a possible correlation between the length of the hydrocarbon chains attached to hydrophilic glucose unit and the water gelation efficacy. The thermal stabilities of the hydrogels would definitely be important regarding the structure–function relationships in LMWGs. Besides their supramolecular gelation efficiencies, the surface active properties such as foaming and emulsifying properties and also the CMCs were determined. The obtained compounds may have potential applications in the area of food, pharmaceuticals and cosmetics.

3.3 *D*-Glucosamine-based surfactants: design, syntheses and characterization

3.3.1 Regioselective *N*-acylation of *D*-glucosamine

The present work was undertaken for the purpose of preparation and investigating on the properties of some *N*-acyl derivatives of *D*-glucosamine (2-amino-2-deoxy-glucose), where the amine group was selectively functionalised by reaction with *O*-acylated hydroxycarboxylic acid anhydrides. It is well known that *D*-glucosamine can be liberated from its salts by treatment of *D*-glucosamine hydrochloride with strong bases. In our case treatment of *D*-glucosamine hydrochloride with triethylamine or pyridine in the presence of DMF led to the in situ generation of *D*-glucosamine where the amine group at the C-2 position is now free. The free amine group serves as a better nucleophile than the other hydroxy groups under the applied reaction conditions and readily undergoes ring opening reaction with *O*-acylated hydroxycarboxylic acid anhydrides in the presence of pyridine as catalyst.

3.3.1.1 General procedure for the syntheses of *N*-acyl-glycopyranosylamines (22–24) derived from *O*-*O'*-di-acylated tartaric acid anhydrides

The regioselective mono-acylation of *D*-glucosamine was achieved by the pyridine catalysed[124] amidation in the presence of DMF as solvent (Scheme 11).

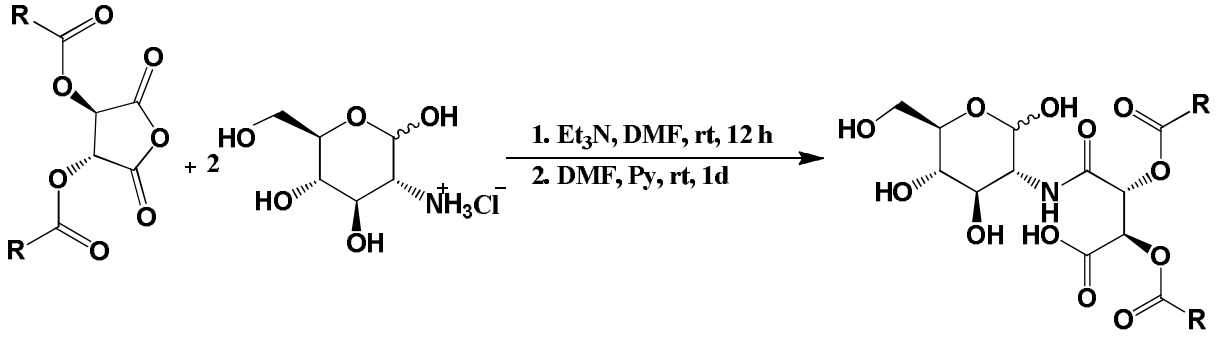

9 R = $C_{11}H_{23}$
10 R = $C_{13}H_{27}$
11 R = $C_{15}H_{31}$

22 R = $C_{11}H_{23}$; 81%
23 R = $C_{13}H_{27}$; 61%
24 R = $C_{15}H_{31}$; 86%

Scheme 11: Syntheses *O*-*O'*-di-acylated tartaric acid derived *D*-glucosamine amphiphiles **22**–**24**.

General procedure for the syntheses of *N*-acylated glucosamine is as follows. *D*-glucosamine hydrochloride (2 eq) in anhydrous DMF was treated with dry triethylamine for deprotonation, followed by the addition of the *O*-*O'*-di-acylated tartaric acid anhydrides (1 eq) in the presence of pyridine (1 eq) to achieve the selective acylation of the amine group leading to **22-24**. The formation of **22-24** was confirmed by ^{1}H NMR and ^{13}C NMR spectra. In the ^{13}C

NMR spectrum the carbon at the C-2 position is shifted downfield by 2 ppm as compared to *D*-glucosamine which essentially implies that the addition took place exclusively on the amine group at C-2. Ewing, Goodby[125] *et al.* and some other groups[126] have also described regioselective functionalisation of the amine group in *D*-glucosamine with fatty acid chlorides in the presence of Et_3N and DMF and NMR data (^1H and ^{13}C NMR spectra) are in close agreement.

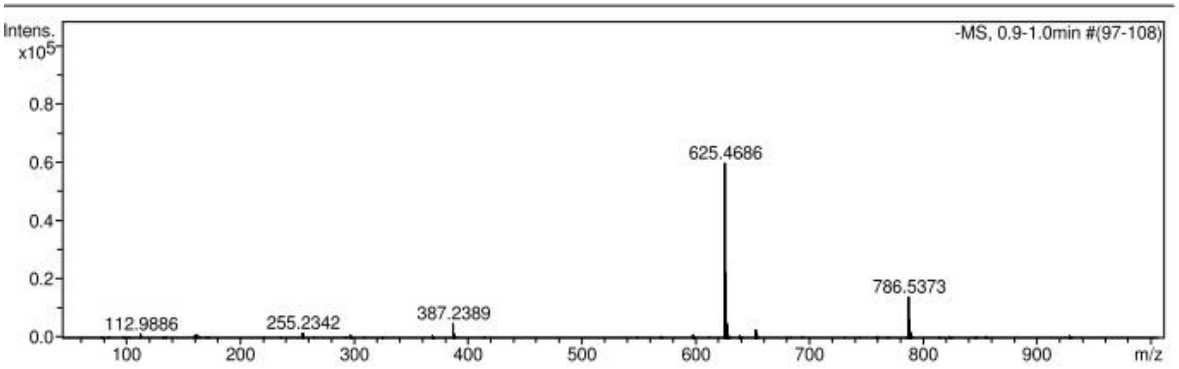

Figure 33: HRMS (ESI$^-$, m/z) spectrum of compound **24**. Calculated for $[M-H]^-$. Calculated 786.5368 Da, found 786.5373 Da.

The high resolution mass spectrum of **24** also supports the assigned structure.

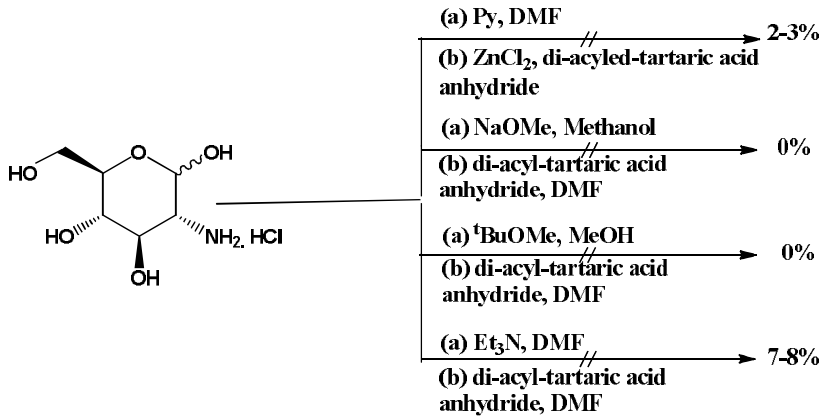

Scheme 12: Alternative attempts to prepare *N*-acylated *D*-glucosamines based on *O*-*O'*-di-acylated hydroxycarboxylic acid anhydrides.

The deprotonation of *D*-glucosamine hydrochloride was also carried out in the presence of several other strong bases like NaOMe/MeOH, KO^{t}Bu/MeOH, Et_3N/DMF to liberate *D*-glucosamine, followed by the addition of *O*-*O'*-di-acyl-tartaric acid anhydrides to obtain *N*-acylated-*D*-glucosamines (Scheme 12). Unfortunately, however the yields were low and/or did not lead to the desired products. The reaction was also attempted in the presence of equivalent amounts of Py/DMF to liberate *in situ D*-glucosamine, followed by addition of anhydrides in the presence of $ZnCl_2$, but the desired *N*-acylated-*D*-glucosamines were obtained only in very low yield.

All these results clearly emphasize the importance and significance of pyridine in this reaction. Pyridine not only serves as a base for the deprotonation of *D*-glucosamine hydrochloride, but also acts as a catalyst to achieve the selective acylation.

3.3.1.1.1 NMR characterisation of 22-24

In Figure 34 the ^{1}H NMR spectrum of **24** is shown, exemplifying this group of compounds. The ^{1}H NMR spectrum shows the characteristic signals of the palmitoyl residue at δ = 2.58 – 2.27 (m, 4H), 1.83 – 1.55 (m, 4H), 1.54 – 1.09 (m, 48H), 0.90 (t, 6H) ppm.

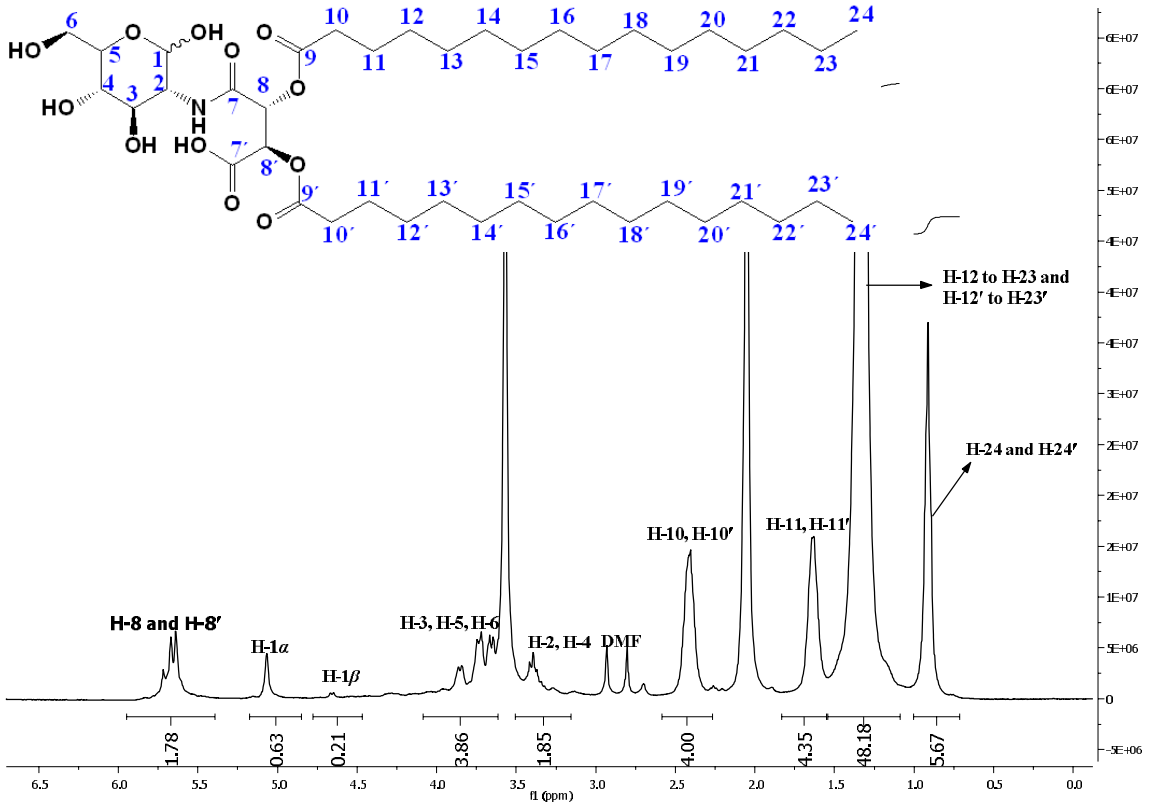

Figure 34: ^{1}H NMR spectrum of **24** in acetone-d_6 recorded at 50 °C in acetone-d_6.

Signals with chemical shifts in the range of 5.07 –3.16 ppm are characteristic for the ring protons at C-1 to C-6 of *D*-glucosamine and all assignments of the proton signals are shown in Figure 34. **24** consists of a diastereomeric mixture of the *α* and *β* anomers and their proportion was determined *via* the integration of the anomeric protons. In *D*-glucosamine, the proton at C-2 display a chemical shift at δ = 3.09 (dd, *J* = 10.4, 3.5 Hz, 1H, H-2*α*) and 2.85 (dd, *J* = 10.2, 8.3 Hz, 1H, H-2*β*) ppm while in **24** the proton at C-2 is shifted downfield to 3.50 – 3.16 (m) ppm, clearly indicating that the acylation took place on the amine group at C-2 position. Protons with the chemical shifts of δ = 5.95 – 5.39 (m, 2H) ppm are the H-8 and H-8′ proton of the tartaric acid unit.

In Figure 35 the ^{13}C NMR spectrum of **24** is shown, exemplifying this group of compounds**.**

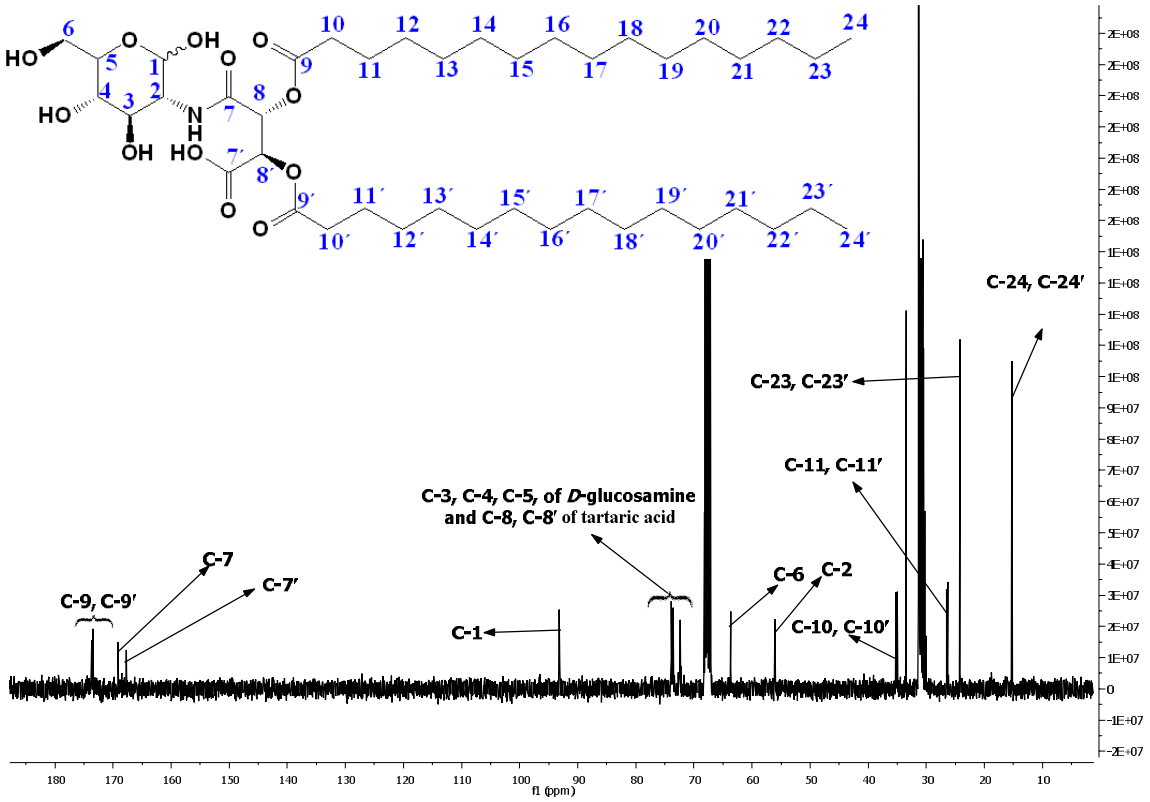

Figure 35: ^{13}C NMR spectrum of **24** recorded at 50 °C in acetone-d_6.

The ^{13}C NMR spectrum shows the characteristic signals of the carbonyl carbons at C-9, C-9′, C-7 and C-7 of **24** which occur at δ = 173.70, 173.45, 169.13, 167.74 ppm, respectively. The characteristic signals of the tartaric acid unit appear at δ = 73.89, 73.72 ppm. The complete assignments of all ring carbons (C-1 to C-6) of the *D*-glucosamine unit in **24** were achieved using 2-D NMR (^{1}H-^{1}H COSY, ^{1}H-^{13}C HSQC) and the chemical shifts of all carbon (C-1 to C-6) signals in the *D*-glucosamine skeleton of **24** are shown in Table 12. That the acylation took place on the amine group at C-2 position was again confirmed by the downfield shift of the C-2 carbon by approximately 3 ppm as compared to *D*-glucosamine.

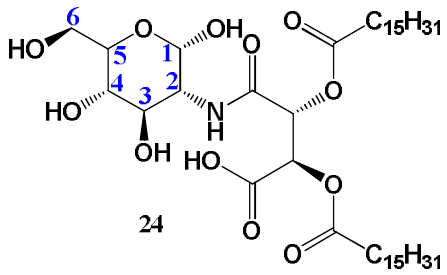

24

compound	C-1α	C-2α	C-3α	C-4α	C-5α	C-6α
24	93.15	56.03	73.72	73.89	73.94	63.65

Table 12: Assignments of the *D*-glucosamine moiety in **24** in ^{13}C NMR spectrum.

3.3.1.2 Syntheses of *N*-acylated-*D*-glucosamines (25–27) derived from *O*-acylated malic acid anhydrides: General procedure

Pyridine (2 eq) was added to the DMF solution of *D*-glucosamine hydrochloride (2 eq) for the deprotonation, followed by addition of the *O*-acylated malic acid anhydrides **3**-**5** (1 eq) as described earlier in section 3.3.1.1 (Scheme 13).

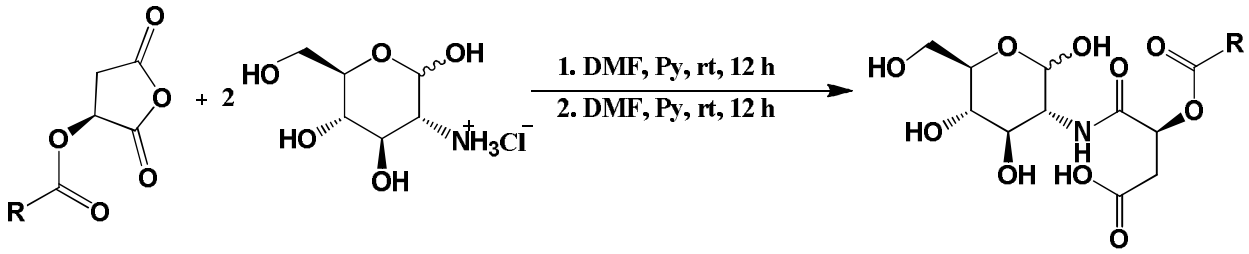

3 R = $C_{11}H_{23}$
4 R = $C_{13}H_{27}$
5 R = $C_{15}H_{31}$

25 R = $C_{11}H_{23}$; 59%
26 R = $C_{13}H_{27}$; 66%
27 R = $C_{15}H_{31}$; 63%

Scheme 13: Syntheses of *N*-acylated-*D*-glucosamines **25**–**27** derived from *O*-acylated malic acid anhydrides.

3.3.1.2.1 Characterisation of 25-27

In Figure 36 the ^{1}H NMR spectrum of **25** is shown, exemplifying this group of compounds**.** The ^{1}H NMR spectrum shows the characteristic signals of the lauroyl residue at δ = 2.76 – 2.33 (m, 2H), 2.00 – 1.70 (m, 2H), 1.67 – 1.30 (m, 16H), 1.08 (t, *J* = 5.3 Hz, 3H) ppm.

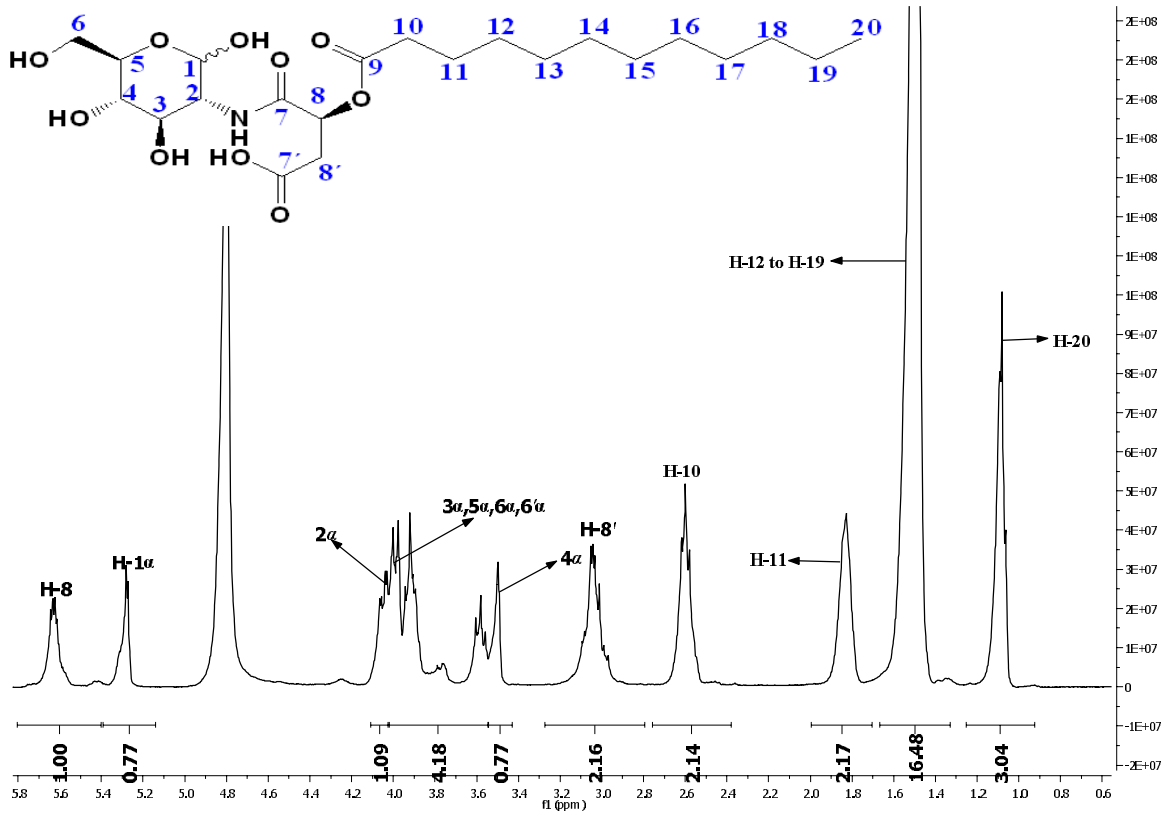

Figure 36: ^{1}H NMR spectrum of **25** in methanol-d_4 recorded at 30 °C.

The signals with chemical shifts in the range of 5.28–3.50 ppm are characteristic for the ring protons at C-1–C-6 of the *D*-glucosamine moiety and the assignment of all proton signals of the *D*-glucosamine unit are shown in Figure 36. In *D*-glucosamine the proton at C-2 is found at 3.09 (dd, J = 10.4, 3.5 Hz, 1H, H-2α), 2.85 (dd, J = 10.2, 8.3 Hz, 1H, H-2β) ppm whereas in **25** the proton at C-2 is shifted downfield to 4.05 (dd, J = 10.5, 3.4 Hz, 1H) ppm clearly indicating that acylation took place on the amine group at C-2. The protons with the chemical shifts of δ = 5.63 (dd, J = 8.0, 4.5 Hz, 1H) and 2.76 – 2.33 (m, 2H) ppm are the H-8 and H-8′ protons, respectively, of the malic acid unit of **25**.

In Figure 37 the ^{13}C NMR spectrum of **25** is shown, exemplifying this group of compounds. The ^{13}C NMR spectrum shows the characteristic signals of the carbonyl groups at C-7, C-9, C-7′ of **25** with chemical shifts of δ = 174.26, 173.06, 171.76 ppm, respectively. The characteristic CH and CH_2 signals of the malic acid unit appear at δ = 71.47, 37.56 ppm, respectively.

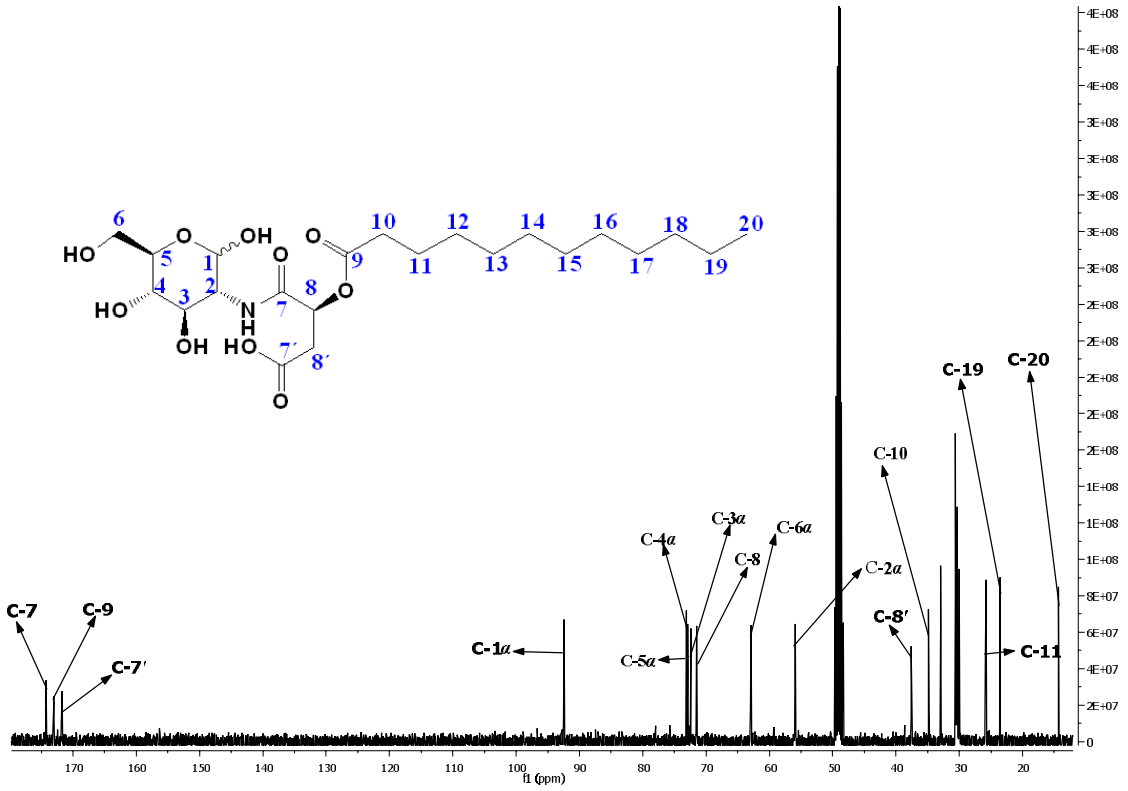

Figure 37: ^{13}C NMR spectrum of **25** in methanol-d_4 recorded at 30 °C.

The complete assignments of all ring carbons (C-1 to C-6) of the *D*-glucosamine unit in **25** were achieved by 2-D NMR (^{1}H-^{1}H COSY, ^{1}H-^{13}C HSQC) and are shown in Figure 37. The acylation clearly took place on the amine group at C-2 position as confirmed by the downfield shift of the C-2 carbon by approximately 3 ppm as compared to pure *D*-glucosamine.

3.3.2 Foaming and emulsifying properties of 22-27

Due to the presence of both hydrophilic hydroxyl groups and hydrophobic fatty acid chains, these amphiphiles are expected to exhibit surface properties.[127] In case of **22-24** due to their extremely low solubilities in water the corresponding triethanolamine salts have been used to measure foaming properties and the results are depicted in Table 13. Despite of the fact that the *O*-*O′*-di-acylated tartaric acid based amphiphiles **22-24** by the virtue of being gemini surfactants are expected to exhibit strong foaming abilities they were actually not foaming at all and this simply because of their low solubilities in water.[120]

The foaming ability is gradually decreasing with increasing hydrocarbon chains length and this fact might be attributed to difference in solubilities of the amphiphiles in water. Among these series of amphiphiles, the malic acid based amphiphile **25** displays the best foaming ability which is comparable to SDS.

compound[a]	foaming ability (mL)	foam stability (mL)	HLB values
22	106	100	12
23	73	69	-
24	69	66	-
25	715	712	not-detectable
26	171	165	not detectable
27	60	49	not detectable
SDS	765	720	-

[a] For foaming properties triethanolamine salts have been used.

Table 13: Foaming and emulsifying properties of the *D*-glucosamine based amphiphiles **22**-**27**.

The HLB values of the amphiphiles ware also determined and are shown in Table 13. Tartaric acid based amphiphile **22** with a C_{12} hydrocarbon chain shows a HLB value of 12 whereas amphiphiles **23** and **24** with C_{14} and C_{16} hydrocarbon chains, respectively, do not show any HLB value due to their extremely low solubilities in water.

3.3.3 Conclusion

A small library of N-acylated-D-glucosamines have been prepared regioselectively with good yield and in just one step by treatment of the corresponding O-acylated hydroxycarboxylic acid anhydrides with D-glucosamine (2-amino-2-deoxy-D-glucopyranose).Their foaming, emulsifying properties and CMCs have been determined. It has been revealed that the N-acylated-D-glucosamines containing O-O′-di-acyl tartaric acid moieties showed poor surface properties in water because of their low solubility in water.128 On the other hand the malic acid based N-acylated glucosamine 25 with C_{12} hydrocarbon chain shows excellent foaming which is comparable to SDS.

3.4 Combination products based on methyl-*α*-*D*-glucopyranoside

3.4.1 General synthetic procedure

Methyl-*α*-*D*-glucopyranoside (5 eq) was acylated with *O*-acylated hydroxycarboxylic acid anhydrides (1 eq) in the presence of DMF and Py (1 eq) in a similar way as described earlier for the syntheses of 6-*O*-acylated fatty acid esters of *D*-glucose in section 3.2.1.2 (Scheme 14).

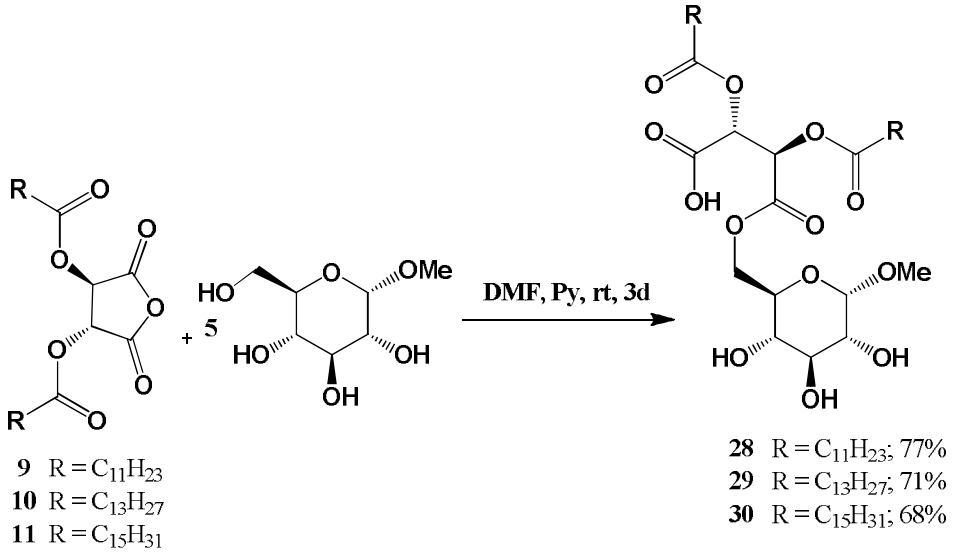

Scheme 14: Syntheses of methyl-*α*-*D*-glucopyranoside based surface active compounds **28**–**30**.

The reaction was monitored by TLC and also by HPLC-MS of the crude reaction mixture. The products were separated by column chromatography using a MeOH/EtOAc (10:90) solvent mixture as eluent and **28-30** were characterised by ^{1}H and ^{13}C NMR spectra. The formation of the 6-*O*-acylated product was confirmed by the downfield shift of the protons at the C-6 position and C-6 carbon in ^{1}H and ^{13}C NMR, respectively (Figure 39 and Figure 41).

3.4.1.1 NMR characterisation of the products

In Figure 38 the ^{1}H NMR spectrum of **30** is shown, exemplifying this group of compounds**.** The ^{1}H NMR spectrum shows the characteristic signals of the palmitoyl residues appear at δ = 2.76 – 2.36 (m, 4H), 1.93 – 1.74 (t, J = 7.2 Hz, 4H), 1.68 – 1.41 (m, 48H), 1.11 (t, J = 6.8 Hz, 6H) ppm. Signals with chemical shifts in the range of 5.75 –3.45 ppm are the characteristic signals for the ring protons at C-1 to C-6 of the methyl-*α*-*D*-glucopyranoside moiety and the complete assignments of all protons are shown in Figure 38.

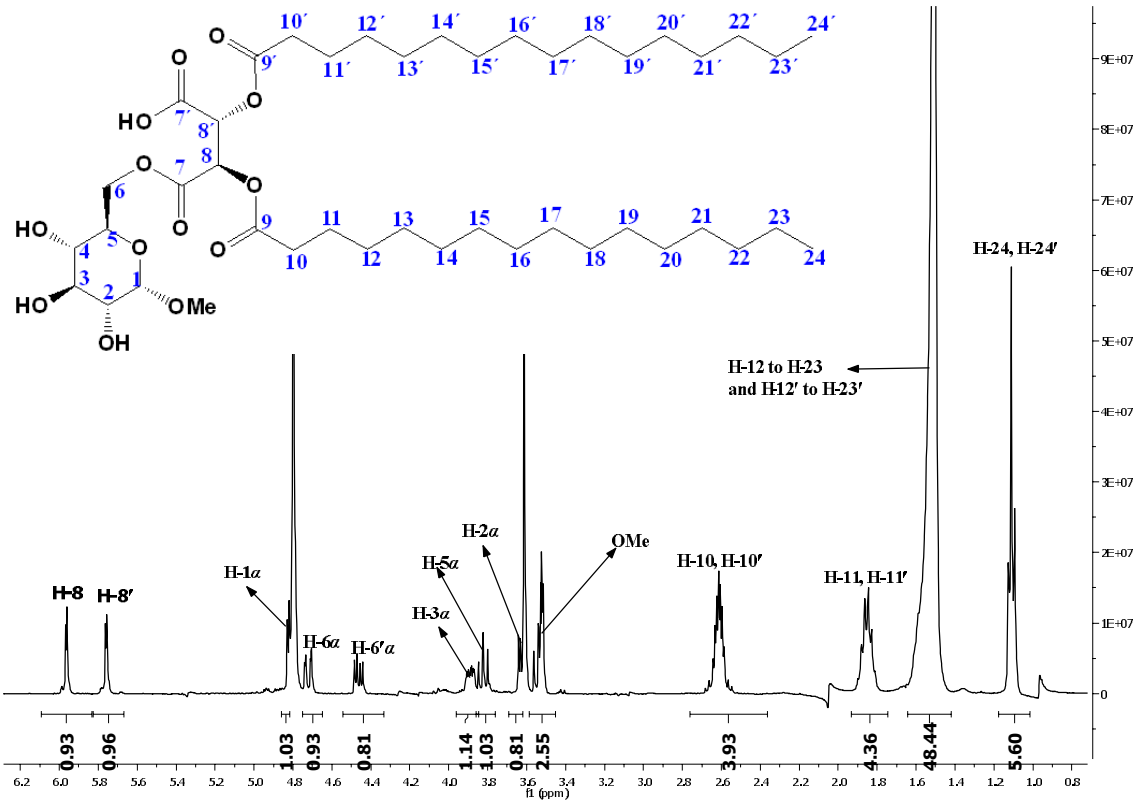

Figure 38: ^{1}H NMR spectrum of **30** in MeOH-d_4.

In methyl-*α*-*D*-glucopyranoside the protons at C-6 position appear at δ = 4.11 (dd, *J* = 11.8, 2.5 Hz, 1H), 3.98 (dd, *J* = 11.8, 5.5 Hz, 1H) ppm whereas in **30** these protons are shifted downfield to δ = 4.79 (dd, *J* = 11.7, 2.0 Hz, 1H), 4.53 (dd, *J* = 11.7, 5.1 Hz, 1H) ppm, clearly indicating that the esterification took place at the C-6 hydroxy group (Figure 39). Protons with chemical shifts at δ = 5.96 (d, *J* = 2.6 Hz, 1H), 5.75 (d, *J* = 2.6 Hz, 1H) ppm are the H-8 and H-8′ protons, respectively of the tartaric acid unit.

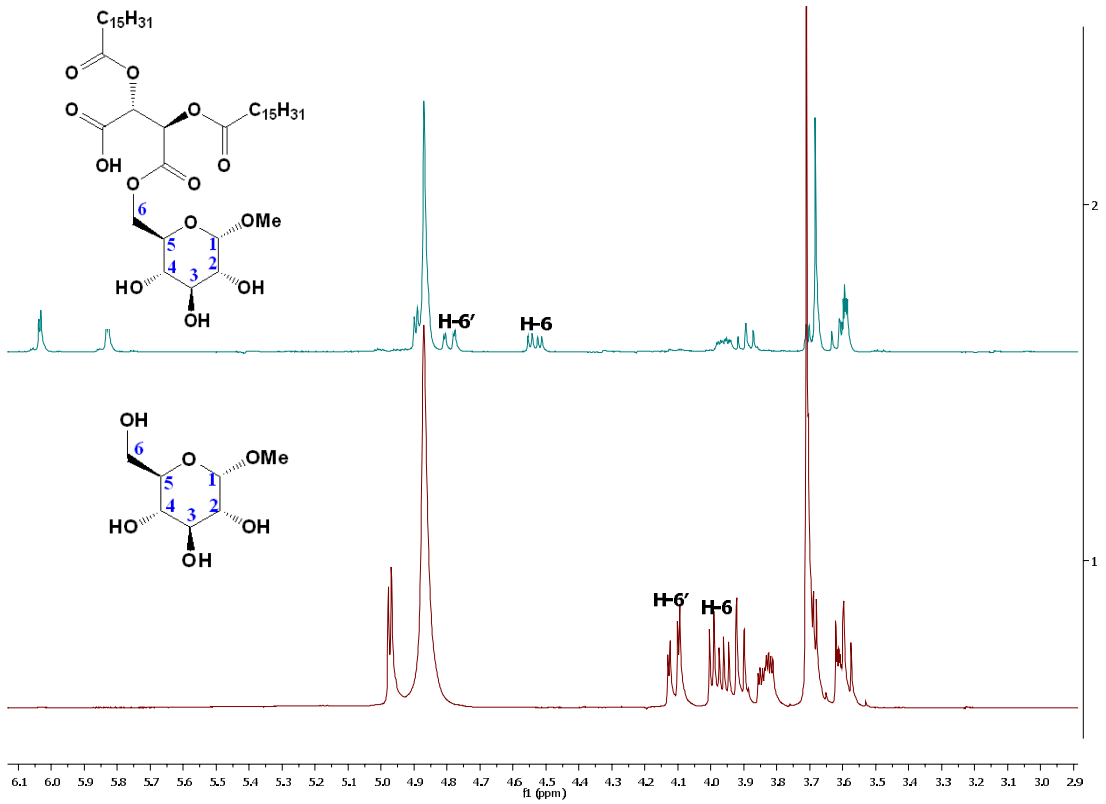

Figure 39: Expanded region of superimposed ^{1}H NMR spectra of methyl-*α*-*D*-glucopyranoside and **30** to demonstrate the downfield shift of H-6 and H-6′ after acylation.

In Figure 40 the ^{13}C NMR spectrum of **30** is shown, exemplifying this group of compounds. The ^{13}C NMR spectrum shows the characteristic carbonyl group signals at C-9, C-9′, C-7, C-7′ with chemical shifts of δ = 174.36, 174.28, 168.55 ppm, respectively. The characteristic CH signals of tartaric acid unit appear at δ = 71.60 ppm. The assignments of all ring carbons (C-1 to C-6) of the methyl-α-D-glucopyranoside unit of 30 were achieved by 2-D NMR (^{1}H-^{1}H COSY, ^{1}H-^{13}C HSQC) and are summarised in Table 14.

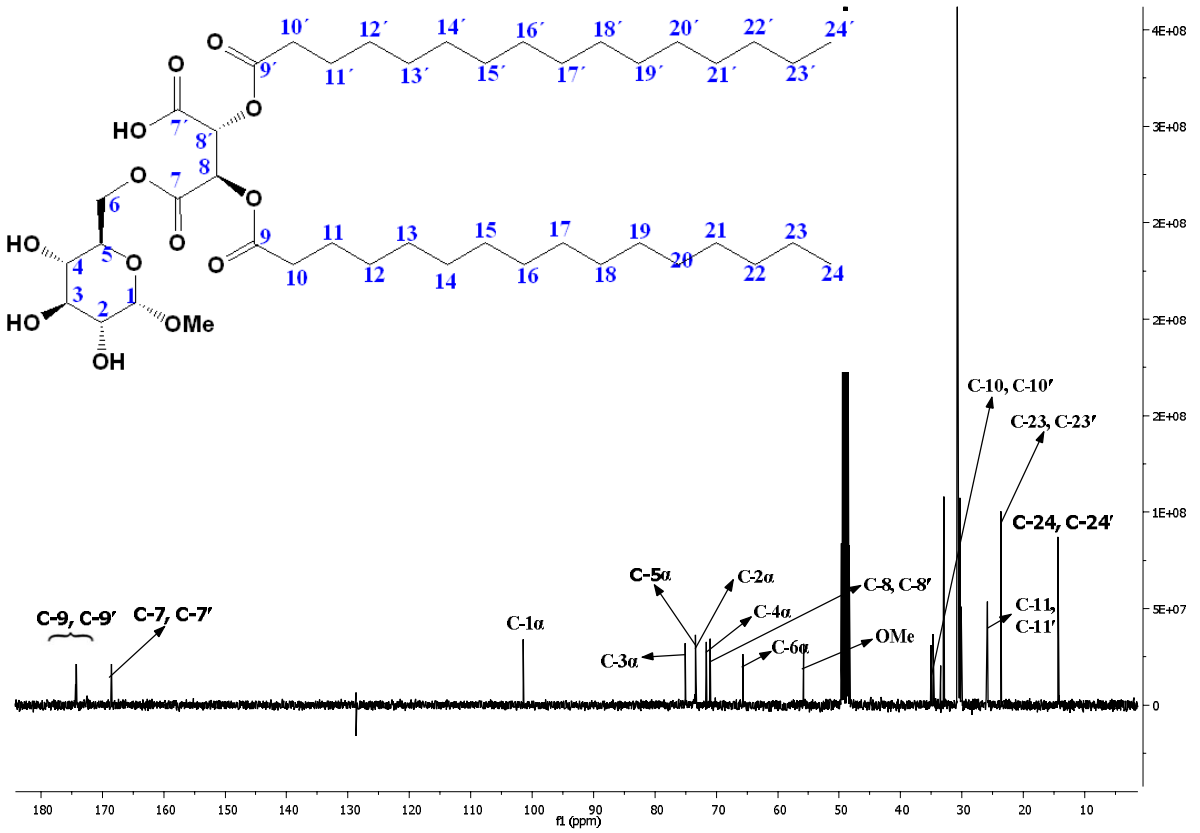

Figure 40: ^{13}C NMR spectrum of **30** in MeOH-d_4.

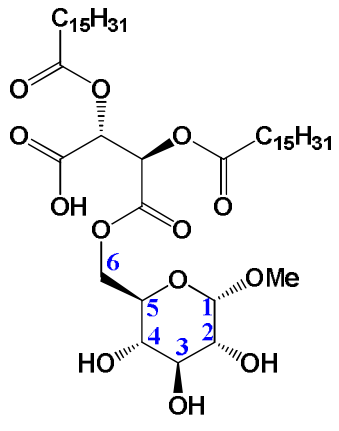

30

compound	C-1*α*	C-2*α*	C-3*α*	C-4*α*	C-5*α*	C-6*α*
30	101.40	73.32	75.07	71.60	73.39	65.69

Table 14: Assignments of the carbons in the methyl-*α*-*D*-glucopyranoside moiety of **30**.

The acylation at the C-6 position was clearly confirmed by the downfield shift of the C-6 carbon by approximately 3 ppm as compared to pure methyl-*α*-*D*-glucopyranoside (Figure 41).

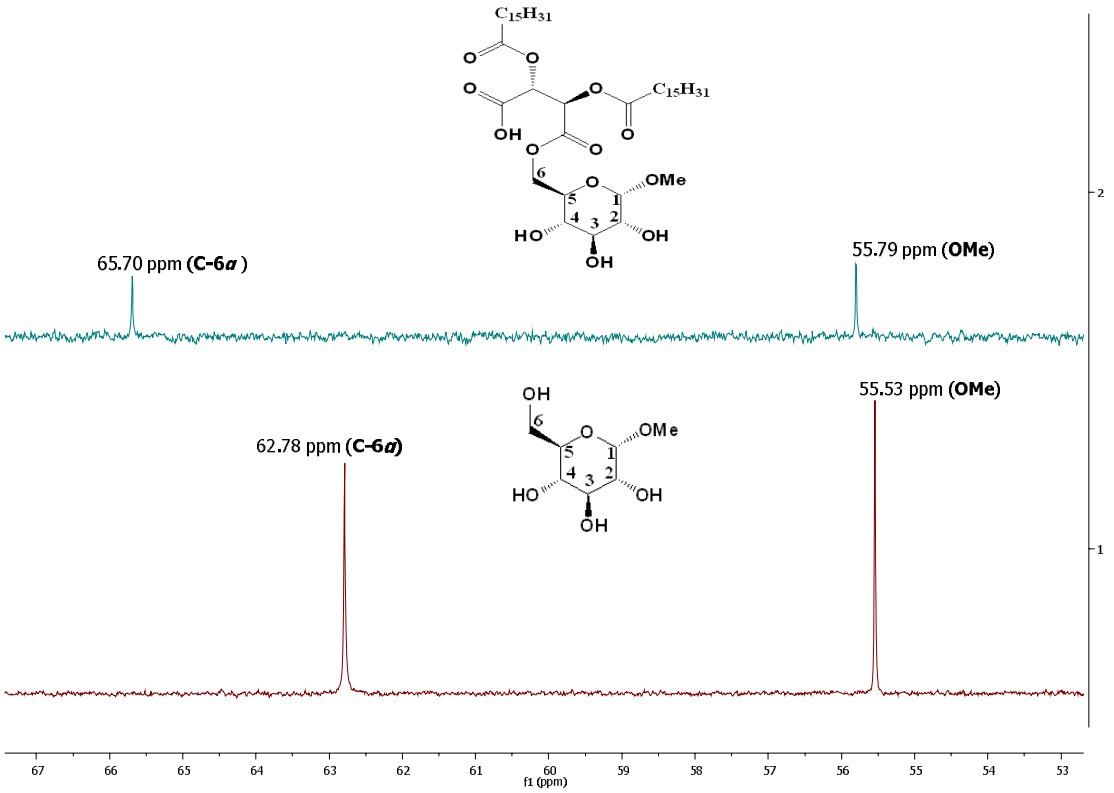

Figure 41: Expanded region of the superimposed ^{13}C NMR spectra of methyl-*α*-*D*-glucopyranoside and **30** to demonstrate the downfield shift of C-6 in **30**.

3.4.2 Surface and interface properties of 28-30

3.4.2.1 Determination of CMC values of 28-30

The CMC values of the triethanolamine salts of **28**-**30** were determined by the ring method[122] based on surface tension measurements. These studies are shown in Figure 42. As described before, the CMCs and γ_{CMC} of the surfactants were obtained from the plots of the surface tensions against the logarithm of concentration (log C, g/L) and the results are shown in Table 15. It is worthy to note that amphiphiles **28**-**30** possess CMC values which are lower than SDS by approximately two to three orders in magnitude. This essentially implies that it is thermodynamically favourable for the hydrophobic domains of these surfactants to leave in the aqueous solution. **28**-**30** are gemini surfactants in which two hydrophobic tails are interconnected by a spacer. They have an inherent tendency to pack tightly at the air/water interface and subsequently display reduced interfacial tension at the air/water interface. In the amphiphiles with increasing hydrocarbon chains the CMCs slightly increase from **28** to **29** and then decrease again from **29** to **30**.

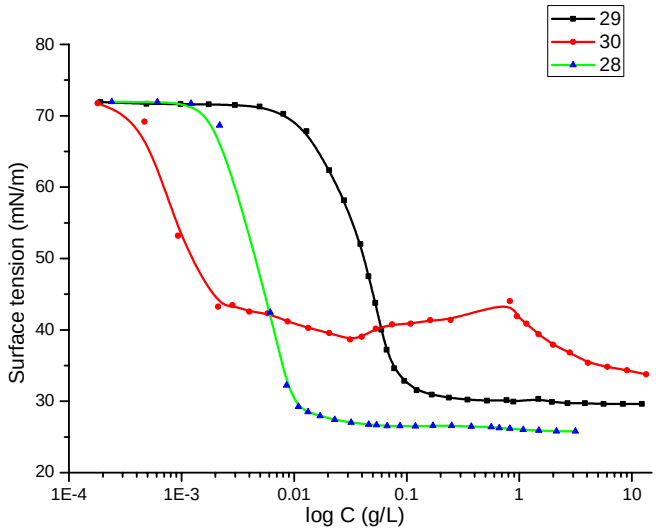

Figure 42: Plot of surface tension *vs.* logarithm of concentration (log C, g/L) for **28**–**30** in water at 25 °C.

compound[a]	CMC (mol/L)	γ_{CMC} (mN/m)
28	1.34×10^{-5}	27.0
29	9.92×10^{-5}	30.4
30	3.78×10^{-6}	36.1
SDS	8.0×10^{-3}	22.1

[a] For CMC determinations triethanolamine salts have been used.

Table 15: CMCs and γ_{CMC} s (mN/m) of **28**–**30** in water.

3.4.2.2 Foaming and emulsifying properties of 28-30

The foaming and emulsifying abilities of **28**-**30** were determined as described before and the results are shown in Table 16. Among this series of amphiphiles the foaming ability of **28** with a C_{12} hydrocarbon chain is higher than that of the corresponding amphiphiles **29** and **30** with C_{14} and C_{16} hydrocarbon chains, respectively. This is due to an increase of the hydrophobic nature of the molecules with increasing hydrocarbon chain length.[120]

compound[a]	foaming ability (mL)	foam stability (mL)	HLB values
28	359	356	not detectable
29	95	92	11
30	86	85	11

[a] For foaming properties triethanolamine salts have been used.

Table 16: Foaming and emulsifying properties of **28**-**30**.

28 does not show an HLB value while **29** and **30** produce very stable oil in water emulsions with characteristic HLB values of 11. Hence they may be useful for the preparation of O/W emulsions, *e.g.* in the food industry or for cosmetics. Due to their facile accessibly and low price they may be attractive for commercial applications.

3.4.3 Gelation abilities of 28-30

The gelation abilities of **28-30** in water were determined by the simple method of being stable to inversion of the container as shown earlier in section 3.2.2 and the results are shown in Table 17.

compound	MGC (minimum gelation concentration, w/v).	T^{a}_{gel}
28	not a gelator	-
29	ND[b]	13 °C
30	1.3%	34 °C

[a] For T_{gel} value 10% (w/v) of each hydrogels was used.
[b] Not determined due to low thermal stability of the hydrogel

Table 17: Minimum gelation concentrations and thermal stabilities of the hydrogels (10%, w/v) derived from **28-30**.

As described before in section 3.2.2.1, the thermal stabilities and minimum gelation concentrations of the amphiphiles in water are strongly influenced by the length of the hydrocarbon chains in the lipophilic part of the molecules. **30** with a longer hydrocarbon chain (C_{16}) produces a very stable hydrogel at room temperature (T_{gel} = 34 °C) with a minimum gelators concentration of 1.3% (w/v), whereas the corresponding amphiphile **29** with a shorter hydrocarbon chain (C_{14}) produces a stable hydrogel only at a low temperature (T_{gel} = 13 °C) while the amphiphile **28** with a C_{12} hydrocarbon chain is not leading to gel in water.

3.4.4 Conclusion

In summary, a small library of amphiphiles based on methyl-*α*-*D*-glucopyranoside was synthesised. They are accessible in just two steps and could thus be produced also on industrial scale. **28-30** are displaying not only good foaming and emulsifying properties, but **30** produces a very transparent gel in water and hence might have potential practical applications.

3.5 Combination products based on *D*-galactose

3.5.1 Reaction of native *D*-galactose with *O*-acylated hydroxycarboxylic acid anhydrides in the presence of pyridine

The solvent free reaction of *D*-galactose (1eq) with *O*-acylated hydroxycarboxylic acid anhydrides (1 eq) in the presence of pyridine at room temperature within 12 h is leading to an almost quantitative conversion of starting materials into a mixture of mono acylated esters of *D*-galactose. The presence of the axial hydroxy group at C-5 makes galactose potentially more reactive but at the same time less selective. Therefore the reaction leads to a mixture of almost all possible diastereomers (mono acylated) of *D*-galactose which are very difficult to separate.

3.5.2 Reaction of protected *D*-galactose

In order to achieve a selective mono-acylation on the hydroxy group at the C-6 position of *D*-galactose a synthetic strategy was devised using 1,2:3,4-di-*O*-isopropylidene-*α*-*D*-galactopyranoside (**31)** as starting material (Scheme15). **31** was obtained in 93% yield by a published procedure[129] in treating *D*-galactose in dry acetone in the presence of sulphuric acid. **31** has only one free hydroxy group at C-6. The solution of **31** in anhydrous chloroform was then treated with *O*-*O′*-di-acylated tartaric acid anhydrides **9**-**11** in the presence of pyridine to obtain the corresponding 6-*O*-(*O*-*O′*-di-acyl tartaryl)1,2:3,4-di-*O*-isopropylidene-*α*-*D*-galactopyranosides **32**–**34** in almost quantitative yield (Scheme15).

These **32**-**34** were treated with 90% trifluoroacetic acid in water at room temperature for 12 h. The corresponding 6-*O*-(*O*-*O′*-di-acyl tartaryl)-*D*-galactose **35-37** were precipitated from the reaction mixture.

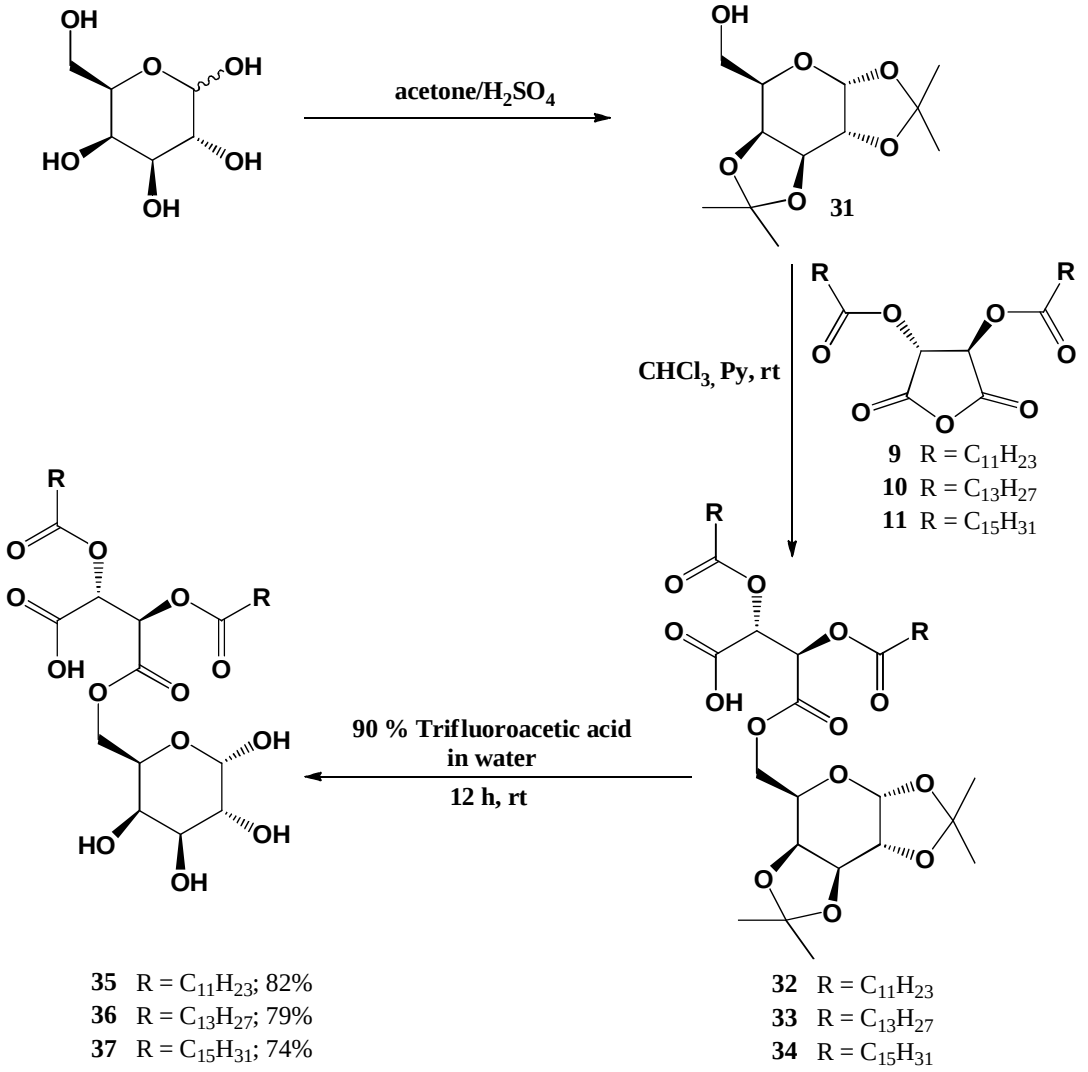

Scheme15: Syntheses of the 6-*O*-acylated fatty acid esters of *D*-galactose **35**–**37**.

35-37 contain always a mixture of pyranosides and furanosides together with their *α*/*β* anomers as shown in Figure 43. This was also confirmed by ^{1}H NMR and HPLC-MS of the pure **35-37** (Figure 43).

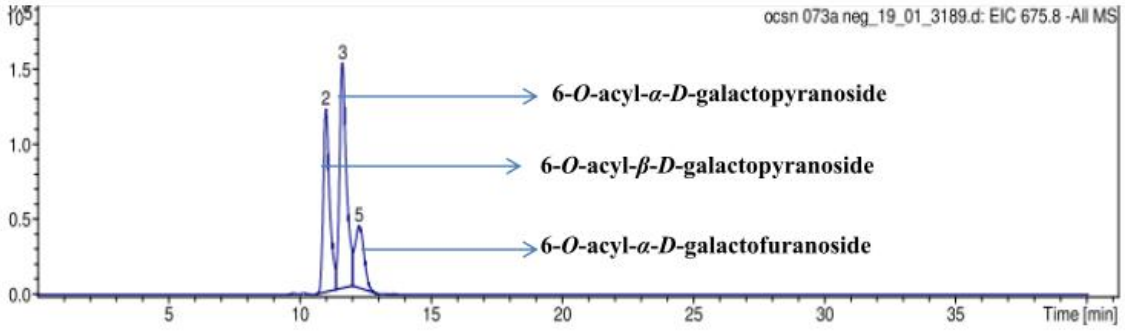

Figure 43: HPLC-MS chromatogram of **35**; eluent: CH_3CN/H_2O (70:30).

3.5.2.1 NMR Characterisation of the products

In Figure 44 the ^{1}H NMR spectrum of **37** is shown, exemplifying this group of compounds**.**

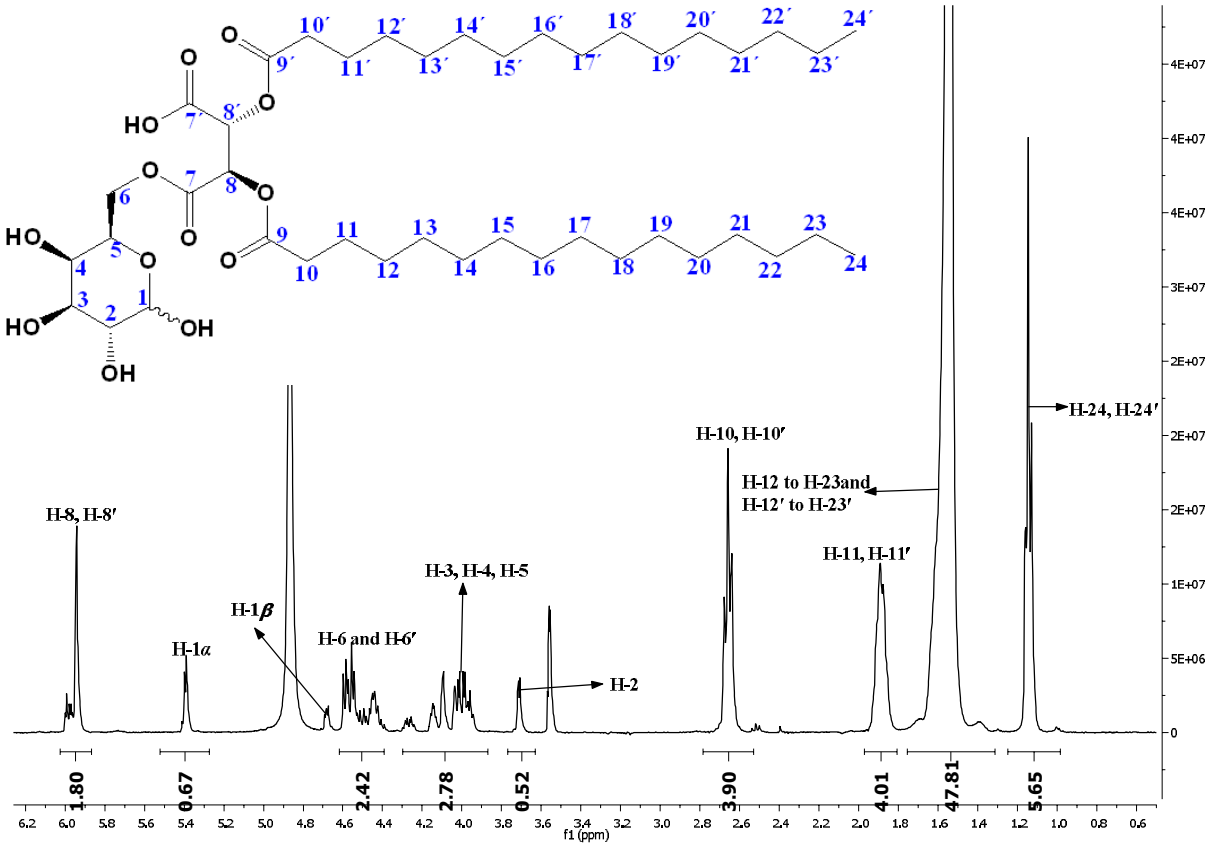

Figure 44: ^{1}H NMR spectrum of **37** in MeOH-d_4

The ^{1}H NMR spectrum shows the characteristic signals of the palmitoyl residue at δ = 2.66 (t, *J* = 7.2 Hz, 4H), 1.97 – 1.80 (m, 4H), 1.75 – 1.31 (m, 48H), 1.14 (t, *J* = 6.2 Hz, 6H) ppm. Signals with chemical shifts in the range of 5.39 –3.63 ppm are characteristic for the ring protons at C-1 to C-6 of *D*-galactose moiety and the assignments of all proton signals are shown in Figure 44. In *D*-galactose, the protons at C-6 show chemical shifts at δ = 4.24 (dd, *J* = 12.1, 5.9 Hz, 1H), 4.12 (dd, *J* = 12.1, 5.9 Hz, 1H) ppm whereas in **37** the protons at C-6 are shifted downfield to δ = 4.62 – 4.39 (m, 2H) ppm, clearly indicating that esterification took place on the hydroxy group at C-6 position (Figure 44). Protons with chemical shifts of δ = 6.03 – 5.88 (m, 2H) ppm are the H-8 and H-8′ protons of the tartaric acid unit.

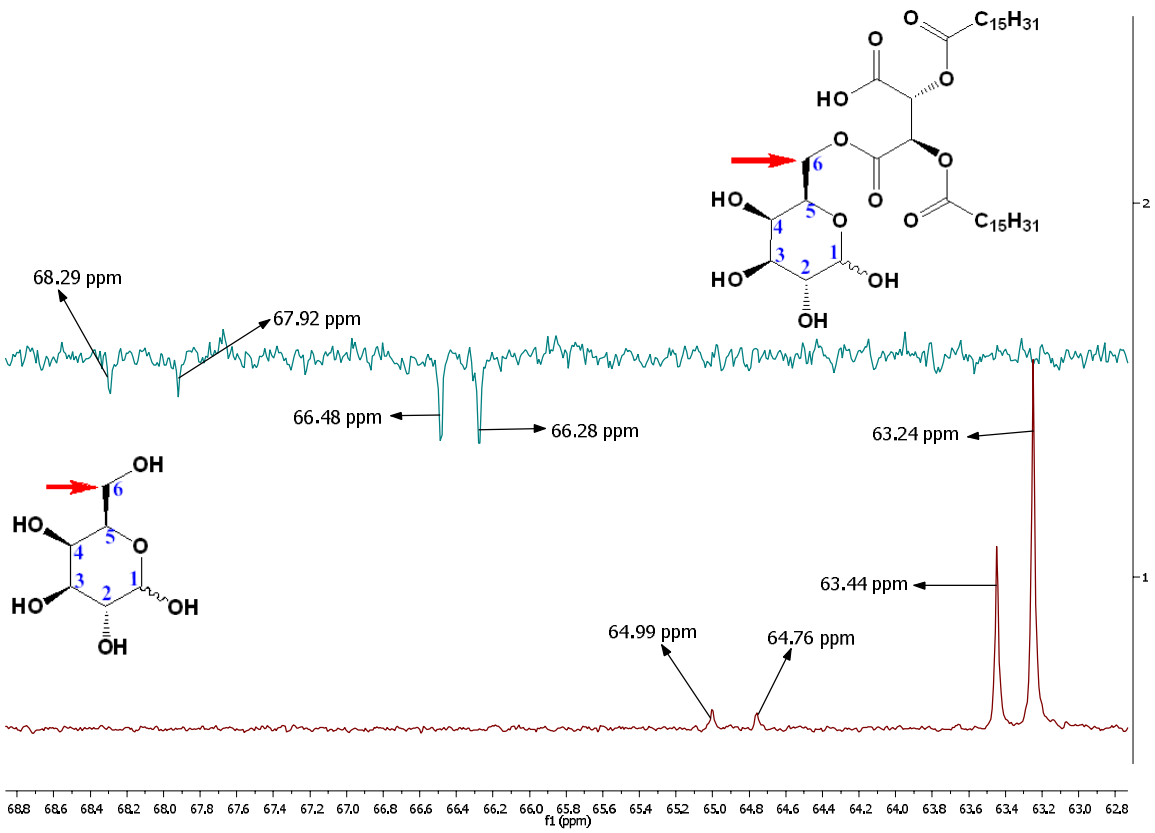

Figure 45: Expanded region of the superimposed DEPT 145 spectrum of **37** and the ^{13}C NMR spectrum of *D*-galactose to demonstrate downfield shift of C-6 carbon of *D*-galactose after substitution.

In pure *D*-galactose the C-6 carbon shows chemical shifts at 63.24 ($^{\beta f}$C-6), 63.44 ($^{\alpha f}$C-6), 64.99 ($^{\beta p}$C-6) and 64.76 ($^{\alpha p}$C-6) whereas in **37** the carbon at the C-6 positions are shifted downfield to 66.28 ($^{\beta f}$C-6), 66.48 ($^{\alpha f}$C-6), 67.92 ($^{\beta p}$C-6), 68.28 ($^{\alpha p}$C-6) ppm, respectively as shown in Figure 45. This clearly indicates that the acylation with *O*-*O'*-di-acylated tartaric acid anhydrides took place at the hydroxy group of C-6.

$^{\beta f}$C-6 = C-6 of β furanoside anomer; $^{\alpha f}$C-6 = C-6 of α furanoside anomer; $^{\beta p}$C-6 = C-6 of β pyranoside anomer; $^{\alpha p}$C-6 = C-6 of α pyranoside anomer.

3.5.3 Conclusion

Regioselective esterification of *D*-galactose was carried out using di-isopropylidene protected *D*-galactose as precursor in order to achieve selective esterification at the hydroxy group of C-6. It was revealed qualitatively that **35**-**37** are also gelators in water although the detailed characterisation of the nature of the gel fibers has to be done yet and need to be studied further in order to determine the influence of the polar head groups on the gelation efficacy in water as well as in organic solvents.

3.6 Combination products based on sucrose

3.6.1 Reactivity of sucrose and properties

3.6.1.1 Comparisons of the reactivities of the different hydroxyl groups

Sucrose is a non-reducing sugar with a unique structure containing nine chiral centres. Due to the presence of eight hydroxy groups having almost comparable reactivities it is practically very difficult in practice to achieve regioselective esterifications of unprotected sucrose. Also the isolation and characterization of each regiomer from the reaction mixture is difficult. In sucrose, even though all the hydroxyl groups are comparable in reactively, there are slight differences in reactivities. In practice the primary hydroxy groups usually react with some preference using suitable electrophiles (Figure 46).[130]

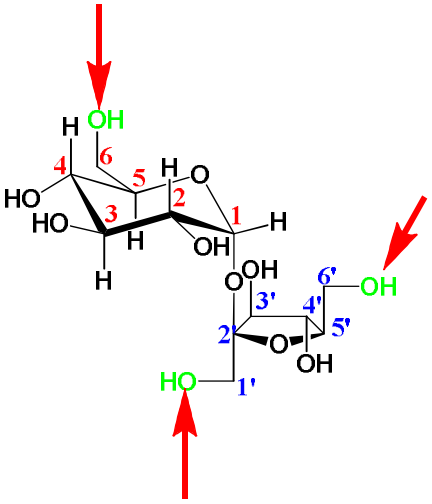

Figure 46: Structural representation of the sucrose with indication of the most reactive hydroxy groups for esterification reactions.

The analysis of the products obtained after tritylation or tosylation indicate that the reactivities decrease in the order 6-OH > 6′-OH > 1′-OH. Reaction with sulphuryl chloride showed the order 6-OH>6′-OH > 4-OH > 1′-OH. Reaction with PPh3, CCl4 in pyridine at 70 °C led to 6,6′-dichloro-6,6′-dideoxysucrose in 92% yield. Treatment of sucrose with acetic anhydride (1.1 mol equiv.) in pyridine at −40 °C is leading to the formation of 6-O-acetyl sucrose in 40% yield. On the other hand, 6′-OH was the most reactive site towards silylating agents. All these examples clearly indicate that 1′-OH is less reactive than 6-OH and 6′-OH presumably due to its neopentyl-like character. As a consequence the products of an equimolar derivatisation reaction are always contaminated with small amounts of other monoesters as well as di- and tri-substituted esters, whereby the composition varies with the reaction conditions and the reactants. To take full advantage of sucrose as a feedstock, it would be

optimal and highly desirable to achieve selective modifications leading to a single product with defined physical, chemical, or biological properties.

3.6.1.2 Reaction of native Sucrose with *O-O'*-di-acylated hydroxycarboxylic acid anhydrides

In a general procedure for the regioselective acylation of sucrose with *O*-acylated hydroxycarboxylic acid anhydrides the following method was employed. A DMF solution of sucrose (5 eq) was treated with *O*-acylated hydroxycarboxylic acid anhydrides (1 eq) in the presence of pyridine (1 eq). The reaction was continued for 3 d in case of tartaric acid anhydrides (Scheme 16) and 12 h in the case of malic acid anhydrides (Scheme 17).

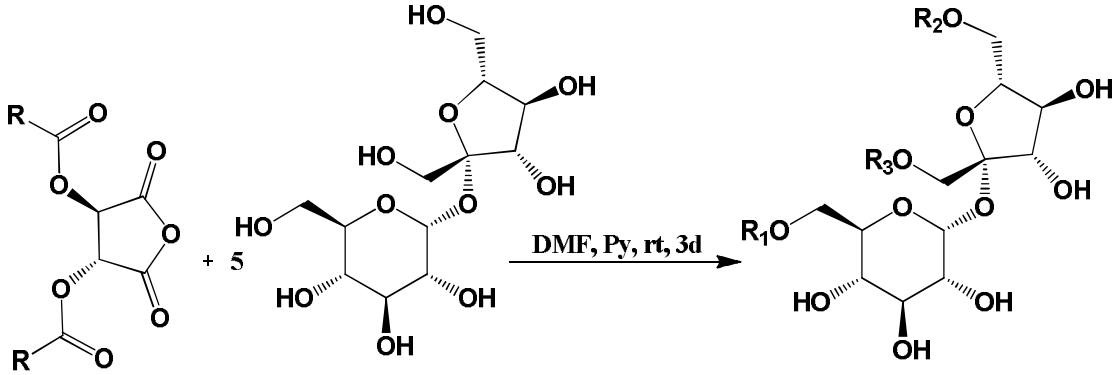

9 R = $C_{11}H_{23}$
10 R = $C_{13}H_{27}$
11 R = $C_{15}H_{31}$

38a,b,c R = $C_{11}H_{23}$; 65%
39a,b,c R = $C_{13}H_{27}$; 39%
40a,b,c R = $C_{15}H_{31}$; 43%

In **a** R_1 = *O-O'*-diacylated tartaric acid; R_2 and R_3 = H (80-85% yield)
In **b** R_2 = *O-O'*-diacylated tartaric acid; R_1 and R_3 = H (5-10 % yield)
In **c** R_3 = *O-O'*-diacylated tartaric acid; R_1 and R_2 = H (5-10% yield)

Scheme 16: Syntheses of mono acylated sucrose products **38a,b,c**–**40a,b,c**.

The reactions were monitored by TLC. The reaction products consists of diastereomeric mixtures of mono-esterified regiomers of sucrose as confirmed by HPLC-MS. The isolation and separation of the regiomers of sucrose is possible by HPLC-MS (Figure 47) using CH_3CN/H_2O as eluent as published in the literature.[131,132]

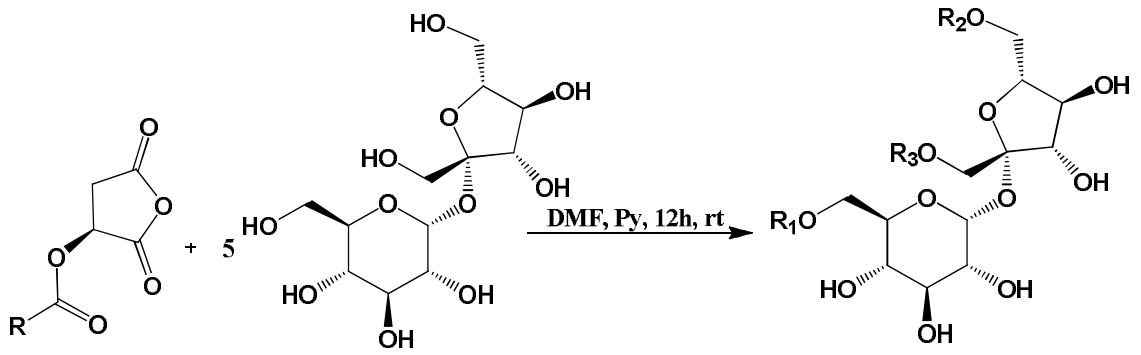

3 R = $C_{11}H_{23}$
4 R = $C_{13}H_{27}$
5 R = $C_{15}H_{31}$

41a,b,c R = $C_{11}H_{23}$; 57%
42a,b,c R = $C_{13}H_{27}$; 61%
43a,b,c R = $C_{15}H_{31}$; 59%

In **a** R_1 = *O*-acylated malic acid; R_2 and R_3 = H (80-85% yield)
In **b** R_2 = *O*-acylated malic acid; R_1 and R_3 = H (5-10 % yield)
In **c** R_3 = *O*-acylated malic acid; R_1 and R_2 = H (5-10% yield)

Scheme 17: Syntheses of sucrose derived esters **41a,b,c**–**43a,b,c**.

As shown in Figure 47 the crude product contains a mixture of 6-*O*-acylated, 6′-*O*-acylated and 1′-*O*-acylated products with ~80% of a single regioisomer which can be identified as 6-*O*-acyl-sucrose as confirmed by TLC and HPLC-MS. The mixture of regioisomers was separated by column chromatography using MeOH/EtOAc (10:90) as eluant. The product was characterised by ^{1}H and ^{13}C NMR.

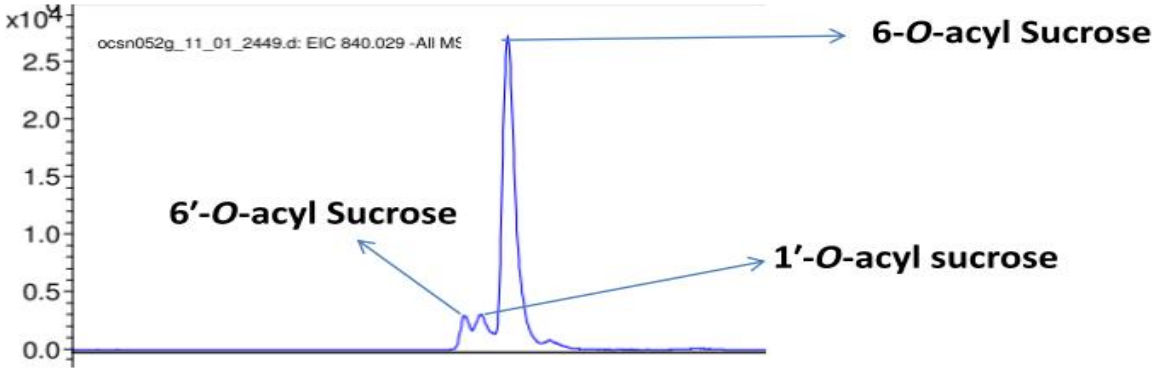

Figure 47: HPLC-MS chromatogram of the crude reaction mixture of sucrose and *O*-*O*′-di-lauroyl-tartaric acid anhydride; eluent: CH_3CN/H_2O (30:70).

3.6.1.3 NMR Characterisation of 38-40

In Figure 48 the ^{1}H NMR spectrum of **38a-b** is shown, exemplifying this group of compounds**.** The ^{1}H NMR spectrum shows the characteristic signals of the lauroyl residue at δ = 2.65 – 2.29 (m, 4H), 1.89 – 1.55 (t, *J* = 6.8 Hz, 4H), 1.54 – 1.14 (m, 32H), 0.98 (t, *J* = 6.0 Hz, 6H) ppm. Signals with chemical shifts in the range of δ = 5.43 –3.41 ppm are the characteristic signals of the ring protons of the sucrose unit. The protons with chemical shifts

of δ = 5.81 (d, *J* = 11.5 Hz, 1H), 5.65 (d, *J* = 12.3 Hz, 1H) ppm are the CH protons of the tartaric acid moiety of **38a-b**.

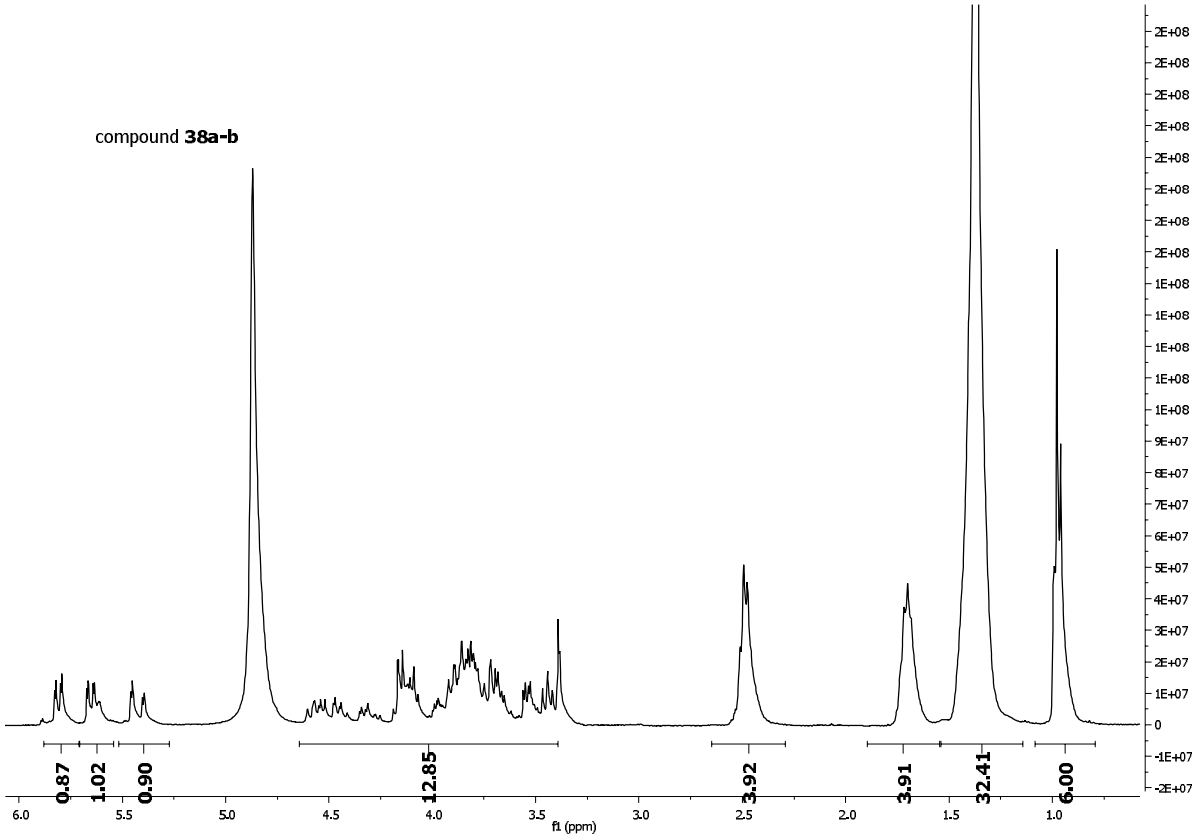

Figure 48: ^{1}H NMR spectrum of **38a-b** in MeOH-d_4 recorded at 30 °C.

38a-b was isolated from the crude mixture by column chromatography as a diastereomeric mixture of 6-*O*-acylated sucrose (**38a**) and 6′-*O*-acylated sucrose (**38b**). The complete assignments of all the carbon signals of the sucrose unit are summarised in Table 18.

compound	C-1	C-2	C-3	C-4	C-5	C-6	C-1′	C-2′	C-3′	C-4′	C-5′	C-6′
sucrose	93.68	73.33	74.48	71.60	74.83	62.47	63.39	105.48	79.78	76.01	83.93	64.38
38a	93.59	71.85	74.47	71.24	73.06	65.49	64.21	105.59	79.56	75.86	83.77	64.26
38b	93.49	73.24	74.24	71.55	74.75	62.52	63.53	105.22	79.62	76.80	80.66	68.03

Table 18: ^{13}C chemical shifts of sucrose[133], **38a** and **38b** in MeOH-d_4 to demonstrate the downfield shift of the C-6 and C-6 ′carbons.

38a-b was isolated as a diastereomeric mixture of 6-*O*-acylated and 6′-*O*-acylated esters of sucrose and the formation of 6-*O* and 6′-*O* acylated products was confirmed by downfield shift of the C-6 and C-6′ of sucrose units, respectively as compared to pure native sucrose (Figure 49).

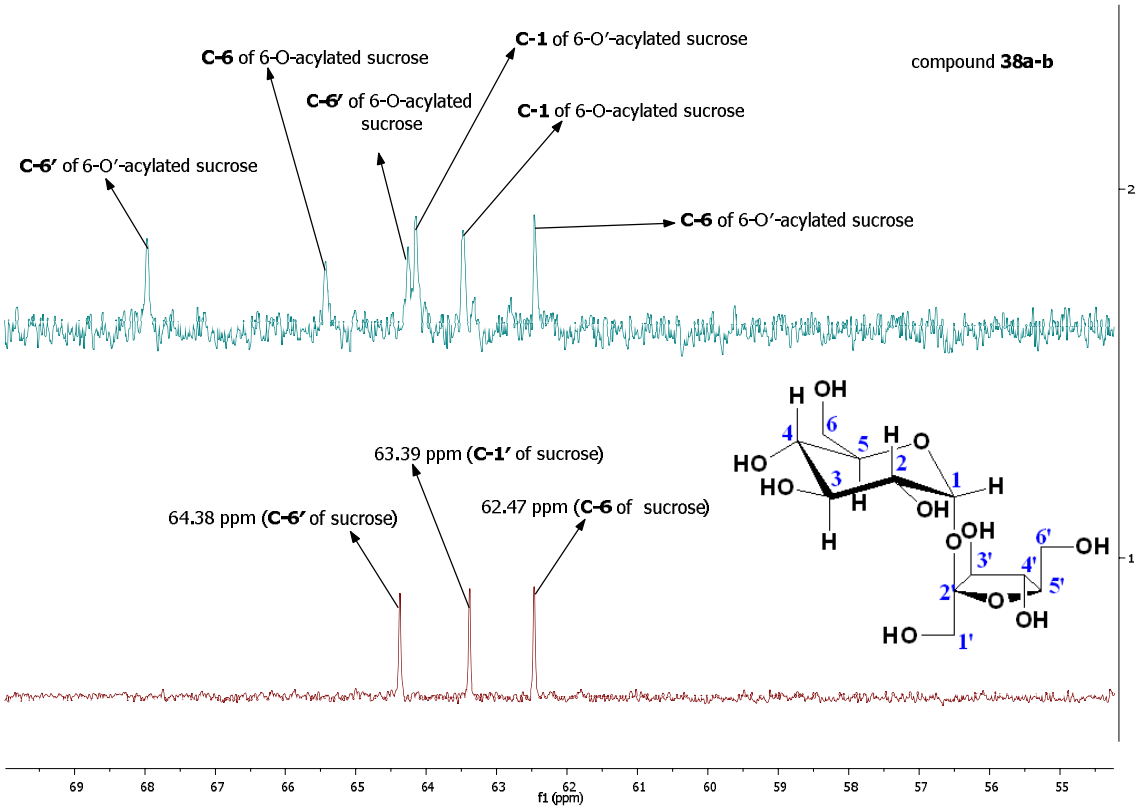

Figure 49: Expanded region of superimposed ^{13}NMR spectra of sucrose and **38a-b** to demonstrate downfield shift of C-6 and C-6′.

3.6.1.4 Surface properties of 38a,b,c–43a,b,c

Due to the presence of numerous hydrophilic hydroxy groups and hydrophobic fatty acid chains these molecules are expected to demonstrate good surface-active properties.

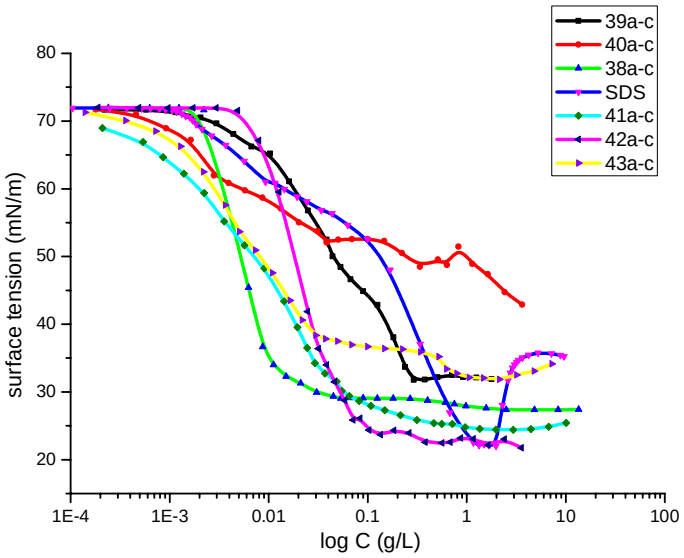

Figure 50: Plot of surface tensions *vs.* the logarithm of concentration (log C, g/L) for **38a,b,c**–**43a,b,c**.

We therefore determined the CMC values of the sucrose esters by the ring method[122] based on surface tension measurements as described before in section 3.2.3.2. The CMC values of the amphiphiles **38a,b,c**–**43a,b,c** were obtained from the plot of the surface tensions *vs.* the logarithm of concentration (Figure 50).The results are shown in Table 19.

compound[a]	CMC (mol/L)	γ_{CMC} (mN/m)
38a-c	1.2×10^{-5}	29.5
39a-c	2.9×10^{-4}	31.7
40a-c	3.4×10^{-4}	48.9
41a-c	1.1×10^{-4}	23.6
42a-c	1.1×10^{-4}	21.9
43a-c	1.4×10^{-4}	24.7
SDS	8.0×10^{-3}	22.1

[a] for CMCs triethanolamine salts have been used.

Table 19: Critical micelle concentrations (CMCs) and γ_{CMC}s at air/water interface of **38a,b,c**–**43a,b,c**.

In the case of the malic acid based amphiphiles **41a,b,c**–**43a,b,c** there is no sharp decrease in the CMCs with increasing hydrocarbon chain whereas in case of tartaric acid based amphiphiles **38a,b,c**–**40a,b,c** there is an increase of the CMC value with increasing carbon chain. This is contrary to the general trend which is normally observed in classical surfactants. This clearly implies the importance of the hydrocarbon tail for the control of the CMC value.[134,135] Similar trends of variations of the CMCs with hydrocarbon chains have been

observed also by other groups.[136,137] In the normal case, with increasing length of the hydrocarbon chain due to the hydrophobic interaction across the hydrocarbon chain facilitate a close packing of the monolayers at an interface. This enables the formation of hydrogen bonding between the carbohydrate head[138] groups across the monomers at the interface. Thus, spherical aggregates can form at the CMC. However, in the case of these tartaric and malic acid based amphiphiles with an increase in the hydrocarbon chain length there seems to be a competition[139] between the hydrophobic effect and the steric factor between the hydrocarbon chains that is entirely governed by the packing parameter (*p*). The packing parameter *p* depends on three factor according to the equation mentioned below

$$p = v/(a.l)$$

v, *a* and *l* are the volume, surface area and lipophilic chain length of the amphiphile molecule, respectively.

In case of the tartaric and malic acid based surfactants **38a,b,c**–**43a,b,c** this packing parameter, *p*, becomes prominent which essentially governs and retards the close packing at the interface for the higher fatty acid chain length. As the chain length increases for a constant polar hydrophilic head group (sucrose moiety) the packing parameter decreases, which would obstruct the formation of spherical aggregates at the interface.

3.6.1.5 Foaming and emulsifying properties of 38a,b,c–43a,b,c

Here the foaming and emulsifying properties of **38a,b,c**–**43a,b,c** were determined and the results are shown in Table 20.

compound[a]	foaming ability (mL)	foam stability (mL)	HLB values
38a-c	351	348	not detectable
39a-c	39	36	not detectable
40a-c	66	65	not detectable
41a-c	645	640	11-12
42a-c	557	548	12
43a-c	247	234	12
SDS	765	720	-

[a] For foaming properties triethanolamine salts have been used.

Table 20: Foaming and emulsifying properties of **38a,b,c**–**43a,b,c**.

The foaming abilities of the malic acid based amphiphiles **41a,b,c**–**43a,b,c** are much higher than those of the corresponding tartaric acid based amphiphiles **38a,b,c**–**40a,b,c** with same hydrocarbon chain length. With an increase in the hydrocarbon chain length for both the

tartaric and malic acid based amphiphiles the foaming abilities are decreasing. This may simply be attributed to the difference of their solubilities in water.[120] The foaming abilities of both the tartaric and malic acid based amphiphiles were compared with the commercially available surfactant SDS. **41a-c** displays excellent foaming ability which is comparable to SDS and hence this compound might be a felicitous alternative of SDS which causes untoward side effects[140]. Fatty acid esters of sucrose are well known as eco-friendly and green surfactants, easily degradable after hydrolysis with a lipase or esterase.[141] **38a-c**, **42a-c** and **43a-c** display foaming abilities in a moderate range whereas **39a-c** and **40a-c** are not foaming at all. Because of the poor solubility of the tartaric acid based amphiphiles **38a,b,c**–**40a,b,c** in water they don't have any characteristic HLB values in the range of 3-18; in contrast malic acid based amphiphiles **41a,b,c**–**43a,b,c** have HLB values in the range between 11-12 and hence they might be useful for the preparation of oil in water emulsions for applications in the food and cosmetics sector.

3.6.2 Conclusion

A regioselective mono-esterification of sucrose was achieved by the pyridine catalysed esterification of sucrose with *O*-acylated hydroxycarboxylic acid anhydrides using anhydrous DMF as solvent. In this way mixtures of 6-*O*-acyl sucrose, 6′-*O*-acyl sucrose and 1′-*O*-acyl sucrose containing *O*-acylated hydroxycarboxylic acid moieties with different hydrocarbon chains were synthesized. The high selectivity of the pyridine catalysed esterification reaction enabled the preparation of a monoester fraction which was strongly enriched with 6-*O*-acyl sucrose (over 80%). The surface properties of these compounds were determined. It was shown that length of the hydrocarbon tails plays a decisive role and has a significance influence on foaming, emulsifying properties and especially the CMC values. Among this series of amphiphiles, **41a-c** displays excellent foaming ability which is comparable to SDS and hence might be an useful alternative to SDS.

3.7 Combination products based on *L*-ascorbic acid

3.7.1 Regioselective esterification of ascorbic acid

We have focused part of these research efforts towards the exploitation of one of the best known natural antioxidants, ascorbic acid (Vitamin C). It inhibits free radical initiated lipid peroxidation, a process presumably also implicated in a variety of chronic health problems such as cancer and cardiovascular diseases.[142] Vitamin C has been used *in vitro* only in aqueous solution as an antioxidant because of its hydrophilic nature. Hence, application of Vitamin C as an antioxidant in lipophilic environment is rare.[143,144] The problem of solubility can be circumvented by converting hydrophilic Vitamin C into hydrophobic ester derivatives which improve its solubility in lipophilic materials as well as potentially retaining its radical scavenging capacity in such a hydrophobic environment.

We have now constructed a library of the corresponding Vitamin C derivatives, combination products of fatty acids and hydroxycarboxylic acids (tartaric acid and malic acid) linked to the primary hydroxy group of ascorbic acid *via* ester bonds (Scheme 18).[145]

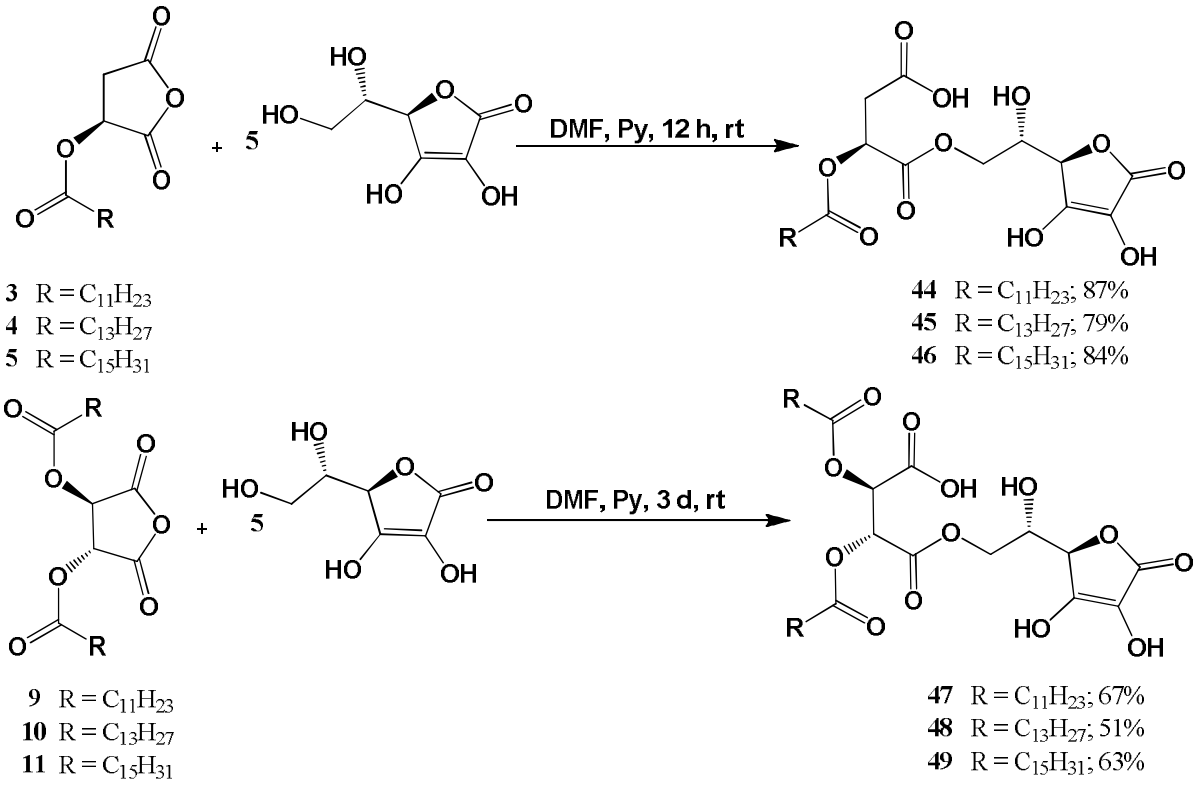

3 R = $C_{11}H_{23}$
4 R = $C_{13}H_{27}$
5 R = $C_{15}H_{31}$

44 R = $C_{11}H_{23}$; 87%
45 R = $C_{13}H_{27}$; 79%
46 R = $C_{15}H_{31}$; 84%

9 R = $C_{11}H_{23}$
10 R = $C_{13}H_{27}$
11 R = $C_{15}H_{31}$

47 R = $C_{11}H_{23}$; 67%
48 R = $C_{13}H_{27}$; 51%
49 R = $C_{15}H_{31}$; 63%

Scheme 18: Syntheses of ascorbic acid based amphiphiles **44-49**.

For this, a DMF solution of ascorbic acid (5 eq) was treated with *O*-acylated hydroxy-carboxylic acid anhydrides (1 eq) in the presence of pyridine (1 eq) which acts as catalyst. The reaction is regioselective and the formation of the 6-*O*-acylated esters was confirmed by

comparing the chemical shifts (ppm) of the C-6 carbons in the ^{13}C NMR spectrum of the products in comparison to *L*-ascorbic acid. Only the primary hydroxy group is esterified, all the other hydroxy groups are still available for the formation of hydrogen bonds, for complex formation or for redox functions.

3.7.1.1 NMR characterisation of 44-49

In Figure 51 the ^{1}H NMR spectrum of **47** is shown, exemplifying this group of compounds**.** The ^{1}H NMR spectrum displays the characteristic signals of the lauroyl residue at δ = 2.51 – 2.28 (m, 4H), 1.72 – 1.56 (m, 4H), 1.51 – 1.13 (m, 32H), 0.90 (t, *J* = 7.0 Hz, 6H) ppm.

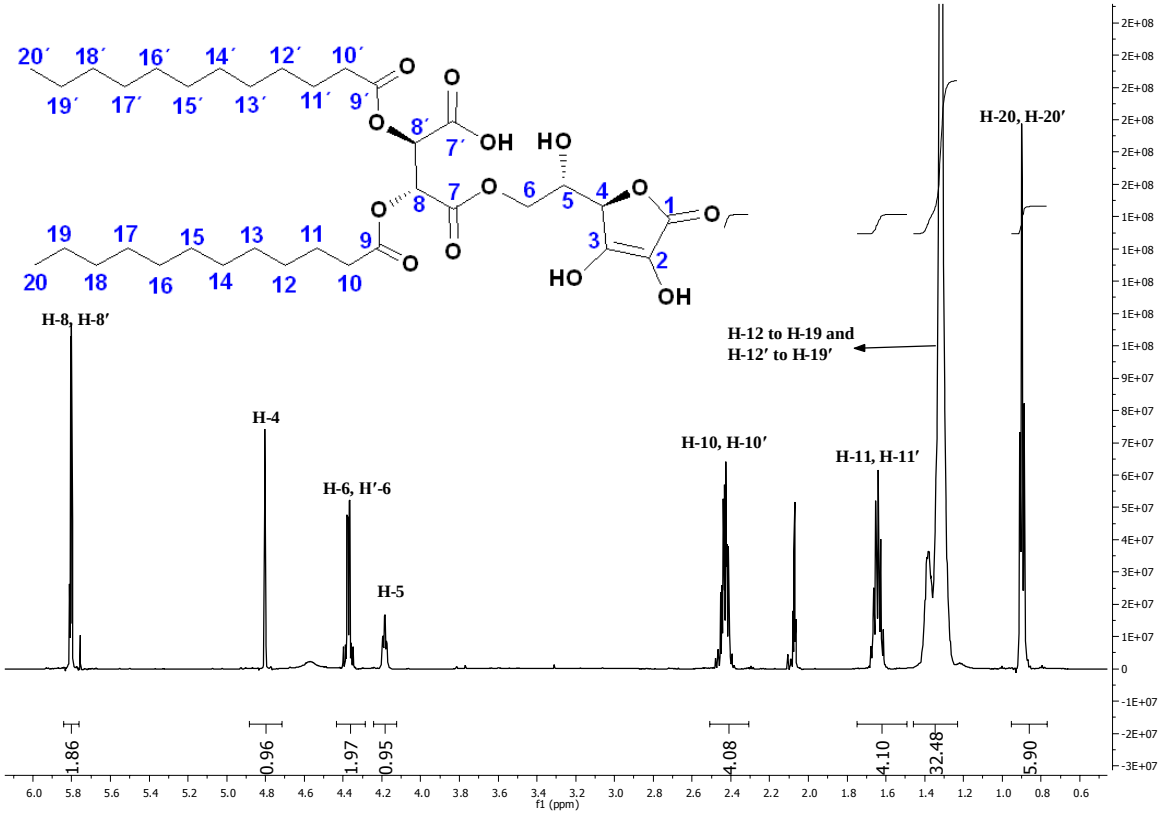

Figure 51: ^{1}H NMR spectrum of **47** in acetone-d_6.

The signals with chemical shifts in the range of 4.80–4.18 ppm are characteristic for the ascorbic acid unit and the assignments of all proton signals are summarised in Figure 51. Protons with the chemical shift of δ = 5.80 (dd, *J* = 5.9, 2.9 Hz, 2H) ppm are the H-8 and H-8′ protons of the tartaric acid moiety.

In Figure 52 the ^{13}C NMR spectrum of **47** is shown, exemplifying this group of compounds**.**

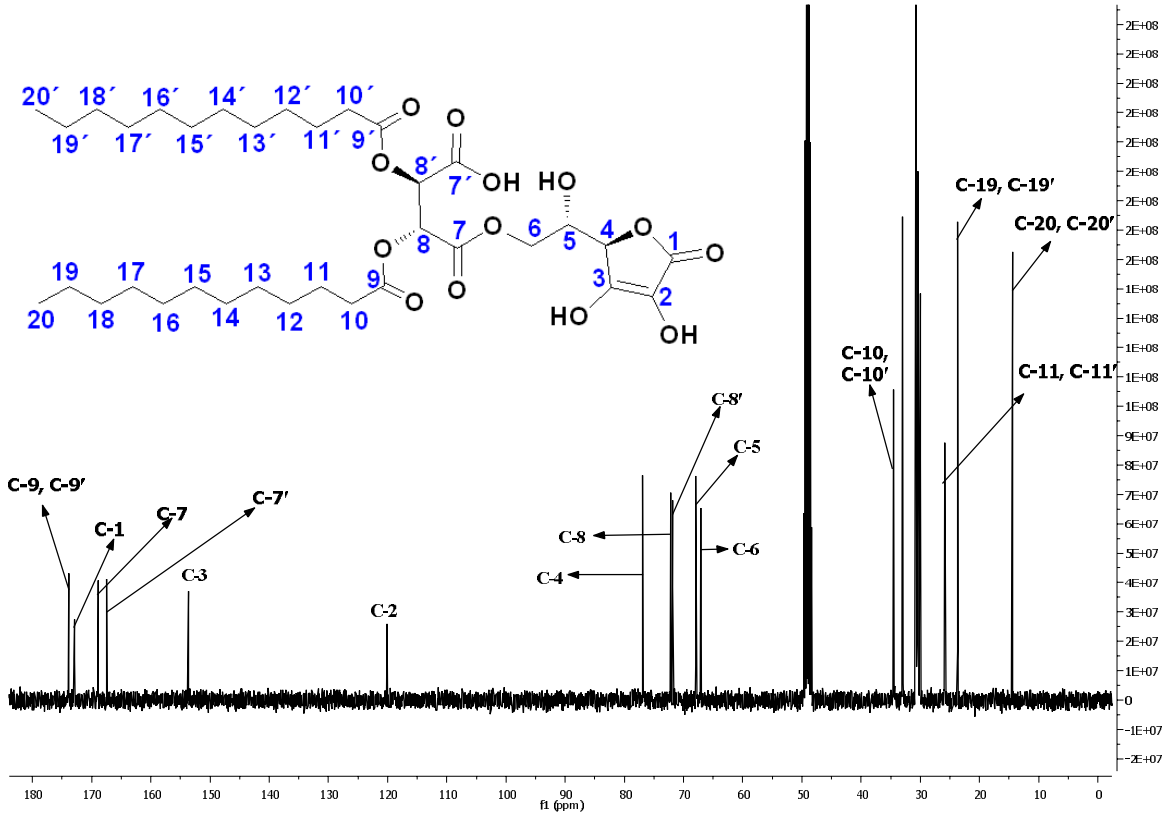

Figure 52: ^{13}C NMR spectrum of **47** in acetone-d_6.

The ^{13}C NMR spectrum shows the characteristic signals of the carbonyl groups at C-9, C-9′, C-1, C-7, C-7′ with chemical shifts of δ = 173.61, 173.38, 168.12, 167.33 ppm, respectively. The characteristic CH signals of tartaric acid unit appear at δ = 72.19, 71.82 ppm. The complete assignments of all carbons of the *L*-ascorbic acid unit of **47** were done based on 2-D NMR (^{1}H-^{1}H COSY, ^{1}H-^{13}C HSQC) as shown in Figure 52.

3.7.2 Gelation properties

3.7.2.1 Gelation abilities of 44-49 in various solvents

The gelation abilities of **44-49** were determined in a variety of solvents by the simple method of being "stable to inversion" of the container.[146] For this, a weighed amount of the corresponding amphiphile (50 mg) was dissolved in 200 µL of an organic solvent or in water and heated in a septum-capped test tube until the solid had dissolved. The resultant mixture was then cooled to room temperature and when the tube could be inverted without any flow, it was determined to be a "*gel*".

compound	**44**	**45**	**46**	**47**	**48**	**49**
Water	TG[a]	G	G	G	G	G
DMF	S	S	S	S	S	S
DMSO	S	S	S	S	S	S
ACN	S	S	AS	S	G	G
Methanol	S	S	S	S	S	S
$CHCl_3$	S	S	PG	S	S	PG
CCl_4	G	TG[a]	PG	PG	G	G
Benzene	S	S	PG	S	G	PG
Toluene	TG	S	PG	S	G	G

G: gel; S: soluble; PG: partially gel; TG: transparent gel; AS: amorphous solid.
[a] at + 5 °C.

Table 21: Gelation abilities of **44**-**49** in different solvents.

The minimum gelation concentration (MGC) in water was determined by adding more water in 50 µL portions. Amphiphiles **46**, **48** and **49** showed excellent gelation abilities in a broad range of solvents (Table 21). Gel-to-solution phase transition temperature for all hydrogels (10%, w/v) was determined using DSC and the DSC thermograms are shown in Figure 53.

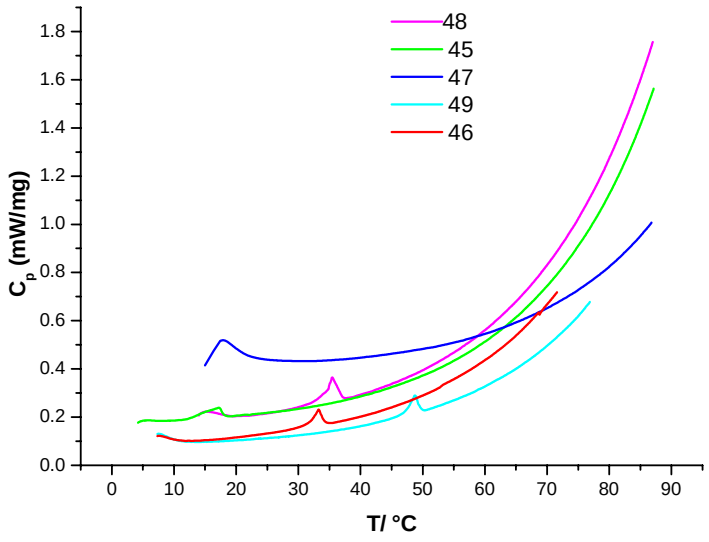

Figure 53: DSC thermographs of the hydrogels derived from **45-49 (**temperature range 10-90 °C).

Solution-to-gel phase transition temperatures and the minimum gelation concentrations in water are shown Table 22. In case of ascorbic acid amphiphiles derived from both *O*-acylated tartaric and malic acid anhydrides it was found that the gelation abilities and gel stabilities in water are highly influenced by the length of the hydrocarbon chains. **46**, **48** and **49** produce

very stable hydrogels at room temperature with minimum gelation concentrations of 0.9%, 4.5% and 1.7% (w/v), respectively.

compound	MGC[a] (minimum gelation concentration, w/v).	T[b]gel
44	10%	5 °C
45	5.2%	17 °C
46	0.9%	33 °C
47	10.4%	18 °C
48	4.5%	36 °C
49	1.7%	49 °C

[a] For **44**, **45** determined at + 5 °C.
[b] For **44** determined by inversion tube method.

Table 22: Minimum gelation concentrations (MGCs) and T_{gel}s values of **44-49** in water.

In contrast, tartaric and malic acid based amphiphiles with shorter hydrocarbon chain (C_{12}) produce stable hydrogels only below room temperature (Figure 54). This might be attributed to structural differences in the self-complementary assembly indicating more significant crystalline packing[147,148] for both tartaric and malic acid amphiphiles with long fatty acid chains as compared to those with shorter chains. Increasing the chain length for both the tartaric and malic acid based amphiphiles promotes more association among the fibers through van der Waals forces of attraction and drives the molecules to arrange in highly ordered layered structures. These ambidextrous gelation properties can possibly be utilized to develop hybrid materials with desired properties in a variety of solvents as well as in water.

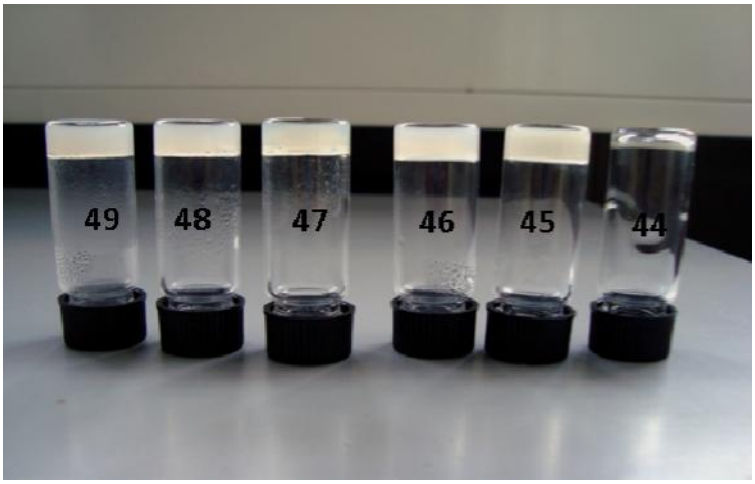

Figure 54: Images of the hydrogels derived from **44-49** (10%, w/v).

3.7.2.2 Morphology of the hydrogels

In order to obtain visual insights into the morphology of the hydrogels SEM measurements of **49** were performed.

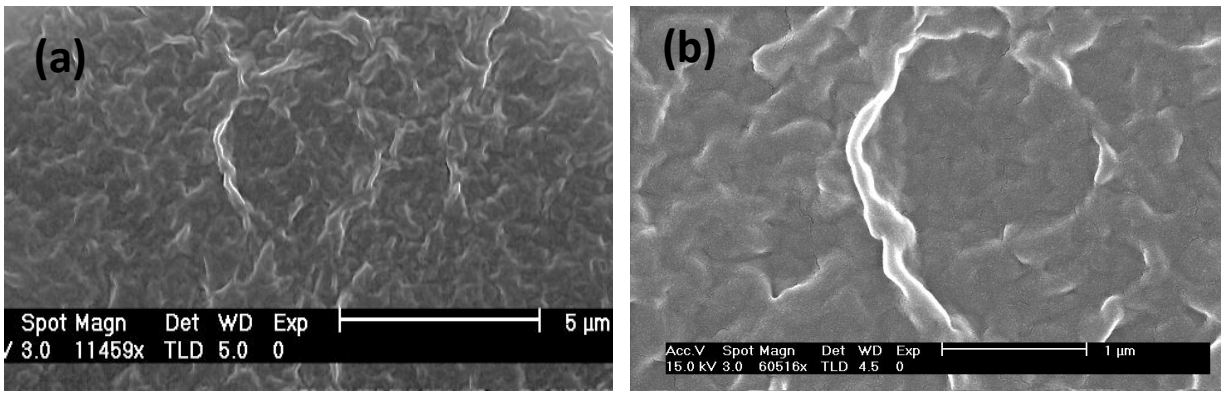

Figure 55: (**a**) SEM image of a xerogel of **49** obtained from water. Scale bar, 5 µm, (**b**) SEM image of the xerogel of compound **49** obtained from water. Scale bar, 1 µm.

The SEM micrographs of the xerogel obtained from 1.7% hydrogel of **49** are shown in Figure 55. The SEM images revealed that the hydrogel of **49** could self-assemble into a three dimensional network structure composed of numerous fibrillar aggregates with 125-300 nm in diameter and several micrometers in length, which were entangled with each other to produce a 3-D network structure.

3.7.2.3 Driving forces leading to the formation of hydrogels

3.7.2.3.1 IR spectroscopic studies

In order to investigate the driving force leading to the formation of a hydrogel, ATR-IR investigations were performed taking again **47**.

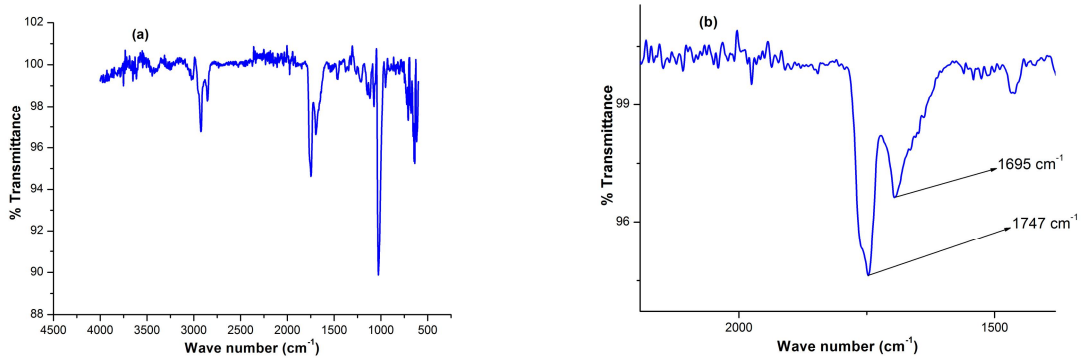

Figure 56: (**a**) FT-IR spectrum of **47** in DMSO; (**b**) expanded region of the FT-IR spectrum of **47** in DMSO.

In DMSO solution the band appearing at 1747 cm^{-1} can be assigned to the stretching vibrations of the ester carbonyl groups and non-hydrogen bonded carboxylic acid group (Figure 56) while the xerogel obtained from D_2O the stretching vibrations of a set of carbonyl groups is shifted to 1713 cm^{-1} (Figure 57), strongly supporting the existence of hydrogen bonding between the carbonyl groups in the gel phase. This implies that the hydrogen bond formation is an important driving force for the aggregation of **47** in water.

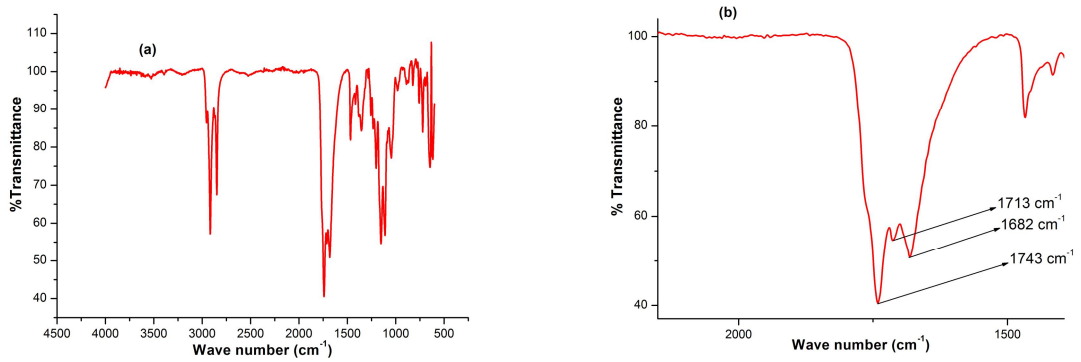

Figure 57: (**a**) FT-IR spectrum of the xerogel obtained from 10% (w/v) hydrogel of compound **47** in D_2O; (**b**) expanded region of the FT-IR spectrum of the xerogel obtained from 10% (w/v) hydrogel of compound **47** in D_2O.

3.7.2.3.2 NMR spectroscopy studies

To gain even more insight into the driving force behind the self-assembly and the orientation of the molecules in the self-assembled state, temperature dependent ^1H NMR measurements of **47** were carried out (Figure 58, Figure 59). In D_2O the gel molecules are organized in a highly rigid network and consequently their signals are broadened and unresolved even at 95 °C. Therefore, the gel sample was prepared in a D_2O/DMSO-d_6 solvent mixture (2.3:1 v/v). With a gradual increase of the temperature from 30 °C to 90 °C the signals for the fatty acid protons were found to be slightly shifted downfield and became sharper as compared to the signals at 30 °C. This indicates that an increase of temperature leads to a disordering of the intermolecular aggregation into the isotopic form.

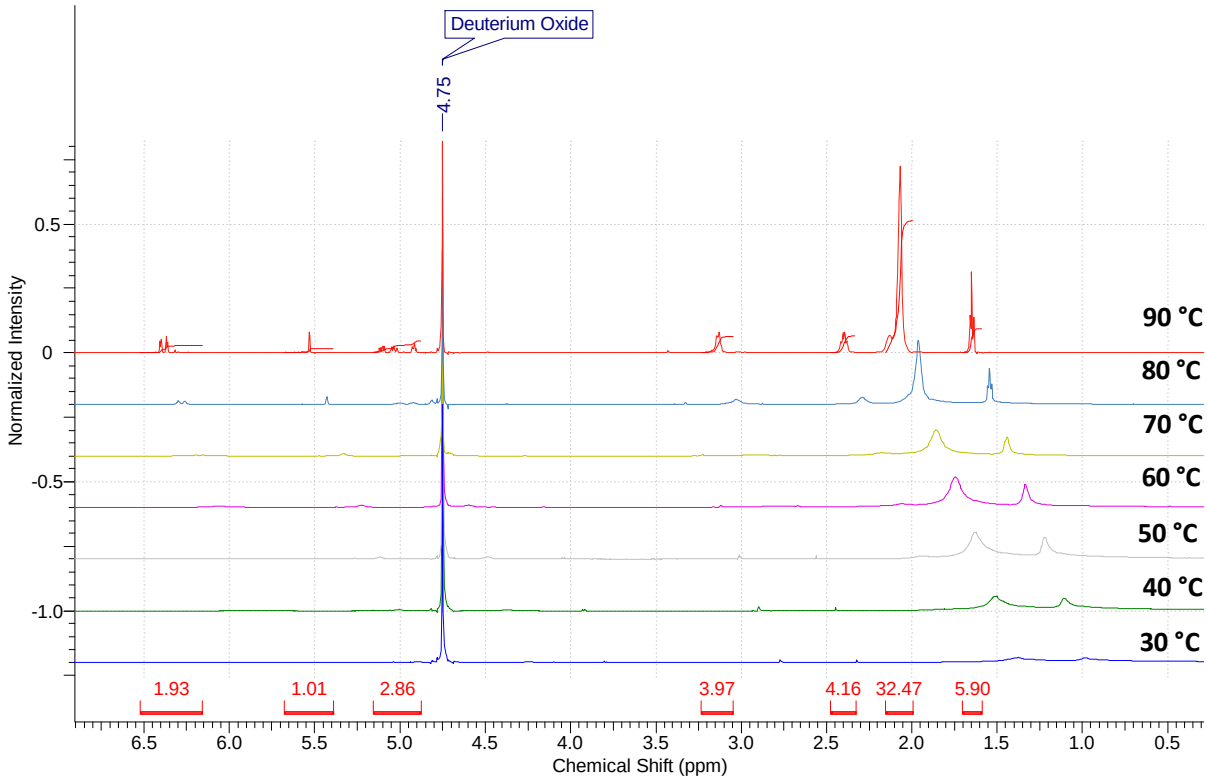

Figure 58: Variable temperature ^{1}H NMR spectra of **47** in a D_2O/DMSO-d_6 solvent mixture (2.3:1 v/v).

In addition, the broadening of the fatty acid proton signals (Figure 59) in the gel phase suggests the existence of van der Waals forces between the carbon chains inside the gel network. These results imply that both intermolecular hydrogen bonding and van der Waals attraction forces are very crucial and act synergistically to stabilize the self-assembled structure.

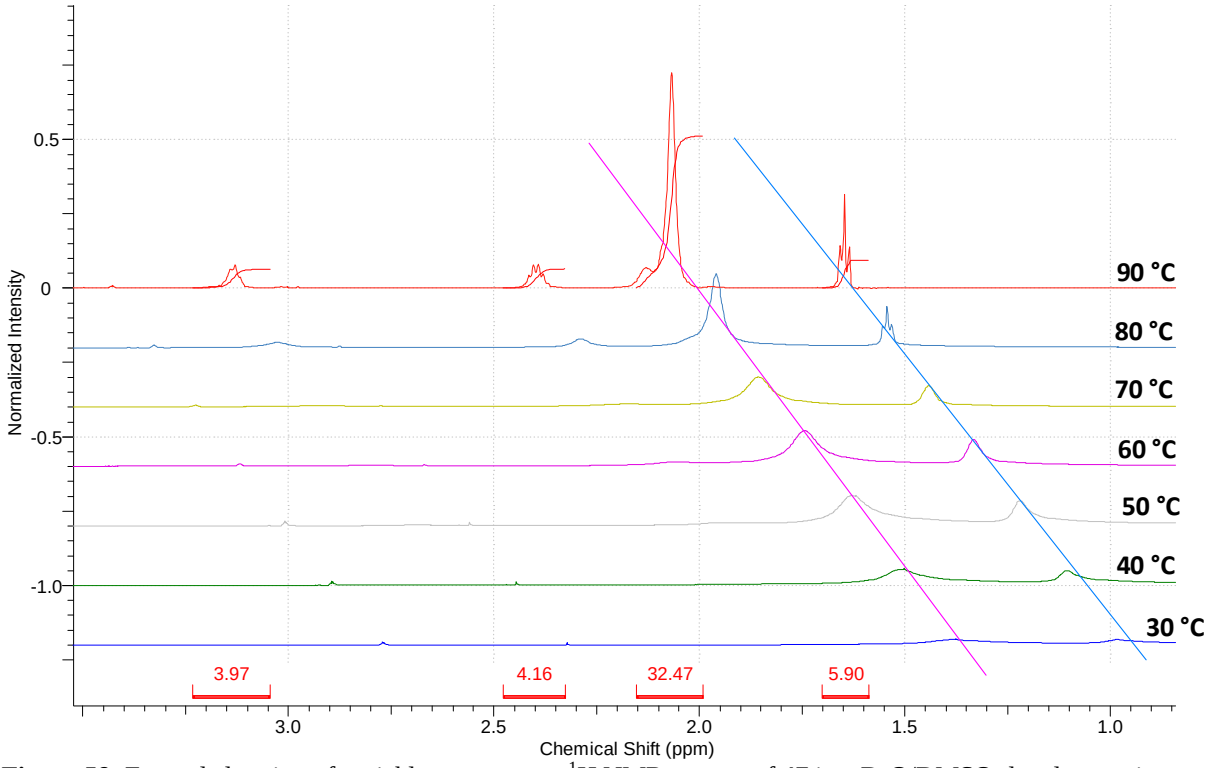

Figure 59: Expanded region of variable temperature ^{1}H NMR spectra of **47** in a D_2O/DMSO-d_6 solvent mixture (2.3:1 v/v).

3.7.3 Active oxygen species and scavenging action of ascorbic acid

Free radicals or more general active oxygen species are mainly responsible to increase the chance for a variety of diseases in the human body and also the aging phenomena. The mechanism of damage which radicals cause on bio-molecules, such as unsaturated lipids and nucleic acids is well established. However deeper studies are still needed in order to estimate and reveal completely the relationship between radicals and various pathologies. Aerobial life needs oxygen for mitochondrial oxidation during metabolism but at the same times O_2 is the origin of the so-called "active oxygen species" (AOS), such as superoxide, $^{\bullet}$OH, $^{\bullet}$OOH, etc. All these chemical species participate in the development or exacerbation of various pathologies, such as the Alzheimer's disease, ischemia-reperfusion disturbances in the brain and heart, rheumatism, inflammatory disorders, gastric ulcer, and cancer. For example hydroxy radicals can damage the cell membrane by a process known as "lipid peroxidation" which is basically a radical chain reaction. After initiation it propagates rapidly and causes significant damage of the lipid molecules. It can also cause disruption of proteins and hence interrupt enzyme activity. Oxidative damage to DNA can also occur at a high rate under normal metabolic conditions.

Ascorbic acid is a naturally occurring antioxidant and can thus scavenge active oxygen species before they cause damage to biological molecules or prevent oxidative damage by interrupting the radical chain reaction of lipid peroxidation.

3.7.3.1 Antioxidant efficiencies of 44–49

The first question to be addressed: will a lipid modified ascorbic acid retain its radical scavenging activity so that these amphiphiles might be useful for the stabilisation of native fats and oils against aerial oxidation. Vitamin E is largely used to stabilise food in lipophilic media. However the highest intake of vitamin E might create some problem. High intake of vitamin E from diet or supplements might increase the risk of dying at any cost[149] including heart disease. Numerous methods have been described in the literature to determine the antioxidant efficiency of an antioxidant. The antioxidant activities of **44-49** were determined based on the DPPH radical. [150] It is a stable radical which displays a violet colour in solution with a characteristic molar absorption maximum at 517 nm (Figure 60).

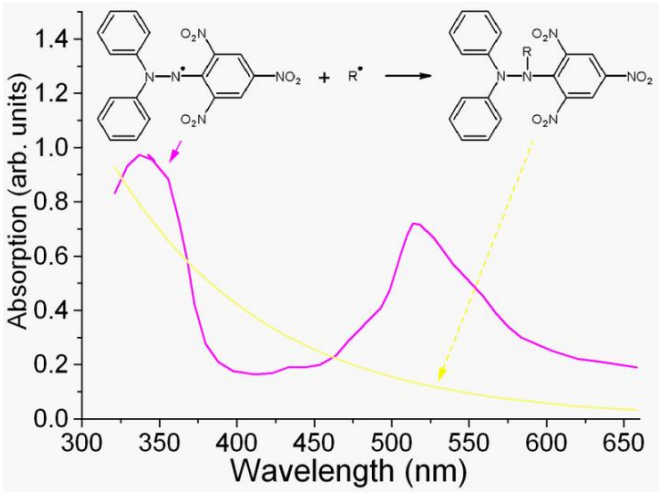

Figure 60: UV-visible absorption spectrum of the DPPH radical (pink) and after trapping one radical (yellow).

Thus one can evaluate the antioxidant efficiency of an antioxidant by following the decrease in absorption of DPPH radical at 517 nm with gradual increase in concentration of an antioxidant (Scheme 19).

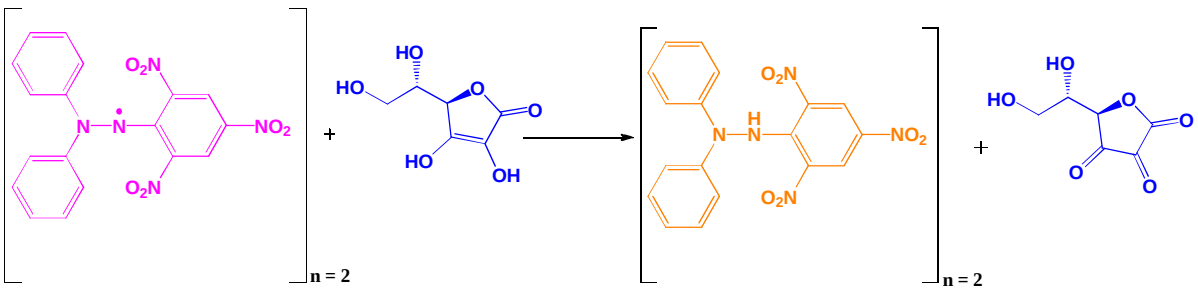

Scheme 19: Trapping of a DPPH radical by ascorbic acid.

3.7.3.1.1 Determination the antioxidant activities of 44-49

The antioxidant activities of **44-49** were determined using the stable free radical DPPH (*α*-*α*-biphenyl-*β*-picrylhydrazyl-radical) according to a slightly modified method as described in the literature.[150]

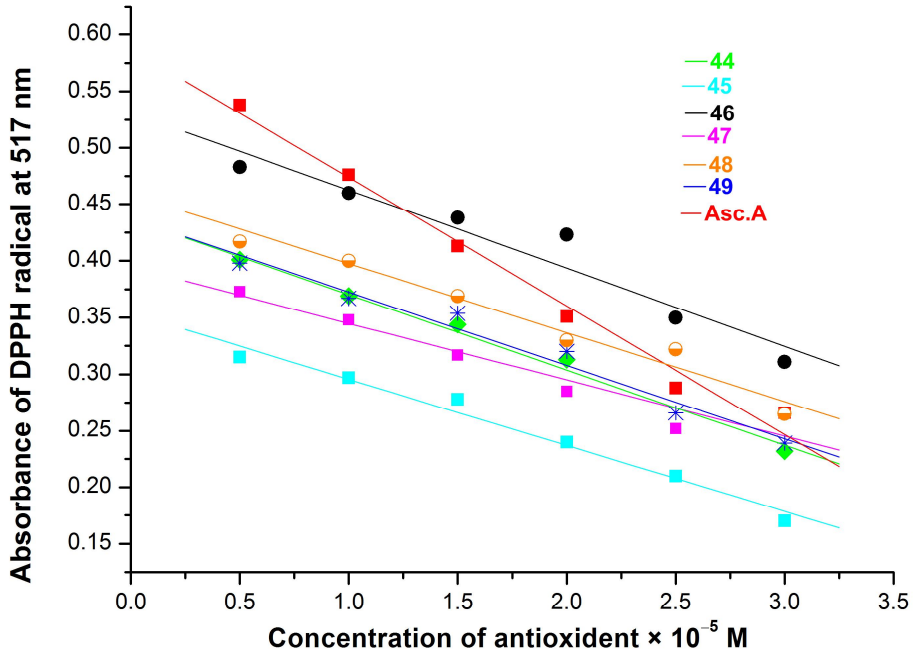

Figure 61: Decolourisation of DPPH-radical (at 517 nm) after addition of various concentrations of antioxidants.

The measured antioxidant activities of **44-49** have been interpreted by comparing their "efficient concentration" or EC_{50} values (concentration of antioxidant which causes 50% loss of the DPPH radical activity). For this 3000 µL portions of the reaction mixture containing 2000 µL DPPH solution (approximately 60-100 µM in methanol) and 1000 µL of **44-49** at different concentrations were incubated at room temperature for 30 min and the absorbance of the test sample was determined at 517 nm using a UV-visible spectrophotometer. The antioxidant activity towards the DPPH radical was determined from the difference in absorbance with and without addition of the corresponding amphiphile. The antioxidant efficiencies of the amphiphiles are shown[151] in Figure 61 and the results from Figure 61 are summarized in Table 23.

antioxidant[a]	$EC_{50}(10^{-5}$ M)	n_{DPPH}
44	3.28 ± 0.01	2
45	3.03 ± 0.01	2
46	3.86 ± 0.02	2
47	3.33 ± 0.00	2
48	3.84 ± 0.01	2
49	3.38 ± 0.01	2
Asc.A	2.59 ± 0.01	2

[a] n_{DPPH} = the number of DPPH radicals reduced by one molecule of antioxidant. Asc.A = ascorbic acid. EC_{50} = concentration of antioxidant that causes 50% loss of the DPPH radical activity. Each value is the average ± S.D of 6 measurements.

Table 23: Antioxidant efficiencies (EC_{50} values) of **44-49** and ascorbic acid.

The antioxidant efficiencies (EC_{50} values) of the above amphiphiles are comparable to ascorbic acid which implies that the lipid modification does not interfere with the radical scavenging properties. Although the hydroxy group at the C-6 seems to have little inhibitory effect towards the reducing activity there is a slight difference in activities between ascorbic acid and these esters as has been also observed[150e–g,152] by other groups. This aspect warrants further studies. Due to the fatty acid residues, their solubilities in hydrophobic environments are clearly increased and hence these amphiphiles could be useful as stabilizers in food related lipophilic media such as native oils.[152]

3.7.4 Foaming and emulsifying properties of 44-49

Last but not least, **44-49** are also interesting surfactants which display good foaming and emulsifying properties. As expected, the foaming and emulsifying properties of these amphiphiles are again strongly influenced by the hydrocarbon chains length (Table 24). By increasing the chain length, their solubility in water is decreased which has an impact on their foaming abilities. Foaming ability of both the malic and tartaric based amphiphiles with shorter chains (C_{12}) is much higher than the corresponding compounds with longer chains (C_{14} and C_{16}). Within this series of amphiphiles **44** is the best foaming agent which is a consequence of its high HLB value (Hydrophilic-Lipophilic-Balance), whereas **49** showed the lowest foaming ability, also corresponding to its low HLB value. **45-48** display HLB values in the range of 8-13 and hence they may be useful for the preparation of O/W emulsions in *e.g.* food industry.

compound[a]	foaming ability (mL)	foam stability (mL)	HLB values
44	719	718	>18
45	528	521	12
46	421	418	8-13
47	700	696	9-10
48	209	206	8-10
49	59	53	3-5
SDS	765	720	-

[a] For the determination of the foaming properties potassium salts have been used.

Table 24: Foaming and emulsifying properties of **44**-**49** in water.

3.7.5 Antimicrobial activities of 44-49 against several microorganisms

The above synthesized amphiphiles **44**-**49** were tested regarding their activities against a series of bacteria (Gram negative: *Pseudomonas putida mt2*, *Escherichia coli*, *Enterobacter aeruginosa*; Gram positive: *Staphylococcus aureus*; *Micrococcus luteus*, and eukaryotic species such as fungi (*Aspergillus niger*, *Candida albicans*).

substance	*Ps. Putida mt2*	*E. coli*	*Enterobacter aer.*	*S. aureus*	*M. luteus*	*Asp. niger*	*Ca. albicans*
44	++	-	++	-	++	-	+++
45	-	++	+++	+	+++	-	++
46	-	(+)	+	(+)	(+)	-	++
47	++	++	++	++	+	-	+
48	-	-	-	-	(+)	-	(+)
49	(+)	-	-	-	-	-	+

- = No spot; (+) = overgrown spot; + = spot with colonies; ++ = spot with only a few colonies; +++ = clear spot without colonies.

Table 25: Antimicrobial properties of the amphiphiles **44**–**49** (inhibition zones).

Amphiphiles **44**, **45** and **47** showed excellent activities against a variety of the above microorganisms, particularly against *Enterobacter aeruginosa* and to some extent against *Micrococcus luteus*, *Candida albicans*. Malic and tartaric acid based amphiphiles with C_{12} hydrocarbon chain have higher activities against microorganisms while the activities are more or less decreasing with increasing hydrocarbon chain length.

3.7.6 Nano particles of noble metals

Nano particles derived from noble metals have received much interest in the past decades on account of their enormous potential and applications in the vast field of optical, biomedical and electronic application.[153] Nano particles are microscopic particles with dimensions of less than 100 nm. Especially gold and silver nano particles by the virtue of being inert and highly biocompatible have received major attention because of their unusual chemical, electronic and optical properties.[153,154] These properties make them useful in biotechnology and biomedicine, all the way from protein and DNA detection to cancer therapy and drug delivery.[154] The amendable size– and shape–dependent properties of the metal nano particle are completely contrary to the properties of the same material in bulk (whereas the physical properties are almost remaining constant regardless to the size of the bulk material). Due to the high surface to volume ratio of metal nano particles which cause confinement of the electrons at the metal surface and therefore exhibit tuneable optical, electron and magnetic properties depending on their size and electron population on the metal surface. Such size-dependant properties leading to surface plasmon resonance in some metal particles and superparamagnetism in magnetic materials.

3.7.6.1 Gold nano particles

Numerous studies have been aimed towards the development of versatile method for the synthesis of gold nano particle with the goal to generate these in a controllable and reproducible size and shape distribution.[154] The most conventional synthesis of gold nano particles (GNPs) was introduced already by *J. Turkevitch et al*. in 1951, the reduction of chloroauric acid by sodium citrate at elevated temperature.[155] Sodium citrate not only acts as a reducing agent for Au (III) to Au (0) but also it is a stabiliser for the naked gold nano particles by preventing their aggregation. The negatively charged citrate ions are strongly adsorbed on the gold metal surface and serve as a repellent to prevent them from aggregation and growth.[156]

Another popular method for the synthesis of gold nano particle in water is the reduction of chloroauric acid by sodium borohydride in the presence of thiol or amine as steric stabiliser.[154,155,156]

However, the above reaction conditions are questionable regarding applications in physiological systems and these make chemically synthesised gold nano particles unsuitable for applications in biological environments.[154]

Therefore one group had the idea to synthesise gold nano particles for physiological applications by means of a two-step procedure. [153]The first step was the *in situ* reduction of

Au (III) to Au (0) by means of sodium tartrate, ascorbic acid or reducing amino acids followed by treatment of the naked gold particles by a variety of reagents such as polyethylene glycol, poly vinyl alcohol, polyvinyl pyrolidone and surface active agents such as sodium dodecyl sulphate, Tween 80, triton and carbohydrates like chitosan which are capable of stabilising gold nano particles.[153]

In this work the gold nano particles were synthesized without any external reducing or capping agent. Ascorbic acid is well known for its capability to reduce metal salts such as chloroauric acid for the synthesis of gold nano particles in solution. As described above (in section 3.7.2.2) we have found that 6-*O*-acylated fatty acid esters of ascorbic acid form highly ordered self-assembled 3-D supramolecular network structures consisting of numerous fibers. Thus we made an effort to combine these two properties in order to acquire the *in situ* synthesis of gold nano particles. The major advantage of this method is the possibility for a selective tailoring of the surface chemical properties of metal nano particles.[156] The gold nano particles are embedded into the hydrogel of self-assembled nano fibers and form a well-ordered, tightly bound film on the gold particle surface thus capping them and preventing their aggregation.

3.7.6.1.1 Preparation of gold nano particles

For the *in situ* synthesis of gold nano particles a weighed amount (0.025 g) of **49** was placed in a septum capped test tube and then 500 µL water were added. The mixture was slowly heated up to 50 °C in an oil bath to dissolve all solid. After complete dissolution the test tube was then cooled to room temperature leading to gelation (Figure 62).

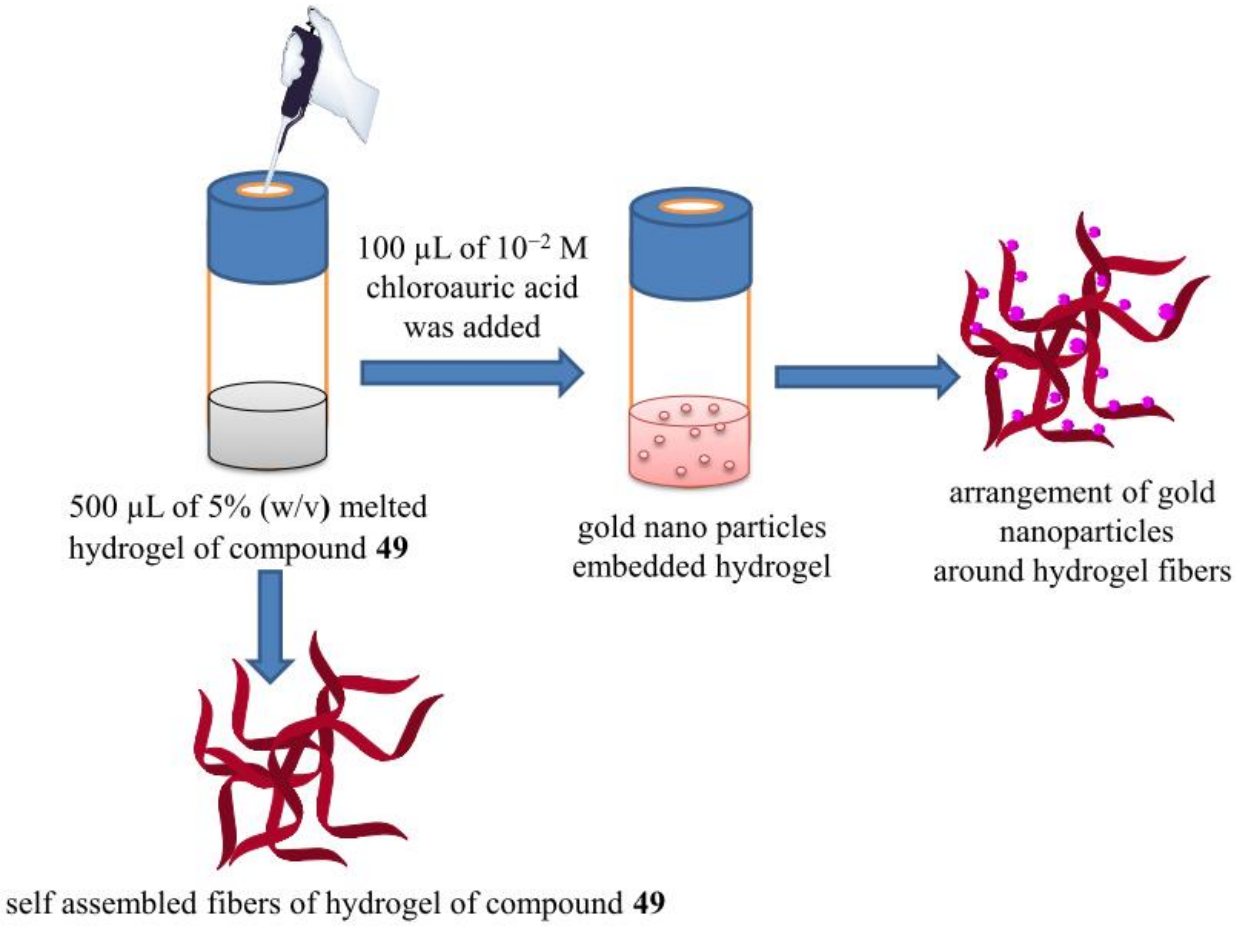

Figure 62: Synthesis of gold nanoparticles and arrangement of gold nano-particles around fibers (schematic).

The process was repeated twice in order to obtain homogeneous hydrogel. Then the gel was melted again at 50 °C and 100 µL of a 10^{-3} M chloroauric acid in water was added under vigorous stirring of the melted hydrogel with a glass rod for a few seconds. The formation of the gold nano particles was confirmed by visual colour change of the solution from light yellow to pink within few seconds (Figure 63). Such change in colour is indicative for the change of oxidation state from Au (III) to Au (0) and for the formation of gold nano particles. After addition of the chloroauric acid the melted gel was immediately cooled to room temperature in order to revert the formation of gold nano particles embedded in the hydrogel.

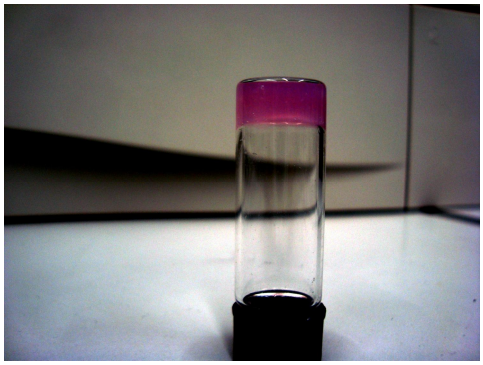

Figure 63 : Gold nano particle embedded in the hydrogel of **49**.

3.7.6.1.2 Characterisation of the gold nano particles

3.7.6.1.2.1 UV–visible spectroscopy studies

UV–visible absorption spectrum was used to monitor surface emission plasmon resonance of gold nano particles embedded in the hydrogel. For this, the GNPs embedded hydrogel was freeze dried and dissolved in acetonitrile[157] and then immediately subjected to UV–visible spectroscopy studies (Figure 64).

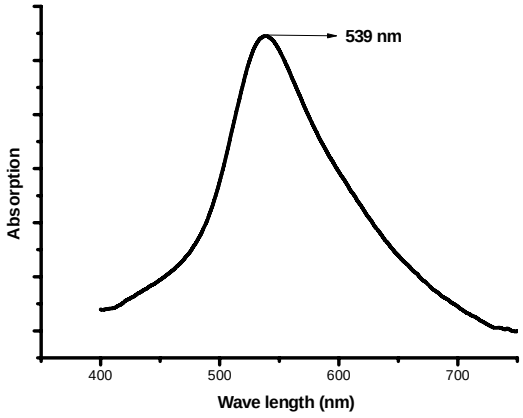

Figure 64: UV-visible spectrum of gold nano particles.

The absorption maximum at 539 nm corresponds to the surface emission plasmon resonance of gold particles having nanoscale dimensions.[157]

3.7.6.1.2.2 Scanning electron microscopic studies

In order to reveal the size distribution and morphology of the gold nano particles SEM measurements were carried out.

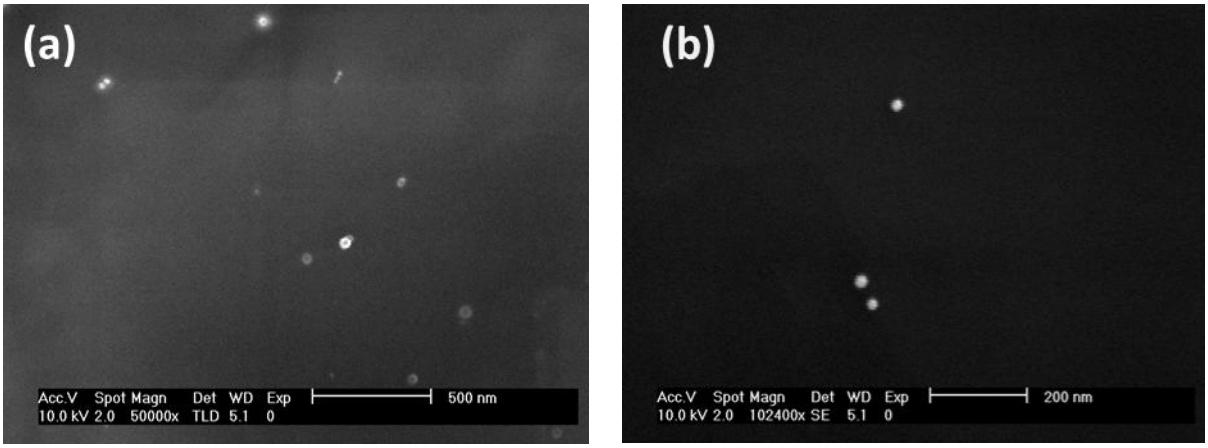

Figure 65: Scanning electron microscopy image of gold nano particles embedded in the hydrogel of **49** under different magnifications (**a**–**b**).

The SEM images revealed that gold nano particle have spherical shape with uniform size distribution in the range of ~25-40 nm (Figure 65).

3.7.6.2 Silver nano particles

3.7.6.2.1 Potential of silver NPs against microorganism

Silver nano particle have received much attention in recent years because they display size dependent optical properties, thereby suggesting the possibility of tuning them. Ag NPs exhibit localised surface plasmon resonance which highly depends upon their sizes, shapes and the surrounding environment.[158] These unique optical properties enable Ag NPs to serve as photo-stable and ultrasensitive optical probes and sensors for detection of single molecules and their binding kinetics, imaging of single receptors on single living cells, and probing fluid dynamics of single embryos in real time at nm scale.[159] Besides their amendable optical properties silver nano particles has also received considerable attention because of their enormous potential against several microorganism including *Escherichia coli* and *Staphylococcus aureus*.[160] Their activities against bacteria are strongly depending on their size. With a decrease in size their activity against microorganisms is higher due to their large surface to volume ratio.[160] They are completely unique as compared to common antibacterial substances to which microorganism can become resistant.[161] In contrast, as silver NPs have nanoscale dimensions and hence they can easily penetrate through the cell wall, rupture, and destroy the physical structure of the cell wall resulting in the destruction of the microorganism.[161] Irrespective of the fact that silver NPs are well known for their potential activity against several microorganisms, their mechanistic action is still full of controversy and must be studied further.[162]

3.7.6.2.2 Synthesis of silver nano particles

For the *in situ* synthesis of silver nano particles a weighed amount (0.025 g) of **49** was placed in a septum capped test tube to which 500 µL water were added. The mixture was heated slowly at 50 °C in an oil bath to dissolve all solids in water. After that the test tube was cooled to room temperature for gelation. The process was repeated twice in order to obtain a homogeneous hydrogel. Then the gel was melted at 50 °C and 100 µL of a 10^{-2} M silver nitrate solution in water was added under vigorously stirring the hydrogel with a glass rod for few seconds. Formation of silver nano particles was confirmed by the visual change in colour of the solution from colourless to black within a few seconds (Figure 66).

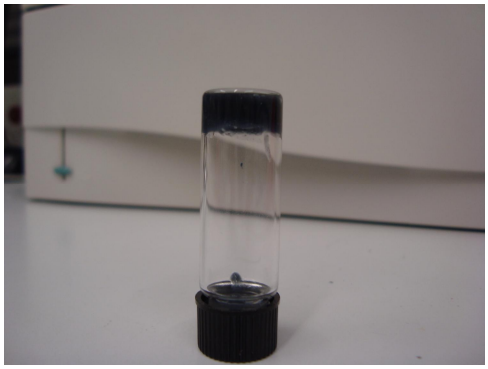

Figure 66: Photographic image of silver nano particles embedded in the hydrogel of **49**.

This change in colour is indicative of (*i*) the change of oxidation state of Ag (I) to Ag (0) and (*ii*) formation of silver nano particles. After addition of silver nitrate to the melted gel, the melted gel was immediately put to room temperature to revert the formation of silver nano particles embedded in the hydrogel.

3.7.6.2.3 Characterisation of the silver nano particles

3.7.6.2.3.1 UV-visible spectroscopic studies

The formation of the silver nano particles was confirmed by UV-visible spectroscopic studies. For the UV-vis. spectroscopic studies the silver nano particle embedded in the hydrogel was freeze dried[157], dissolved in acetonitrile and immediately subjected to UV-visible spectroscopic studies.

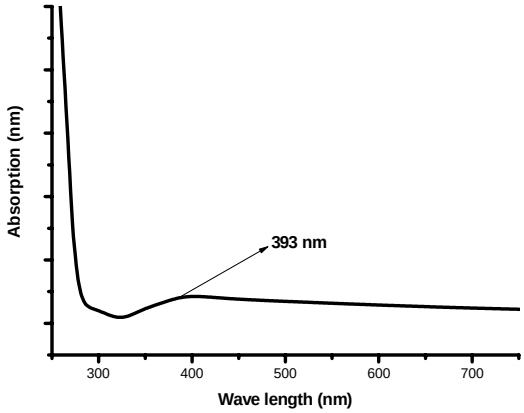

Figure 67: UV-visible absorption spectrum of silver nano particles embedded hydrogel of **49**.

The absorption maximum at 393 nm corresponds to the surface emission plasmon resonance of silver particles of nanoscale dimension. Based on a relevant literature[159] search related to size distribution of the silver nano particles it was found that there is a close relationship between the absorption maximum in the UV-visible spectrum and the corresponding size distribution of the silver nano particles. The absorption maximum at 393 nm corresponds to the surface emission plasmon resonance of silver nano particles having a size distribution of approximately 63 nm.

3.7.6.2.3.2 Scanning electron microscopic studies

In order to obtain a clear visualisation of shape and size distribution of the silver nano particles, scanning electron microscopic measurements have been performed.

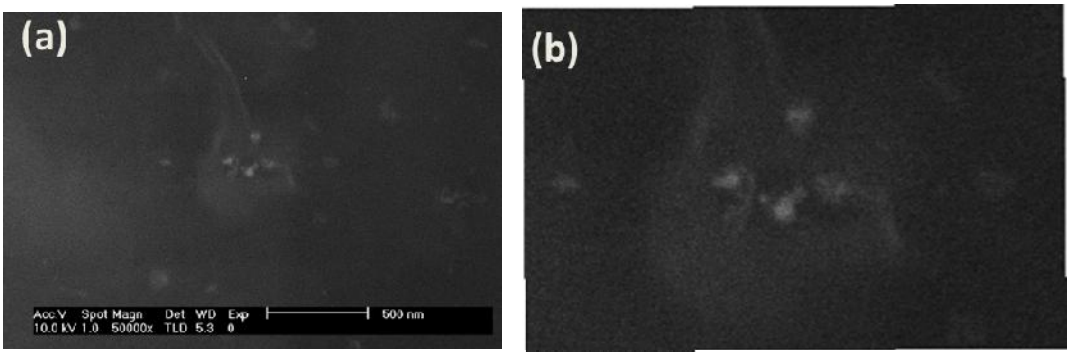

Figure 68: Scanning electron microscopic images of the silver nano particles embedded in the hydrogel of **49** under different magnifications (**a**-**b**). Scale bar, 500 nm.

The scanning electron microscopic image (Figure 68) revealed that the silver nano particles display a size distribution in the range of 60-80 nm.

3.8 Conclusion

In summary, we have synthesised a small library of ascorbic acid amphiphiles largely derived from renewable resources. Some of these amphiphiles display robust gelation abilities in a wide range of solvents and the ambidextrous gelation properties of these amphiphiles may be useful for the development of hybrid materials in a variety of solvents. The thermal stabilities of the gelators in water are strongly affected by the length of the hydrocarbon chains of the lipophilic part of the molecule. This implies that one could regulate the structure and stability of a gel system by tuning the hydrocarbon chains length of the gelator molecules for desired applications. Besides their supramolecular gelation properties we have also determined their antioxidant, foaming and emulsifying properties which may find applications in the fields of food industry and cosmetics.

Besides that we have also provided a suitable synthetic procedure for the *in situ* synthesis of gold and silver nano particles which might have potential biological applications.

3.9 Combination products based on *D*-sorbitol

3.9.1 Regioselective esterification of *D*-sorbitol

D-sorbitol was regioselectively acylated with *O*-acylated hydroxycarboxylic acid anhydrides in the presence of DMF and pyridine according to Scheme 20.

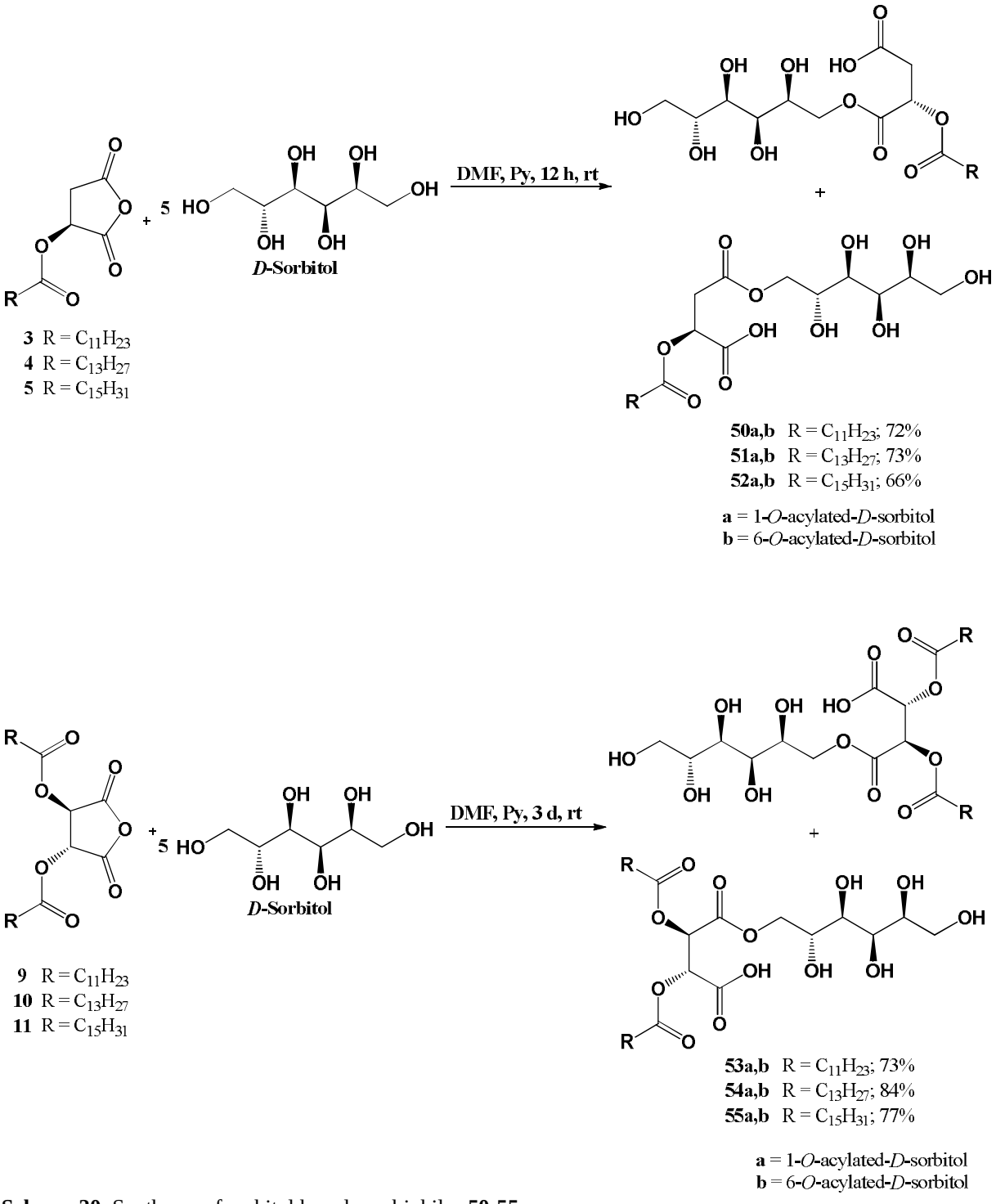

Scheme 20: Syntheses of sorbitol based amphiphiles **50**-**55**.

For this, a DMF solution of *D*-sorbitol (5 eq) was treated with *O*-acylated hydroxycarboxylic acid anhydrides (1 eq) in the presence of pyridine (1 eq). The reaction was continued for 3 d

in case of the tartaric acid anhydrides while in case of the malic acid anhydrides only for 12 h. The products were characterised by ^{1}H and ^{13}C NMR. The formation of the 6-*O* and 1-*O* acylated products was confirmed by the downfield shift of the protons at C-6 and C-1 positions.

3.9.1.1 NMR characterisation of 50a,b–55a,b

In Figure 69 the ^{1}H NMR spectrum of **53a-b** is shown, exemplifying this group of compounds**.** The ^{1}H NMR spectrum reveals the characteristic signals of the lauroyl residue at δ = 2.52 – 2.28 (m, 4H), 1.78 – 1.51 (m, 4H), 1.28 (m, 32H), 1.00 – 0.77 (m, 6H) ppm.

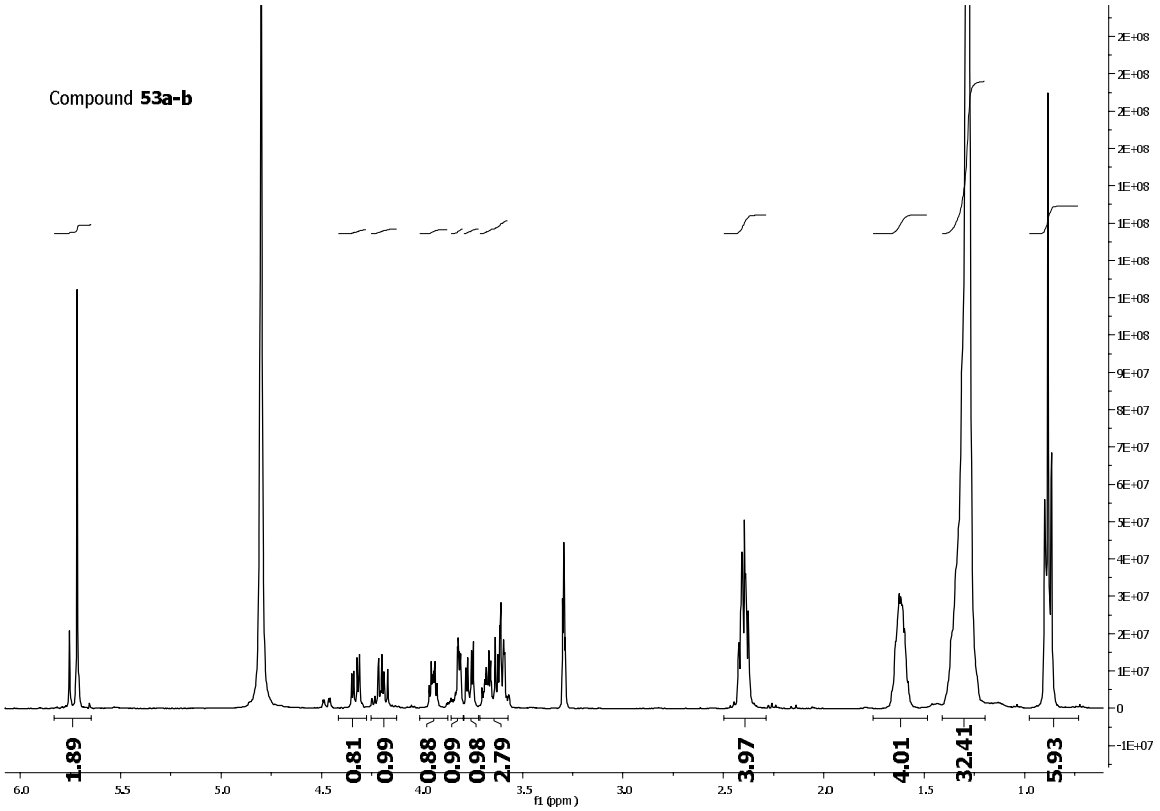

Figure 69: ^{1}H NMR spectrum of **53a-b** in MeOH-d_4.

Signals with chemical shifts in the range of 4.35 –3.51 ppm are characteristic for the *D*-sorbitol moiety. In *D*-sorbitol, the protons at C-1 display chemical shifts at δ = 3.65 – 3.61 (m, 2H) ppm whereas in **53a-b** the protons at the C-1 position are shifted downfield to 4.35 (dd, *J* = 11.3, 4.2 Hz, 1H), 4.21 (dd, *J* = 11.3, 7.0 Hz, 1H) ppm, clearly implying that esterification took place on the hydroxy group at C-6. The protons with chemical shift of δ = 5.74 (d, *J* = 15.2 Hz, 2H) ppm are the CH protons of the tartaric acid moiety.

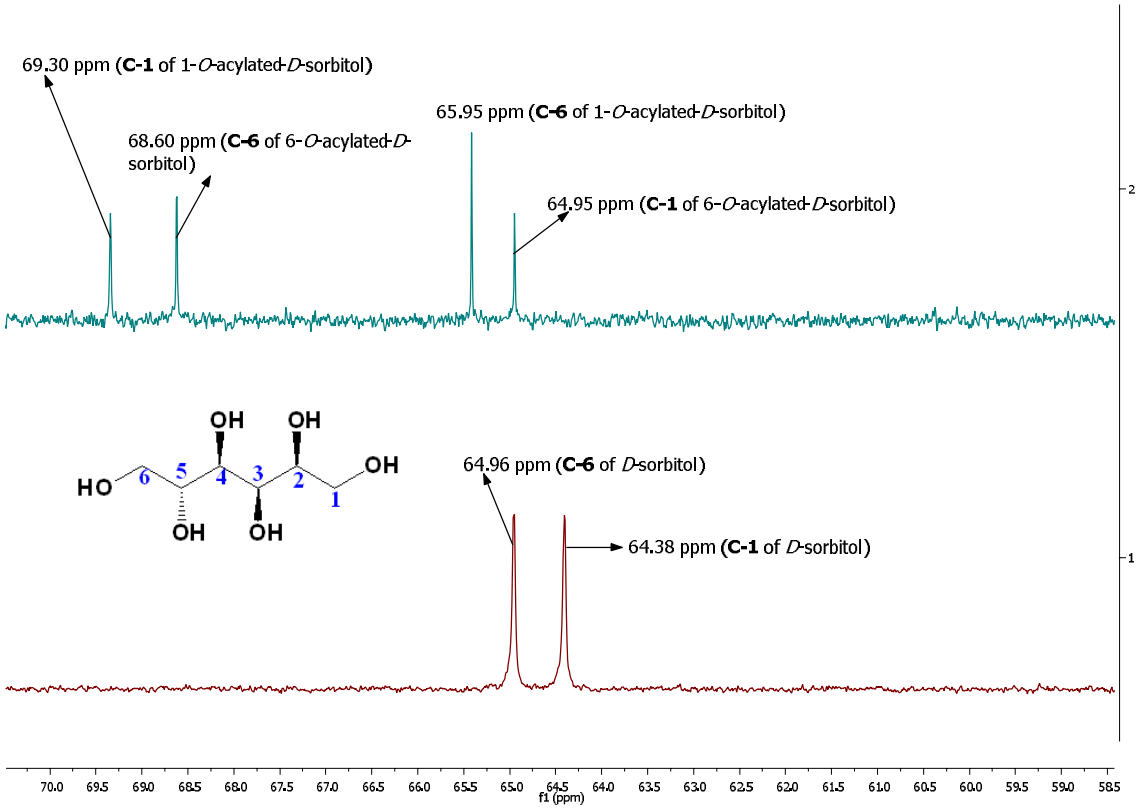

Figure 70: Expanded region of superimposed ^{13}C NMR spectra of *D*-sorbitol and the mixture of fatty acid esters of sorbitol (6-*O* and 1-*O*-acyl-*D*-sorbitol) to demonstrate the downfield shift of C-1 and C-6 of **53a-b**.

In pure *D*-sorbitol C-1 and C-6 display chemical shifts 64.96 and 64.38 ppm, respectively whereas in compound **53a-b** the chemical shifts of the C-1 carbon in 1-*O*-acyl-*D*-sorbitol and the C-6 carbon in 6-*O*-acyl-*D*-sorbitol are shifted downfield to 69.31 and 68.60 ppm, respectively (Figure 70). This clearly indicates that the esterification of sorbitol with *O*-acylated hydroxycarboxylic acid anhydrides took place on hydroxy groups at C-1 and C-6 of *D*-sorbitol.

3.9.2 Gelation properties of 50a,b–55a,b

3.9.2.1 Gelation properties in various solvents

The gelation abilities of **50a,b**-**55a,b** were determined in various solvents by the simple method[163] of being "stable-to-inversion" of the container and the results are summarised in Table 26. For this, a weighed amount of the corresponding sorbitol based amphiphile (25 mg) and the solvent (500 µL) were placed into a septum-capped test tube and heated slowly in an oil bath until the solid was dissolved. The resultant mixture was allowed to cool to room temperature. Gelation is considered to have occurred if the solid aggregate mass was stable to inversion when the sample test tube was turned upside down.

compound	**50a-b**	**51a-b**	**52a-b**	**53a-b**	**54a-b**	**55a-b**
Water	S	G	G	G	G	G
DMF	S	S	S	S	S	S
DMSO	S	S	S	S	S	S
ACN	P	P	P	P	P	p
Methanol	S	S	S	S	S	S
$CHCl_3$	SS	SS	S	P	P	SS
CCl_4	G[a]	G[c]	S	SS	SS	G[c]
Benzene	PG[b]	P	S	S	S	S
Toluene	S	S	S	S	S	G[c]
Hexane	I[d]	I[d]	I[d]	P	PG	G
Acetone	S	S	S	S	S	p

G: gel; S: soluble; I: insoluble; PG: partially gel; AS: amorphous solid, SS: suspended solution. P: precipitation.
[a] Gel at +5 °C but not gel at room temperature.
[b] Partially gel at + 5 °C but not gel at room temperature.
[c] Gel at + 5 °C but partially gel at room temperature.
[d] Insoluble even at the boiling point of the solvent.

Table 26: Gelation abilities of **50a,b**–**55a,b**.

The gel to solution phase transition temperature of the hydrogels derived from **50a,b**–**55a,b** (10%, w/v) was determined using DSC. DSC thermographs of the hydrogels are shown in Figure 71.

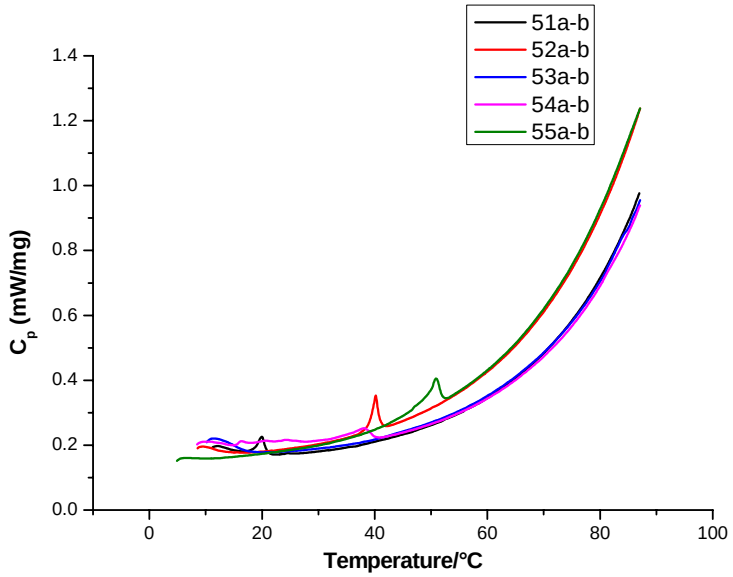

Figure 71: DSC thermographs of the hydrogels derived from **51a,b**–**55a,b** (10%, w/v) in the temperature range of 10–90 °C.

The minimum gelation concentrations (MGCs) of the hydrogels were determined by addition of additional water in 100µL portions until the concentration was insufficient to form a stable gel.

All gels are thermoreversible as they melt when heated above the gelation temperature and reverted to gel again through supramolecular interactions upon cooling. Among the series of tartaric and malic acid based amphiphiles, **55a-b** can gelatinise some nonpolar solvents as well as water, whereas **50a-b**, **51a-b**, **52a-b**, **53a-b** and **54a-b** can gelatinise only a few among the tested solvents in addition to water (Table 26). This implies that the attachment of C_{16} hydrocarbon chains at the tartaric acid unit not only enhances its solubility in organic solvents but also renders more associations among the fibers through van der Waals forces of attraction leading eventually to gel formation.[164] The ambidextrous gelation properties of this amphiphile might be useful for the development of hybrid materials in a variety of solvents as well as in water.[165]

3.9.2.2 Thermal stabilities of the hydrogels–relation to the hydrocarbon chains

Robustness and embodiment of gelation abilities in water can be illustrated by considering three parameters: (i) minimum gelation concentration, (ii) thermal stability of the hydrogel (T_{gel}) (iii) number of water molecules entrapped by one gelator molecule. All three parameters are strongly influenced by the length of hydrocarbon chain in the lipophilic part of the molecule (Table 27).

compound	MGC[a] (minimum gelation concentration, w/v).	Tgel[b]	ımber of water molecule entrapped[c]
50a-b	non-gelator	-	-
51a-b	3.6%	20 °C	~800
52a-b	2.5%	40 °C	~1200
53a-b	3.2%	13-14 °C	~1150
54a-b	3.4%	38 °C	~1200
55a-b	1.7%	51 °C	~2600

[a] For **51a-b, 53a-b** MGCs were determined at +5 °C.
[b] For **53a-b** T_{gel} value was determined by inversion tube method.
[c] For **51a-b, 53a-b** determined at + 5 °C.

Table 27: Minimum gelation concentrations (MGCs) and the thermal stabilities (Tgels) of the hydrogels derived from **50a,b-55a,b.**

The malic acid based amphiphile **52a-b** with a C_{16} hydrocarbon chain produces a very stable hydrogel at room temperature (T_{gel} = 40 °C) with a minimum gelator concentration of 2.5%, (w/v) thus ~1200 water molecules are immobilized by one gelator molecule. In contrast, the corresponding amphiphile with a shorter hydrocarbon chains such as C_{14} produces a stable

hydrogel only at low temperatures (T_{gel} = 20 °C) with a minimum gelator concentration of 3.6%, while compound with a C_{12} hydrocarbon chain is not leading to a gel at all (Figure 72). Similar trends of alkyl chain length dependences of MGCs and T_{gel}s have also been observed in case of the tartaric acid based amphiphiles. This implies that one can regulate the structure and thermal stability of the hydrogel by tuning the length of the hydrocarbon chains for desired and specific applications.[166] The high and low melting points of the hydrogels might be attributed to structural differences in the self-complementary assembly indicating more significant and adequate crystalline packing for amphiphiles with long fatty acid chains as compared to the shorter ones. An increase in chain length promotes more association among the fibers through van der Waals forces of attractions which drive the molecule to arrange in highly ordered, layered structures and hence are contributing to the higher thermal stabilities of the hydrogels.

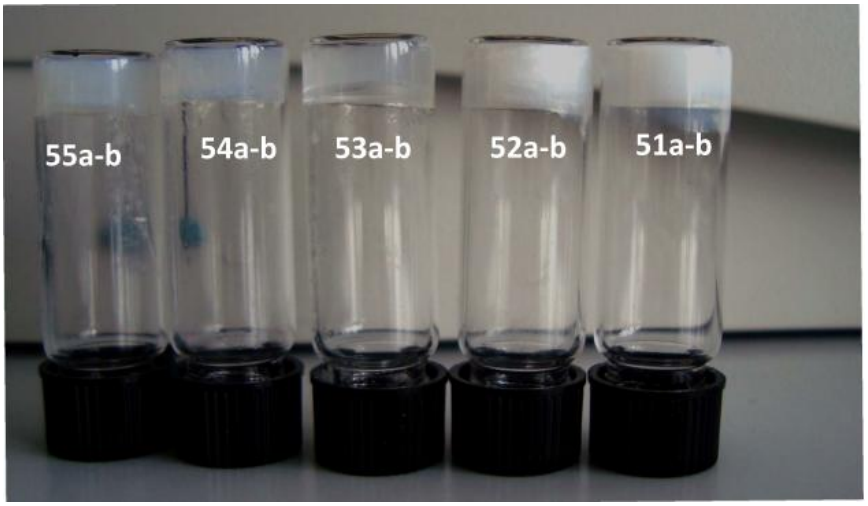

Figure 72: Images of the hydrogels derived from **51a,b**–**55a,b** (10%, w/v).

3.9.3 Driving forces leading to the formation of hydrogels

3.9.3.1 IR spectroscopic studies

In order to investigate the driving force leading to the formation of a hydrogel, ATR-IR investigations were performed taking **55a-b** as an example. In DMSO solution the band appearing at 1745 cm^{-1} can be assigned to the stretching vibrations of the ester carbonyl groups and non-hydrogen bonded carboxylic acid group, whereas in the xerogel obtained from D_2O the stretching vibrations of a set of carbonyl groups is shifted to 1720 cm^{-1}, strongly supporting the existence of hydrogen bonding between the carbonyl groups in the gel phase. This clearly implies that hydrogen bond formation is an important driving force for the aggregation of **55a-b** in water.

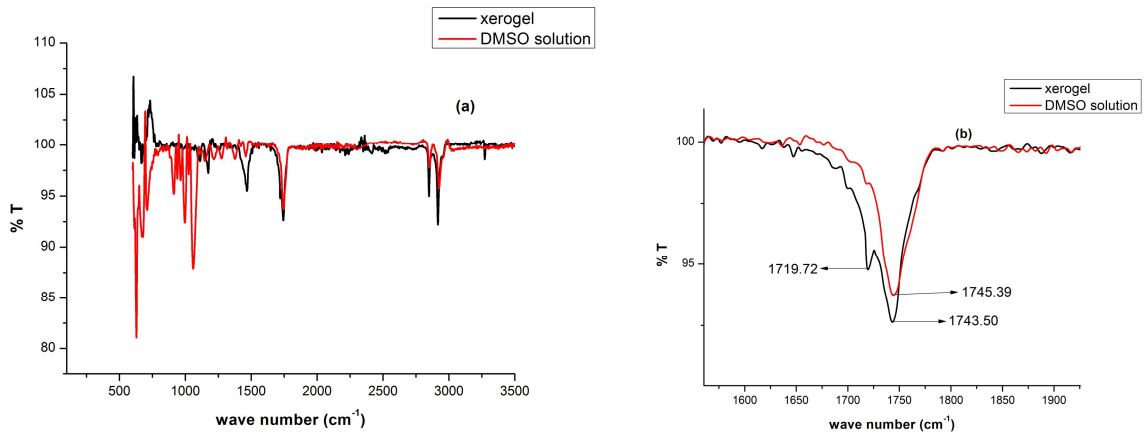

Figure 73: (**a**) Superimposed FT-IR spectra of **55a-b** in DMSO solution and the xerogel obtained from hydrogel; (**b**) expanded region of superimposed FT-IR spectra of **55a-b** in DMSO solution and the xerogel obtained from hydrogel.

3.9.3.2 NMR spectroscopy studies

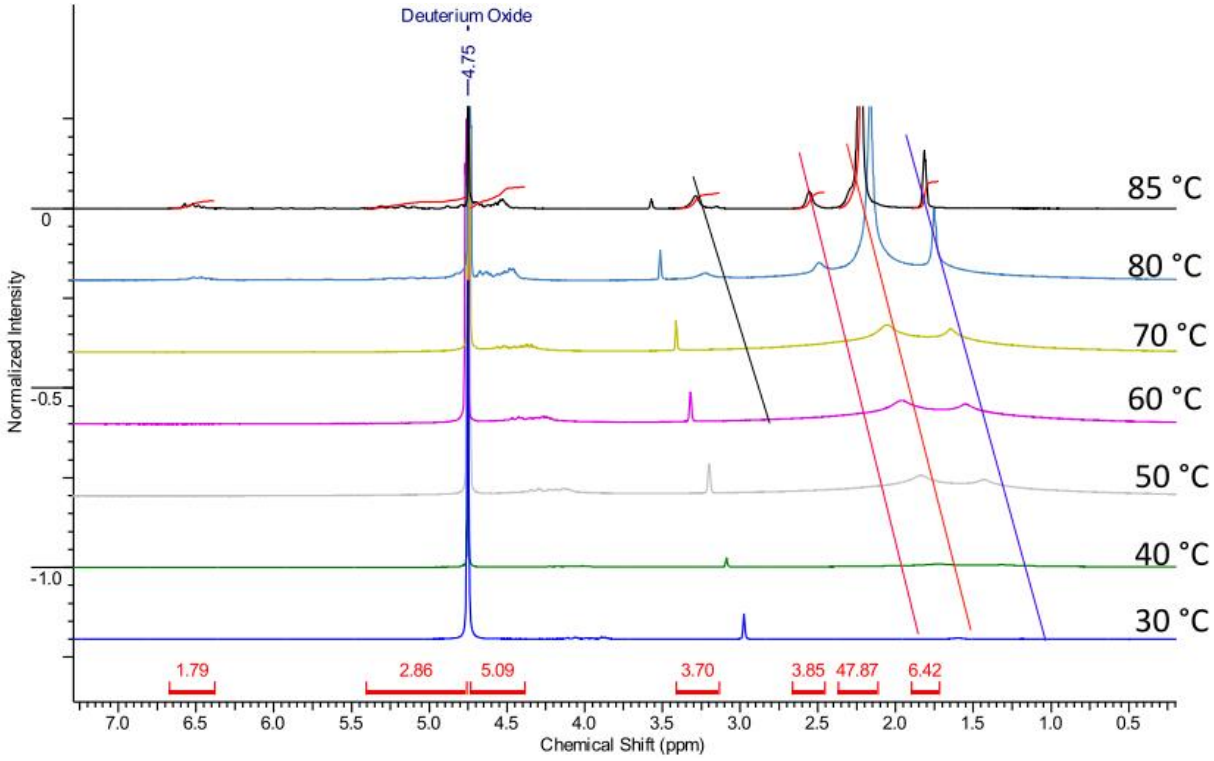

Figure 74: Variable temperature ^{1}H NMR spectra of **55a-b** (5.3%, w/v) in D_2O/DMSO-d_6 solvent mixture (2.9:1, v/v).

In order to obtain a deeper insight into the orientation of the molecules with respect to each other in the self-assembled state and the contributions of the different groups through selective supramolecular interactions within the gel network, temperature-dependent ^{1}H NMR spectroscopic measurements were carried out using **55a-b**, a representative gelator, in a D_2O/DMSO-d_6 solvent mixture (Figure 74, Figure 75). In the D_2O gel, the molecules are self-

assembled into a highly organized rigid network and consequently their signals are quite broad and unresolved even at 95 °C and therefore, the gel sample was prepared in a D_2O/DMSO-d_6 solvent mixture in order to obtain a relatively less rigid gel network.

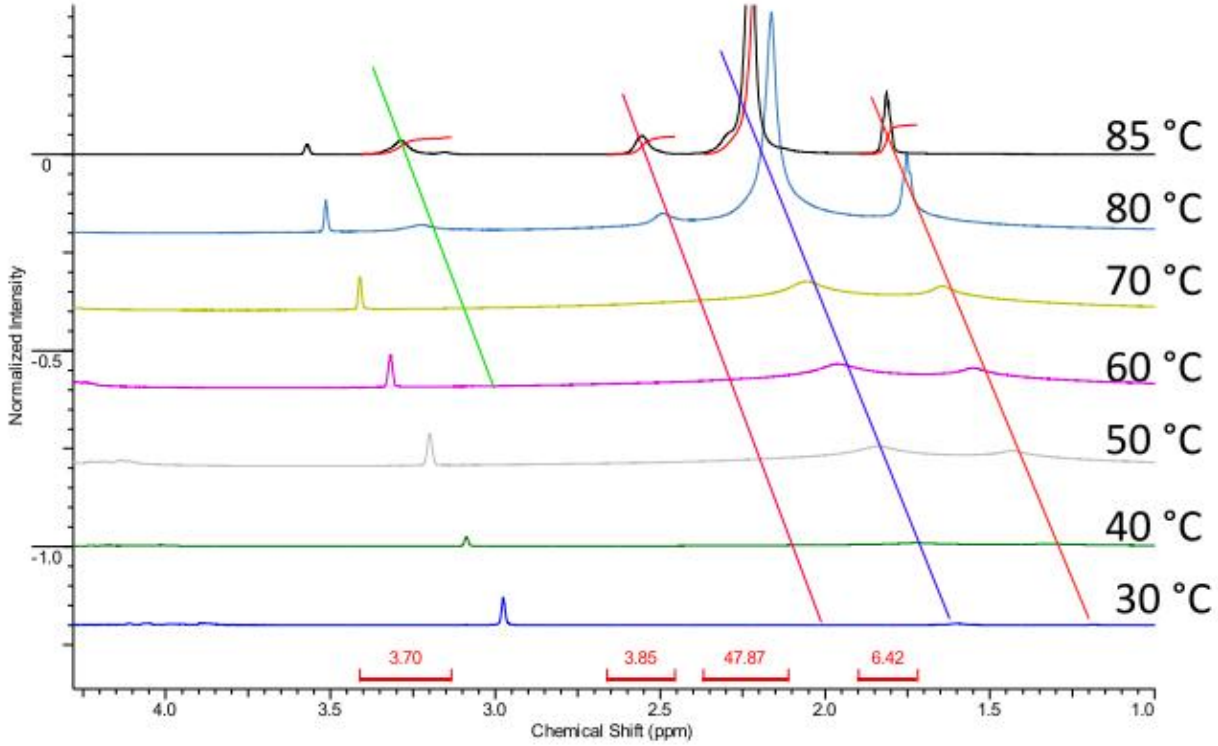

Figure 75: Expanded region of variable temperature ^{1}H NMR spectra of **55a-b** (5.3%, w/v) in D_2O/DMSO-d_6 solvent mixture (2.9:1, v/v).

With a gradual increase in temperature from 30 to 90 °C the signals for the fatty acid protons were found to be slightly shifted downfield and becoming sharper as compared to the signals at 30 °C (Figure 75). This indicates that a gradual increase in temperature is leading to disordering of the self-assembled gel network into its isotopic form. In addition, broadening of the fatty acid proton signals in the gel phase also suggests the existence of van der Waals forces between the hydrocarbon chains inside the gel network.

3.9.4 Surface and interface properties of 50a,b–55a,b

3.9.4.1 Foaming and emulsifying properties of 50a,b–55a,b

Amphiphiles **50a,b**–**55a,b** are surface active agents which display good foaming and emulsifying properties. In case of both the tartaric and malic acid based amphiphiles with shorter hydrocarbon chain the foaming ability is much higher than that of the corresponding compounds with longer carbon chains (only exception is from **50a,b** to **51a,b**). For a given hydrocarbon chain length the foaming abilities of the malic acid based amphiphiles are much higher than those of the corresponding tartaric acid based amphiphiles (Table 28).

compound[a]	foaming ability (mL)	foam stability (mL)	HLB values
50a-b	710	700	not detectable
51a-b	940	934	not detectable
52a-b	452	442	not detectable
53a-b	542	540	13
54a-b	65	53	10
55a-b	I	I	11-12
SDS	765	720	-

[a] For foaming properties triethanolamine salts have been used. I: Insoluble in water

Table 28: Foaming and emulsifying properties of **50a,b**–**55a,b**.

This might be attributed mainly to the difference in solubilities of the amphiphiles in water since this is highly influenced by the hydrocarbon chains length. Among the above series of amphiphiles **50a-b**, **51a-b** display excellent foaming ability which is even higher than commercially available surfactant sodium dodecyl sulphate (SDS). Hence these compounds might be useful alternatives to SDS.[167] **52a-b** and **53a-b** possess foaming abilities in the moderate range whereas **54a-b**, **55a-b** are not foaming at all. The foaming abilities of these amphiphiles are strongly reflected in their HLB values (Table 28). Amphiphiles **53a-b**, **54a-b** and **55a-b** possess HLB values in the range of 10-13 and hence they might be useful for the preparation of O/W emulsions *e.g.*in food industry and cosmetics.

3.9.4.2 CMC values of 50a,b–55a,b in water

The CMCs of **50a,b**–**55a,b** have been determined by the ring method[168] based on surface tension measurements (Figure 76).

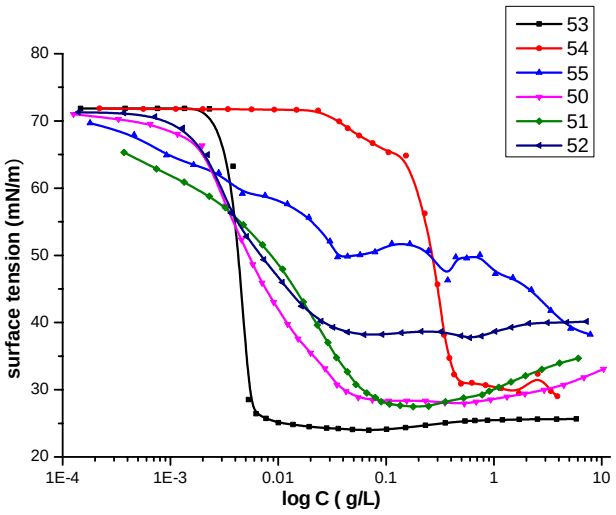

Figure 76: Plot of surface tension *vs.* the logarithm of concentration for **50a,b**–**55a,b** in water at 25 °C.

The CMCs and γ_{CMC} (surface tension at CMC) of the amphiphiles were obtained from a curve of the surface tensions γ (mN/m) against log C (g/L) and the results are summarized in Table 29. In case of the malic acid based amphiphiles **50a,b**–**52a,b** there is a slight decrease in CMC with an increase in hydrocarbon chain length from **50a,b** to **51a,b** and notably there is low value of γ_{CMC} especially in the case of **50a-b** and **51a-b**. This essentially implies that these amphiphiles have an inherent and excellent tendency to adsorb strongly at air/water interface and orient themselves in a proper way to reduce the surface tension at the air/water interface. In case of the tartaric acid based amphiphile **53a-b** the CMC value is much lower than that of the malic acid based amphiphiles which essentially implies that **53a-b** is basically a gemini surfactant. In the structure core of **53a-b** two hydrocarbon chains are connected by a spacer which facilitates the close packing of the surfactant monomers at the air/water interface due to the interactions between the hydrocarbon chains[169] It should be noted that **53a-b** has a CMC value which is 3 orders of magnitude lower than that of SDS and hence might be useful as an alternative to SDS.

compound[a]	CMC (mol/L)	γ_{CMC} (mN/m)
50a-b	9.42×10^{-5}	27.1
51a-b	1.38×10^{-4}	27.2
52a-b	6.99×10^{-5}	33.6
53a-b	7.01×10^{-6}	24.4
54a-b	5.18×10^{-4}	30.5
55a-b	3.90×10^{-4}	47.7
SDS	8.0×10^{-3}	22.1

[a] For CMCs triethanolamine salts have been used.

Table 29: CMCs and the corresponding surface tensions (γ_{CMC}) at the air/water interface of **50a,b**–**55a,b**.

3.9.5 Conclusion

The regioselective esterification of *D*-sorbitol has been accomplished by reacting *D*-sorbitol with *O*-acylated hydroxycarboxylic acid anhydrides in the presence of pyridine. A methodical investigation was carried out to reveal their gelation efficacy in water as well as in some other organic solvents. Besides this, their potent activities as surfactants and emulsifiers were investigated. It is worthy to note that some of the amphiphiles possess foaming abilities higher than that of SDS and CMC values which are lower than SDS. Some of the compounds could serve as stable emulsifiers for the preparation of oil in water emulsions. Since sorbitol and its derivatives are low calorie sweeteners and low digestible carbohydrates they are widely used

with the objective to control caloric intake and body weight in people with diabetes. So these derivatives of sorbitol in the place of sugar might be useful in providing a wider variety of reduced calorie and sugar-free choices.

3.10 Combination products based on *D*-mannitol

3.10.1 Regioselective esterification of *D*-mannitol

3.10.1.1 Syntheses of 1-*O*-acylated fatty acid esters of *D*-mannitol

As it turned out, *D*-mannitol is more reactive than *D*-sorbitol and therefore reaction of *D*-mannitol (5 eq) with *O*-acylated hydroxycarboxylic acid anhydrides (1 eq) in the presence of DMF and pyridine (1 eq) leads to an almost quantitative conversion into 1-6-di-*O*-*O*-acylated fatty acid esters in case of the malic acid anhydrides. In case of the tartaric acid anhydrides a mixture of mono- and di-*O*-acylated fatty acid esters is obtained ((Figure 77).

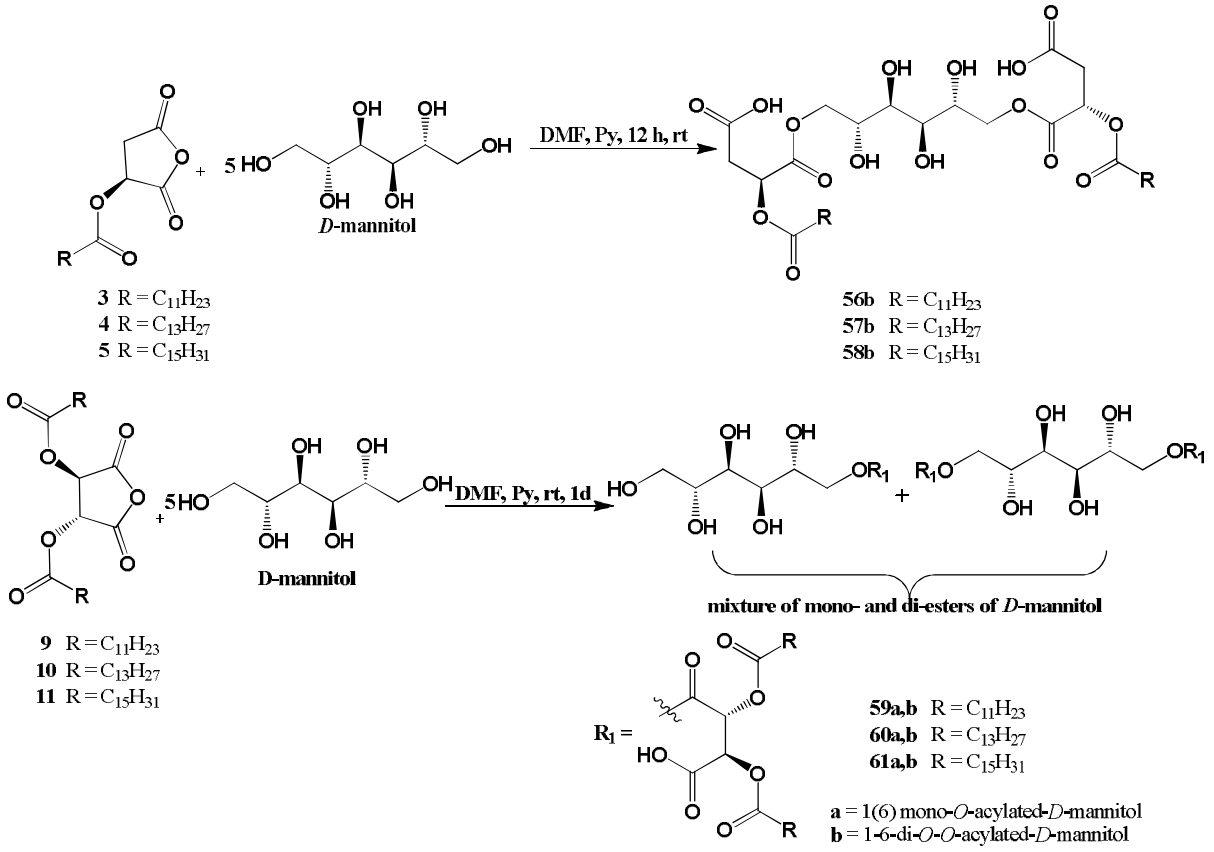

Figure 77: Reaction of *D*-mannitol with *O*-acylated malic and tartaric acid anhydride in the presence of DMF.

While di-esters **56b**–**61b** are completely soluble in *n*-hexane, the corresponding mono-esters **59a**–**61a** are not. Thus the product mixtures can be separated simply by washing them with *n*-hexane.

As it is turned out, the selectivity regarding mono-and di-acylation depends very much on the employed solvent. Thus, acylation of *D*-mannitol in the presence of DMA (instead of DMF) is leading exclusively to the 1(6)-mono-acylated-*D*-mannitol (Figure 76).

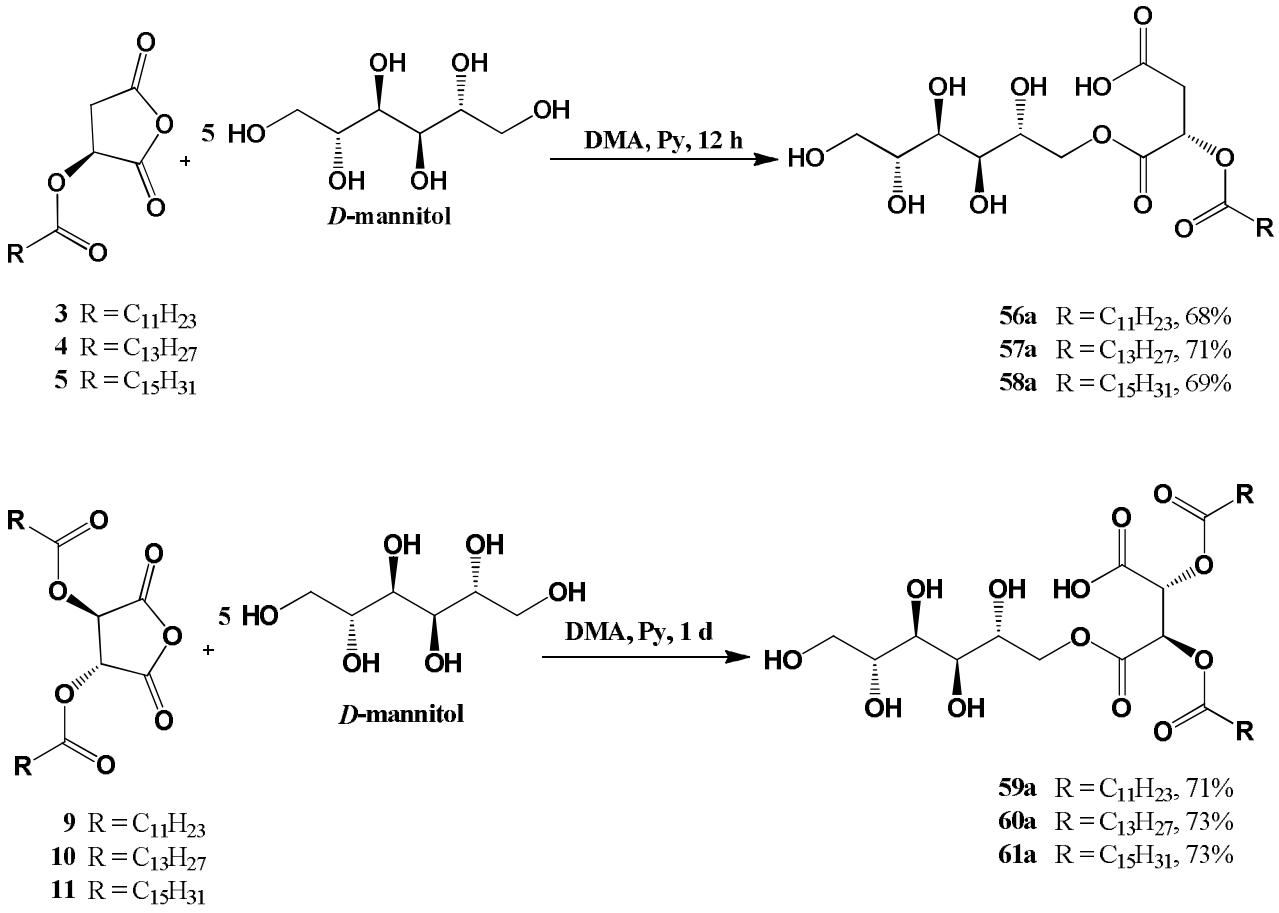

Figure 78: Reaction of *D*-mannitol in the presence of DMA and pyridine.

3.10.2 Characterisation of 56b-61b by NMR

Using **59b** as example, the ^{1}H NMR spectrum shows the protons with chemical shifts at δ = 4.52 (dd, *J* = 11.2, 2.5 Hz, 1H), 4.27 (dd, *J* = 11.2, 6.5 Hz, 1H) ppm characteristic for the H-1 and H-1′ proton of the mannitol unit. The protons with the chemical shifts at δ = 3.90 (m, 2H) ppm are characteristic for the H-2 and H-3 protons of **59b**.

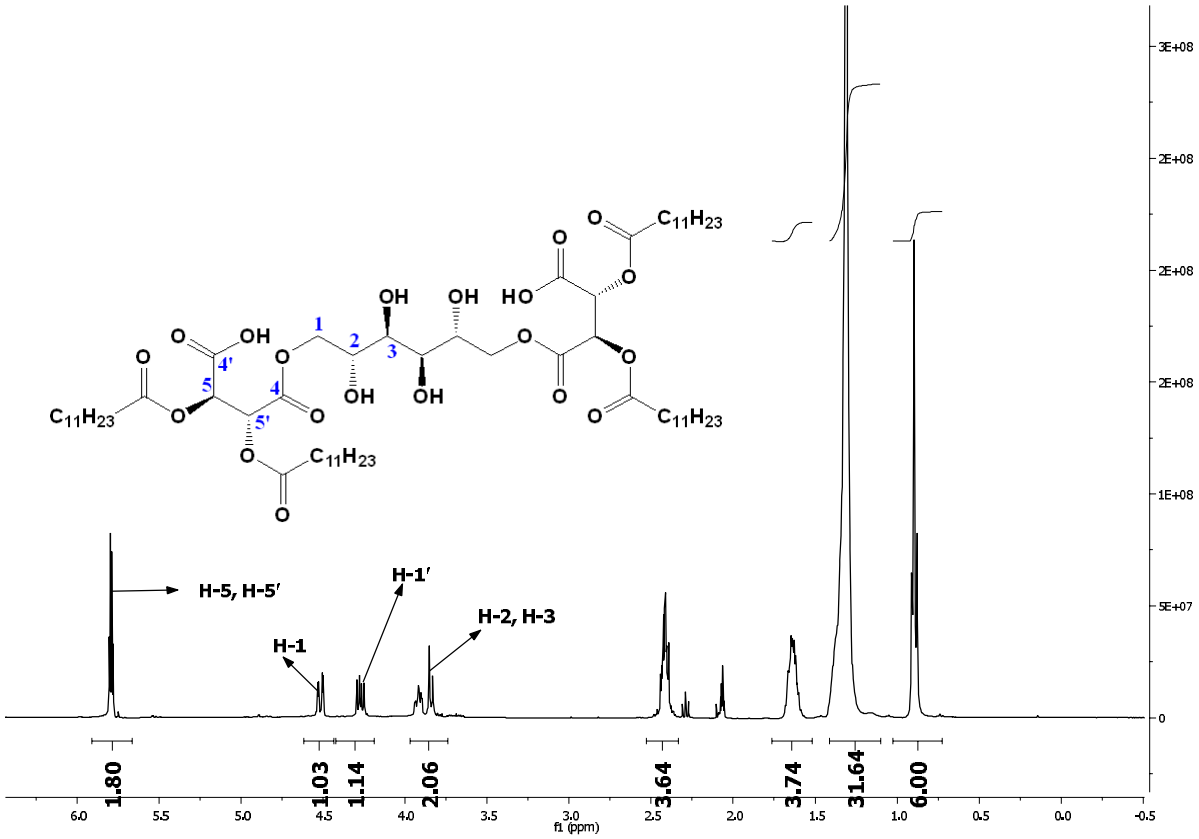

Figure 79: ^{1}H NMR spectrum of **59b** in acetone-d_6.

The ^{13}C NMR spectrum of **59b** is shown in Figure 80. The carbons with the chemical shifts of δ = 173.50, 173.41, 168.14, 167.45 ppm are characteristic for the carbonyl groups at the C-6, C-6′, C-4, C-4′, respectively. The carbons displaying chemical shifts at δ = 72.24, 71.98, 69.83 ppm are characteristic for the C-1, C-2, C-3 carbons of mannitol unit.

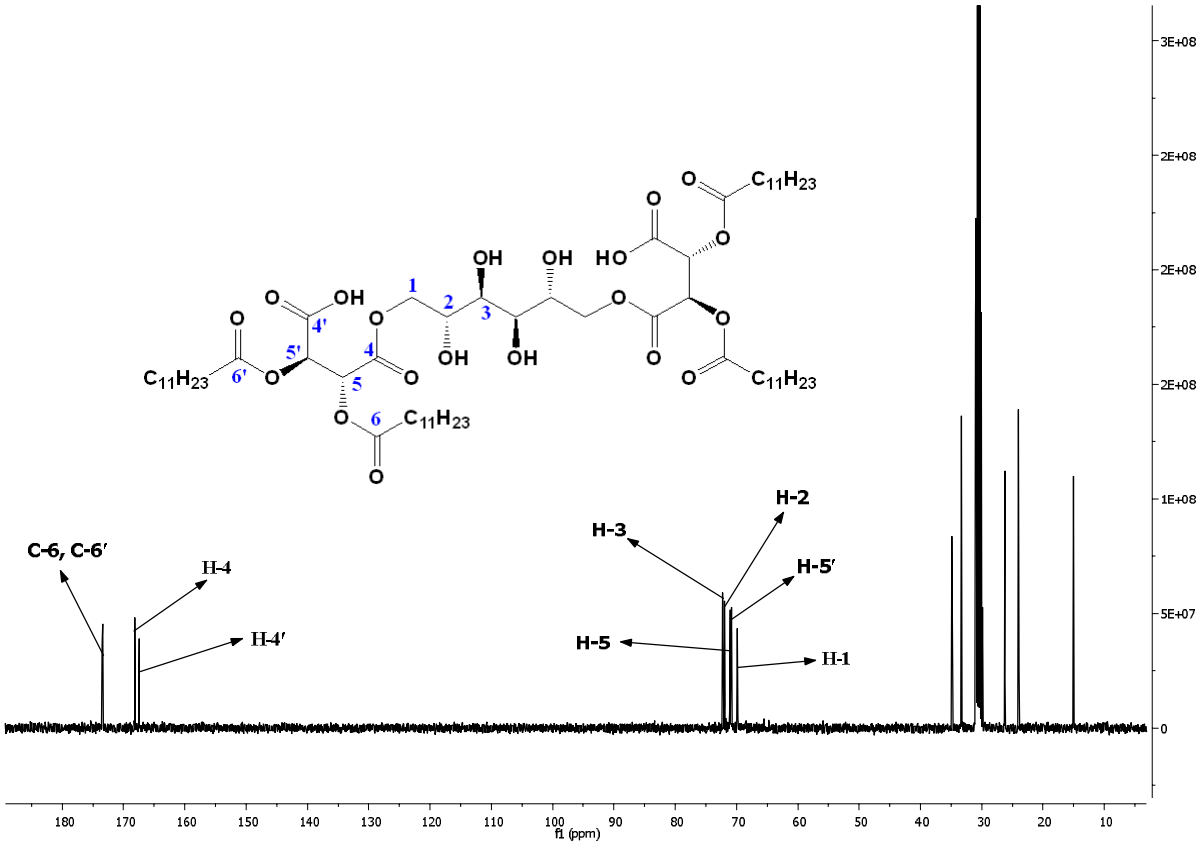

Figure 80: ^{13}C NMR spectrum of **59b** in acetone-d_6.

3.10.3 Characterisation of 56a-61a by NMR

In Figure 81 the ^{1}H NMR spectrum of **59a** is shown, exemplifying this group of compounds**.** The ^{1}H NMR spectrum shows characteristic signals for the lauroyl residue at δ = 2.49 – 2.30 (m, 4H), 1.78 – 1.50 (m, 4H), 1.33 (m, 32H), 0.91 (t, *J* = 6.8 Hz, 6H) ppm. Protons with the chemical shifts in the range of 4.53 – 3.66 ppm are characteristic signals for the *D*-mannitol moiety of **59a** and the complete assignment of all protons is summarized in Figure 81.

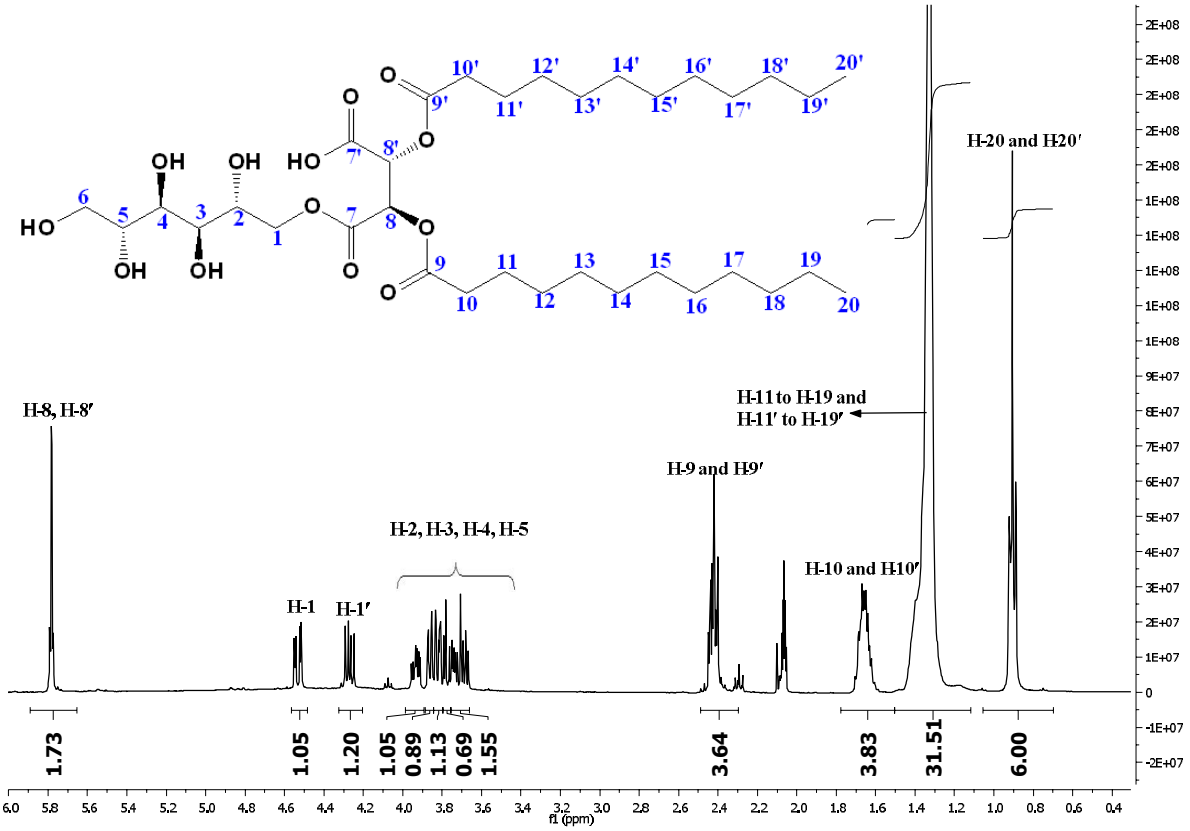

Figure 81: ^{1}H NMR spectrum of **59a** in MeOH-d_4.

In *D*-mannitol, the protons at the C-1(6) position are having a chemical shift of δ = 3.86 (dd 2H) ppm whereas in **59a** these protons are shifted downfield to 4.53 (dd, *J* = 11.2, 2.8 Hz, 1H), 4.27 (dd, *J* = 11.2, 6.4 Hz, 1H) ppm, clearly implying that esterification took place on the hydroxy group at the C-1(6) position. The protons with chemical shifts of δ = 5.89 – 5.65 (m, 2H) ppm are the H-8 and H-8′ protons of the tartaric acid moiety in **59a**.

In Figure 82 the ^{13}C NMR spectra of both *D*-mannitol and **59a** are shown to demonstrate the downfield shift of the C-1(6) carbon in *D*-mannitol by 4.9 ppm after esterification.

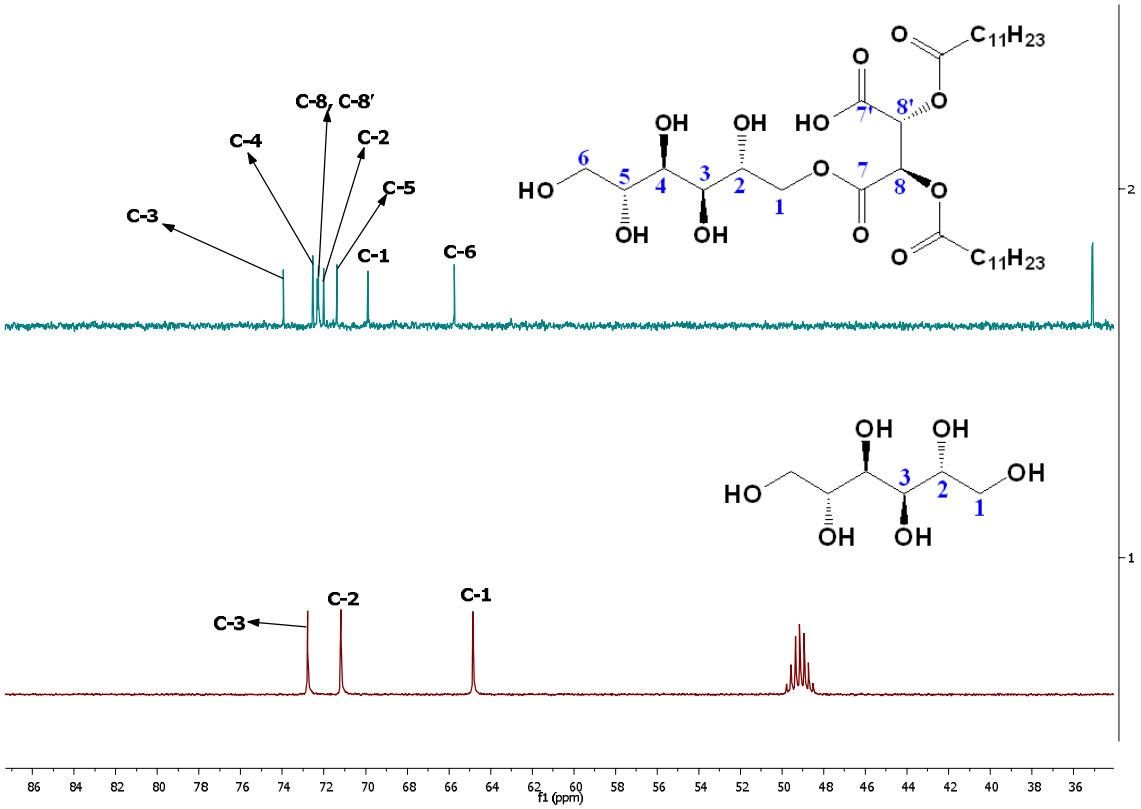

Figure 82: Superimposed ^{13}C NMR spectra of *D*-mannitol and **59a** to demonstrate the downfield shift of the C-1(6) carbon.

3.10.4 Gelation properties of 56a-61a in water

The gelation abilities of **56a-61a** in water (10%, w/v) were determined by the simple method of being stable to inversion of the container and the results are shown in Table 30. In case of both the tartaric and malic acid based amphiphiles thermal stabilities and minimum gelation concentrations in water are again strongly influenced by the length of the hydrocarbon chains in the lipophilic part of the molecules.

compound	MGC[a] (minimum gelation concentration, w/v).	T^{b}_{gel}
56a	PG[c]	-
57a	2.9%	19.8 °C
58a	6.4%	40.0 °C
59a	13.5%	20 °C
60a	4.3%	38 °C
61a	0.7%	50.2°C

[a] For **57a** determined at + 5 °C. PG = partially gel.
[b] 5% (w/v) hydrogel of **61b** was used for T_{gel} measurement because of its low solubility in water.
[c] Not gel at room temperature bur partially gel at + 5 °C.

Table 30: Thermal stabilities and minimum gelation concentrations of the hydrogels derived from **56a-61a**.

The malic acid based amphiphile **58a** with a longer hydrocarbon chain (C_{16}) produces a very stable hydrogel at room temperature (T_{gel} = 40 °C) with a minimum gelation concentration of 6.4% (w/v), whereas the corresponding amphiphile **57a** with a shorter hydrocarbon chain (C_{14}) produces a stable hydrogel only at low temperatures (T_{gel} = 19.8 °C) while **56a** with a C_{12} hydrocarbon chain is not leading to a gel at all A similar trend in the alkyl chain length dependence of the thermal stability and the MGC was also observed in case of the tartaric acid based amphiphiles.

3.10.5 Conclusion

In summary, a small library of mannitol based amphiphiles has been synthesised. They can be afforded in a simple two step reaction and hence could be produced also on industrial scale. On the other hand they exhibit gelation abilities in water and hence they might have numerous potential applications.

4 Conclusions

As outlined in the aim of the thesis (chapter 2) several libraries of compounds–combination products of fatty acids, carbohydrates and hydroxycarboxylic acids–were synthesized (Scheme 21). The majority of the shown molecules can be synthesised in just two simple steps and could thus be produces on an industrial scale. It is worthy to note that all the synthesised compounds are composed from renewable resources and, due to their molecular constitution all of them are potentially highly biodegradable.

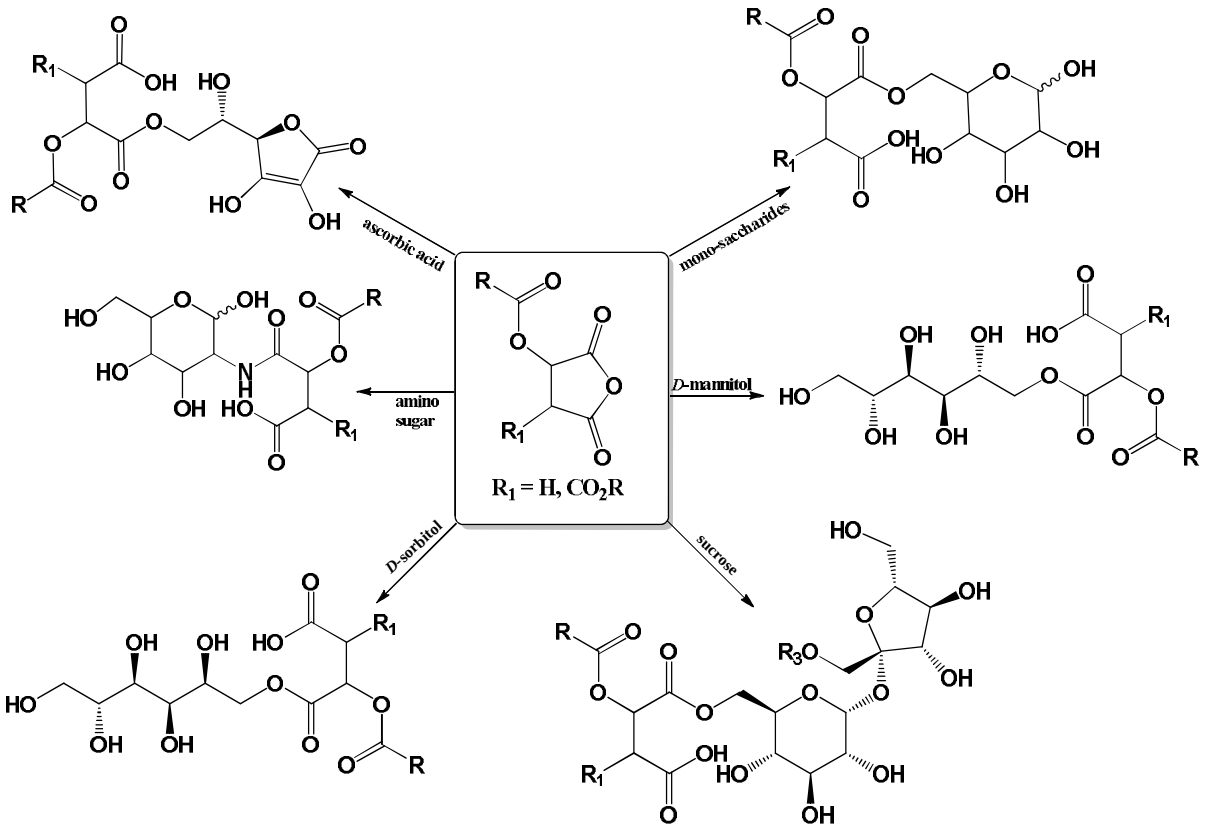

Scheme 21: Lipid modification of carbohydrates based on *O*-acylated hydroxycarboxylic acid anhydrides as key intermediates.

All of these obtained molecules were fully characterised by ^{1}H, ^{13}C NMR and high resolution mass spectroscopy. Their properties such as surfactants, emulsifiers, self-assembled supramolecular gelators and antioxidants were studied in detail.

4.1 Derivatives of *D*-glucose

Several of the derivatives of *D*-glucose **16**-**21** displayed interesting properties as gelators in water or organic solvents. Especially, **18** and **21**, containing a C_{16} hydrocarbon chain display robust gelation abilities in water, producing hydrogels with high thermal stability and very low minimum gelation concentrations. The increase in thermal stabilities of the hydrogels

with an increase in the hydrocarbon chain length clearly indicates that van der Waals interactions between the hydrocarbon chain play an important role for the self-assembly of these molecules in water.

Also the crude diastereomeric mixture shows unprecedented gelation abilities which are comparable to the isomerically pure 6-*O*-acylated product. Thus the crude product mixture might be useful for practical and industrial applications.

Beside gelation, these amphiphiles also show excellent foaming abilities. **16** possesses a foaming ability which is comparable to SDS. We also found that for a defined hydrocarbon chain length, the foaming abilities of the malic acid based amphiphiles are considerably higher than those of the tartaric acid based amphiphiles. Notably **18** has a CMC value which is 3 orders of magnitude lower than that of the commercially available surfactant SDS and hence might be a useful alternative to SDS. **18** is a quasi-gemini surfactant; in the core of the molecule two hydrocarbon chains are connected with a spacer and hence facilitate the surfactant molecules to pack closely at the air/water interface.

4.2 Derivatives of *D*-galactose and methyl-*α*-*D*-glucopyranoside

Beside glucose we have also taken other mono-sugar liked *D*-galactose and methyl-*α*-*D*-glucopyranoside as starting material to make lipid modification with *O*-acylated hydroxycarboxylic acid anhydrides. Some of the methyl-*α*-*D*-glucopyranoside based amphiphiles also show very promising gelation ability in water with high thermal stability and low minimum gelation concentration.

We have found in all derivatives of mono-saccharides the polar head group seems to have a very little effect on the gelation efficacies in water. All derivatives of *D*-glucose (**16**-**21**), *D*-galactose (**35**-**37**) and methyl-*α*-*D*-glucopyranoside (**28**-**30**) containing C_{16} hydrocarbon chains show strong gelation ability in water irrespective of the polar heads groups.

4.3 Derivatives of *D*-glucosamines

All products derived from *D*-glucosamines **22**-**27** display extremely low solubilities in water and hence they do not form gels in water. With the exception of **25** which shows excellent foaming ability in water, none of the derivatives **22**-**24** and **26**, **27** are foamers.

4.4 Derivatives of sucrose

A series of sucrose derivatives **38a,b,c**-**43a,b,c** containing both malic or tartaric acid moieties have been synthesised. The amphiphiles **38a,b,c**-**43a,b,c** do not exhibit any gelation efficacy

in water, which implies that there must be a well-balanced combination of both the H-bonding and hydrophobic interactions for the induction of gelation in water.

38a,b,c-40a,b,c which contain with a tartaric acid unit do not have any emulsifying properties due to their extremely low solubilities in water. On the contrary amphiphiles **41a,b,c-43a,b,c** containing malic acid moieties have emulsifying properties with characteristic HLB values in the range of 11-12. Notably malic acid based amphiphile **38a,b,c** with a C_{12} hydrocarbon chain exhibits foaming ability which is comparable to SDS.

4.5 Derivatives of *L*-ascorbic acid

A library of ascorbic acid based amphiphiles **44-49** –combination products of fatty acids and hydroxycarboxylic acids (tartaric acid and malic acid) linked to the primary hydroxy group of ascorbic acid−were synthesised. With the exception of **44** all of the amphiphiles exhibited robust gelation abilities in water. **48** and **49** display ambidextrous gelation properties and are not only inducing gelation in water but also several other polar aprotic and non-polar solvents like acetonitrile, carbon tetrachloride, and toluene. These ambidextrous gelation properties can be utilized to develop hybrid materials in a variety of solvents as well as in water.

SEM measurements have been performed in order to investigation the nature of the gel fibers. The images revealed that the hydrogels derived from **44-49** are composed of numerous cross linked fibers. Intermolecular hydrogen bonding and van der Waals forces act synergistically to induce gelation and stabilise the gel fibers in water as confirmed by spectroscopic studies.

The antioxidant efficiencies of **44-49** have been determined, showing that antioxidant efficiencies (EC_{50} values) are comparable to ascorbic acid. This implies that the lipid modification of ascorbic acid on the C-6 position does not interfere with the radical scavenging action of ascorbic acid. Since **44-49** are soluble in native oils, they might be useful as food stabilisers to prevent out oxidation.

Using the combination properties (gelation, antioxidant) of these molecules, organic-inorganic hybrid nanocomposites were prepared by *in situ* reduction of Au (III) in hydrogels. Gold nano particles of 25-40 nm were obtained which are stabilised by the fibrillar network of the hydrogel. In a similar way *in situ* fabrication of stabilized silver nano particles was achieved.

44 shows excellent foaming ability which is comparable to SDS. **45**, **46**, **47** and **48** show HLB values in the range of 8-13 and hence they may be useful for the preparation of O/W emulsions in *e.g.* food industry.

4.6 Derivatives of polyols (*D*-sorbitol and *D*-mannitol)

A series of amphiphiles based on *D*-sorbitol (**50a,b-55a,b**) and *D*-mannitol (**56a-61a**) were synthesised. In case of *D*-sorbitol the products **50a,b-55a,b** contain always a mixture of 1 and 6-*O*-acylated esters, while in case of *D*-mannitol the reaction **56a-61a** product consists of 1(6)-*O*-acylated esters. However in the reaction with *D*-mannitol 1,6-*O*-*O*-di-acylated mannitol is observed, depends on the choice of the solvent used. The amphiphiles based on *D*-sorbitol and *D*-mannitol show excellent gelation abilities in water.

Amphiphiles **51a,b-55a,b** form stable gels in water. **53a,b**, **54a,b**, **55a,b** display HLB values in the range of 10-13 and hence they might be useful for the preparation of O/W emulsion especially to control caloric intake and body weight of the people with diabetes.

Again the contribution of both H-bonding and van der Waals interactions for the stabilisation of the self-assembled gel fibers was confirmed by spectroscopic studies. In case of both *D*-sorbitol and *D*-mannitol it was found that the hydrocarbon chains lengths have a decisive role and strong impact on the thermal stabilities of the hydrogels.

4.7 Molecule with potential industrial applications

4.7.1 Excellent hydrogelators with high thermal stability

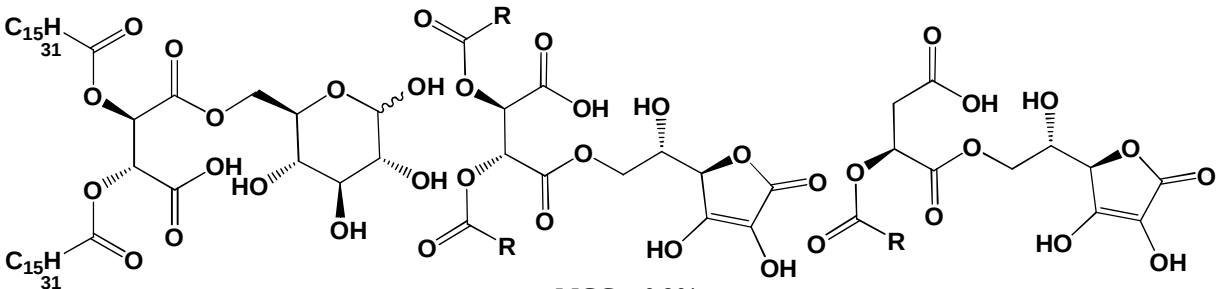

MGC = 2.5%
Tgel = 67 °C

MGC = 0.9%
Tgel = 33 °C

MGC = 1.7%
Tgel = 49 °C

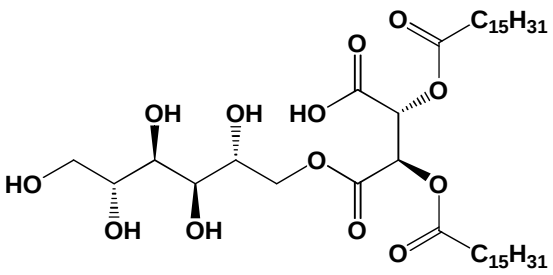

MGC = 0.7%
Tgel = 50 °C

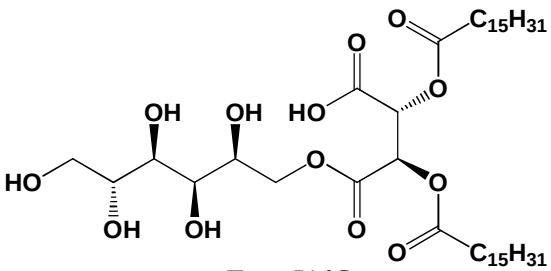

T_{gel} = 51 °C
MGC = 1.7%

4.7.2 Excellent foaming properties comparable to SDS

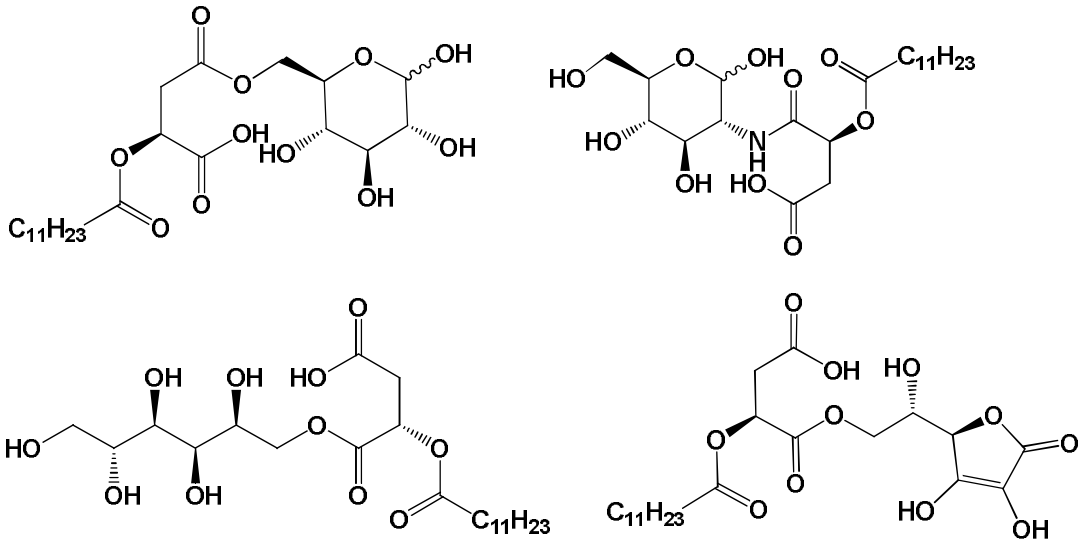

4.7.3 Antioxidants and hence might be useful as food stabiliser in lipophilic media

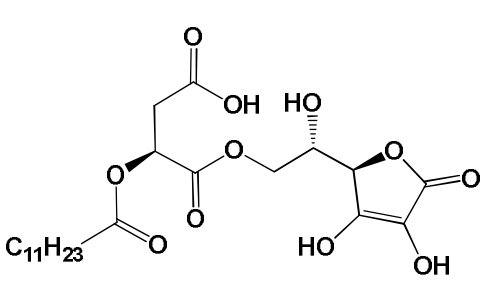

R = $C_{11}H_{23}$, $C_{13}H_{27}$, $C_{15}H_{31}$

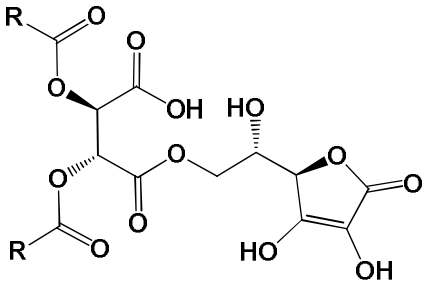

R = $C_{11}H_{23}$, $C_{13}H_{27}$, $C_{15}H_{31}$

5 Experimental Section

5.1 General remarks

All solvents were reagent grade and were directly used without distillation. Reagents were purchased from Acros, Aldrich or Fluka and used without purification unless stated otherwise. ^{1}H NMR (400 or 600 MHz) and ^{13}C NMR (101 MHz) spectra were recorded at ambient temperature unless stated otherwise. Tetramethylsilane (TMS) served as the internal standard. Chemical shifts are reported in ppm downfield with respect to the internal standard TMS or the solvent peaks. Designation of splitting patterns: s (singlet), d (doublet), t (triplet), dt (double of triplets), q (quartet), m (multiplet) and bs (broad signal). Mass spectra were obtained from Bruker microTOF mass spectroscopy.

5.2 Used equipment and reagents

^{1}H-NMR-spectra:	Bruker WM 400 (400.130 MHz). Bruker WM 600 (600.130 MHz).
^{13}C-NMR-spectra:	Bruker WM 400 (100.612 MHz). Bruker WM 600 (150.902 MHz).
Column chromatography:	Silica gel 60 (Merck, 0.063-200 mm, 230-400 mesh,).
Thin layer chromatography:	Silica gel 60. F254 on Al foil (Merck).
Surface tension and CMC measurements:	Company Imeter GmbH (Augsburg): Imeter 4 (De Noüy Ring method); measure resolution 0.01 mN/m; measure range 15-100mN/m. Software: imeter4.1.156, Fa. Imeter.
IR spectra	Attenuated total reflectance (ATR) mode using a JASCO FT/IR-4200 infrared spectrometer
CD spectra	Jasco J-810 spectropolarimeter

5.3 Determination of foaming ability

The forming ability and stability of the surfactant solutions in water were determined according to a literature procedure[170,171]. For this, 0.1% solutions of the corresponding surfactants were prepared in doubly distilled water. 200 mL of such freshly prepared solution were manually beaten in a 1 litre graduated cylinder with a standard perforated disc with a frequency of 60 beats in one minute (Figure 83).[171]

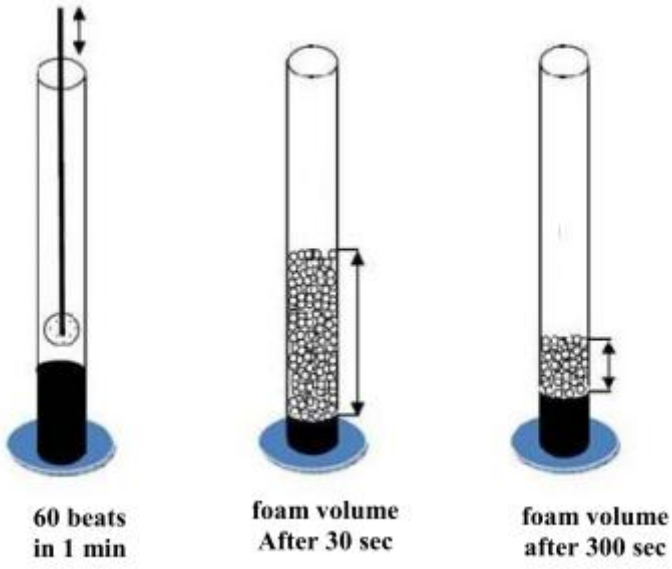

Figure 83: Determination of foaming ability and foam stability –schematic.

The volume of such produced foam was measured after 30 seconds and 5 minutes later and the values (mL) corresponding to the foaming ability and stability of the foam, respectively.

5.4 Differential scanning calorimetry

The gel-to-solution phase transition temperatures (T_{gel}) for all hydrogels (10%, w/v) were measured using a DSC instrument (NETZSCH DSC 204). For this, the hydrogel sample was heated in the temperature range between 10-90 °C with a heating rate of 2 °K/min and the temperature dependent heat capacity was measured. The exothermic maxima in the DSC thermogram correspond to the phase transition from the highly viscous gel state to the solution state.

5.5 Determination of HLB values

Numerous compounds with surface-active properties are useful for the preparation of emulsions such as oil in water (O/W) or water in oil (W/O). Emulsifier properties are closely related to the so-called HLB value, which describes the Hydrophilic-Lipophilic Balance of a surface active molecule.[171,172,173]

HLB values were determined using an emulsion comparative method for oil/water emulsions 20:80 (O/W) based on a published procedure[171,174] as follows: To 2 g of the corresponding oil, 200 mg of a mixture of two emulsifiers, one with a known HLB-value and one for which the HLB-value is unknown, were added. The mixture was heated to 70–80 °C until the

emulsifiers were fully dispersed. Using this approach, a series of mixtures with different weight proportions were prepared (normally 3–18). To these mixtures 8 mL portions of hot (70–80 °C) water were added and the mixtures were shaken intensively for 10 s or treated with an Ultra Turrax high performance disperser for 10 s. The thus prepared samples were subsequently stored at room temperature and inspected visually after 24h. As oil phases, paraffin oil (r*HLB = 10), canola oil (r^*_{HLB} = 7) and toluene (r^*_{HLB} = 15) were employed.

r^*_{HLB} = required HLB value.

$r^*_{HLB} = W_1 \times HLB_1 + W_2 \times HLB_2$

Figure 84: Determination of HLB values by visual inspection.

5.6 Determination of surface tensions and CMCs of the amphiphiles

The CMC values of the amphiphiles were determined using the ring method[171,175] based on surface tension measurements. For this, a series of standard solutions of the corresponding amphiphiles in doubly distilled water were prepared. The standard solutions were kept for 20 min at 25 °C in order to allow the solution to attain equilibrium before conducting measurements. CMC (critical micelle concentration) values and γ_{CMC} (surface tension at CMC) of the amphiphiles were obtained from the minima in the plot of the surface tension γ (mN/m) *vs.* the logarithm of concentration log C (g/L).

5.7 Antimicrobial Properties

All synthesized compounds were tested regarding their activities against a series of bacteria (Gram negative: *Pseudomonas putida mt2* (DSM3931), *Escherichia coli* (DSM498), *Enterobacter aeruginosa* (DSM30053); Gram positive: *Staphylococcus aureus* (DSM346); *Micrococcus luteus* (DSM20030)) and eukaryotic species such as fungi (*Aspergillus niger*

(DSM63263), *Candida albicans* (DSM1386)). For the antimicrobial tests, standard agar plates were employed which were prepared in the following way:

a. For bacteria, by suspending 37 g LB-agar (Bertani-agar after Miller) containing 5 g of yeast extract, 10 g of peptone, 10 g of NaCl, and 12 g agar in 800 mL of bi-distilled water.
b. For fungi by suspending 4 g of peptone, 24 g of malt extract, and 25 g agar in 800 mL of bi-distilled water. The mixtures were heated until all components were dissolved and afterwards sterilized for 15 min at 121 °C. Afterwards ca. 20 mL of the resulting mixture was poured onto a standard agar plate which was allowed to cool for 2 days.

In every agar plate 100 µL of the corresponding cell suspension (105–106 cells/mL) was plated out with a glass spatula and allowed to dry for ca. 30 min. Then, 10 µL of a 1% solution of the corresponding test samples were applied to defined areas of the agar plates which were then incubated (a) for bacteria at 30 °C for 24 and 48 h and (b) for fungi and yeasts at room temperature for 48 and 72 h, respectively. The agar plates were inspected visually at regular intervals and the inhibition zones were measured.

5.8 Detection of spots in TLC

Vanillin (250 mg) was dissolved in ethanol (100 mL) and sulphuric acid (2.5 mL) was added cautiously with stirring and cooling. After immersion, the sorbent layers were dried at 80 °C for 1 minute. Zones are highly coloured on a white background. The reagent is best when prepared fresh and used immediately.

5.9 Preparation of probes for optical and scanning microscopic studies

Xerogels obtained from the corresponding hydrogels were used for both optical and scanning electron microscopy (SEM) studies. The samples of each hydrogel were prepared based on a spin-casting technique by placing the hydrogel (at minimum gelation concentrations to avoid stacking of layers) onto freshly cleaned silicon dioxide wafers to obtain a thin nano-layer of the corresponding hydrogels on the silica surfaces. Each silicon dioxide wafer was then frozen by immersion into liquid nitrogen; the contained water was evaporated by a vacuum pump prior to examination. The thus obtained xerogel was directly subjected to optical electron microscopic studies. Scanning electron microscopy (SEM) images were recorded using a Philips SFEG 30 instrument. The accelerating voltage was 15 kV, with 4.7 mm working distance. For Scanning electron microscopic studies the xerogel was attached to a copper

holder by using a conductive adhesive tape, and then coated with a thin layer of gold by the sputtering technique and was then observed in a SEM apparatus.

5.10 Syntheses of *O*-acylated malic acid anhydrides 1-6

5.10.1 (*S*)-2,5-Dioxotetrahydrofuran-3-yl octanoate (1)

5.5 g (41 mmol) of finely powdered *L*-malic acid and 14 mL (82 mmol) of octanoyl chloride were placed in a 100 mL round bottom equipped with a magnetic stirrer bar and an air bubbler. The mixture was heated slowly up to 70 °C for 4 hours and then the reaction mixture was allowed to cool to room temperature. The crude mixture was dissolved in *n*-hexane and cooled to -10 °C, whereby the product was precipitated. The product was filtered and washed with *n*-hexane (previously cooled at − 10 °C) to obtain 4.2 g (42%) of **1 (**90% purity as confirmed by ^{1}H NMR).

Melting point: 25-28 °C.

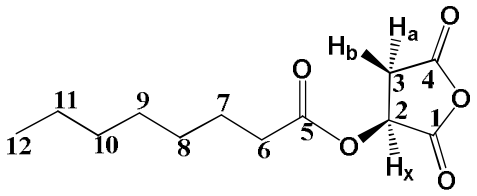

^{1}H-NMR (400,13 MHz, $CDCl_3$) δ =5.51ppm, dd (H_x), at **C-2**; 3.36 ppm, dd (H_b), at **C-3**; 2.96 ppm, dd (H_a), at **C-3;** 2.40 ppm, t (2H), at **C-6;** 1.62 ppm, m (2H), at **C-7**; 1.26 ppm, m (8H), at **C-8** to **C-11**; 0.86 ppm, t, 3H at **C-12**.

^{13}C-NMR; DEPT; COSY ^{1}H/**^{13}C** (MHz, $CDCl_3$): δ = 172.61 ppm **C-4**; δ = 168.02 ppm **C-1;** δ = 166.66 ppm **C-5**; δ = 67.48 ppm **C-2**; δ = 35.03 ppm **C-3**; δ = 33.33 ppm **C-6;** δ = 31.46 ppm **C-8**; δ = 28.76 ppm **C-9**; δ = 28.68 ppm **C-10**; δ = 24.48 ppm **C-7**; δ = 22.44 ppm **C-11**; δ = 13.89 ppm **C-12**.

5.10.2 (*S*)-2,5-Dioxotetrahydrofuran-3-yl decanoate (2)

7.0 g (52 mmol) of finely powered *L*-malic acid and 22 mL (0.1 mol) decanoyl chloride were reacted as described above for **1** (section 5.10.1). 9.9 g (70%) of **2** was obtained as colorless solid.

Melting point: 37-38 °C.

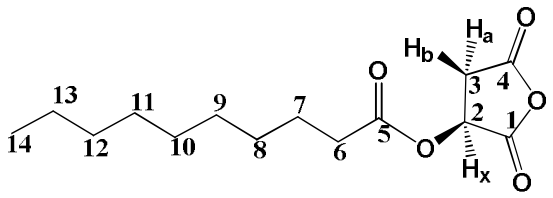

^{1}H-NMR (400,13 MHz, $CDCl_3$): δ = 5.51 ppm, dd (H_x), at **C-2**; δ = 3.36 ppm, dd (H_b), at **C-3**; δ = 2.96 ppm, dd (H_a), at **C-3**; δ = 2.39 ppm, t (2H), at **C-6**; δ = 1.62 ppm, m (2H), at **C-7**; δ = 1.25 ppm, m (12H), at **C-8** to **C-13**; δ = 0.85 ppm, t (3H), at **C-14**.

^{13}C-NMR; DEPT; COSY ^{1}H/^{13}C (100,625 MHz, $CDCl_3$): δ = 172.63 ppm **C-4**; δ = 168.06 ppm **C-1**; δ = 166.73 ppm **C-5**; δ = 67.49 ppm **C-2**; δ = 35.00 ppm **C-3**; δ = 33.32 ppm **C-6**; δ = 31.72 ppm **C-8**; δ = 29.22 ppm **C-9**; δ = 28.81- 29.09 ppm **C-10** to **C-12**; δ = 24.47 ppm **C-7**; δ = 22.52 ppm **C-13**; δ = 13.94 ppm **C-14**.

5.10.3 (*S*)-2,5-Dioxotetrahydrofuran-3-yl dodecanoate (3)

In a 500 mL round bottom flask equipped with a magnetic stirrer bar and air bubbler, 30 g (0.22 mol) of finely powdered *L*-malic acid and 133 mL (0.55 mol) of lauroyl chloride were mixed and heated slowly up to 70 °C for 4 h. Then the reaction mixture was allowed to cool to room temperature. Lauric acid and excess lauroyl chloride was removed from the crude mixture as follows: the crude mixture was dissolved in a minimum amount of *n*-hexane under reflux condition and kept at room temperature for 12 h causing the product to precipitate. It was filtered and washed thoroughly with cold *n*-hexane and dried under vacuum. 60 g of **3** (90%) was obtained as white powder.

Melting point: 43- 44 °C.

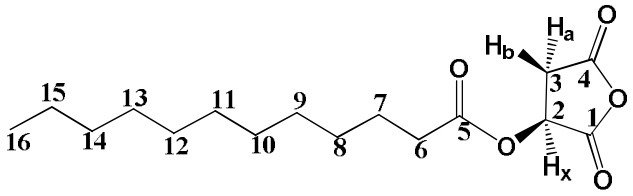

^{1}H-NMR (400,13 MHz, $CDCl_3$): δ = 5.51 ppm, dd (H_x), at **C-2**; δ = 3.36 ppm, dd (H_b), at **C-3**; δ = 2.99 ppm, dd (H_a), at **C-3**; δ = 2.42 ppm, t (2H), at **C-6**; δ = 1.65 ppm, m (2H), at **C-7**; δ = 1.26 ppm, m (16H), at **C-8** to **C-15**; δ = 0.88 ppm, t (3H), at **C-16**.

^{13}C-NMR; DEPT; COSY ^{1}H/^{13}C (100,625 MHz, $CDCl_3$): δ = 172.55 ppm **C-4**; δ = 167.74 ppm **C-1**; δ = 166.31 ppm **C-5**; δ = 67.40 ppm **C-2**; δ = 35.16 ppm **C-3**; δ = 33.32 ppm **C-6**; δ = 28.90- 31.86 ppm **C-14** to **C-8**; δ = 24.57 ppm **C-7**; δ = 22.64 ppm **C-15**; δ = 14.05 ppm **C-16**.

5.10.4 (*S*)-2,5-Dioxotetrahydrofuran-3-yl tetradecanoate (4)

5.0 g (37 mmol) of finely powered *L*-malic acid was reacted as described for **3** (section 5.10.3) using 20 mL (74 mmol) of myristoyl chloride to obtain 9.5 g (78%) of **4** as white amorphous solid.

Melting point: 63-64 °C.

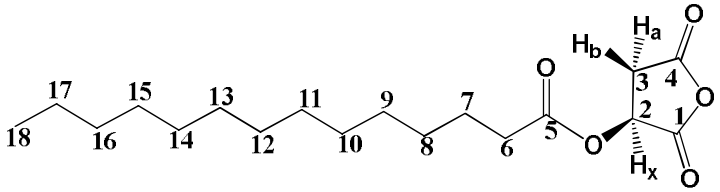

^{1}H-NMR (400,13 MHz, $CDCl_3$): δ = 5.51 ppm, dd (H_x), at **C-2**; δ = 3.35 ppm, dd (H_b), at **C-3**; δ = 2.97 ppm, dd (H_a), at **C-3**; δ = 2.40 ppm, t (2H), at **C-6**; δ = 1.63 ppm, m (2H), at **C-7**; δ = 1.24 ppm, m (20H), at **C-8** to **C-17**; δ = 0.86 ppm, t (3H) at **C-18**.

^{13}C-NMR; DEPT; COSY ^{1}H/^{13}C (100,625 MHz, $CDCl_3$): δ = 172.59 ppm **C-4**. δ = 167.98 ppm **C-1**; δ = 166.61 ppm **C-5**; δ = 67.48 ppm **C-2**; δ = 35.05 ppm **C-3**; δ = 33.36 ppm **C-6**; δ = 28.86- 31.84 ppm **C-16** to **C-8**; δ = 24.51 ppm **C-7**; δ = 22.59 ppm **C-17**; δ = 14.00 ppm **C-18**.

5.10.5 (*S*)-2,5-Dioxotetrahydrofuran-3-yl palmitate (5)

18 mL (59 mmol) of palmitoyl chloride was reacted with 4.0 g (30 mmol) of finely powdered *L*-malic acid as described for **3** (section 5.10.3) yielding 8.1 g (76%) of **5** as white amorphous solid.

Melting point: 65-66 °C.

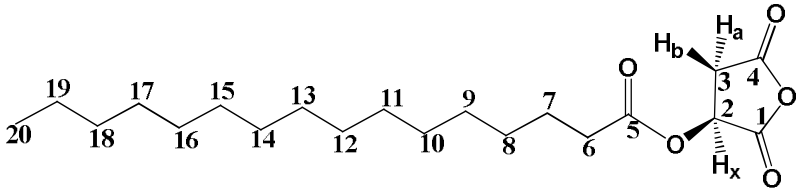

^{1}H-NMR (400,13 MHz, $CDCl_3$): δ = 5.52 ppm, dd (H_x), at **C-2**; δ = 3.36 ppm, dd (H_b), at **C-3**; δ = 2.99 ppm, dd (H_a), at **C-3**; δ = 2.42 ppm, t (2H), at **C-6**; δ = 1.65 ppm, m (2H), at **C-7**; δ = 1.26 ppm, m (24H), at **C-8** to **C-19**; δ = 0.88 ppm, t (3H), at **C-20**.

^{13}C-NMR; DEPT; COSY ^{1}H/^{13}C (100,625 MHz, $CDCl_3$): δ = 172.55 ppm **C-4**. δ = 167.73 ppm **C-1**; δ = 166.28 ppm **C-5**; δ = 67.40 ppm **C-2**; δ = 35.17 ppm **C-3**; δ = 33.43 ppm **C-6**; δ = 28.91- 31.90 ppm **C-8** to **C-18**; δ = 24.57 ppm **C-7**; δ = 22.66 ppm **C-19**; δ = 14.06 ppm **C-20**.

5.10.6 (*S*)-2,5-Dioxotetrahydrofuran-3-yl stearate (6)

4.0 g (30 mmol) of finely powered *L*-malic acid was reacted with 20 mL (59 mmol) of stearoyl chloride as described for **3** (section 5.10.3) to obtain 9.4 g (82%) of **6**.

Melting point: 88-90 °C.

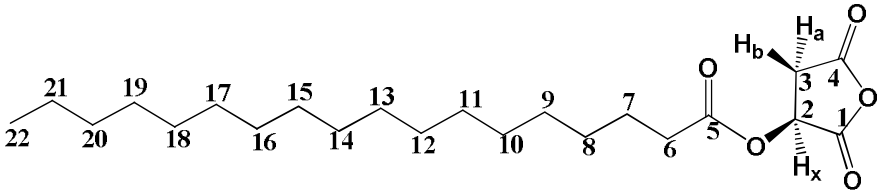

^{1}H-NMR (400,13 MHz, $CDCl_3$): δ = 5.51 ppm, dd (H_x), at **C-2**; δ = 3.36 ppm, dd (H_b), at **C-3**; δ = 2.99 ppm, dd (H_a), at **C-3**; δ = 2.42 ppm, t (2H), at **C-6**; δ = 1.64 ppm, m (2H), at **C-7**; δ = 1.25 ppm, m (28H), at **C-8** to **C-21**; δ = 0.87 ppm, t (3H), at **C-22**.

^{13}C-NMR; DEPT; COSY ^{1}H/^{13}C (100,625 MHz, $CDCl_3$): δ = 172.56 ppm **C-4**; δ = 167.81 ppm **C-1**; δ = 166.39 ppm **C-5**; δ = 67.43 ppm **C-2**; δ = 35.17 ppm **C-3**; δ = 33.41 ppm **C-4**; δ = 28.89- 31.89 ppm **C-8** to **C-20**; δ = 24.56 ppm **C-7**; δ = 22.64 ppm **C-21**; δ = 14.04 ppm **C-22**.

5.11 Syntheses of *O*-*O'*-di-acylated tartaric acid anhydrides 7-12

5.11.1 (3*R*,4*R*)-2,5-Dioxotetrahydrofuran-3,4-diyl-dioctanoate (7)

19.9 mL (117 mmol) of octanoyl chloride was added to 5.0 g (33 mmol) finely powdered *L*-tartaric acid in a round bottom flask under stirring and the reaction mixture was heated at 90 °C for 24 h and then cooled to rt. The product was precipitated with *n*-hexane in the following manner: the crude mixture was dissolved in a minimum amount of *n*-hexane and kept at rt for overnight, the precipitate was filtered, washed thoroughly with *n*-hexane, and dried under vacuum. 7.9 g (62%) of **7** was obtained as white powder.

Melting point: 35-36 °C.

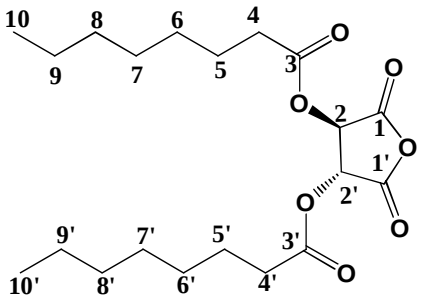

^{1}H-NMR (400.13 MHz, $CDCl_3$): δ = 5.65 ppm, s (2H), at **C-2+C-2´**; δ = 2.45 ppm, t (4H), at **C-4+C-4´**; δ = 1.66 ppm, m (4H), at **C-5+C-5´**; δ = 1.28 ppm, m (16H), at **C-6** to **C-9** and **C-6´**to **C-9´**; δ = 0.88 ppm, t (6H), at **C-10+C-10´**.

^{13}C-NMR; DEPT; COSY ^{1}H/^{13}C (MHz, $CDCl_3$): δ = 172.59 ppm **C-1+C-1´**;δ = 163.48 ppm **C-3+C-3´**;δ = 72.04 ppm **C-2+C-2´**;δ = 33.28 ppm **C-4+C-4´**;δ = 31.52 ppm **C-6+C-6´**;δ = 28.77 ppm **C-7+C-7´**;δ = 28.75 ppm **C-8+C-8´**;δ = 24.50 ppm **C-5+C-5´**;δ = 22.51 **C-9+C--9´**;δ = 13.96 ppm **C-10+C-10´**.

5.11.2 (3*R*,4*R*)-2,5-Dioxotetrahydrofuran-3,4-diyl-didecanoate (8)

4.6 g (31 mmol) of finely powered *L*-tartaric acid was allowed to react with 22.3 mL (0.11 mol) of caprinoyl chloride at 90 °C for 24 h as described for **7** (section 5.11.1) to obtain 10.1 g (86%) of **8** as colourless solid.

Melting point: 56-57 °C.

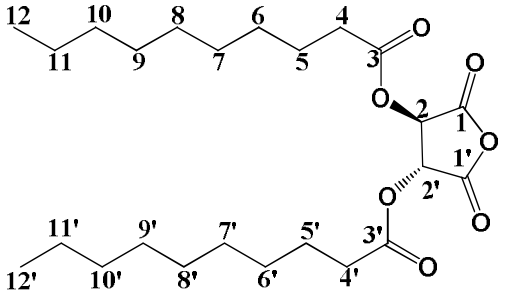

^{1}H-NMR (400,13 MHz, $CDCl_3$): δ = 5.64 ppm, s (2H), at **C-2+C-2´**; δ = 2.44 ppm, t (4H), at **C-4+C-4´**; δ = 1.65 ppm, m (4H), at **C-5+C-5´**; δ = 1.26 ppm, m (20H), at **C-6** to **C-11** and **C-6´**to **C-11´**; δ = 0.87 ppm, t (6H), at **C-12+C-12´**.

^{13}C-NMR; DEPT; COSY ^{1}H/^{13}C (100,625 MHz, $CDCl_3$): δ = 172.57 ppm **C-1+C-1´**; δ = 163.49 ppm **C-3+C-3´**; δ = 72.04 ppm **C-2+C-2´**; δ = 33.28 ppm **C-4+C-4´**; δ = 28.83- 31.79 ppm **C-6** to **C-10** and **C-6´** to **C-10**; δ = 24.49 ppm **C-5+C-5´**; δ = 22.60 **C-11+C-11´**;δ = 14.00 ppm **C-12+C-12´**.

5.11.3 (3*R*,4*R*)-2,5-dioxotetrahydrofuran-3,4-diyl-didodecanoate (9)

5.3 g (35 mmol) of finely powered *L*-tartaric acid was allowed to react with 29.4 mL (0.12 mol) of lauroyl chloride at 90 °C for 24 h as described for **7 (**section 5.11.1) to yield 14.4 g (82%) of **9** as colourless solid.

Melting point: 65-66 °C.

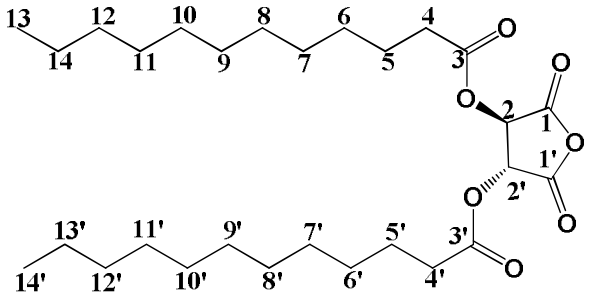

^{1}H-NMR (400,13 MHz, $CDCl_3$): δ = 5.65 ppm, s (2H), at **C-2** to **C-2´**; δ = 2.46 ppm, t (4H), at **C-4** to **C-4´**; δ = 1.66 ppm, m (4H), at **C-5** and **C-5´**; δ = 1.26 ppm, m (32H), at **C-6** to **C-13** and **C-6´** to **C-13´**; δ = 0.88 ppm, t (6H), at **C-14+C-14´**.

^{13}C-NMR; DEPT; COSY ^{1}H/^{13}C (100,625 MHz, $CDCl_3$): δ = 172.59 ppm **C-1+C-1´**, δ = 163.45 ppm **C-3+C-3´**; δ = 72.07 ppm **C-2+C-2´**; δ = 33.32 ppm **C-4+C-4´**; δ = 28.86- 31.88 ppm **C-6+C-12** and **C-6´+C-12´**; δ = 24.52 ppm **C-5+C-5´**; δ = 22.65 **C-13+C-13´**; δ = 14.06 ppm **C-14+C-14´**.

5.11.4 (3*R*,4*R*)-2,5-Dioxotetrahydrofuran-3,4-diyl-ditetradecanoate (10)

4.1 g (27.3 mmol) of finely powered *L*-tartaric acid was allowed to react with 25.85 mL (95.6 mmol) of myristoyl chloride at 90 °C for 24 h as described for **7** (section 5.11.1) to obtain 12.8 g (85%) of **10** as colourless solid.

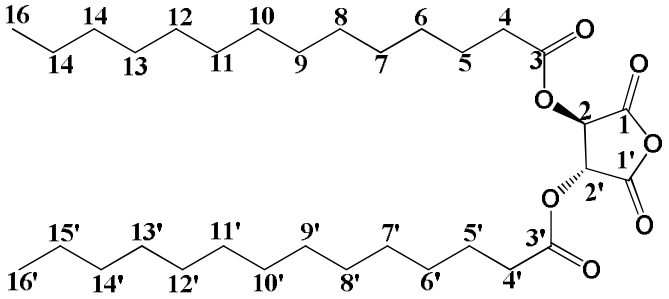

Melting point: 74-76 °C.

^{1}H-NMR (400,13 MHz, $CDCl_3$): δ = 5.65 ppm, s (2H), at **C-2+C-2´**; δ = 2.46 ppm, t (4H), at **C-4+C-4´**; δ = 1.67 ppm, m (4H), at **C-5+C-5´**; δ = 1.26 ppm, m (40H), at **C-6** to **C-15** and **C-6´** to **C-15´**; δ = 0.88 ppm, t (6H), at **C-16+C-16´**.

^{13}C-NMR; DEPT; COSY ^{1}H/^{13}C (100,625 MHz, $CDCl_3$): δ = 172.57 ppm **C-1+C-1´**; δ = 163.44 ppm **C-3+C-3´**; δ = 72.08 ppm **C-2+C-2´**; δ = 33.33 ppm **C-4+C-4´**; δ = 28.86- 31.90 ppm **C-6** to **C-14** and **C-6´** to **C-14´**; δ = 24.54 ppm **C-5+C-5´**; δ = 22.67 ppm **C-15+C-15´**; δ = 14.07 ppm **C-16+C-16´**.

5.11.5 (3*R*,4*R*)-2,5-Dioxotetrahydrofuran-3,4-diyl-dipalmitate (11)

4.0 g (27 mmol) of finely powered *L*-tartaric acid was allowed to react with 28.5 mL (93.3 mmol) of palmitoyl chloride at 90 °C for 24 h as described above for **7** (section 5.11.1) to yield 14.4 g (89%) of **11** as colourless solid.

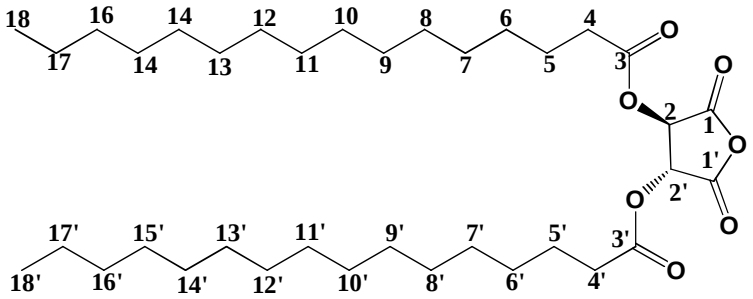

Melting point: 83-84 °C.

^{1}H-NMR (400,13 MHz, $CDCl_3$): δ = 5.65 ppm, s (2H), at **C-2+C-2´**; δ = 2.46 ppm, t (4H), at **C-4+C-4´**; δ = 1.67 ppm, m (4H), at **C-5+C-5´**; δ = 1.26 ppm, m (48H), at **C-6** to **C-17** and **C-6´** to **C-17´**; δ = 0.88 ppm, t (6H), at **C-18+C-18´**.

^{13}C-NMR; DEPT; COSY ^{1}H/^{13}C (100,625 MHz, $CDCl_3$): δ = 172.56 ppm **C-1+C-1´**; δ = 163.44 ppm **C-3+C-3´**; δ = 72.08 ppm **C-2+C-2´**; δ = 33.33 ppm **C-4+C-4´**; δ = 28.87- 31.91 ppm **C-6** to **C-16** and **C-6´** to **C-16´**; δ = 24.54 ppm **C-5+C-5´**; δ = 22.67 ppm **C-17+C-17´**; δ = 14.07 ppm **C-18+C-18´**.

5.11.6 (3*R*,4*R*)-2,5-Dioxotetrahydrofuran-3,4-diyl-distearate (12)

4.0 g (27 mmol) of finely powered *L*-tartaric acid was allowed to react with 32 mL (93 mmol) of stearoyl chloride at 90 °C for 24 h as described for **12** (section 5.11.1) to obtain 14.0 g (79%) of **12** as colourless solid.

Melting point: 93- 95 °C.

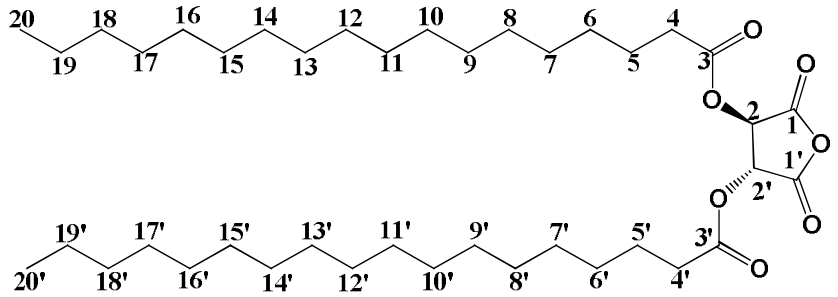

^{1}H-NMR (400,13 MHz, $CDCl_3$): δ = 5.67 ppm, s (2H), at **C-2+C-2´**; δ = 2.48 ppm, t (4H), at **C-4+C-4´**; δ = 1.69 ppm, m (4H), at **C-5+C-5´**; δ = 1.28 ppm, m (56H), at **C-6** to **C-19** and **C-6´**to **C-19´**; δ = 0.90 ppm, t (6H), at **C-20+C-20´**.

^{13}C-NMR; DEPT; COSY ^{1}H/^{13}C (100,625 MHz, $CDCl_3$): δ = 172.61 ppm **C-1+C-1´**; δ = 163.46 ppm **C-3+C-3´**; δ = 72.07 ppm **C-2+C-2´**; δ = 33.33 ppm **C-4+C-4´**; δ = 28.87- 31.92 ppm **C-6** to **C-18** and **C-6´** to **C-18´**; δ = 24.53 ppm **C-5+C-5´**; δ = 22.69 ppm **C-19+C-19´**; δ = 14.10 ppm **C-20+C-20´**.

5.12 Syntheses of *D*-glucose based amphiphiles 16-21

5.12.1 (*S*)-3-(Dodecanoyloxy)-4-oxo-4-(((2*R*,3*S*,4*S*,5*R*)-3,4,5,6-tetrahydroxytetrahydro-2H-pyran-2-yl)methoxy)butanoic acid (16)

To a solution of *D*-glucose (5 g, 0.028 mol) in absolute DMF (45 mL) *O*-lauroyl malic acid anhydride (**3)** (1.7 g, 5.6 mmol) was added with stirring under argon. The reaction mixture was allowed to cool to 0 °C followed by addition of dry pyridine (0.45 mL, 5.6 mmol) under an argon atmosphere. The reaction was continued under the argon atmosphere at 0 °C for 2-3 hours, followed by an additional 12 hours at room temperature. After completion of the reaction, the mixture was poured into an ice-water mixture and 2 N HCl was added at 0 °C under vigorous stirring. The product was extracted with ethyl acetate, washed four times with brine solution, dried over sodium sulphate and the organic solvent was removed under reduced pressure to obtain the crude product. This contains a mixture of regioisomers (monoesters) of *D*-glucose (as confirmed by TLC and HPLC-MS) and trace amounts of lauric acid. Lauric acid was removed from the crude mixture in the following manner: the crude mixture was dissolved in a minimum amount of chloroform under reflux conditions and then *n*-hexane was added slowly to precipitate the mixture of regioisomers from the solution. The precipitation was filtered and dried under reduced pressure yielding 2.2 g (81%) of the regioisomers. The 6-substituted monoester **16** was isolated from the mixture of regioisomers in the following manner: the mixture was dissolved in a minimum amount of acetonitrile

under reflux conditions and kept at room temperature for 12 h leading to the precipitation of **16**. The precipitation was then filtered and dried to obtain 0.7 g (26%, α/β = 4/1) of **16** as a mixture of anomers.

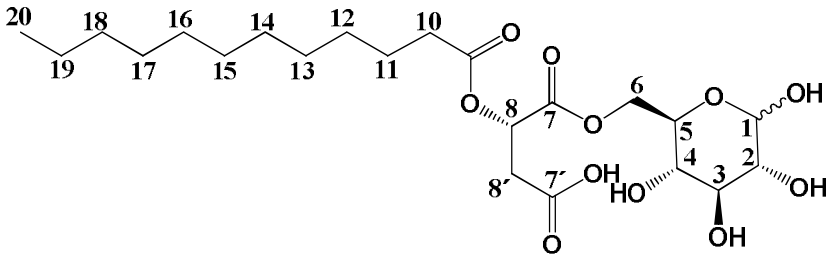

^{1}H NMR (400 MHz, MeOH-d_4) δ = 5.46 – 5.17 (m, 1H, H-**8**), 4.96 (d, *J* = 2.3 Hz, 1H, H-**1*α***), 4.37 – 4.30 (m, 1H, H-**6**), 4.26 – 4.10 (m, 1H, H-**6′**), 3.99 – 3.73 (m, 1H, H-**5**), 3.57 – 3.51 (m, 1H, H-**3**), 3.26 – 3.10 (m, 2H, H-**2** and H-**4**), 2.91 – 2.56 (m, 2H, H-**8′**), 2.26 (t, *J* = 7.2 Hz, 2H, H-**10**), 1.59 – 1.30 (m, 2H, H-**11**), 1.30 – 0.94 (m, 16H, H-**12** to H-**19**), 0.77 (t, *J* = 6.8 Hz, 3H, H-**20**) ppm.

^{13}C NMR (101 MHz, MeOH-d_4) δ = 177.70, 174.35, 174.31, 172.78, 170.60, 170.54 (C-**7**, C-**9**, C-**7′**), 98.15 (C-**1*β***), 93.92 (C-**1*α***), 77.80 (C-**3*β***), 76.09 (C-**2*β***), 75.07 (C-**5*β***), 74.66 (C-**3*α***), 73.65 (C-**2*α***), 71.69 , 71.58 (C-**8*α*** and C-**8*β***), 71.50(C-**4*α***), 70.45 (C-**4*β***), 69.82 (C-**5*α***), 65.92 (C-**6*β***), 65.75 (C-**6*α***), 36.76, 34.92, 34.59, 33.04, 30.72, 30.57, 30.45, 30.38, 30.21, 30.04, 26.06, 25.85, 23.71, 14.45.

HRMS (ESI$^-$, m/z, $[M-H]^-$) calculated for $C_{22}H_{37}O_{11}$: 477.2336 Found: 477.2329

5.12.2 (*S*)-4-Oxo-3-(tetradecanoyloxy)-4-(((2*R*,3*S*,4*S*,5*R*)-3,4,5,6-tetrahydroxytetrahydro-2H-pyran-2-yl)methoxy)butanoic acid (17)

To a solution of *D*-glucose (5 g, 0.028 mol) in anhydrous DMF (45 mL) *O*-tetradecanoyl malic acid anhydride (**4**) (1.8 g, 5.6 mmol) was added with stirring under argon and then the reaction mixture was allowed to cool to 0 °C followed by addition of dry pyridine (0.45 mL, 5.6 mmol) under the argon atmosphere. The reaction was continued under the argon atmosphere at 0 °C for 2-3 hours, followed by an additional 12 hours at room temperature. After completion of the reaction, the mixture was poured into an ice-water mixture and 2 N HCl was added at 0 °C under vigorous stirring. The product was extracted with ethyl acetate, washed four times with brine solution, dried over sodium sulphate and the organic solvent was removed under reduced pressure to obtain the crude product. The crude product contains a mixture of regioisomers (monoesters) of *D*-glucose (as confirmed by TLC and ^{13}C NMR) and trace amounts of tetradecanoic acid. Tetradecanoic acid was removed by washing the

crude mixture several times with *n*-hexane yielding 2.3 g (82%) of the regioisomers. The 6-substituted monoester **17** was isolated from the mixture of regioisomers in the following manner: the mixture was dissolved in a minimum amount of acetonitrile under reflux condition and kept at room temperature for 12 h from which **17** was precipitated. The precipitation was then filtered and dried to obtain 0.8 g (29%, α/β = 4.3/1) of **17** as a mixture of anomers.

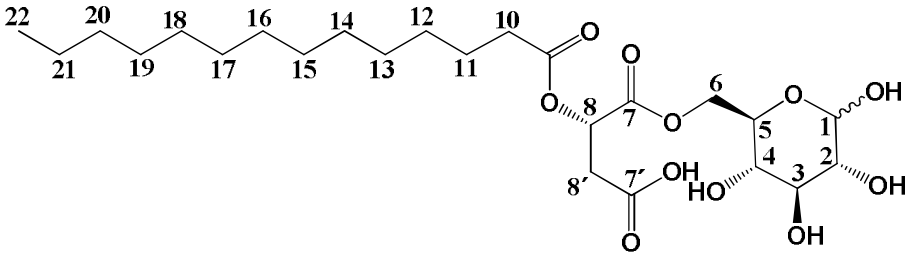

^{1}H NMR (400 MHz, MeOH-d_4) δ = 5.49 – 5.16 (m, 1H, H-**8**), 5.13 – 4.88 (m, 1H, H-**1**), 4.65 – 4.03 (m, 2H, H-**6**, H-**6′**), 3.87 – 3.40 (m, 2H, H-**5**, H-**3**), 3.26 – 3.03 (m, 2H, H-**2**, H-**4**), 3.00 – 2.57 (m, 2H, H-**8′**), 2.31 – 2.08 (m, 2H, H-**10**), 1.53 – 1.33 (m, 2H, H-**11**), 1.23 – 0.99 (m, 16H, H-**12** to H-**21**), 0.77 – 0.61 (m, 3H, H-**22**) ppm.

^{13}C NMR (101 MHz, MeOH-d_4) δ = 174.37, 174.29, 174.27, 172.78, 170.56, 170.50 (C-**7**, C-**9,** C-**7′**), 98.03 (C-**1*β***), 93.75 (C-**1*α***), 77.70 (C-**3*β***), 76.00 (C-**2*β***), 74.98 (C-**5*β***), 74.61 (C-**3*α***), 73.55 (C-**2*α***), 71.72, 71.67 (C-**8*β***, C-**8*α***), 71.50 (C-**4*α***), 70.41 (C-**4*β***), 69.77 (C-**5*α***), 65.87 (C-**6*β***), 65.83 (C-**6*α***), 36.76, 34.57, 32.97, 30.71, 30.67, 30.50, 30.38, 30.31, 29.98, 25.78, 23.63, 14.43 ppm.

HRMS (ESI$^-$, m/z, [M−H]$^-$) calculated for $C_{24}H_{41}O_{11}$: 505.2649 Found: 505.2658

5.12.3 (*S*)-4-Oxo-3-(palmitoyloxy)-4-(((2*R*,3*S*,4*S*,5*R*)-3,4,5,6-tetrahydroxytetrahydro-2H-pyran-2-yl)methoxy)butanoic acid (18)

To a solution of *D*-glucose (10 g, 0.055 mol) in absolute DMF (45 mL) *O*-palmitoyl malic acid anhydride (**5)** (3.93 g, 0.011 mol) was added with stirring under argon and then the reaction mixture was allowed to cool to 0 °C followed by addition of dry pyridine (0.9 mL, 0.011 mol) under the argon atmosphere. The reaction was continued under the argon atmosphere at 0 °C for 2-3 hours, followed by an additional 12 hours at room temperature. After completion of the reaction, the mixture was poured into an ice-water mixture and 2 N HCl was added at 0 °C under vigorous stirring. The product was extracted with ethyl acetate, washed four times with brine solution, dried over sodium sulphate and the organic solvent was removed under reduced pressure to obtain the crude product. The crude product contains

a mixture of regioisomers (monoesters) of *D*-glucose (as confirmed by ^{13}C NMR spectrum of the crude mixture and TLC) and also palmitic acid. Palmitic acid was removed from the crude mixture by washing several times with hexane and the residue was dried yielding 4.6 g (76%) of the regioisomers. The 6-substituted monoester **18** was isolated from the mixture of regioisomers in the following manner: the mixture was dissolved in a minimum amount of acetonitrile and kept at room temperature for 12 h from which **18** was precipitated. The precipitation was then filtered and dried to obtain 1.5 g (26%, α/β = 4.7/1) of **18** as a mixture of anomers.

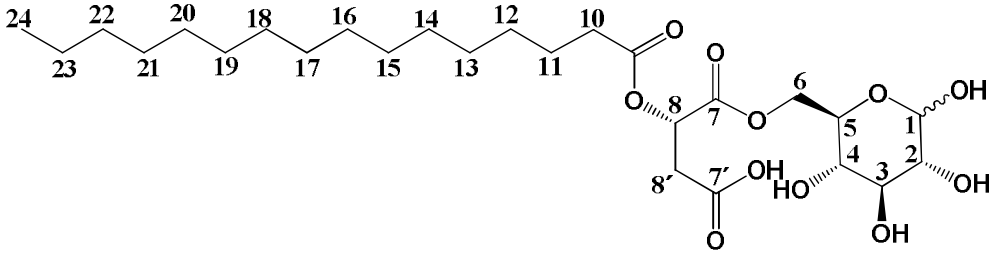

^1H NMR (600 MHz, MeOH-d_4) δ = 5.67 – 5.36 (m, 1H, H-**8**), 5.11 (d, J = 3.7 Hz, 1H, H-**1*α***), 4.48 – 4.22 (m, J = 2.4 Hz, 1H, H-6), 4.04 – 3.79 (m, 1H, H-6′), 3.78 – 3.66 (m, 1H, H-**5**), 3.64 – 3.46 (m, 1H, H-**3**), 3.45 – 3.34 (m, 1H, H-**2**), 3.32 – 3.13 (m, 1H, H-**4**), 3.10 – 2.75 (m, 2H, H-**8′**), 2.40 (m, 2H, H-**10**), 1.66 (t, J = 5.8 Hz, 2H, H-**11**), 1.46 – 1.22 (m, 24H, H-**12** to H-**23**), 0.91 (t, J = 7.0 Hz, 3H, H-**24**) ppm.

^{13}C NMR (101 MHz, MeOH-d4) δ = 174.52, 174.44, 174.41, 172.98, 170.71, 170.65 (C-**7**, C-**9,** C-**7′**), 98.35 (C-**1*β***), 94.07 (C-**1*α***), 78.09 (C-**3*β***), 76.37 (C-**2*β***), 75.29 (C-**5*β***), 74.94 (C-**3*α***), 73.90 (C-**2*α***), 72.25, 72.03 (C-**8*α*** and C-**8*β***), 71.86 (C-**4*α***), 70.70 (C-**4*β***), 69.99 (C-**5*α***), 66.09 (C-**6*β***), 66.06 (C-**6*α***), 34.73, 32.95, 30.65, 30.62, 30.45, 30.31, 30.25, 30.02, 25.84, 23.58, 20.76, 14.25.

HRMS (ESI^-, m/z, $[M-H]^-$) calculated for $C_{26}H_{45}O_{13}$: 787.5208 Found: 787.5206

5.12.4 (2*R*,3*R*)-2,3-Bis(dodecanoyloxy)-4-oxo-4-(((2*R*,3*S*,4*S*,5*R*)-3,4,5,6-tetrahydroxytetrahydro-2H-pyran-2-yl)methoxy)butanoic acid (19)

To a solution of *D*-glucose (20 g, 0.11 mol) in anhydrous DMF (150 mL) *O*-*O′*-di-lauroyl-tartaric acid anhydride (**9**) (11 g, 0.022 mol) was added with stirring under argon and the reaction mixture was allowed to cool down to 0 °C, followed by addition of dry pyridine (1.8 mL, 0.022 mol). The reaction was continued under an argon atmosphere at 0 °C for 2-3 h and an additional 3 days at room temperature. After completion of the reaction, the mixture was poured into ice-water mixture and then 2 N HCl was added at 0 °C under vigorous stirring.

The product was extracted with ethyl acetate, washed four times with brine solution, dried over sodium sulphate and the organic solvent was removed under reduced pressure to obtain the crude product (12.5 g, 83%). The crude product contains a mixture of regioisomers (monoesters) of *D*-glucose (as confirmed by TLC and HPLC-MS and also ^{13}C NMR). The 6-substituted monoester **19** (~ 80%) was precipitated from the mixture in the following manner: the crude mixture was dissolved in a minimum amount of *n*-hexane under reflux conditions and then a half volume of acetone was added. The solution was cooled to 0°C in an ice-water bath and then kept 12 hours at room temperature leading to the precipitation of **19**. The precipitated was filtered and dried to obtain 3.1 g (21%, α/β = 1.8/1) of **19** as a mixture of anomers.

The selective precipitation of 6-*O*-acylated-*D*-glucose by pure acetone, or a mixture of solvents was already published in the literature[176] and was therefore also used here. The NMR spectra of the synthesised amphiphiles were compared with the published NMR spectra of 6-*O*-octanoyl-*D*-glucopyranose and the values are in perfect agreement with those reported previously.[177]

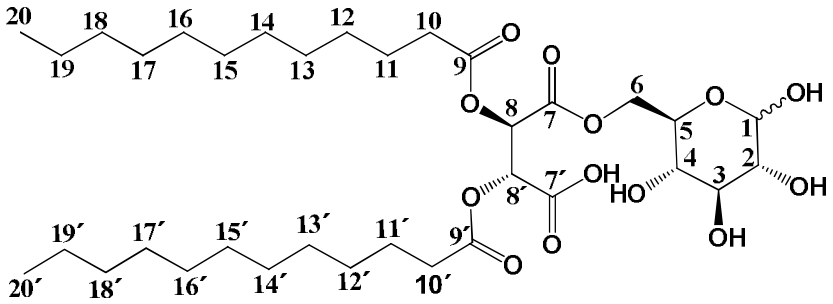

^{1}H NMR (400 MHz, acetone-d$_6$) δ = 5.88 (d, *J* = 2.8 Hz, 1H, H-**8**), 5.85 (d, *J* = 2.6 Hz, 1H, H-**8′**), 5.24 (d, *J* = 3.6 Hz, 1H, H-**1***α*), 4.64 (dd, *J* = 8.1, 4.9 Hz, 1H, H-**6**), 4.46 – 4.32 (m, 1H, H-**6′**), 4.09 (ddd, *J* = 9.8, 4.7, 1.9 Hz, 1H, H-**5**), 3.84 (t, *J* = 9.2 Hz, 1H, H-**3**), 3.57 – 3.47 (m, 2H, H-**2**, H-**4**), 2.55 (m, 4H, H-**10**, H-**10′**), 1.78 (d, *J* = 7.2 Hz, 4H, H-**11**, H-**11′**), 1.66 – 1.27 (m, 32H, H-**12** to H-**19** and H-**12′** to H-**19′**), 1.03 (t, *J* = 6.7 Hz, 6H, H-**20** and H-**20′**) ppm.

^{13}C NMR (101 MHz, acetone-d$_6$) δ = 173.61, 173.38 (C-**9** and C-**9′**), 168.12, 167.33 (C-**7** and C-**7′**), 98.95 (C-**1*β***), 94.49 (C-**1*α***), 78.54 (C-**3*β***), 76.92 (C-**2*β***), 75.64 (C-**5*β***), 75.37 (C-**3*α***), 74.28 (C-**2*α***), 72.31, 72.08 (C-**8** and C-**8′**), 72.05 (C-**4*α***), 72.01 (C-**4*β***), 70.96 (C-**5*α***), 66.59 (C-**6*β***), 66.41 (C-**6*α***), 34.97, 34.92, 33.29, 30.88, 30.67, 30.35, 30.33, 29.86, 26.21, 26.19, 23.95, 14.94 ppm.

HRMS (ESI$^-$, m/z, [M−H]$^-$) calculated for $C_{34}H_{59}O_{13}$: 675.3956 Found: 675.3951

5.12.5 (2*R*,3*R*)-4-Oxo-2,3-bis(tetradecanoyloxy)-4-(((2*R*,3*S*,4*S*,5*R*)-3,4,5,6-tetrahydroxytetrahydro-2H-pyran-2-yl)methoxy)butanoic acid (20)

To a solution of *D*-glucose (10 g, 0.055 mol) in anhydrous DMF (75 mL) *O*-*O′*-di-tetradecanoyl tartaric acid anhydride (**10)** (6.14 g, 0.011 mol) was added with stirring under an argon atmosphere and then the reaction mixture was allowed to cool down to 0 °C, followed by addition of dry pyridine (0.9 mL, 0.011 mol) under an argon atmosphere. The reaction was continued under an argon atmosphere at 0 °C for 2-3 hours, followed by an additional 3 days at room temperature. After completion of the reaction, the mixture was poured into ice-water mixture with 2 N HCl at 0 °C under vigorous stirring. The product was extracted with ethyl acetate, washed four times with brine solution, dried over sodium sulphate and the organic solvent was removed under reduced pressure to obtain the crude product 6.1 g, 74%) which consists of a mixture of regioisomers (monoesters) of *D*-glucose (as confirmed by TLC and HPLC-MS). The 6-substituted monoester **20** (~ 80%) was isolated from the crude mixture in the following manner: a total of 30 mL acetone was added to dissolve the crude mixture and **20** precipitated from the mixture after 12 hours standing at room temperature. The precipitate was filtered and dried to obtain 2.4 g (29%, α/β = 2.2/1) of **20** as a mixture of anomers.

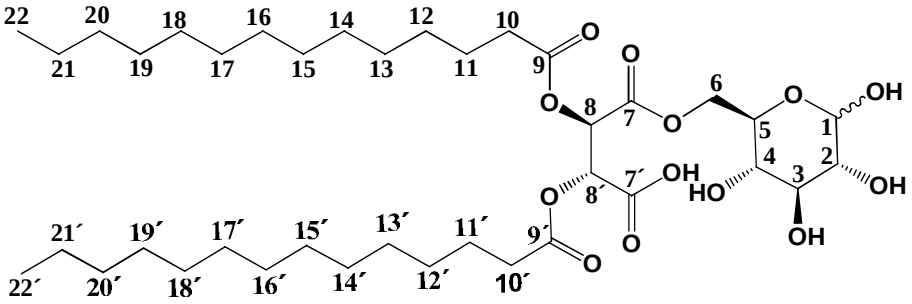

^{1}H NMR (400 MHz, acetone-d_6) δ = 5.91 – 5.81 (m, 2H, H-**8** and H-**8′**), 5.23 (d, *J* = 3.6 Hz, 1H, H-**1*α***), 4.67 – 4.59 (m, 1H, H-**6**), 4.38 (m, 1H, H-**6′**), 4.09 (ddd, *J* = 9.8, 4.8, 2.1 Hz, 1H, H-**5**), 3.83 (t, *J* = 9.1 Hz, 1H, H-**3**), 3.56 – 3.45 (m, 2H, H-**2**, H-**4**), 2.54 (m, 4H, H-**10**, H-**10′**), 1.92 – 1.66 (m, 4H, H-**11**, H-**11′**), 1.48 (m, 40H, H-**12** to H-**21**, H-**12′** to H-**21′**), 1.03 (t, *J* = 6.8 Hz, 6H, H-**22** and H-**22′**) ppm.

^{13}C NMR (101 MHz, acetone-d_6) δ = 173.43, 173.21 (C-**9** and C-**9′**), 167.93, 167.06 (C-**7** and C-**7′**), 98.70 (C-**1*β***), 94.27 (C-**1*α***), 78.25 (C-**3*β***), 76.51 (C-**2*β***), 75.33 (C-**5*β***), 75.03 (C-**3*α***), 73.99 (C-**2*α***), 72.05 , 71.79 (C-**8** and C-**8′**), 71.70 (C-**4*α***), 71.63 (C-**4*β***), 70.63 (C-**5*α***), 66.33 (C-**6*β***), 66.09 (C-**6*α***), 34.69, 34.66, 33.12, 30.76, 30.74, 30.16, 29.74, 26.03, 25.99, 23.80, 14.84 ppm.

HRMS (ESI⁻, m/z, [M−H]⁻) calculated for $C_{38}H_{67}O_{13}$: 731.4582 Found: 731.4588

5.12.6 (2*R*,3*R*)-4-Oxo-2,3-bis(palmitoyloxy)-4-(((2*R*,3*S*,4*S*,5*R*)-3,4,5,6-tetrahydroxytetrahydro-2H-pyran-2-yl)methoxy)butanoic acid (21)

To a solution of *D*-glucose (20 g, 0.11 mol) in absolute DMF (150 mL) *O*-*O*′-di-palmitoyl tartaric acid anhydride (**11**) (13.5 g, 0.022 mol) was added with stirring under argon and then the reaction mixture was allowed to cool down to 0 °C followed by addition of dry pyridine (1.8 mL, 0.02 mol) under an argon atmosphere. The reaction was continued under an argon atmosphere at 0 °C for 2 hours, followed by an additional 3 days at room temperature. After completion of the reaction, the mixture was poured into 2 N HCl at 0 °C under vigorous stirring. The product was extracted with ethyl acetate, washed four times with brine solution, dried over sodium sulphate and the organic solvent was removed under reduced pressure to afford the crude product (14.7 g, 84%). This contains a mixture of regioisomers (monoesters) of *D*-glucose (as confirmed by TLC and HPLC-MS). The 6-substituted monoester **21** (~ 80 %) was isolated from the mixture in the following manner: a total of 30 mL acetone was added to dissolve the crude mixture. The solution was cooled to 0 °C under ice-water bath and then kept overnight at room temperature. **21** was precipitated from the mixture after 12 hours standing at room temperature. The precipitate was then filtered and dried to obtain 5.8 g (33%, α/β = 2.1/1) of **21** as a mixture of anomers.

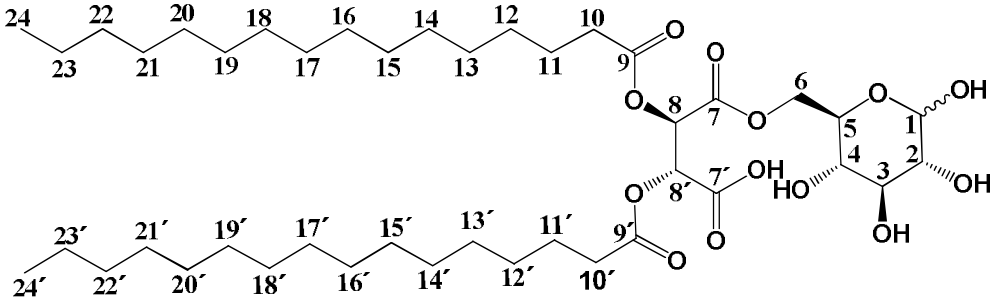

^{1}H NMR (400 MHz, acetone-d_6) δ = 5.89 – 5.81 (m, 2H, H-**8** and H-**8′**), 5.23 (d, *J* = 3.6 Hz, 1H, H-**1*α***), 4.64 (dd, *J* = 9.1, 4.8 Hz, 1H, H-**6**), 4.38 (dd, *J* = 9.1, 4.8 Hz, 1H H-**6′**), 4.09 (ddd, *J* = 9.9, 4.7, 2.0 Hz, 1H, H-**5**), 3.84 (t, *J* = 9.2 Hz, 1H, H-**3**), 3.56 – 3.40 (m, 2H, H-**2**, H-**4**), 2.60 – 2.46 (m, 4H, H-**10**, H-**10′**), 1.89 – 1.67 (m, 4H, H-**11**, H-**11′**), 1.48 (m, 48H, H-**12** to H-**23** and H-**12′** to H-**23′**), 1.03 (t, *J* = 6.8 Hz, 6H, H-**24**, H-**24′**) ppm.

^{13}C NMR (101 MHz, acetone-d_6) δ = 173.69, 173.46 (C-**9** and C-**9′**), 168.31, 167.43 (C-**7** and C-**7′**), 99.01 (C-**1*β***), 94.55 (C-**1*α***), 78.60 (C-**3*β***), 76.91 (C-**2*β***), 75.70 (C-**5*β***), 75.44 (C-**3*α***),

74.34 (C-**2*α***), 72.42, 72.19 (C-**8** and C-**8′**), 72.16 (C-**4*α***), 72.08 (C-**4*β***), 71.04 (C-**5*α***), 66.64 (C-**6*β***), 66.46 (C-**6*α***), 30.97, 30.94, 30.73, 30.44, 30.42, 29.92, 15.01 ppm.

HRMS (ESI$^-$, m/z, [M−H]$^-$) calculated for $C_{42}H_{75}O_{13}$: 787.5208 Found: 787.5206

5.13 Syntheses of *D*-glucosamine based amphiphiles 22-27

5.13.1 (2*R*,3*R*)-4-Oxo-2,3-bis(dodecanoyloxy)-4-((3*R*,4*R*,5*S*)-2,4,5-trihydroxy-6-(hydroxymethyl)tetrahydro-2H-pyran-3-ylamino)butanoic acid (22)

In a 100 mL round bottom flask equipped with a magnetic stirrer bar 2 g (0.009 mol) of *D*-glucosamine hydrochloride and 75 mL DMF were added and the mixture was stirred for an hour after which dry Et_3N (2mL) was added while stirring under an argon atmosphere. The reaction was continued at room temp for the next 12 h for the *in situ* liberation of *D*-glucosamine. The excess of Et_3N was nearly completely removed from the reaction mixture by distillation under reduced pressure, since in presence of Et_3N would lead to a significant elimination in the *O*-*O′*-di-lauroyl tartaric acid anhydride in the next step. The thus *in situ* prepared solution of *D*-glucosamine in DMF was further used without purification. To this solution of *D*-glucosamine (1.6 g, 0.009 mol) 2.3 g (0.0046 mol) of *O*-*O′*-di-lauroyl tartaric acid anhydride (**9**) was added and then the reaction was continued at 0 °C (ice-water bath) with stirring under argon. To the reaction mixture 0.37 mL (0.0046 mol) of pyridine was added. The reaction was allowed to continue to 0 °C for 2 h followed by an additional day at room temperature. After completion of the reaction, the mixture was poured into a conical flask containing an ice-water mixture and then 2 N HCl was added at 0 °C under vigorous stirring to neutralize excess pyridine. The precipitation was filtered, washed with water and then *n*-hexane. The reaction product behaved like a gel in *n*-hexane and therefore the mixture was centrifuged and hexane was decanted. The precipitate was dried to obtain **22** in a yield of 2.5 g (81%, α/β = 7/1).

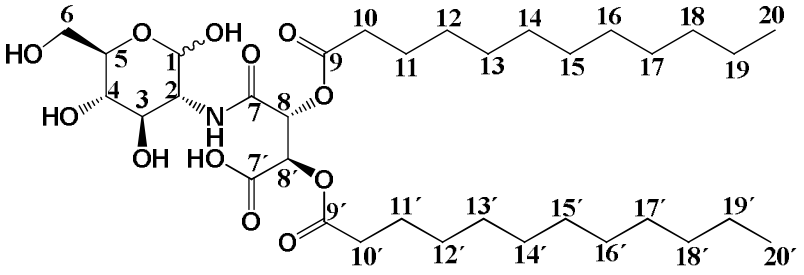

^{1}H NMR (400 MHz, MeOH-d_4) δ = 5.83 – 5.54 (m, 2H, H-**8**, H-**8′**), 5.08 (d, *J* = 3.3 Hz, 1H, H-**1**), 4.20 – 3.34 (m, 6H, H-**2**, H-**3**, H-**4**, H-**5**, H-**6**, H-**6′**), 2.55 – 2.29 (m, 4H, H-**10** and H-

10′), 1.77 – 1.47 (m, 4H, H-**11** and H-**11′**), 1.47 – 1.11 (m, 32H, H-**12** to H-**19** and H-**12′** to H-**19′**), 1.01 – 0.79 (m, 6H, H-**20** and H-**20′**) ppm.

^{13}C NMR (101 MHz, MeOH-d_4) δ = 174.30, 173.77, 169.72 (C-**7**, C-**9**, C-**9′**, C-**7′**), 92.52 (C-**1**), 73.52 (C-**5**), 73.26 (C-**4**), 72.77, 72.68 72.33 (C-**3, C-8, C-8′**), 63.02 (C-**6**), 56.10 (C-**2**), 35.89, 34.80, 34.63, 33.06, 30.75, 30.63, 30.55, 30.43, 30.38, 30.17, 30.14, 25.94, 25.86, 23.70, 14.41 ppm.

HRMS (ESI$^-$, m/z, [M−H]$^-$) calculated for $C_{34}H_{60}NO_{12}$: 674.4116 Found: 674.4109

5.13.2 (2*R*,3*R*)-4-Oxo-2,3-bis(tetradecanoyloxy)-4-((3*R*,4*R*,5*S*)-2,4,5-trihydroxy-6-(hydroxymethyl)tetrahydro-2H-pyran-3-ylamino)butanoic acid (23)

In a 100 mL round bottom flask equipped with a magnetic stirrer bar 2 g (0.009 mol) of *D*-glucosamine hydrochloride and 75 mL anhydrous DMF were added and the mixture was stirred for an hour and then dry Et_3N (2mL) was added to the mixture with stirring under an argon atmosphere. The reaction was further continued at room temp for the next 12 h for the *in situ* liberation of *D*-glucosamine. Then the excess of Et_3N was nearly completely removed from the reaction mixture by distillation under reduced pressure as described above (section 5.13.1). The thus *in situ* prepared solution of *D*-glucosamine in DMF was further used without purification. To this solution of *D*-glucosamine (1.6 g, 0.009 mol) in DMF 2.5 g (0.0046 mol) of *O*-*O′*-di-tetradecanoyl tartaric acid anhydride (**10**) was added and then the reaction was continued at 0 °C (ice-water bath) with stirring under argon. To the reaction mixture 0.37 mL (0.0046 mol) of pyridine was added. The reaction was allowed to continue at 0 °C for 2 h followed by an additional one day at room temperature. After completion of the reaction, the mixture was poured into a conical flask containing ice-water mixture and then 2 N HCl was added at 0 °C under vigorous stirring to neutralize the excess pyridine. The precipitate was filtered, washed with water and then acetone to obtain pure **23** in a yield of 2 g (61%, α/β = 4.5/1)

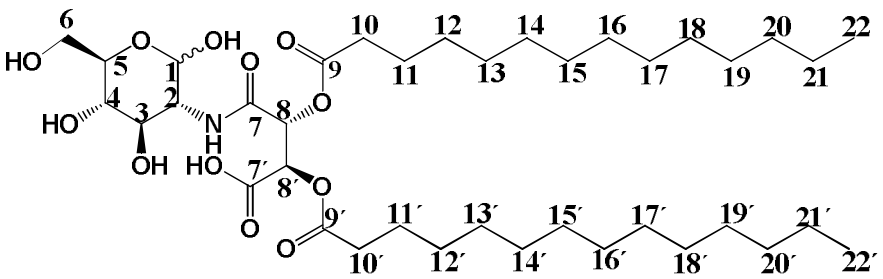

^{1}H NMR (600 MHz, MeOH-d_4) δ = 5.79 – 5.51 (m, 2H, H-**8**, H-**8´**), 5.08 (d, *J* = 3.5 Hz, 1H, H-**1**), 4.06 – 3.33 (m, 5H, H-**3**, H-**4**, H-**5**, H-**6**, H-**6′**), 2.81 – 2.60 (m, 1H, H-**2**), 2.52 – 2.30 (m, 4H, H-**10** and H-**10′**), 1.76 – 1.51 (m, 4H, H-**11** and H-**11′**), 1.48 – 1.08 (m, 40H, H-**12** to H-**21** and H-**12′** to H-**21′**), 1.00 – 0.71 (m, 6H, H-**22**, H-**22′**) ppm.

^{13}C NMR (151 MHz, MeOH-d_4) δ = 174.32, 173.73, 169.72, 168.74 (C-**7**, C-**9**, C-**9′**, C-**7′**), 92.57 (C-**1**), 73.58 (C-**5**), 73.51 (C-**4**), 73.29, 72.87, 72.36 (C-**3,** C-**8,** C-**8′**), 63.11 (C-**6**), 56.14 (C-**2**), 34.84, 34.67, 33.06, 30.79, 30.76, 30.64, 30.56, 30.43, 30.38, 30.20, 30.16, 25.96, 25.88, 23.69, 14.38 ppm.

HRMS (ESI$^-$, m/z, [M−H]$^-$) calculated for $C_{38}H_{68}NO_{12}$: 730.4742 Found: 730.4751

5.13.3 (2*R*,3*R*)-4-Oxo-2,3-bis(palmitoyloxy)-4-((3*R*,4*R*,5*S*)-2,4,5-trihydroxy-6-(hydroxymethyl)tetrahydro-2H-pyran-3-ylamino)butanoic acid (24)

In a 100 mL round bottom flask equipped with a magnetic stirrer bar 2 g (0.009 mol) of *D*-glucosamine hydrochloride and 75 mL anhydrous DMF were added and the mixture was stirred for an hour and then dry Et_3N (2mL) was added to the mixture with stirring under an argon atmosphere. The reaction was further continued at room temp for the next 12 h for the *in situ* liberation of *D*-glucosamine. Then the excess of Et_3N was nearly completely removed from the reaction mixture by distillation under reduced pressure as described above (section 5.13.1). The thus *in situ* prepared solution of *D*-glucosamine in DMF was further used without purification. To this solution of *D*-glucosamine (1.6 g, 0.009 mol) in DMF 2.8 g (0.0046 mol) of *O*-*O′*-di-palmitoyl tartaric acid anhydride (**11**) was added and then the reaction was continued to 0 °C (ice-water bath) with stirring under argon. To the reaction mixture 0.37 mL (0.0046 mol) of pyridine was added. The reaction was allowed to continue to 0 °C for 2 h followed by an additional day at room temperature. After completion of the reaction, the mixture was poured into a conical flask containing ice-water mixture and then 2 N HCl was added at 0 °C under vigorous stirring to neutralize the excess pyridine. The precipitate was filtered, washed with water and then chloroform and dried to obtain pure **24** with a yield of 3.1 g (86%, α/β = 5/1).

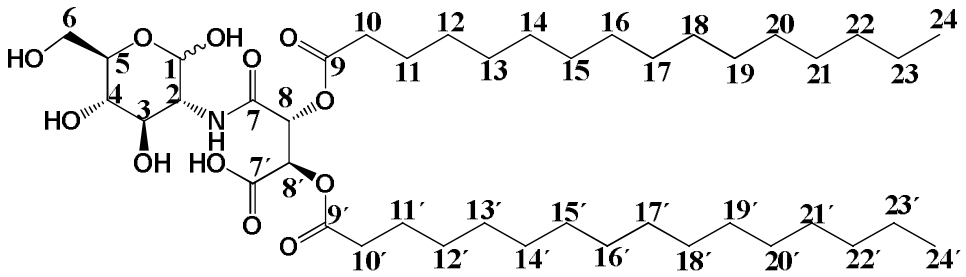

^{1}H NMR (400 MHz, acetone-d_6) δ = 5.64 (m, 2H, H-**8** and H-**8′**), 5.07 (d, *J* = 3.6 Hz 1H, H-**1*α***), 3.72 (s, 4H, H-**3**, H-**5**, H-**6**, H-**6**′), 3.50 – 3.16 (m, 2H, H-**2**, H-**4**), 2.41 (m, 4H, H-**10** and H-**10′**), 1.63 (m, 4H, H-**11** and H-**11′**), 1.32 (m, 48H, H-**12** to H-**23** and H-**12′** to H-**23′**), 0.91 (m, 6H, H-**24** and H-**24′**) ppm.

^{13}C NMR (101 MHz, acetone-d_6) δ = 173.70, 173.45, 169.13, 167.74 (C-**7**, C-**9**, C-**9′, C-7′**), 93.15 (C-**1**), 73.94 (C-**5**), 73.89, 73.72 (C-**8** and C-**8′**), 73.54 (C-**4**), 72.41 (C-**3**), 63.65 (C-**6**), 56.03 (C-**2**), 35.25, 34.99, 33.51, 31.19, 31.13, 31.08, 31.02, 30.97, 30.89, 30.50, 30.26, 26.51, 26.35, 24.18, 15.23 ppm.

HRMS (ESI$^-$, m/z, [M−H]$^-$) calculated for $C_{42}H_{76}NO_{12}$: 786.5368 Found: 786.5373

5.13.4 (2*S*)-2-(Dodecanoyloxy)-4-oxo-4-(((3*R*,4*R*,5*S*)-2,4,5-trihydroxy-6-(hydroxymethyl)tetrahydro-2H-pyran-3-yl)amino)butanoic acid (25)

In a 100 mL round bottom flask equipped with a magnetic stirrer bar 2 g (0.009 mol) of *D*-glucosamine hydrochloride and 75 mL DMF were added and the mixture was stirred for an hour and then dry pyridine (0.73 mL, 0.009 mol) was added to the mixture with stirring under an argon atmosphere. The reaction was further continued at room temp for the next 12 h for the deprotonation of *D*-glucosamine hydrochloride. The thus *in situ* prepared solution of *D*-glucosamine in DMF was used without further purification. To this solution of *D*-glucosamine (1.6 g, 0.009 mol) in DMF 1.4 g (0.0047 mol) of *O*-lauroyl malic acid anhydride (**3)** was added and then the reaction was continued to 0 °C under ice-water bath with stirring under argon. To the reaction mixture 0.38 mL (0.0047 mol) of pyridine was added. The reaction was allowed to continue to 0 °C for 2 h followed by an additional 12 h at room temperature. After completion of the reaction, the mixture was poured into a conical flask containing ice-water mixture and then 2 N HCl was added at 0 °C under vigorous stirring to neutralize the excess pyridine. The product was extracted with ethyl acetate (2 × 250 mL) and then the combined organic fractions were washed with brine and dried over sodium sulphate. The organic solvent was removed under reduced pressure to obtain the crude product. The crude product was dissolved in a minimum amount of acetonitrile and the solution was kept at room for 2 d

temperature leading to the precipitation of **25**. The precipitate was filtered and dried to obtain pure **25** in a yield of 1.3 g (59%, only *α* anomer).

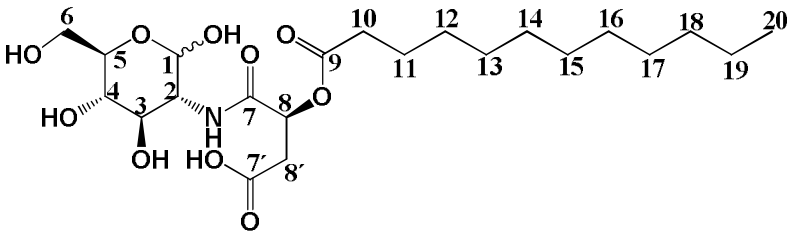

^{1}H NMR (400 MHz, MeOH-d_4) δ = 5.63 (dd, *J* = 8.0, 4.5 Hz, 1H, H-**8**), 5.28 (d, *J* = 3.3 Hz, 1H, H-**1*α***), 4.05 (dd, *J* = 10.5, 3.4 Hz, 1H, H-**2*α***), 3.83 (m, 4H, H-**3*α***, H-**5*α***, H-**6*α***, H-**6′*α***), 3.50 (dd, *J* = 3.1, 1.5 Hz, 1H, H-**4*α***), 3.27 – 2.80 (m, 2H, H-**8′**), 2.76 – 2.33 (m, 2H, H-**10**), 2.00 – 1.70 (m, 2H, H-**11**), 1.67 – 1.30 (m, 16H, H-**12** to H-**19**), 1.08 (t, *J* = 5.3 Hz, 3H, H-**20**) ppm.

^{13}C NMR (101 MHz, MeOH-d_4) δ = 174.26, 173.06, 171.76 (C-**7**, C-**9,** C-**7′**), 92.40 (C-**1*α***), 73.13 (C-**5*α***), 72.90 (C-**4*α***), 72.41 (C-**3*α***), 71.47 (C-**8**), 62.92 (C-**6*α***), 55.89 (C-**2*α***), 37.56 (C-**8′**), 34.82, 32.95, 30.62, 30.44, 30.31, 30.27, 30.07, 25.82, 23.58, 14.29 ppm.

HRMS (ESI$^-$, m/z, [M−H]$^-$) calculated for $C_{22}H_{38}NO_{10}$: 476.2496 Found: 476.2506

5.13.5 (2*S*)-4-Oxo-2-(tetradecanoyloxy)-4-(((3*R*,4*R*,5*S*)-2,4,5-trihydroxy-6-(hydroxymethyl)tetrahydro-2H-pyran-3-yl)amino)butanoic acid (26)

In a 100 mL round bottom flask equipped with a magnetic stirrer bar 2 g (0.009 mol) of *D*-glucosamine hydrochloride and 75 mL DMF were added and the mixture was stirred for an hour and then dry pyridine (0.73 mL, 0.009 mol) was added to the mixture with stirring under argon atmosphere. The reaction was further continued at room temp for next 12 h for the deprotonation of *D*-glucosamine hydrochloride. The thus *in situ* prepared solution of *D*-glucosamine in DMF was used without further purification. To this solution of *D*-glucosamine (1.6 g, 0.009 mol) in DMF 1.5 g (0.0047 mol) of *O*-tetradecanoyl malic acid anhydride (**4**) was added and then the reaction was continued to 0 °C (ice-water bath) with stirring under argon. To the reaction mixture 0.38 mL (0.0047 mol) of pyridine was added. The reaction was allowed to continue to 0 °C for 2 h followed by an additional 12 h at room temperature. After completion of the reaction, the mixture was poured into a conical flask containing ice-water mixture and then 2 N HCl was added at 0 °C under vigorous stirring to neutralize the excess pyridine. The product was extracted with ethyl acetate (2 × 250 mL) and then the combined organic fractions were washed with brine, dried over sodium sulphate. The organic solvent was removed under reduced pressure to obtain the crude product. The crude product was

dissolved in a minimum amount of acetonitrile and then the solution was kept for 2 d at room temperature from which **26** precipitated. The precipitate was filtered and dried to obtain **26** in a yield of 1.5 g (65%, α/β = 7.2/1).

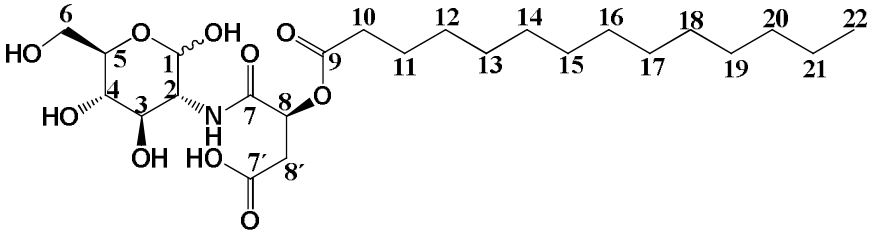

^{1}H NMR (400 MHz, MeOH-d_4) δ = 5.70 (dd, *J* = 8.0, 4.5 Hz, 1H, H-**8**), 5.35 (d, *J* = 3.3 Hz, 1H, H-**1*α***), 4.35 – 3.40 (m, 6H, H-**2*α***, H-**3*α***, H-**4*α***, H-**5*α***, H-**6*α***, H-**6′*α***), 3.34 – 2.87 (m, 2H, H-**8′**), 2.83 – 2.45 (m, 2H, H-**10**), 1.90 (m, 2H, H-**11**), 1.55 (m, 20H, H-**12** to H-**21**), 1.15 (t, *J* = 5.3 Hz, 3H, H-**22**) ppm.

^{13}C NMR (101 MHz, MeOH-d_4) δ = 174.55, 173.36, 172.05 (C-**7**, C-**9,** C-**7′**), 92.70 (C-**1*α***), 73.42 (C-**5*α***), 73.20 (C-**4*α***), 72.71 (C-**3*α***), 71.76 (C-**8**), 63.22 (C-**6*α***), 56.19 (C-**2*α***), 36.76 (C-**8′**), 34.57, 32.97, 30.71, 30.67, 30.50, 30.38, 30.31, 29.98, 25.78, 23.63, 14.43 ppm.

HRMS (ESI$^-$, m/z, $[M-H]^-$) calculated for $C_{24}H_{42}NO_{10}$: 504.2809 Found: 504.2827

5.13.6 (2*S*)-4-Oxo-2-(palmitoyloxy)-4-(((3*R*,4*R*,5*S*)-2,4,5-trihydroxy-6-(hydroxymethyl)tetrahydro-2H-pyran-3-yl)amino)butanoic acid (27)

In a 100 mL round bottom flask equipped with a magnetic stirrer 2 g (0.009 mol) of *D*-glucosamine hydrochloride and 75 mL DMF were added and the mixture was stirred for an hour and then dry pyridine (0.73 mL, 0.009 mol) was added to the mixture with stirring under argon. The reaction was further continued at room temp for next 12 h for the deprotonation of *D*-glucosamine hydrochloride. The thus *in situ* prepared solution of *D*-glucosamine in DMF was further used without purification. To this solution of *D*-glucosamine (1.8 g, 0.009 mol) in DMF 1.7 g (0.0047 mol) of *O*-palmitoyl malic acid anhydride (**5**) was added and then the reaction was continued at 0 °C under ice-water bath with stirring under argon. To the reaction mixture 0.38 mL (0.0047 mol) of pyridine was added. The reaction was allowed to continue to 0 °C for 2 h and an additional 12 h at room temperature. After completion of the reaction, the mixture was poured into a conical flask containing ice-water mixture and then 2 N HCl at 0 °C was added with vigorous stirring to neutralize the excess pyridine. The product was extracted with ethyl acetate (2 × 250 mL) and then the combined organic fractions were washed with brine and dried over sodium sulphate. The organic solvent was removed under

reduced pressure to obtain the crude product. The crude product was dissolved in a minimum amount of acetonitrile and then the solution was kept for 2 d at room temperature and then the precipitate was filtered off to obtain **27** with a yield of 1.6 g (63%, α/β = 8/1.

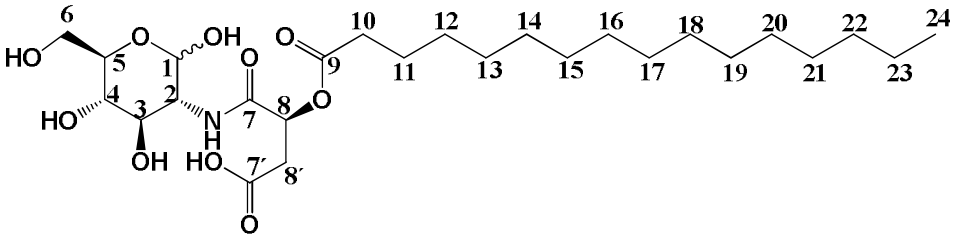

^{1}H NMR (400 MHz, MeOH-d_4) δ = 5.47 – 5.33 (m, 1H, H-**8**), 5.10 (d, 3.5 Hz, 1H, H-**1*α***), 3.91 – 3.84 (m, 1H, H-**2*α***), 3.84 – 3.64 (m, 4H, H-**3*α***, H-**5*α***, H-**6*α***, H-**6′*α***), 3.37 (t, *J* = 9.2 Hz, 1H, H-**4*α***), 2.94 – 2.72 (m, 2H, H-**8′**), 2.48 – 2.17 (m, 2H, H-**10**), 1.78 – 1.44 (m, 2H, H-**11**), 1.45 – 1.09 (m, 24H, H-**12** to H-**23**), 0.90 (t, *J* = 6.9 Hz, 3H, H-**24**) ppm.

^{13}C NMR (101 MHz, MeOH-d_4) δ = 174.58, 174.32, 173.30, 173.17, 171.97, 171.61 (C-**7**, C-**9**, C-**7′**), 92.66 (C-**1*β***), 92.49 (C-**1*α***), 78.01, 73.16, 73.05, 72.75, 72.47, 72.38, 71.37, 70.54 (C-**3*α***, C-**3*β***, C-**4*α***, C-**4*β***, C-**5*α***, C-**5*β***,C-**8**) 62.85 (C-**6*β***), 62.77 (C-**6*α***), 55.96 (C-**2*β***), 55.78 (C-**2*α***), 38.49 (C-**8′**), 37.49, 34.74, 34.67, 33.05, 30.77, 30.73, 30.62, 30.57, 30.44, 30.40, 30.12, 30.09, 25.86, 25.84, 23.70, 14.42 ppm.

HRMS (ESI$^-$, m/z, [M−H]$^-$) calculated for $C_{26}H_{46}NO_{10}$: 532.3122 Found: 532.3128

5.14 Syntheses of methyl-*α*-*D*-glucopyranoside based amphiphiles 28-30

5.14.1 (2*R*,3*R*)-2,3-Bis(dodecanoyloxy)-4-oxo-4-(((2*R*,3*S*,4*S*,5*R*,6*S*)-3,4,5-trihydroxy-6-methoxytetrahydro-2H-pyran-2-yl)methoxy)butanoic acid (28)

To a solution of methyl-*α*-*D*-glucopyranoside (15 g, 0.077 mol) in anhydrous DMF, *O*-*O′*-dilauroyl tartaric acid anhydride (**9)** (7.7 g, 0.015 mol) was added and the reaction mixture was stirred under an argon atmosphere for an hour. The reaction mixture was cooled to 0 °C, followed by addition of dry pyridine (1.21 mL, 0.015 mol) with stirring under argon. The reaction was further continued at 0 °C for the next 3 h followed by an additional 3 d at room temperature. The formation of the *O*-acylated methyl-*α*-*D*-glucopyranoside was confirmed by TLC and also HPLC-MS of the crude mixture. After completion of the reaction, the mixture was poured into a beaker containing 200 mL ice-water mixture, followed by addition of 2 N

HCl under vigorous stirring . The product was extracted with ethyl acetate (2 × 250 mL) and then the combined organic fractions were washed with brine solution (3 ×150 mL), dried over sodium sulphate and concentrated under reduced pressure to obtain the crude product (8.3 g, 77%). The crude product contains a mixture of mono-esters of methyl-*α*-*D*-glucopyranoside and the 6-*O*-acylated methyl-*α*-*D*-glucopyranoside (**28)** was isolated by silica gel column chromatography using methanol/ethyl acetate solvent mixture (20:80) for elution and characterised by NMR. Yield: 2.8 g (33%).

R_f value: 0.06 (MeOH/EtOAc = 20:80)

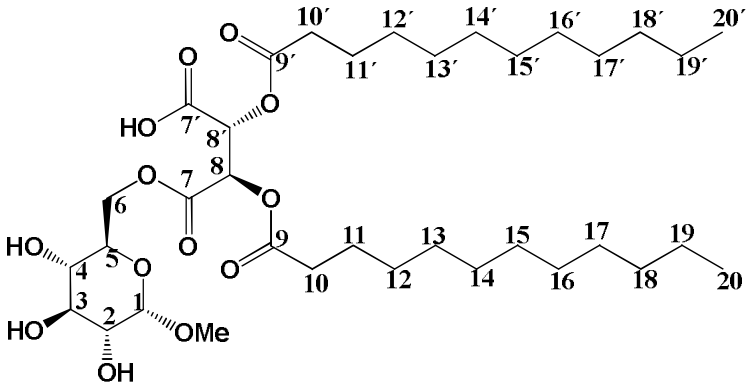

^{1}H NMR (400 MHz, MeOH-d_4) δ = 5.93 (d, *J* = 2.6 Hz, 1H, H-**8**), 5.77 (d, *J* = 2.5 Hz, 1H, H-**8´**), 4.98 – 4.81 (m, 1H, H-**1**), 4.70 (dd, *J* = 11.7, 1.9 Hz, 1H, H-**6**), 4.44 (dd, *J* = 11.7, 5.1 Hz, 1H, H-**6′**), 3.91 – 3.83 (m, 1H, H-**3**), 3.80 (t, *J* = 9.3 Hz, 1H, H-**5**), 3.64 – 3.59 (m, 1H, H-**2**), 3.58 (s, 3H, O**CH$_3$**), 3.55 – 3.50 (m, 1H, H-**4**), 2.69 – 2.37 (m, 4H, H-**10** and H-**10′**), 1.94 – 1.71 (m, 4H, H-**11** and H-**11′**), 1.62 – 1.25 (m, 32H, H-**12** to H-**19** and H-**12′** to H-**19′**), 1.08 (t, *J* = 6.8 Hz, 6H, H-**20** and H-**20′**) ppm.

^{13}C NMR (101 MHz, MeOH-d_4) δ = 174.13, 174.08, 168.21 (C-**9**, C-**9´**, C-**7** and C-**7**), 101.33 (C-**1**), 75.02 (C-**3**), 73.31 (C-**2**), 73.13 (C-**4**), 72.93(C-**8**), 71.54 (C-**8´**), 70.96 (C-**5**), 65.73 (C-**6**), 55.77 (O**CH$_3$**), 34.84, 34.61, 32.95, 30.63, 30.49, 30.47, 30.33, 30.28, 30.09, 30.02, 25.81, 23.59, 14.33 ppm.

HRMS (ESI$^-$, m/z, [M−H]$^-$) calculated for $C_{35}H_{61}O_{13}$: 689.4118 Found: 689.4108

5.14.2 (2*R*,3*R*)-4-Oxo-2,3-bis(tetradecanoyloxy)-4-(((2*R*,3*S*,4*S*,5*R*,6*S*)-3,4,5-trihydroxy-6-methoxytetrahydro-2H-pyran-2-yl)methoxy)butanoic acid (29)

To a solution of methyl-*α*-*D*-glucopyranoside (15 g, 0.077 mol) in anhydrous DMF, *O*-*O′*-ditetradecanoyl tartaric acid anhydride (**10)** (8.5 g, 0.015 mol) was added and the reaction

mixture was stirred under an argon atmosphere and then cooled to 0 °C, followed by addition of dry pyridine (1.24 mL, 0.015 mol) with stirring under argon. The reaction was further continued at 0 °C for the next 3 h followed by an additional 3 d at room temperature. The formation of the *O*-acylated methyl-*α*-*D*-glucopyranoside was confirmed by TLC and also HPLC-MS of the crude mixture. After completion of the reaction, the mixture was poured into a beaker containing 200 mL ice-water mixture, followed by addition of 2 N HCl to the mixture under vigorous stirring . The product was extracted with ethyl acetate (2 × 250 mL) and then the combined organic fractions were washed with brine solution (3 ×150 mL), dried over sodium sulphate and concentrated under reduced pressure to obtain the crude product (8.1 g, 71%). The crude product contains a mixture of mono-esters of methyl-*α*-*D*-glucopyranoside and the 6-*O*-acylated methyl-*α*-*D*-glucopyranoside (**29)** was isolated in the following manner: the crude mixture was dissolved in a minimum amount of acetonitrile under reflux conditions and then the solution was kept at room temp for 2 d. The 6-*O*-acylated methyl-*α*-*D*-glucopyranoside (**29**) was precipitated from the solution, filtered and dried under reduced pressure to yield 4.5 g (40%).

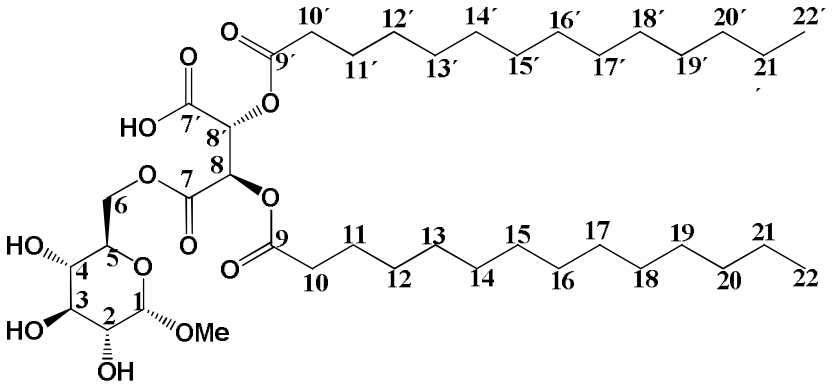

^{1}H NMR (400 MHz, MeOH-d_4) δ = 5.87 – 5.52 (m, 2H, H-**8**, H-**8′**), 4.87(m, 1H, H-**1**), 4.72 (m, 1H, H-**6**), 4.57 (m, 1H, H-**6′**), 4.22 (dd, *J* = 11.7, 4.8 Hz, 1H, H-**3**), 3.78 (m, 1H, H-**5**), 3.65 (m, 1H, H-**2**), 3.58 (t, *J* = 9.3 Hz, 1H, H-**4**), 3.42 – 3.23 (s, 3H, O**CH$_3$**), 2.38 (m, 4H, H-**10** and H-**10′**), 1.79 – 1.44 (m, 4H, H-**11** and H-**11′**), 1.30 (m, 40H, H-**12** to H-**21** and H-**12′** to H-**21′**), 0.88 (t, *J* = 6.8 Hz, 6H, H-**22** and H-**22′**) ppm.

^{13}C NMR (101 MHz, MeOH-d_4) δ = 173.72, 173.68, 168.91, 167.41 (C-**9**, C-**9′**, C-**7** and C-**7′**), 101.39 (C-**1**), 74.91(C-**3**), 73.22 (C-**2**), 72.13 (C-**4**), 71.85 (C-**8**), 71.33 (C-**8′**), 70.85 (C-**5**), 65.69 (C-**6**), 55.76 (O**CH$_3$**), 34.65, 34.54, 33.07, 30.81, 30.80, 30.78, 30.61, 30.58, 30.48, 30.43, 30.38, 30.08, 30.02, 25.91, 25.87, 23.72, 14.48 ppm.

HRMS (ESI$^-$, m/z, [M−H]$^-$) calculated for $C_{39}H_{69}O_{13}$: 745.4744 Found: 745.4742

5.14.3 (2R,3R)-4-Oxo-2,3-bis(palmitoyloxy)-4-(((2R,3S,4S,5R,6S)-3,4,5-trihydroxy-6-methoxytetrahydro-2H-pyran-2-yl)methoxy)butanoic acid (30)

To a solution of methyl-*α*-*D*-glucopyranoside (15 g, 0.077 mol) in anhydrous DMF *O*-*O′*-dipalmitoyl tartaric acid anhydride (**11)** (9.40 g, 0.015 mol) was added and the reaction mixture was stirred under an argon atmosphere and then cooled to 0 °C, followed by addition of pyridine (1.24 mL, 0.015 mol) with stirring the reaction mixture under argon. The reaction was further continued at 0 °C for next 3 h followed by an additional 3 d at room temperature. The formation of *O*-acylated methyl-*α*-*D*-glucopyranoside was confirmed by TLC and also HPLC-MS of the crude mixture. After completion of the reaction, the mixture was poured into a beaker containing 200 mL ice-water mixture, followed by addition of 2 N HCl to the mixture under vigorous stirring . The product was extracted with ethyl acetate (2 × 250 mL) and then the combined organic fractions were washed with brine solution (3 ×150 mL), dried over sodium sulphate and concentrated under reduced pressure to obtain the crude product (8.4 g, 68%). The crude product contains a mixture of mono-esters of methyl-*α*-*D*-glucopyranoside. The 6-*O*-acylated methyl *α*-*D*-glucopyranoside (**30)** was isolated from the crude mixture by silica gel column chromatography using methanol/ethyl acetate solvent mixture (20:80) as eluent with a yield of 2.6 g (32%). Besides the isolation of **30** by column chromatography it is also possible to selectively precipitate **30** (with trace amount of other regioisomers) in the following manner: the crude mixture was dissolved in a minimum amount of acetonitrile under reflux conditions and then kept at room temp for 2 d. **30** (90% purity) was precipitated from the mixture yielding 6.3 g (51%).

R_f value: 0.07 (MeOH:EtOAC = 20:80)

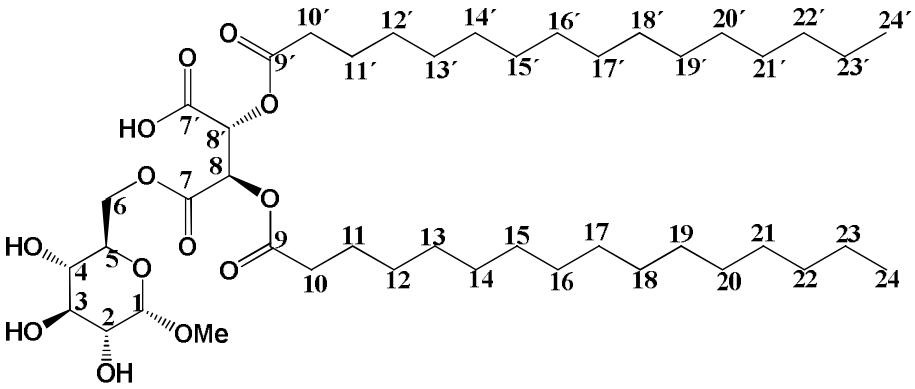

^{1}H NMR (400 MHz, MeOH-d_4) δ = 5.96 (d, *J* = 2.6 Hz, 1H, H-**8**), 5.75 (d, *J* = 2.6 Hz, 1H, H-**8′**), 4.82 (d, *J* = 3.7 Hz, 1H, H-**1*α***), 4.72 (dd, *J* = 11.7, 2.0 Hz, 1H, H-**6*α***), 4.46 (dd, *J* = 11.7, 5.1 Hz, 1H, H-**6′*α***), 3.98 – 3.85 (m, 1H, H-**3*α***), 3.82 (t, 1H, *J* = 9.2 Hz, H-**5*α***), 3.69 – 3.62 (m, 1H, H-**2*α***), 3.61 (s, 3H, O**CH$_3$**), 3.58 – 3.53 (m, 1H, H-**4*α***), 2.76 – 2.36 (m, 4H, H-**10** and H-

10′), 1.93 – 1.74 (m, 4H, H-**11** and H-**11′**), 1.68 – 1.41 (m, 48H, H-**12** to H-**23** and H-**12′** to H-**23′**), 1.11 (t, *J* = 6.8 Hz, 6H, H-**24** and H-**24′**) ppm.

^{13}C NMR (101 MHz, MeOH-d_4) δ = 174.36, 174.28, 168.55 (C-**9**, C-**9′,** C-**7** and C-**7′**), 101.40 (C-**1*α***), 75.07 (C-**3*α***), 73.39 (C-**2*α***), 73.32 (C-**4*α***), 71.60 (C-**8** and C-**8′**), 71.03 (C-**5*α***), 65.57 (C-**6*α***), 55.80 (O**CH$_3$**), 34.98, 34.69, 33.46, 32.99, 30.72, 30.68, 30.54, 30.39, 30.37, 30.18, 30.09, 25.86, 23.63, 14.34 ppm.

HRMS (ESI$^-$, m/z, [M−H]$^-$) calculated for $C_{43}H_{77}O_{13}$: 801.5370 Found: 801.5385

5.15 Syntheses of *D*-galactose based amphiphiles 35-37

5.15.1 1,2:3,4-Di-isopropylidene-*α*-*D*-galactopyranoside (31)

The synthesis of **31** was achieved using a literature procedure.[178] In a 250 mL two neck round bottom flask equipped with a dropping funnel fitted with calcium chloride tube and a reflux condenser containing a water cooling system, 185 mL dry acetone was added and cooled to 0 °C (ice-water bath) to which 5.5 mL of concentrated sulphuric acid was added from the dropping funnel under stirring at 0 °C. Then 10 g of anhydrous *D*-galactose was added under continuous stirring. The ice-water bath was removed and the mixture was kept at room temperature for 3-4 h. After completion of the reaction, the mixture was neutralised with sodium carbonate, filtered and evaporated under reduced pressure, yielding **31** as syrup, 13.4 g (93%).

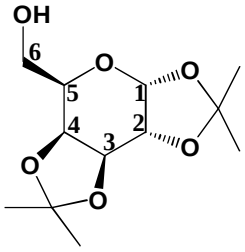

^{1}H NMR ($CDCl_3$,400 MHz) δ =5.53 (d, 3*J* = 5.0 Hz, 1H, H-**1***α*), 4.60 (dd, 3*J* = 2.4, 7.9 Hz, 1H, H-**3***α*), 4.39 (dd, 3*J* = 1.8, 7.9 Hz, 1H, H-**2***α*), 4.29 (dd, 3*J* = 2.4, 5.0 Hz, 1H, H-**4***α*), 3.93 (td, 3*J* = 1.8, 7.0 Hz, 1H, H-**5***α*), 3.31 (dd, 2*J* = 9.9 Hz, 3*J* = 7.0 Hz, 1H, H-**6***α*), 3.20 (dd, 2*J* = 9.9 Hz, 3*J* = 7.0 Hz, 1H, H-**6′***α*), 1.53 (s, 3H), 1.43 (s, 3H),1.34 (s, 3H), 1.32 (s, 3H) ppm.

^{13}C NMR (101 MHz, $CDCl_3$) δ = 109.62 (**C**Me$_2$), 108.83 (**C**Me$_2$), 96.48(C-**1*α***), 71.70, 70.96 (C-**2*α***, C-**4*α***) 70.81(C-**3*α***), 68.42(C-**5*α***), 62.34(C-**6*α***) ppm.

5.15.2 6-*O*-(*O*-*O′*-Di-lauroyl-tartaryl)-1,2:3,4-di-isopropylidene-*α*-*D*-galactopyranoside (32)

In a 100 mL round bottom flask equipped with a magnetic stirrer bar **31** (1 g, 3.84 mmol) was dissolved in 30 mL chloroform and then 2.1 g (4.23 mmol) of *O*-*O′*-di-lauroyl-tartaric acid anhydride (**9**) was added. The mixture was stirred to bring the anhydride into solution and then 0.34 mL of pyridine (4.23 mmol) was added. The reaction was continued at rt for 12 h. After completion, the chloroform was removed under reduced pressure to obtain the crude product of **32** as pyridinium salt in almost quantitative yield (3.5 g).

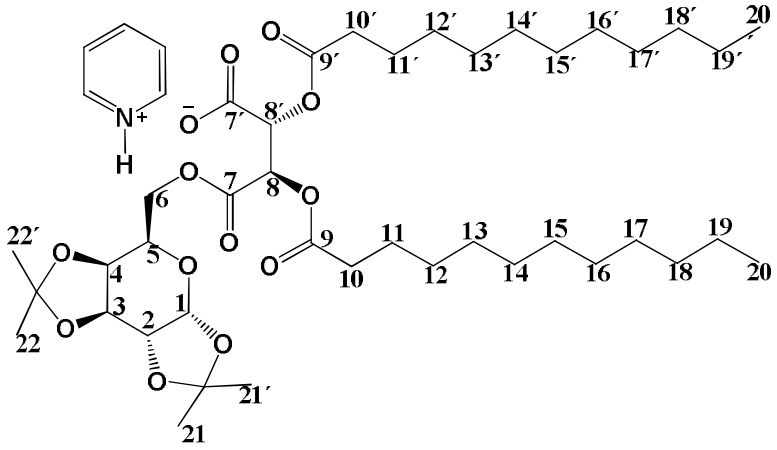

^{1}H NMR ($CDCl_3$,400 MHz) δ = 5.65 (m, 2H, H-**8** and H-**8′**), 5.48 (d, 3*J* = 5.0 Hz, 1H, H-**1***α*), 4.58 (dd, 3*J* = 2.4, 7.9 Hz, 1H, H-**3***α*), 4.30 (dd, 3*J* = 1.8, 7.9 Hz, 1H, H-**2***α*), 4.24 (dd, 3*J* = 2.4, 5.0 Hz, 1H, H-**4***α*), 4.17 (dd, 2*J* = 9.9 Hz, 3*J* = 7.0 Hz, 1H, H-**6***α*), 4.09 (dd, 2*J* = 9.9 Hz, 3*J* = 7.0 Hz, 1H, H-**6′***α*), 3.95 (td, 3*J* = 1.8, 7.0 Hz, 1H, H-**5***α*), 2.36 (m, 4H, H-**10** and H-**10′**), 1.60 (m, 4H, H-**11** and H-**11′**), 1.55-1.32 (m, 12H, H-**21**, H-**21′**, H-**22**, H-**22′**), 1.24 (m, 32H, H-**12** to H-**19**, H-**12′** to H-**19′**), 0.86 (t, 6H, H-**20** and H-**20′**) ppm.

^{13}C NMR (101 MHz, $CDCl_3$) δ = 179.91, 172.48 (C-**9** and C-**9′**), 169.71 (C-**7**), 165.73 (C-**7′**), 109.67 (CMe_2), 108.87 (CMe_2), 96.16(C-**1***α*), 71.61, 70.68, 70.56, 70.36, 70.24 (C-**2***α*, C-**3***α*, C-**4***α*, C-**8**, C-**8′**), 65.37 (C-**5***α*), 64.54 (C-**6***α*), 33.91, 33.56, 31.82, 29.51, 29.49, 29.37, 29.32, 29.23, 29.14, 28.96, 28.89, 25.79, 25.76, 24.76, 24.62, 24.60, 24.53, 24.33, 22.56, 13.96 ppm.

5.15.2.1 6-*O*-(*O*-*O′*-Di-lauroyl-tartaryl)-*D*-galactopyranoside (35)

1 g (1.32 mmol) of **32** was placed into a 100 mL round bottom flask and then 10 mL of 90% (v/v) trifluoroacetic acid in water was added and the mixture was shaken for 12 h at rt. The product precipitated from the mixture, was filtered and washed with chloroform and *n*-hexane to obtain **35** with a yield of 0.73 g (82%).

The reaction time for the deprotection reaction can be reduced from 12 h to 2-3 h by heating the reaction mixture at 50 °C. However at 50 °C interconversion of 6-*O*-acyl-*D*-galactopyranose to the five membered furanoside is observed.

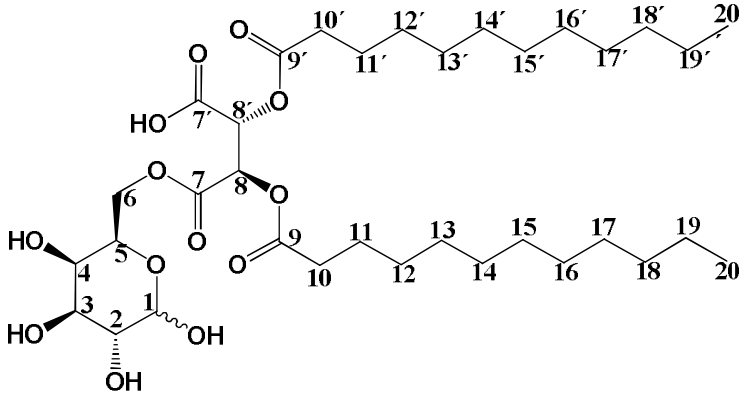

^{1}H NMR (400 MHz, MeOH-d_4) δ = 5.79 – 5.56 (m, 2H, H-**8**, H-**8′**), 5.13 (d, *J* = 3.4 Hz, 1H, H-**1***α*), 4.31 (m, 1H, H-**3**), 4.30 – 4.09 (m, 2H, H-**6**, H-**6′**), 3.85 – 3.63 (m, 2H, H-**4**, H-**5**), 3.51 – 3.38 (m, 1H, H-**2**), 2.40 (t, *J* = 6.9 Hz, 4H, H-**10**, H-**10′**), 1.74 – 1.49 (m, *J* = 6.3 Hz, 4H, H-**11**, H-**11′**), 1.43 – 1.09 (m, 32H, H-**12** to H-**19**, H-**12′** to H-**19′**), 0.88 (t, *J* = 6.7 Hz, 6H, H-**20**, H-**20′**) ppm.

^{13}C NMR (101 MHz, MeOH-d_4) δ = 173.98, 173.96, 173.86, 173.84, 168.91, 167.59 (C-**9**, C-**9′**, C-**7**, C-**7′**), 98.70 (C-**1***β*), 94.23 (C-**1***α*), 74.78 (C-**5***β*), 73.62 (C-**3***β*), 73.57 (C-**2***β*), 72.20 (C-**4***α*), 71.82 (C-**3***α*), 71.74 (C-**4***β*), 70.94 (C-**2***α*), 70.29, 70.25 (C-**8**, C-**8′**), 68.92 (C-**5***α*), 66.51 (C-**6***β*), 66.31 (C-**6***α*), 34.56, 34.52, 33.03, 30.72, 30.57, 30.53, 30.43, 30.36, 30.33, 30.01, 29.99, 25.88, 23.68, 14.42 ppm.

5.15.3 6-*O*-(*O*-*O′*-Di-tetradecanoyl-tartaryl)-1,2:3,4-di-isopropylidene-*α*-*D*-galactopyranoside (33)

In a 100 mL round bottom flask equipped with a magnetic stirrer **31** (1 g, 3.84 mmol) was dissolved in 30 mL chloroform and then 2.3 g (4.23 mmol) of *O*-*O′*-di-tetradecanoyl tartaric acid anhydride (**10)** was added. The reaction mixture was stirred to bring all anhydride into solution and then 0.34 mL (4.23 mmol) of pyridine was added. The reaction was continued at rt for 12 h. After completion the chloroform was removed under reduced pressure to obtain crude **33** as pyridinium salt (3.7 g) in almost quantitative yield.

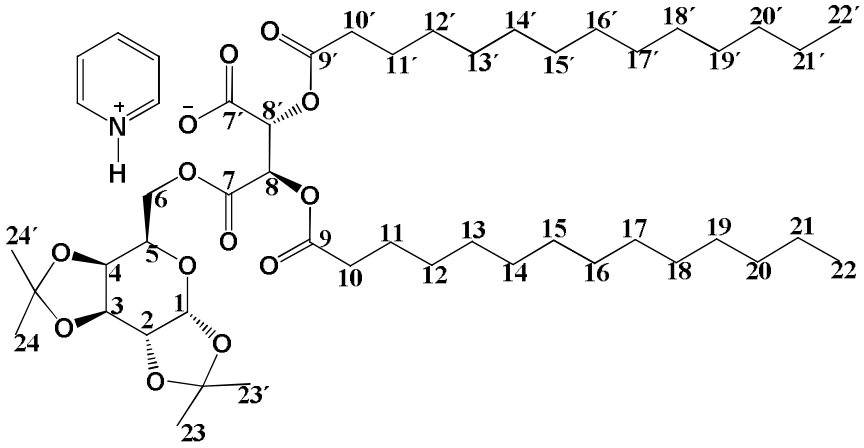

^{1}H NMR ($CDCl_3$,400 MHz) δ = 5.61 (m, 2H, H-**8** and H-**8′**), 5.48 (d, 3*J* = 4.7 Hz, 1H, H-**1***α*), 4.59 (dd, 3*J* = 2.7, 7.8 Hz, 1H, H-**3***α*), 4.32 (dd, 3*J* = 1.8, 7.3 Hz, 1H, H-**2***α*), 4.22 (m, H-**4***α*), 4.19 (dd, 2*J* = 9.9 Hz, 3*J* = 7.0 Hz, 1H, H-**6*α***), 4.12 (dd, 2*J* = 9.9 Hz, 3*J* = 7.0 Hz, 1H, H-**6′***α*), 3.99 (m, H-**5***α*), 2.36 (m, 4H, H-**10** and H-**10′**), 1.63 (m, 4H, H-**11** and H-**11′**), 1.55-1.32 (m, 12H, H-**23**, H-**23′**, H-**24**, H-**24′**), 1.27 (m, 40H, H-**12** to H-**21**, H-**12′** to H-**21′**), 0.86 (t, 6H, H-**22** and H-**22′**) ppm.

^{13}C NMR (101 MHz, $CDCl_3$) δ = 179.96, 172.43 (C-**9** and C-**9′**), 169.76 (C-**7**), 165.79 (C-**7′**), 109.75 (CMe_2), 108.78 (CMe_2), 96.26(C-**1***α*), 71.59, 70.63, 70.57, 70.33, 70.22 (C-**2***α*, C-**3***α*, C-**4***α*, C-**8**, C-**8′**), 65.39 (C-**5***α*), 64.49 (C-**6***α*), 33.91, 33.56, 31.82, 29.51, 29.49, 29.37, 29.32, 29.23, 29.14, 28.96, 28.89, 25.79, 25.76, 24.76, 24.62, 24.60, 24.53, 24.33, 22.56, 13.96 ppm.

5.15.3.1 6-*O*-(*O*-*O′*-Di-tetradecanoyl-tartaryl)-*D*-galactopyranoside (36)

3.7 g (4.6 mmol) of **33** was placed into a 100 mL round bottom flask and 15 mL of 90% (v/v) trifluoroacetic acid in water was added. The mixture was stirred at room temperature for 12 h. The product precipitated from the mixture was filtered and washed with chloroform and *n*-hexane to obtain **36** with a yield of 2.7 g (79%).

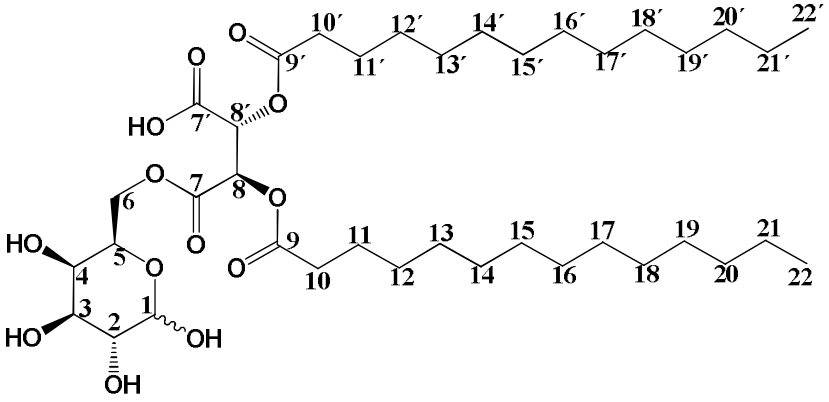

^{1}H NMR (400 MHz, MeOH-d_4) δ = 5.76 – 5.52 (m, 2H, H-**8**, H-**8′**), 5.09 (d, *J* = 3.7 Hz, 1H, H-**1***α*), 4.28 (m, 1H, H-**3**), 4.30 – 4.12 (m, 2H, H-**6**, H-**6′**), 3.86 – 3.57 (m, 2H, H-**4**, H-**5**), 3.51 – 3.38 (m, 1H, H-**2**), 2.47 (t, *J* = 6.7 Hz, 4H, H-**10**, H-**10′**), 1.77 – 1.53 (m, *J* = 6.3 Hz, 4H, H-**11**, H-**11′**), 1.47 – 1.12 (m, 40H, H-**12** to H-**21**, H-**12′** to H-**21′**), 0.87 (t, *J* = 6.9 Hz, 6H, H-**22**, H-**22′**) ppm.

^{13}C NMR (101 MHz, MeOH-d_4) δ = 173.99, 173.91, 173.89, 173.81, 168.88, 167.57 (C-**9**, C-**9′**, C-**7**, C-**7′**), 98.77 (C-**1***β*), 94.27 (C-**1***α*), 74.87 (C-**5***β*), 73.65 (C-**3***β*), 73.59 (C-**2***β*), 72.23 (C-**4***α*), 71.86 (C-**3***α*), 71.77 (C-**4***β*), 70.96 (C-**2***α*), 70.29, 70.23 (C-**8**, C-**8′**), 68.95 (C-**5***α*), 66.52 (C-**6***β*), 66.35 (C-**6***α*), 34.56, 34.52, 33.03, 30.72, 30.57, 30.53, 30.43, 30.36, 30.33, 30.01, 29.92, 25.89, 23.64, 14.49 ppm.

5.15.4 6-*O*-(*O*-*O′*-Di-palmitoyl-tartaryl)-1,2:3,4-di-isopropylidene-*α*-*D*-galactopyranoside (34)

In a 100 mL round bottom flask equipped with a magnetic stirrer **31** (1 g, 3.84 mmol) was dissolved into 30 mL chloroform and then 2.6 g (4.23 mmol) of *O*-*O′*-di-palmitoyl tartaric acid anhydride (**11)** was added. The reaction mixture was stirred to bring all anhydride into solution and then 0.34 mL (4.23 mmol) of pyridine was added. The reaction was continued at rt for 12 h. After completion the chloroform was removed under reduced pressure to obtain crude **34** as pyridinium salt (3.9 g) in almost quantitative yield.

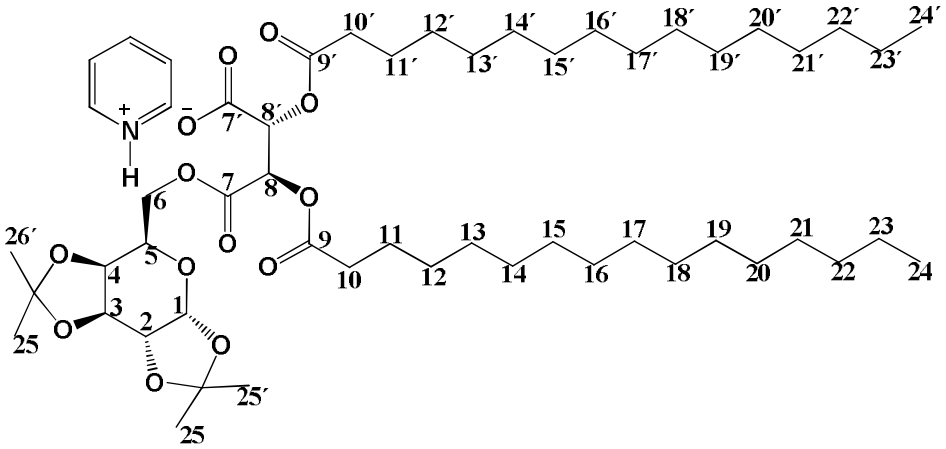

5.15.4.1 6-*O*-(*O*-*O′*-Di-palmitoyl-tartaryl)-*D*-galactopyranoside (37)

3.9 g (4.5 mmol) of crude **34** was placed into a 100 mL round bottom flask and 15 mL of 90% (v/v) trifluoroacetic acid in water was added. The mixture was stirred at rt for 12 h. The product precipitated from the mixture, was filtered and washed with chloroform and *n*-hexane to obtain pure **37** with a yield of 2.6 g (74%).

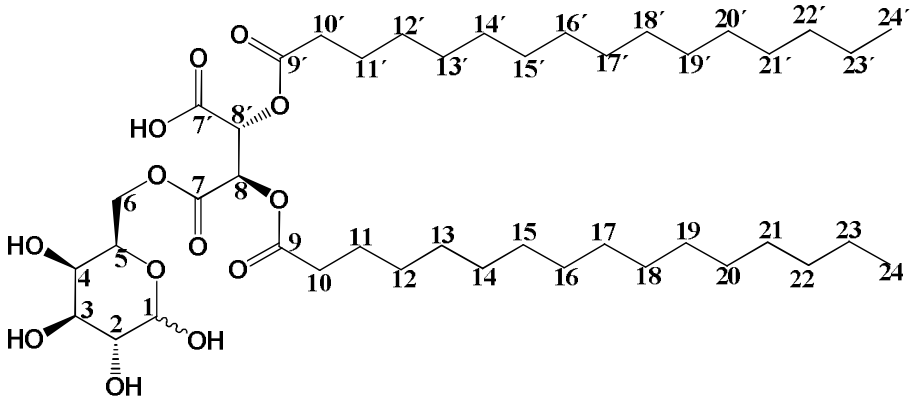

^{1}H NMR (400 MHz, MeOH-d_4) δ = 5.78 – 5.63 (m, 2H,H-**8**, H-**8′**), 5.14 (d, *J* = 3.5 Hz, 1H, H-**1*α***), 4.38 – 4.31 (m, 1H, H-**3**), 4.31 – 4.14 (m, 2H, H-**6**, H-**6′**), 3.87 – 3.62 (m, 2H, H-**4**, H-**5**), 3.52 – 3.38 (m, 1H, H-**2**), 2.41 (t, *J* = 7.2 Hz, 4H, H-**10**, H-**10′**), 1.72 – 1.55 (m, 4H, H-**11**, H-**11′**), 1.50 – 1.06 (m, 48H, H-**12** to H-**23** and H-**12′** to H-**23′**), 0.89 (t, *J* = 6.2 Hz, 6H, H-**24**, H-**24′**) ppm.

^{13}C NMR (101 MHz, MeOH-d_4) δ = 174.00, 173.89, 173.86, 168.90, 167.63 (C-9, C-9′, C-7, C-7′), 98.74 (C-**1*β***), 94.26 (C-**1*α***), 74.81 (C-**5*β***), 73.70 (C-**3*β***), 73.57 (C-**2*β***) 72.25 (C-**4*α***), 71.87 (C-**3*α***), 71.80 (C-**4*β***), 71.01 (C-**2*α***), 70.93, 70.35 (C-**8**, C-**8′**),69.00 (C-**5*α***), 66.48 (C-**6β**), 66.27 (C-**6*α***), 34.62, 34.57, 32.98, 30.71, 30.67, 30.52, 30.48, 30.36, 30.31, 30.28, 29.99, 25.86, 23.62, 14.34 ppm.

5.16 Syntheses of sucrose based amphiphiles 38-43

5.16.1 Reaction product 38a-c resulting from sucrose and *O-O′*-di-lauroyl tartaric acid anhydride (9)

In a 250 mL round bottom flask equipped with a magnetic stirrer, 20 g of sucrose (0.058 mol) and 150 mL anhydrous DMF were mixed and stirred under an argon atmosphere. To this, 5.8 g (0.012 mol) of **9** was added with stirring under argon. The reaction mixture was cooled to 0 °C and 0.94 mL (0.012 mol) of dry pyridine was added. Stirring was continued under an argon atmosphere at 0 °C for the next 3 h, followed by an additional 3 d at rt. After completion of the reaction, the mixture was poured into a 500 mL Erlenmayer flask containing 150 mL ice-water mixture to which 2 N HCl was added under vigorous stirring. The obtained reaction mixture was extracted with ethyl acetate (2 × 250 mL) and the combined organic fractions were washed with brine (3 × 150 mL), dried over Na_2SO_4, filtered and the solvent was removed under reduced pressure to obtain the crude product (8.7 g, 89%). This was partially dissolved in 75 mL acetonitrile under reflux condition and kept at room

temperature for 2 d. The precipitate was filtered to remove lauric acid and dried under reduced pressure to obtain pure **38a-c** (6.4 g, 65%). The crude product contains a mixture of diastereomers (mono-acylated fatty acid esters of sucrose) which is highly enriched in 6-*O*-acyl sucrose (over 80%) and minor quantities of 6′-*O*-acyl sucrose and 1′-*O*-acyl sucrose.
From the crude mixture 6-*O*-(*O*-*O′*-di-lauroyl-tartaryl)-sucrose and 6′-O-(*O*-*O′*-di-lauroyl-tartaryl)-sucrose were isolated by silica gel column chromatography using a mixture of methanol/ethyl acetate (10:90) as eluent.

^{1}H NMR (400 MHz, MeOH-d_4) δ = 5.81 (d, *J* = 11.5, 1H), 5.65 (d, *J* = 12.3, 1H), 5.52 – 5.33 (m, 1H), 4.64 – 3.41 (m, 13H), 2.65 – 2.29 (m, 4H), 1.89 – 1.55 (m, 4H), 1.54 – 1.14 (m, 32H), 0.98 (t, *J* = 6.0 Hz, 6H) ppm.

^{13}C NMR (101 MHz, MeOH-d_4) δ = 174.73, 174.64, 174.62, 174.55, 174.46, 168.71, 168.57, 105.68, 105.32, 93.69, 93.59, 83.86, 80.75, 79.71, 79.51, 76.90, 74.85, 74.57, 74.34, 73.71, 73.67, 73.38, 73.34, 73.06, 71.95, 71.65, 71.34, 68.12, 65.59, 64.41, 64.30, 63.63, 62.62, 34.98, 34.75, 33.17, 30.86, 30.71, 30.58, 30.53, 30.31, 30.23, 25.99, 23.83, 14.57ppm.

HRMS (ESI$^-$, m/z, [M-H]$^-$) calculated for $C_{40}H_{69}O_{18}$: 837.4484 Found: 837.4502

5.16.2 Reaction product 39a-c resulting from sucrose and *O-O′*-di-tetradecanoyl tartaric acid anhydride (10)

In a 250 mL round bottom flask equipped with a magnetic stirrer bar 20 g of sucrose (0.058 mol) and 150 mL anhydrous DMF were mixed and the mixture was stirred under an argon atmosphere. To this *O*-*O′*-di-tetradecanoyl tartaric acid anhydride (**10)** (6.5 g, 0.012 mol) was added with stirring under argon. The reaction mixture was cooled to 0 °C and 0.94 mL (0.012 mol) of dry pyridine was added. Stirring was continued under an argon atmosphere at 0 °C for the next 3 h, followed by an additional 3 d at rt. After completion of the reaction, the mixture was poured into a 500 mL Erlenmayer flask containing 150 mL ice-water mixture to which 2 N HCl was added under vigorous stirring. The obtained reaction mixture was extracted with ethyl acetate (3 × 250 mL) and the combined organic fractions were washed with brine (3 × 150 mL), dried over Na_2SO_4, filtered and the solvent was removed under reduced pressure to obtain the crude product (8.5 g, 81%). This was dissolved in a minimum amount of acetonitrile under reflux conditions and kept at room temperature for 2 d. The precipitate was filtered to remove tetradecanoic acid and dried under reduced pressure to obtain **39a-c** (3.4 g, 32%). The crude product contains a mixture of diastereomers (mono-acylated fatty acid esters

of sucrose) which is highly enriched in 6-*O*-acyl sucrose (over 80%) and minor amounts of 6′-*O*-acyl sucrose and 1′-*O*-acyl sucrose.
6-*O*-(*O*-*O′*-di-tetradecanoyl-tartaryl)-sucrose (**39a**) was isolated from the crude mixture by column chromatography using a mixture of methanol/ethyl acetate (20:80) as eluent.

^{1}H NMR (600 MHz, MeOH-d_4) δ = 5.91 – 5.50 (m, 2H), 5.27 (m, 1H), 4.75 – 2.91 (m, 13H), 2.35 (t, *J* = 6.5 Hz, 4H), 1.50 (m, 4H), 1.47 – 0.98 (m, 40H), 0.97 – 0.63 (t, *J* = 6.0 Hz, 6H) ppm.

HRMS (ESI$^-$, m/z, [M-H]$^-$) calculated for $C_{44}H_{77}O_{18}$: 893.5110, Found: 893.5117

5.16.3 Reaction product 40a-c resulting from sucrose and *O*-*O′*-di-palmitoyl tartaric acid anhydride (11)

In a 250 mL round bottom flask equipped with a magnetic stirrer bar 20 g sucrose (0.058 mol) and 150 mL anhydrous DMF were placed and the mixture stirred under an argon atmosphere. To this 7.1 g (0.012 mol) of *O*-*O′*-di-palmitoyl tartaric acid anhydride (**11)** was added with stirring under an argon atmosphere. The reaction mixture was cooled to 0 °C and 0.94 mL (0.012 mol) of dry pyridine was added. Stirring was continued under an argon atmosphere at 0 °C for the next 3 h, followed by an additional 3 d at rt. After completion of the reaction, the mixture was poured into a 500 mL Erlenmayer flask containing 150 mL ice-water mixture to which 2 N HCl was added under vigorous stirring. The obtained reaction mixture was extracted with ethyl acetate (3 × 250 mL) and the combined organic fractions were washed with brine (3 × 150 mL), dried over Na_2SO_4, filtered and the solvent was removed under reduced pressure to obtain the crude product (8.6 g, 77%). This was dissolved in a minimum amount of acetonitrile under reflux conditions and kept at room temperature for 2 d. The precipitate was filtered to remove palmitic acid and dried under reduced pressure to obtain **40a-c** (3.4 g, 32%). The crude product contains a mixture of diastereomers (mono-functionalised fatty acid esters of sucrose) which is highly enriched in 6-*O*-acyl sucrose (over 80%) and minor amounts of 6′-*O*-acyl sucrose and 1′-*O*-acyl sucrose.
6-*O*-(*O*-*O*-di-palmitoyl-tartaryl)-sucrose (**40a**) was isolated separately from the crude mixture by column chromatography using a mixture of methanol/ethyl acetate (10:90) as eluent.

^{1}H NMR (400 MHz, MeOH-d_4) δ = 5.80 (d, *J* = 14.5 Hz, 1H), 5.73 (d, *J* = 14.5 Hz, 1H), 5.40 (d, *J* = 3.4 Hz, 1H), 4.76 – 3.36 (m, 13H), 2.46 (t, *J* = 6.5 Hz, 4H), 1.80 – 1.45 (m, 4H), 1.45 – 1.25 (m, 48H), 0.94 (t, *J* = 6.0 Hz, 6H) ppm.

^{13}C NMR (101 MHz, MeOH-d_4) δ = 174.10, 173.88, 169.81, 167.70, 102.81, 98.18, 93.93, 77.88, 76.06, 75.09, 74.75, 73.56, 72.39, 71.51, 70.43, 66.12, 65.84, 64.76, 34.65, 34.53, 32.91, 30.65, 30.60, 30.47, 30.43, 30.29, 30.26, 30.23, 29.94, 25.77, 23.55, 14.31ppm.

HRMS (ESI$^-$, m/z, [M-H]$^-$) calculated for $C_{48}H_{85}O_{18}$: 949.5736, Found: 949.5723

5.16.4 Reaction product 41a-c resulting from sucrose and *O*-lauroyl malic acid anhydride (3)

In a 250 mL round bottom flask equipped with a magnetic stirrer bar 20 g of sucrose (0.058 mol) and 150 mL anhydrous DMF were placed and the mixture stirred under an argon atmosphere. To this 3.5 g (0.012 mol) of *O*-lauroyl malic acid anhydride (**3)** was added with stirring under argon. The reaction mixture was allowed to cool to 0 °C and then 0.94 mL (0.012 mol) of dry pyridine was added. Stirring was continued under an argon atmosphere at 0 °C for the next 3 h and then for an additional 12 h at rt. After completion, the mixture was poured into a 500 mL Erlenmayer flask containing 150 mL ice-water mixture to which 2 N HCl was added under vigorous stirring. The reaction mixture was extracted with ethyl acetate (2 × 250 mL) and the combined organic fractions were washed with brine (3 × 150 mL), dried over Na_2SO_4, filtered and the solvent was removed under reduced pressure to obtain the crude product (4.9 g, 66 %). The crude mixture was washed several times with *n*-hexane to remove lauric acid and dried under reduced pressure to obtain **41a-c** (4.2 g, 57%). The product contains a mixture of diastereomers (mono-acylated fatty acid esters of sucrose) which is highly enriched in 6-*O*-acyl sucrose (over 80%) and minor amounts of 6′-*O*-acyl sucrose and 1′-*O*-acyl sucrose, which are difficult to separate by silica gel column chromatography. Hence the mixture of mono-esterified diastereomers was used for the investigation of surface active properties.

HRMS (ESI$^-$, m/z, [M-H]$^-$) calculated for $C_{28}H_{47}O_{16}$: 639.2864, Found: 639.2884

5.16.5 Reaction product 42a-c resulting from sucrose and *O*-tetradecanoyl malic acid anhydride (4)

20 g of sucrose (0.058 mol) was allowed to react with 3.9 g (0.012 mol) of *O*-tetradecanoyl malic acid anhydride (**4)** as described for **41** (section 5.16.4) to obtain the crude product. The crude product was washed several times with *n*-hexane to remove tetradecanoic acid yielding **42a-c** (4.8 g, 61%) as a diastereomeric mixture of 6-*O*-acyl sucrose (over 80%) and minor amounts of 6′-*O*-acyl sucrose and 1′-*O*-acyl sucrose, which are not separable by silica gel

column chromatography. Hence the diastereomeric mixture was used for the investigation of surface active properties.

HRMS (ESI$^-$, m/z, [M-H]$^-$) calculated for $C_{30}H_{51}O_{16}$: 667.3177, Found: 667.3187

5.16.6 Reaction product 43a-c resulting from sucrose and *O*-palmitoyl malic acid anhydride (5)

20 g of sucrose (0.058 mol) was allowed to react with 4.3 g (0.012 mol) of *O*-palmitoyl malic acid anhydride (**5)** as described for **41** (section 5.16.4) to obtain the crude product. The crude product was washed several times with *n*-hexane to remove palmitic acid to obtain **43a-c** (4.9 g, 59%) as a diastereomeric mixture of 6-*O*-acyled sucrose (over 80%) and minor amounts of 6′-*O*-acyled sucrose and 1′-*O*-acyled sucrose which are not separable by silica gel column chromatography. Hence the diastereomeric mixture was used for the investigation of surface active properties.

HRMS (ESI$^-$, m/z, [M-H]$^-$) calculated for $C_{32}H_{55}O_{16}$: 695.3490, Found: 695.3463

5.17 Syntheses of ascorbic acid based amphiphiles 44-49

5.17.1 (*S*)-4-((*S*)-2-((*R*)-3,4-Dihydroxy-5-oxo-2,5-dihydrofuran-2-yl)-2-hydroxyethoxy)-3-(dodecanoyloxy)-4-oxobutanoic acid (44)

To a solution of 20 g *L*-ascorbic acid (0.114 mol) in 75 mL anhydrous DMF, 6.8 g of *O*-lauroyl malic acid anhydride (**3)** (0.023 mol)was added. The reaction mixture was cooled to 0 °C and 1.83 mL of dry pyridine (0.023 mol) was added. Stirring was continued under an argon atmosphere at 0 °C for 30 minutes followed by an additional 12 hours at room temperature. After completion the reaction mixture was poured into 2 N HCl at 0 °C under vigorous stirring. It was extracted with ethyl acetate and the organic fraction was washed 3 times with brine, dried over Na_2SO_4, filtered and the solvent was removed under reduced pressure. The residue was washed twice with *n*-hexane to obtain 9.4 g of **44** (87%) as white solid. The product was purged with nitrogen and stored frozen to prevent oxidation.

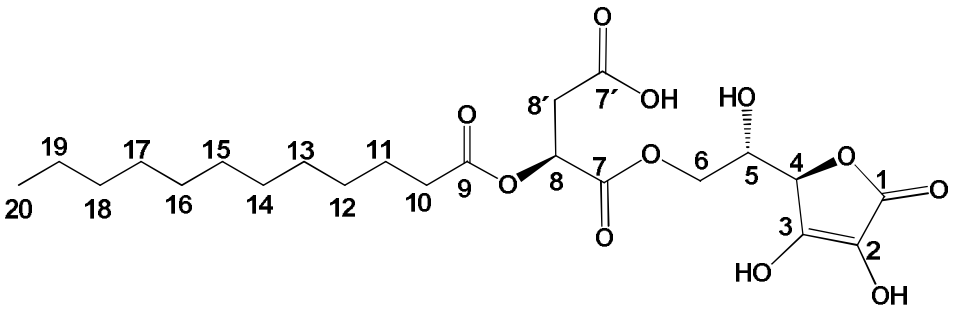

^{1}H NMR (400 MHz, MeOH-d_4) δ = 5.47 (dd, *J* = 7.1, 4.9 Hz, 1H, H-**8**), 4.76 (d, *J* = 2.1 Hz, 1H, H-**4**), 4.34 (dd, *J* = 6.4, 4.3 Hz, 2H, H-**6**, H-**6′**), 4.14 (td, *J* = 6.4, 2.1 Hz, 1H, H-**5**), 2.94 (dd, *J* = 6.0, 3.0 Hz, 2H, H-**8′**), 2.45 – 2.36 (m, 2H, H-**10**), 1.69 – 1.60 (m, 2H, H-**11**), 1.43 – 1.25 (m, 16H, H-**12** to H-**19**), 0.92 (t, *J* = 6.9 Hz, 3H, H-**20**) ppm.

^{13}C NMR (101 MHz, MeOH-d_4) δ = 174.33 (C-**7**), 173.04, 172.71, 170.34 (C-**9**, C-**1,** C-**7′**), 153.85 (C-**3**), 120.05 (C-**2**), 76.98 (C-**4**), 69.72 (C-**8**), 67.71 (C-**5**), 66.72 (C-**6**), 36.67 (C-**8′**), 34.58, 33.00, 30.67, 30.51, 30.40, 30.33, 30.01, 25.82, 23.67, 14.42 ppm.

HRMS (ESI$^-$, m/z, [M-H]$^-$) calculated for $C_{22}H_{33}O_{11}$: 473.2023. Found: 473.2016.

$[\alpha]^{20}_D$ -4.1 (c 0.6, MeOH).

5.17.2 (*S*)-4-((*S*)-2-((*R*)-3,4-Dihydroxy-5-oxo-2,5-dihydrofuran-2-yl)-2-hydroxyethoxy)-4-oxo-3-(tetradecanoyloxy)butanoic acid (45)

To a solution of 20 g *L*-ascorbic acid (0.114 mol) in 75 mL anhydrous DMF, 7.4 g of *O*-tetradecanoyl malic acid anhydride (0.023 mol) (**4**) was added. The reaction mixture was cooled to 0 °C and 1.83 mL of dry pyridine (0.023 mol) was added. Stirring was continued under an argon atmosphere at 0 °C for 30 minutes followed by an additional 12 hours at room temperature. After completion the reaction mixture was poured into 2 N HCl at 0 °C under vigorous stirring. This was extracted with ethyl acetate, the organic fraction was washed 3 times with brine, dried over Na_2SO_4, filtered, and the solvent was removed under reduced pressure. The residue was washed twice with *n*-hexane to obtain 9 g of **45** (79%) as white solid. The product was purged with nitrogen and stored frozen to prevent oxidation.

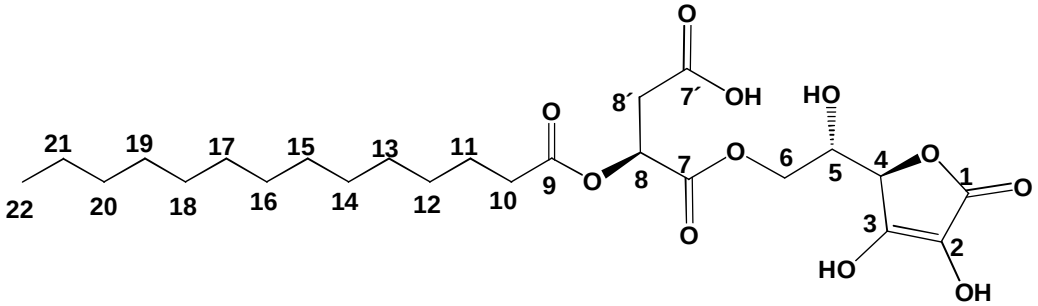

^{1}H NMR (600 MHz, MeOH-d_4) δ = 5.48 (dd, *J* = 7.5, 4.6 Hz, 1H, H-**8**), 4.76 (d, *J* = 2.1 Hz, 1H, H-**4**), 4.34 (dd, *J* = 8.2, 6.5 Hz, 2H, H-**6**, H-**6′**), 4.14 (td, *J* = 6.4, 2.0 Hz, 1H, H-**5**), 3.08 – 2.68 (m, 2H, H-**8′**), 2.51 – 2.33 (m, 2H, H-**10**), 1.65 (m, 2H, H-**11**), 1.53 – 1.09 (m, 20H, H-**12** to H-**21**), 0.92 (t, *J* = 7.1 Hz, 3H, H-**22**) ppm.

^{13}C NMR (151 MHz, MeOH-d_4) δ = 174.34 (C-**7**), 173.04, 172.71, 170.36 (C-**9**, C-**1,** C-**7′**), 153.86 (C-**3**), 120.08 (C-**2**), 77.00 (C-**4**), 69.74 (C-**8**), 67.74 (C-**5**), 66.73 (C-**6**), 36.70 (C-**8′**), 34.60, 33.02, 30.75, 30.71, 30.68, 30.53, 30.42, 30.33, 30.03, 25.83, 23.67, 14.41 ppm.

HRMS (ESI$^-$, m/z, [M-H]$^-$) calculated for $C_{24}H_{37}O_{11}$: 501.2341. Found: 501.2340.

$[\alpha]^{20}_D$ -1.4 (c 0.6, MeOH).

5.17.3 (*S*)-4-((*S*)-2-((*R*)-3,4-Dihydroxy-5-oxo-2,5-dihydrofuran-2-yl)-2-hydroxyethoxy)-4-oxo-3-(palmitoyloxy)butanoic acid (46)

To a solution of 20 g *L*-ascorbic acid (0.114 mol) in 75 mL anhydrous DMF 8.1 g (0.023 mol) of *O*-tetradecanoyl malic acid anhydride (**5)** was added. The reaction mixture was cooled to 0 °C and 1.85 mL of dry pyridine (0.023 mol) were added. Stirring was continued under an argon atmosphere at 0 °C for 30 minutes followed by an additional 12 hours at room temperature. After completion the reaction mixture was poured into 2 N HCl at 0 °C under vigorous stirring. This was extracted with ethyl acetate and the organic fraction was washed 3 times with brine, dried over Na_2SO_4, filtered and the solvent was removed under reduced pressure. The residue was washed twice with *n*-hexane to obtain 10.1 g of **46** (84%) as white solid. The product was purged with nitrogen and stored frozen to prevent oxidation.

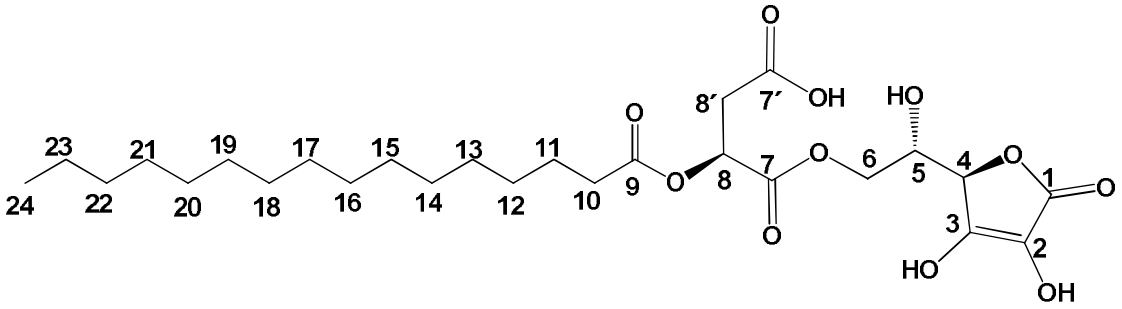

^{1}H NMR (400 MHz, MeOH-d_4) δ = 5.47 (dd, *J*=7.2, 4.9, 1H, H-**8**), 4.76 (d, *J*=2.1, 1H, H-**4**), 4.33 (dd, *J*=6.4, 4.4, 2H, H-**6**, H-**6′**), 4.14 (d, *J*=2.1, 1H, H-**4**), 2.94 (dd, *J*=6.0, 3.3, 2H, H-**8′**), 2.41 (t, *J*=7.3, 2H, H-**10**), 1.72 – 1.59 (m, 2H, H-**11**), 1.48 – 1.16 (m, 24H, H-**12** to H-**23**), 0.92 (t, *J*=6.8, 3H, H-**24**) ppm.

^{13}C NMR (101 MHz, MeOH-d_4) δ = 174.34 (C-**7**), 173.06, 172.71, 170.36 (C-**9**, C-**1,** C-**7′**), 153.86 (C-**3**), 120.08 (C-**2**), 77.00 (C-**4**), 69.74 (C-**8**), 67.73 (C-**5**), 66.74 (C-**6**), 36.69 (C-**8′**), 34.61, 33.04, 30.76, 30.73, 30.70, 30.55, 30.44, 30.36, 30.05, 25.85, 23.69, 14.43 ppm.

HRMS (ESI$^-$, m/z, [M-H]$^-$) calculated for $C_{26}H_{41}O_{11}$: 529.2649. Found: 529.2653.

$[\alpha]^{20}_{D}$ -1.7 (c 0.6, MeOH).

5.17.4 (2*R*,3*R*)-4-((*S*)-2-((*R*)-3,4-Dihydroxy-5-oxo-2,5-dihydrofuran-2-yl)-2-hydroxyethoxy)-2,3-bis(dodecanoyloxy)-4-oxobutanoic acid (47)

To a solution of 20 g (0.114 mol) *L*-ascorbic acid in 75 mL anhydrous DMF 11.3 g (0.023 mol) of *O*-*O'*-di-lauroyl tartaric acid anhydride (**9)** was added. The reaction mixture was cooled to 0 °C and 1.83 mL (0.023 mol) of dry pyridine was added. Stirring was continued under an argon atmosphere at 0 °C for 30 minutes followed by 3 days at room temperature. After completion the reaction mixture was poured into 2 N HCl at 0 °C under vigorous stirring. This was extracted with ethyl acetate and the organic fraction was washed 3 times with brine, dried over Na_2SO_4, filtered and the solvent was removed under reduced pressure. The residue was dissolved in hot *n*-hexane and precipitated at rt. This process was repeated one more time to obtain 10.2 g of **47 (**67%) as white amorphous solid. The product was purged with nitrogen and stored frozen to prevent oxidation.

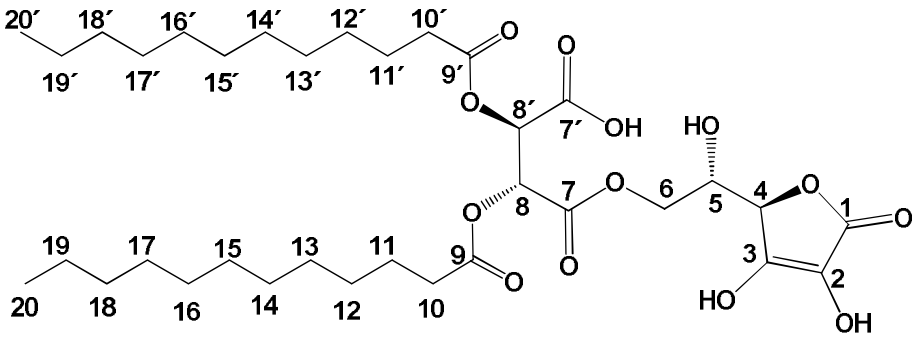

^{1}H NMR (600 MHz, acetone-d_6) δ = 5.80 (dd, *J* = 5.9, 2.9 Hz, 2H, H-**8**, H-**8′**), 4.80 (d, *J* = 2.2 Hz, 1H, H-**4**), 4.37 (dd, *J* = 6.5, 2.8 Hz, 2H, H-**6**, H′-**6**), 4.18 (td, *J* = 6.6, 2.0 Hz, 1H, H-**5**), 2.51 – 2.28 (m, 4H, H-**10**, H-**10′**), 1.72 – 1.56 (m, 4H, H-**11**, H-**11′**), 1.51 – 1.13 (m, 32H, H-**12** to H-**19**, H-**12′** to H-**19′**), 0.90 (t, *J* = 7.0 Hz, 6H, H-**20**, H-**20′**) ppm.

^{13}C NMR (101 MHz, MeOH-d_4) δ = 173.92, 173.86 (C-**9** and C-**9′**), 172.92, 168.91, 167.44 (C-**7**, C-**1,** C-**7′**), 153.67 (C-**3**), 120.12 (C-**2**), 76.88 (C-**4**), 72.19, 71.82 (C-**8** and C-**8′**), 67.90 (C-**5**), 67.08 (C-**6**), 34.53, 33.05, 30.74, 30.59, 30.54, 30.45, 30.40, 30.35, 30.02, 25.88, 25.81, 23.70, 14.44 ppm.

HRMS (ESI$^-$, m/z, $[M-H]^-$) calculated for $C_{34}H_{55}O_{13}$: 671.3643. Found: 671.3638.

$[\alpha]^{20}_{D}$ +10.4 (c 0.6, MeOH).

5.17.5 (2*R*,3*R*)-4-((*S*)-2-((*R*)-3,4-Dihydroxy-5-oxo-2,5-dihydrofuran-2-yl)-2-hydroxyethoxy)-4-oxo-2,3-bis(tetradecanoyloxy)butanoic acid (48)

To a solution of 20 g (0.114 mol) *L*-ascorbic acid in anhydrous DMF (75 mL) 12.6 g (0.023 mol) of *O*-*O*-di-tetradecanoyl tartaric acid anhydride (**10)** was added. The reaction mixture was cooled to 0 °C in an ice-water bath and 1.83 mL (0.023 mol) of dry pyridine was added. Stirring was continued under an argon atmosphere at 0 °C for 30 minutes followed by an additional 3 days at room temperature. After completion the reaction mixture was poured into 2 N HCl at 0 °C under vigorous stirring. The reaction mixture was extracted with ethyl acetate, the organic fraction was washed 3 times with brine, dried over Na_2SO_4, filtered and the solvent was removed under reduced pressure. The residue was dissolved in hot *n*-hexane and precipitated at rt. This process was repeated one more time to obtain 8.4 g (51%) of **48** as a while solid. The product was purged with nitrogen and stored frozen to prevent oxidation.

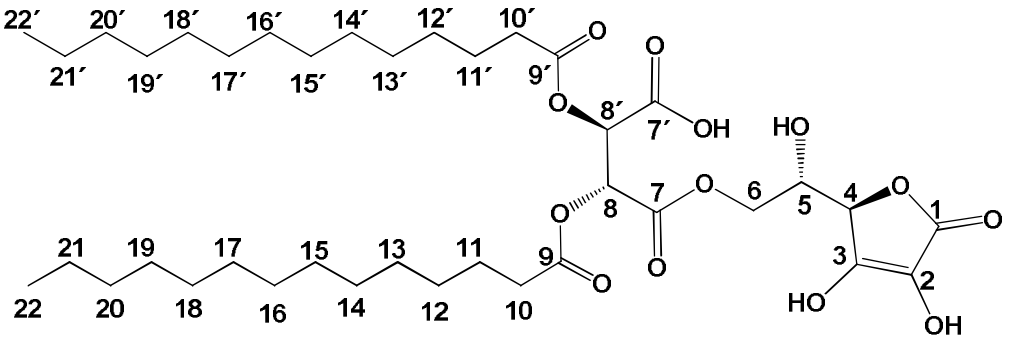

^{1}H NMR (600 MHz, acetone-d_6) δ = 5.79 (m, 2H, H-**8**, H-**8′**), 4.80 (d, *J* = 2.2 Hz, 1H, H-**4**), 4.37 (dd, *J* = 6.4, 3.8 Hz, 2H, H-**6**, H-**6′**), 4.18 (td, *J* = 6.5, 2.2 Hz, 1H, H-**5**), 2.48 – 2.25 (m, 4H, H-**10**, H-**10′**), 1.71 – 1.50 (m, 4H, H-**11**, H-**11′**), 1.51 – 1.05 (m, 40H, H-**12** to H-**21**, H-**12′** to H-**21′**), 0.90 (t, *J* = 7.0 Hz, 6H, H-**22**, H-**22′**) ppm.

^{13}C NMR (151 MHz, acetone-d_6) δ = 173.40, 170.93 (C-**9** and C-**9′**), 168.16, 168.03, 167.27 (C-**7**, C-**1,** C-**7′**), 151.51 (C-**3**), 120.78 (C-**2**), 76.58 (C-**4**), 72.22, 71.87 (C-**8**, C-**8′**), 68.18 (C-**5**), 67.55 (C-**6**), 34.80, 33.28, 31.25, 31.07, 31.04, 31.02, 30.89, 26.19, 26.15, 23.96, 23.96, 15.01ppm.

HRMS (ESI$^-$, m/z, [M-H]$^-$) calculated for $C_{38}H_{63}O_{13}$: 727.4274. Found: 727.4271.

$[\alpha]^{20}_D$ +7.2 (c 0.6, MeOH).

5.17.6 (2*R*,3*R*)-*4*-((*S*)-*2*-((*R*)-3,4-Dihydroxy-5-oxo-2,5-dihydrofuran-2-yl)-2-hydroxyethoxy)-4-oxo-2,3-bis(palmitoyloxy)butanoic acid (49)

To a solution of 20 g (0.114 mol) *L*-ascorbic acid in anhydrous DMF(75 mL), 13.8 g (0.023 mol) of *O*-*O'*-di-palmitoyl tartaric acid anhydride (**11)** was added. The reaction mixture was cooled to 0 °C in an ice-water bath and 1.83 mL (0.023 mol) of dry pyridine was added. Stirring was continued under an argon atmosphere at 0 °C for 30 minutes followed by an additional 3 days at room temperature. After completion the reaction mixture was poured into 2 N HCl at 0 °C under vigorous stirring. This was extracted with ethyl acetate and the organic fraction was washed 3 times with brine, dried over Na_2SO_4, filtered and the solvent was removed under reduced pressure. The residue was dissolved in hot *n*-hexane and precipitated at rt. This process was repeated one more time to obtain 11.2 g (63%) of **49** as a while solid. The product was purged with nitrogen and stored frozen to prevent oxidation.

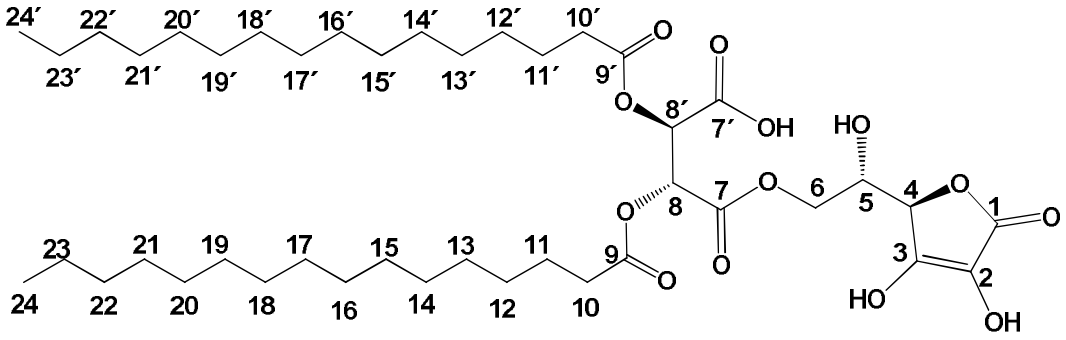

^{1}H NMR (400 MHz, acetone-d_6) δ = 5.81 – 5.77 (m, 2H, H-**8,** H-**8′**), 4.79 (d, *J* = 2.2 Hz, 1H, H-**4**), 4.37 (dd, *J* = 6.5, 3.8 Hz, 2H, H-**6**, H-**6′**), 4.19 (td, *J* = 6.4, 2.1 Hz, 1H, H-**5**), 2.46 – 2.38 (m, 4H, H-**10**, H-**10′**), 1.71 – 1.60 (m, 4H, H-**11**, H-**11′**), 1.53 – 1.11 (m, 48H, H-**12** to H-**23** and H-**12′** to H-**23′**), 0.90 (t, *J* = 6.8 Hz, 6H, H-**24**, H-**24′**) ppm.

^{13}C NMR (101 MHz, acetone-d_6) δ = 173.49, 173.48 (C-**9**, C-**9′**), 170.85, 168.13, 167.44 (C-**7**, C-**1,** C-**7′**), 151.48 (C-**3**), 121.01 (C-**2**), 76.69 (C-**4**), 72.40, 72.04 (C-**8**,C-**8′**), 68.44 (C-**5**), 67.68 (C-**6**), 34.96, 33.35, 31.25, 31.12, 31.08, 30.95, 30.92, 30.88, 30.76, 29.92, 26.29, 26.26, 24.01, 15.01 ppm.

HRMS (ESI$^-$, m/z, [M-H]$^-$) calculated for $C_{42}H_{71}O_{13}$:783.4895. Found: 783.4886.

$[\alpha]^{20}_D$ +4.4 (c 0.6, MeOH).

5.18 Syntheses of sorbitol based amphiphiles 50a,b–55a,b

5.18.1 *O*-Lauroyl malic acid *D*-sorbitol-6-yl ester and *O*-lauroyl malic acid *D*-sorbitol-1-yl ester (50a,b)

10 g (0.055 mol) of *D*-sorbitol was dissolved in 75 mL anhydrous DMF in a round bottom flask equipped with a magnetic stirrer. To this 3.27 g (0.011 mol) of *O*-lauroyl malic acid anhydride (**3)** was added and the reaction mixture was cooled to 0 °C under an argon atmosphere. Then 0.89 mL (0.011 mol) of dry pyridine was added with stirring under argon. The reaction was continued at 0 °C for 2-3 hours followed by an additional 12 hrs. at room temperature. The reaction was monitored by HPLC-MS of the crude mixture. After completion the reaction mixture was poured into a 250 mL Erlenmayer flask containing ice-water to which 2 N HCl was added under vigorous stirring. The product was extracted with ethyl acetate (2 × 250 mL) and then the combined organic fractions were washed with brine and dried over sodium sulphate. The organic solvent was removed under reduced pressure to afford the crude product. This contains a mixture of diastereomers consisting of the 6-*O* and 1-*O*-acylated fatty acid esters of *D*-sorbitol. The crude mixture was washed several times with *n*-hexane to obtain a mixture of **50a-b** (**50a**/**50b** = 0.96/1) with a combined yield of 3.8 g (72%).

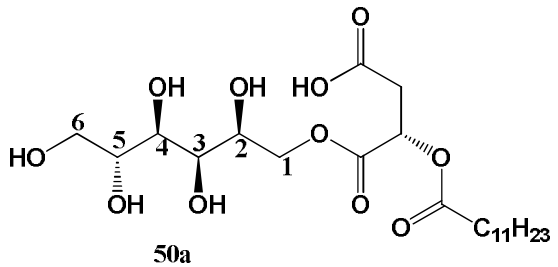

50a

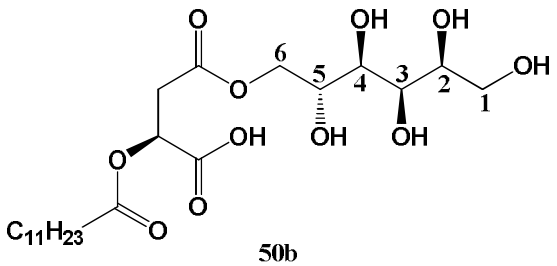

50b

^{1}H NMR (600 MHz, MeOH-d_4) δ = 5.58 – 5.29 (m, 1H), 4.40 (m, 1H), 4.33 – 4.22 (m, 1H), 4.04 – 3.90 (m, 1H), 3.90 – 3.86 (m, 1H), 3.85 – 3.75 (m, 1H), 3.71 (m, 1H), 3.69 – 3.55 (m, 2H), 3.02 – 2.86 (m, 2H), 2.48 – 2.33 (m, 2H), 1.77 – 1.54 (m, 2H), 1.40 – 1.26 (m, 16H), 0.92 (t, *J* = 7.1 Hz, 3H) ppm.

^{13}C NMR (151 MHz, MeOH-d_4) δ = 174.40, 172.92, 172.84, 170.83, 170.66, 74.97, 73.29, 73.21, 72.99, 72.32, 70.88, 70.57, 70.40, 69.91, 69.86, 68.60, 67.79, 64.73, 64.12, 36.78, 36.77, 34.62, 33.02, 30.69, 30.54, 30.42, 30.35, 30.03, 25.84, 23.68, 14.42 ppm.

HRMS (ESI$^-$, m/z, [M-H]$^-$) calculated for $C_{22}H_{39}O_{11}$: 479.2492. Found: 479.2488.

5.18.2 *O*-tetradecanoyl malic acid *D*-sorbitol-6-yl ester and *O*- tetradecanoyl malic acid *D*-sorbitol-1-yl ester (51a,b)

10 g (0.055 mol) of *D*-sorbitol was dissolved in 75 mL anhydrous DMF in a round bottom flask equipped with a magnetic stirrer. To this 3.6 g (0.011 mol) of *O*-tetradecanoyl malic acid anhydride (**4)** was added and the mixture cooled to 0 °C under an argon atmosphere, followed by the additional of 0.89 mL (0.011 mol) pyridine with stirring under argon. The reaction was continued at 0 °C for 2-3 hours, followed by an additional 12 hours at room temperature. The reaction was monitored by HPLC-MS of the crude mixture. After completion the reaction mixture was poured into a 250 mL Erlenmayer flask containing ice-water mixture to which 2 N HCl was added under vigorous stirring. The product was extracted with ethyl acetate (2 × 250 mL) and the combined organic fractions were washed with brine and dried over sodium sulphate. The organic solvent was removed under reduced pressure to afford the crude product. This was washed several times wish *n*-hexane to obtain a mixture of **51a-b** (**51a**/**51b** = 0.75/1) with a combined yield of 4.1 g (73%).

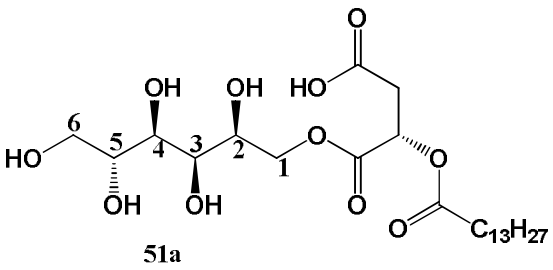

51a

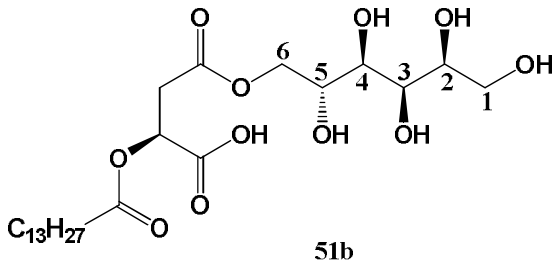

51b

^{1}H NMR (400 MHz, acetone-d_6) δ = 5.59 – 5.27 (m, 1H), 4.57 – 3.42 (m, 8H), 3.19 – 2.73 (m, 2H), 2.38 (t, *J* = 7.4 Hz, 2H), 1.78 – 1.51 (m, 2H), 1.46 – 1.18 (m, 20H), 0.89 (t, *J* = 6.7 Hz, 3H) ppm.

^{13}C NMR (101 MHz, MeOH-d_4) δ = 174.37, 172.86, 172.78, 170.80, 170.63, 74.97, 73.27, 73.20, 72.97, 72.32, 70.87, 70.57, 70.38, 69.87, 69.81, 68.59, 67.78, 64.73, 64.10, 36.71, 34.62, 33.03, 30.76, 30.73, 30.55, 30.44, 30.37, 30.04, 25.85, 23.69, 14.43 ppm.

HRMS (ESI$^-$, m/z, [M-H]$^-$) calculated for $C_{24}H_{43}O_{11}$: 507.2805. Found: 507.2815.

5.18.3 *O*-palmitoyl malic acid *D*-sorbitol-6-yl ester and *O*-palmitoyl malic acid *D*-sorbitol-1-yl ester (52a,b)

10 g (0.055 mol) of *D*-sorbitol was dissolved in 75 mL anhydrous DMF in a round bottom flask equipped with a magnetic stirrer. To this 3.9 g (0.011 mol) of *O*-palmitoyl malic acid anhydride (**5)** was added and the reaction mixture was cooled to 0 °C under an argon

atmosphere, followed by the addition of 0.89 mL (0.011 mol) pyridine with stirring under argon. The reaction was continued at 0 °C for 2-3 hours, followed by next 12 hours at room temperature. The reaction was monitored by HPLC-MS of the crude mixture. After completion of the reaction, the mixture was poured into a 250 mL Erlenmayer flask containing an ice-water mixture to which 2 N HCl was added under vigorous stirring. The product was extracted with ethyl acetate (2 × 250 mL) and the combined organic layers were washed with brine and dried over sodium sulphate. The organic solvent was removed under reduced pressure to afford the crude product. This was washed several times with *n*-hexane to obtain a mixture **52a-b** (**52a**/**52b** = 0.74/1) with a combined yield of 3.9 g (66%).

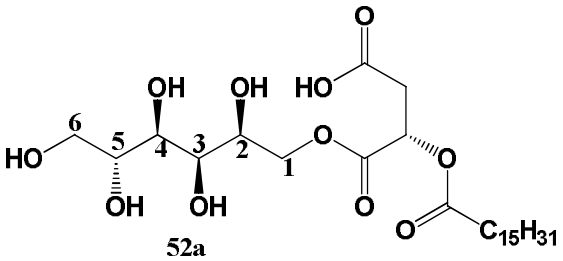

52a

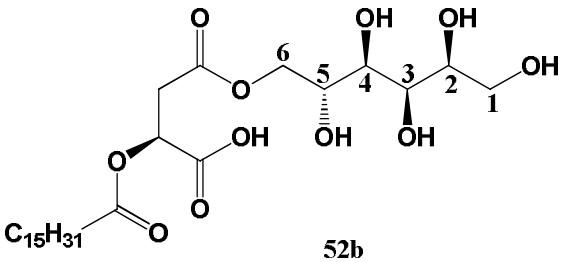

52b

^{1}H NMR (400 MHz, MeOH-d_4) δ = 5.47 (dd, *J* = 8.1, 4.2 Hz, 1H), 4.44 (dd, *J* = 11.4, 2.8 Hz, 1H), 4.28 (dd, *J* = 11.5, 6.4 Hz, 1H), 4.00 – 3.89 (m, 1H), 3.88 – 3.81 (m, 1H), 3.78 (dd, *J* = 10.4, 4.7 Hz, 1H), 3.65 (m, 3H), 2.91 (m, 2H), 2.39 (t, *J* = 7.3 Hz, 2H), 1.80 – 1.54 (m, 2H), 1.43 – 1.21 (m, 24H), 0.89 (t, *J* = 6.8 Hz, 3H) ppm.

^{13}C NMR (101 MHz, MeOH-d_4) δ = 174.42, 172.73, 172.65, 170.82, 170.65, 74.92, 73.63, 73.42, 73.23, 72.31, 71.09, 70.90, 70.76, 70.00, 69.95, 68.66, 67.85, 64.83, 64.32, 36.90, 34.70, 32.94, 30.64, 30.61, 30.59, 30.44, 30.30, 30.24, 30.00, 25.81, 23.57, 14.27 ppm.

HRMS (ESI$^-$, m/z, [M-H]$^-$) calculated for $C_{26}H_{47}O_{11}$: 535.3118. Found: 535.3108.

5.18.4 6-*O* and 1-*O*-(*O*-*O'*-di-lauroyl tartaryl)-*D*-sorbitol (53a-b):

To a solution of *D*-sorbitol (15 g, 0.082 mol) in anhydrous DMF (150 mL) *O*-*O'*-di-lauroyl tartaric acid anhydride (**9)** (8.2 g, 16.47 mmol) was added with stirring under an argon atmosphere. The reaction mixture was allowed to cool down to 0 °C followed by the addition of dry pyridine (1.3 mL, 16.47 mmol). The reaction was continued under an argon atmosphere at 0 °C for 2-3 h followed by an additional 3 days at room temperature. After completion of the reaction, the mixture was poured into an ice-water mixture to which 2 N HCl was added at 0 °C under vigorous stirring. The product was extracted with ethyl acetate (2 × 250 mL), and the combined organic layers were washed four times with brine solution, dried over sodium

sulphate and the organic solvent was removed under reduced pressure to obtain the crude product. The crude product consists of diastereomeric mixture of 6-*O* and 1-*O*-acylated esters of *D*-sorbitol which was isolated from the crude mixture in the following manner: the crude mixture was dissolved in a minimum amount of *n*-hexane under reflux conditions and the solution was kept at room temperature for 2 d. The diastereomeric mixture (**53a-b**) of 6-*O* and 1-*O*-acylated esters of *D*-sorbitol was precipitated from the solution. The precipitation was filtered and dried to obtain **53a-b** (**53a**/**53b** = 0.8/1) with a combined yield of 8.2 (73%). A selective precipitation of **53a** from the diastereomeric mixture is possible by dissolving the diastereomeric mixture (**53a-b**) in a minimum amount of acetone. **53a** with trace amount of **53b** was precipitated from the solution after 12 hrs standing at room temperature.

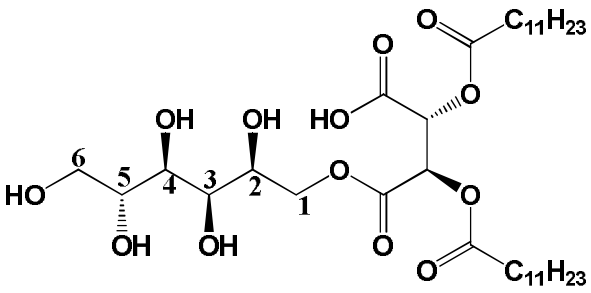

53a

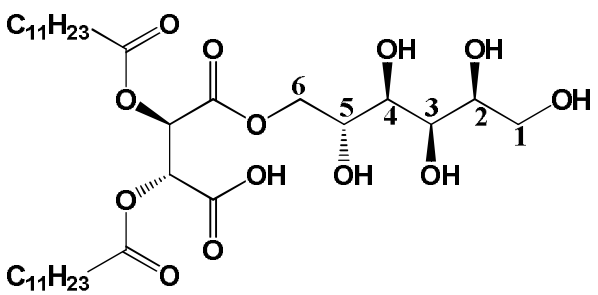

53b

^{1}H NMR (400 MHz, MeOH-d_4) δ = 5.74 (d, *J* = 15.2 Hz, 2H), 4.33 (dd, *J* = 11.3, 4.2 Hz, 1H), 4.19 (dd, *J* = 11.3, 7.0 Hz, 1H), 3.94 (m, 1H), 3.82 (dd, *J* = 4.4, 2.0 Hz, 1H), 3.76 (dd, *J* = 10.8, 3.5 Hz, 1H), 3.71 – 3.57 (m, 3H), 2.40 (m, 4H), 1.61 (m, 4H), 1.28 (m, 32H), 0.88 (t, *J* = 6.8 Hz, 6H) ppm.

^{13}C NMR (151 MHz, acetone-d_6) δ = 173.63, 173.57, 173.52, 173.48, 168.29, 168.27, 167.60, 167.56, 75.54, 74.68, 74.18, 73.62, 72.95, 72.47, 72.43, 72.14, 71.35, 71.15, 71.14, 69.40, 68.68, 65.47, 65.00, 35.02, 33.35, 31.07, 31.05, 30.93, 30.90, 30.88, 30.75, 30.73, 30.70, 30.63, 30.50, 30.40, 30.39, 30.37, 30.24, 30.11, 26.27, 24.01, 15.01 ppm.

^{13}C NMR (101 MHz, MeOH-d_4) δ = 173.99, 173.91, 169.05, 167.72, 73.36, 73.03, 72.35, 72.26, 71.90, 70.90, 68.27, 64.76, 34.54, 33.04, 30.73, 30.57, 30.54, 30.43, 30.38, 30.35, 30.04, 30.00, 25.88, 25.86, 23.69, 14.41 ppm.

HRMS (ESI$^-$, m/z, [M-H]$^-$) calculated for $C_{34}H_{61}O_{13}$: 677.4112. Found: 677.4115.

5.18.5 6-*O* and 1-*O*-(*O*-*O*′-di-tetradecanoyl tartaryl)-*D*-sorbitol (54a-b)

To a solution of *D*-sorbitol (15 g, 0.082 mol) in anhydrous DMF (150 mL) *O*-*O*′-di-tetradecanoyl tartaric acid anhydride (**10)** (9.1 g, 16.47 mmol) was added with stirring under an argon atmosphere. The reaction mixture was cooled to 0 °C followed by the addition of dry pyridine (1.3mL, 16.47 mmol). The reaction was continued under an argon atmosphere at 0 °C for 2-3 h followed by an additional 3 days at room temperature. After completion the reaction mixture was poured into an ice-water mixture to which 2 N HCl was added at 0 °C under vigorous stirring. The product was extracted with ethyl acetate (2 × 250 mL), the combined organic layers were washed four times with brine solution, dried over sodium sulphate and the organic solvent was removed under reduced pressure to obtain the crude product. The crude product consists of diastereomeric mixture of 6-*O* and 1-*O*-acylated esters of *D*-sorbitol which were isolated from the crude product in the following manner: the crude product was dissolved in a minimum amount of *n*-hexane under reflux conditions and the solution was kept at room temperature for 3 d. The diastereomeric mixture (**54a-b**) was precipitated as part gel after 2 d standing at room temperature. The solvent was decanted from the precipitate which was dried under reduced pressure to obtain 10.2 g (84%) of **54a-b** (**54a**/**54b** = 1:1).

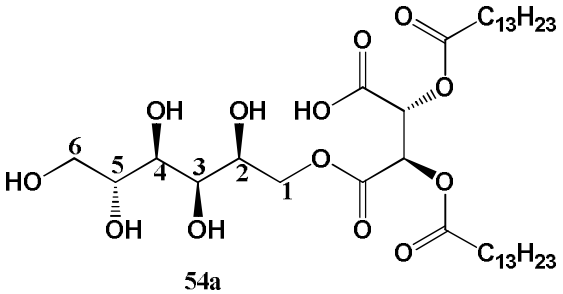

54a

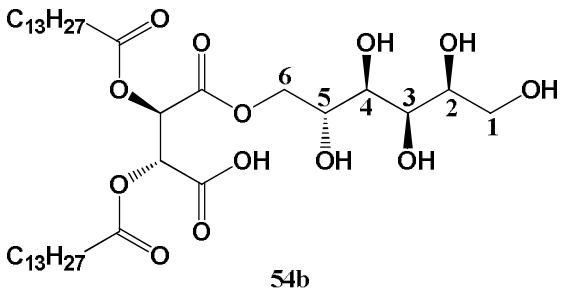

54b

^{1}H NMR (400 MHz, acetone-d_6) δ 5.75 (d, *J* = 20.0 Hz, 2H), 4.59 – 4.21 (m, 2H), 4.04 (m, 1H), 3.98 – 3.79 (m, 2H), 3.70 (m, 3H), 2.42 (t, *J* = 7.0 Hz, 4H), 1.66 (s, 4H), 1.32 (m, 40H), 0.90 (t, *J* = 6.9 Hz, 6H).

^{13}C NMR (101 MHz, Acetone) δ 173.41, 173.35, 173.29, 173.25, 168.13, 168.10, 167.37, 167.33, 75.29, 74.42, 73.92, 73.37, 72.69, 72.25, 72.21, 71.92, 71.11, 70.92, 70.90, 69.14, 68.42, 65.22, 64.77, 34.78, 33.13, 30.88, 30.86, 30.72, 30.69, 30.54, 30.50, 30.30, 30.18, 30.11, 29.92, 29.73, 26.06, 26.02, 23.79, 14.81.

HRMS (ESI$^-$, m/z, [M-H]$^-$) calculated for $C_{38}H_{69}O_{13}$: 733.4738. Found: 733.4740.

5.18.6 6-*O* and 1-*O*-(*O*-*O'*-di-palmitoyl tartaryl)-*D*-sorbitol (55a-b):

To a solution of *D*-sorbitol (15 g, 0.082 mol) in anhydrous DMF (150 mL) *O*-*O'*-di-palmitoyl tartaric acid anhydride (**11)** (10 g, 16.47 mmol) was added with stirring under an argon atmosphere. The reaction mixture was cooled down to 0 °C followed by the addition of dry pyridine (1.3mL, 16.47 mmol). The reaction was continued under an argon atmosphere at 0 °C for 2-3 h and additional 3 days at room temperature. After completion the reaction mixture was poured into an ice-water mixture to which 2 N HCl was added at 0 °C under vigorous stirring. The product was extracted with ethyl acetate (2 × 250 mL), the combined organic layers were washed four times with brine solution, dried over sodium sulphate and the organic solvent was removed under reduced pressure to obtain the crude product. The crude product consists of a diastereomeric mixture (**55a-b**) of 6-*O* and 1-*O*-acylated esters of *D*-sorbitol which was isolated from the crude mixture in the following manner: the crude mixture was dissolved in a minimum amount of *n*-hexane under reflux conditions and the solution was kept at room temperature for 2 d. The diastereomeric mixture (**55a-b**) was precipitated as gel from the solution after 2 d standing at room temperature. The solvent was decanted from the precipitate which was dried under reduced pressure yielding 10 g (77%) of **55a-b** (**55a**/**55b** = 1.1/1). A selective precipitation of **55a** from the mixture of **55a-b** is possible in the following manner: the mixture is dissolved in a minimum amount of acetone and kept at room temperature for 12 h. **55a** precipitated from the solution after 12 h standing at room temperature.

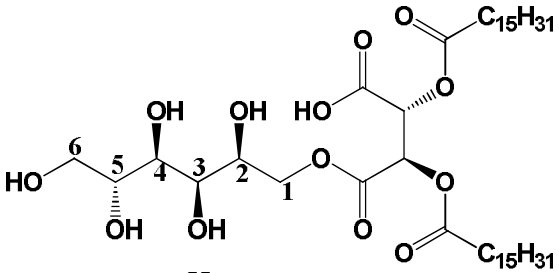

55a

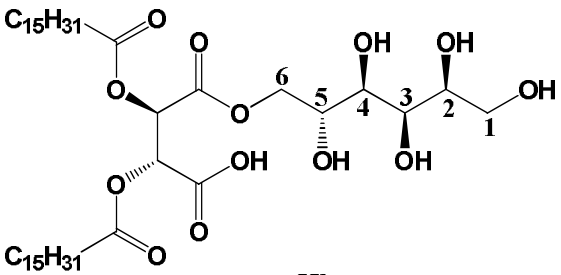

55b

^{1}H NMR (400 MHz, MeOH-d_4) δ = 5.75 (dd, *J* = 5.6, 2.8 Hz, 2H), 4.48 (dd, *J* = 11.4, 2.8 Hz, 1H), 4.26 (dd, *J* = 11.4, 6.0 Hz, 1H), 3.96 – 3.73 (m, 3H), 3.73 – 3.57 (m, 3H), 2.41 (t, *J* = 7.1 Hz, 4H), 1.78 – 1.48 (m, 4H), 1.22 (m, 50H), 0.90 (t, *J* = 6.8 Hz, 6H) ppm.

^{13}C NMR (101 MHz, MeOH-d_4) δ = 173.99, 173.92, 173.83, 173.80, 169.10, 169.05, 167.73, 167.66, 75.06, 73.18, 72.99, 72.90, 72.35, 72.21, 71.88, 70.80, 70.41, 70.11, 68.66, 68.24, 64.70, 64.11, 34.57, 33.11, 30.87, 30.64, 30.53, 30.47, 30.08, 28.01, 25.93, 14.53 ppm.

HRMS (ESI$^-$, m/z, [M-H]$^-$) calculated for $C_{42}H_{77}O_{13}$: 789.5364. Found: 789.5373.

5.19 Syntheses of mannitol based amphiphiles 56a-61a

5.19.1 (*S*)-3-(Dodecanoyloxy)-4-oxo-4-(((2*R*,3*R*,4*R*,5*R*)-2,3,4,5,6-pentahydroxyhexyl)oxy)butanoic acid (56a)

In a 100 mL round bottom flask equipped with a magnetic stirrer bar 10 g (0.055 mol) of finely powered and dried *D*-mannitol and anhydrous DMA (50 mL) were placed. To this *O*-lauroyl-malic acid anhydride (**3**) (3.3 g, 0.011 mol) was added under an argon atmosphere. The reaction mixture was cooled to 0 °C and then 0.89 mL (0.011 mol) of dry pyridine was added under stirring under an argon atmosphere. The reaction was continued at 0 °C for 2-3 h, followed by an additional 12 h at rt. After completion the reaction mixture was poured into a 500 mL beaker containing an ice-water mixture to which 2 N HCl was added under vigorous stirring. The product was extracted with ethyl acetate (2 × 250 mL) and the combined organic layers were washed with brine. The organic solvent was removed under reduced pressure to afford the crude product which was repetitively washed with *n*-hexane to obtain pure **56a** with a yield of 3.6 g (68%).

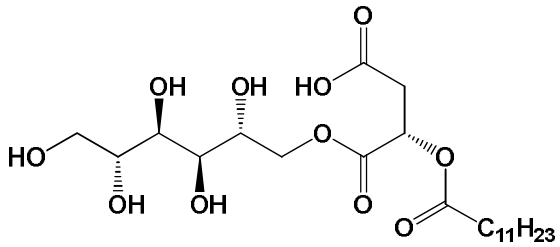

56a

^{1}H NMR (600 MHz, MeOH-d_4) δ = 5.49 (dd, *J* = 8.4, 4.0 Hz, 1H), 4.49 (dd, *J* = 11.4, 2.7 Hz, 1H), 4.31 (dd, *J* = 11.4, 6.4 Hz, 1H), 3.98 – 3.87 (m, 2H), 3.86 – 3.76 (m, 2H), 3.75 – 3.62 (m, 2H), 2.94 (m, 2H), 2.46 – 2.33 (m, 2H), 1.91 – 1.45 (m, 2H), 1.53 – 1.11 (m, 16H), 0.91 (t, *J* = 7.0 Hz, 3H) ppm.

^{13}C NMR (151 MHz, MeOH-d_4) δ = 174.44, 172.73, 170.83, 73.17, 71.35, 71.27, 70.65, 70.00, 68.96, 65.11, 36.86, 34.69, 32.93, 30.59, 30.43, 30.29, 30.24, 29.99, 25.80, 23.57, 14.28 ppm.

HRMS (ESI$^-$, m/z, [M-H]$^-$) calculated for $C_{22}H_{39}O_{11}$: 479.2492. Found: 479.2512.

5.19.2 (*S*)-4-Oxo-4-(((2*R*,3*R*,4*R*,5*R*)-2,3,4,5,6-pentahydroxyhexyl)oxy)-3-(tetradecanoyloxy)butanoic acid (57a)

10 g of *D*-mannitol (0.055 mol) was allowed to react with 3.6 g (0.011 mol) of *O*-tetradecanoyl-malic acid anhydride (**4)** as described above for the synthesis of **56a** yielding 4 g (71%) of **57a**.

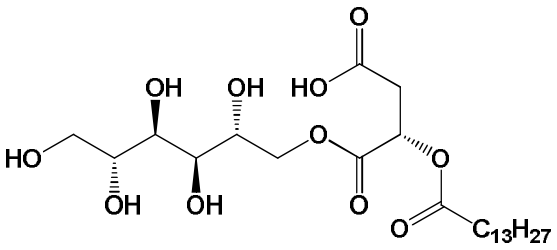

57a

^{1}H NMR (600 MHz, MeOH-d_4) δ = 5.53 (dd, *J* = 8.7, 3.7 Hz, 1H), 4.43 (dd, *J* = 11.4, 2.6 Hz, 1H), 4.30 (dd, *J* = 11.4, 6.4 Hz, 1H), 3.97 (ddd, *J* = 8.9, 6.4, 2.6 Hz, 1H), 3.86 – 3.75 (m, 3H), 3.74 – 3.62 (m, 2H), 3.04 – 2.85 (m, 2H), 2.46 (m, 2H), 1.74 – 1.58 (m, 2H), 1.46 – 1.14 (m, 20H), 0.96 (t, *J* = 7.0 Hz, 3H) ppm.

^{13}C NMR (151 MHz, MeOH-d_4) δ = 173.89, 172.43, 170.63, 72.97, 71.65, 71.33, 70.35, 70.23, 68.01, 65.19, 36.96, 34.79, 32.96, 30.49, 30.33, 30.49, 30.74, 29.31, 25.68, 23.74, 14.38 ppm.

HRMS (ESI$^-$, m/z, [M-H]$^-$) calculated for $C_{24}H_{43}O_{11}$: 507.2805. Found: 507.2813.

5.19.3 (*S*)-4-Oxo-3-(palmitoyloxy)-4-(((2*R*,3*R*,4*R*,5*R*)-2,3,4,5,6-pentahydroxyhexyl)oxy)butanoic acid (58a)

10 g (0.055 mol) of *D*-mannitol was allowed to react with 3.9 g (0.011 mol) of *O*-palmitoyl-malic acid anhydride (**5**) as described above for the synthesis of **56a** yielding 4.1 g (69%) of **58a**.

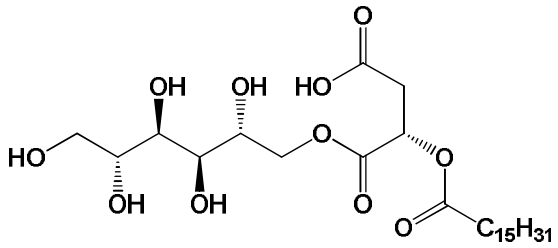

58a

^{1}H NMR (600 MHz, MeOH-d_4) δ = 5.49 (dd, *J* = 8.4, 4.1 Hz, 1H), 4.49 (dd, *J* = 11.4, 2.9 Hz, 2H), 4.31 (dd, *J* = 11.4, 6.4 Hz, 1H), 3.99 – 3.88 (m, 1H), 3.85 – 3.76 (m, 2H), 3.76 – 3.61 (m, 2H), 3.04 – 2.76 (m, 2H), 2.50 – 2.33 (m, 2H), 1.76 – 1.49 (m, 2H), 1.42 – 1.21 (m, 24H), 1.01 – 0.74 (m, 3H) ppm.

^{13}C NMR (151 MHz, MeOH-d_4) δ = 174.46, 172.74, 170.86, 73.24, 71.44, 71.35, 70.74, 70.04, 68.97, 65.13, 36.91, 34.71, 32.93, 30.63, 30.60, 30.58, 30.43, 30.29, 30.24, 30.00, 25.81, 23.56, 14.25 ppm.

HRMS (ESI$^-$, m/z, [M-H]$^-$) calculated for $C_{26}H_{47}O_{11}$: 535.3118. Found: 535.3122.

5.19.4 (2*R*,3*R*)-2,3-Bis(dodecanoyloxy)-4-oxo-4-(((2*R*,3*R*,4*R*,5*R*)-2,3,4,5,6-pentahydroxyhexyl)oxy)butanoic acid (59a)

10 g (0.055 mol) of *D*-mannitol was reacted with 5.5 g (0.011 mol) of *O*-*O'*-di-lauroyl tartaric acid anhydride (**9)** according to the reaction procedure described above for **56a** to afford **59a** with a yield of 5.3 g (71%).

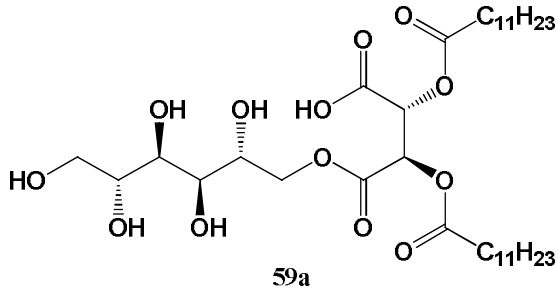

59a

^{1}H NMR (400 MHz, acetone-d_6) δ = 5.78 (m, 2H), 4.53 (dd, *J* = 11.2, 2.8 Hz, 1H), 4.27 (dd, *J* = 11.2, 6.4 Hz, 1H), 3.97 – 3.88 (m, 6H), 2.48 – 2.36 (m, 4H), 1.74 – 1.57 (m, 4H), 1.33 (s, 32H), 0.91 (t, *J* = 6.8 Hz, 6H) ppm.

^{13}C NMR (101 MHz, acetone-d_6) δ = 173.66, 173.53, 168.30, 167.66, 73.89, 72.48, 72.25, 72.21, 71.95, 71.33, 69.83, 65.68, 35.03, 33.38, 30.96, 30.93, 30.78, 30.74, 30.44, 30.42, 29.92, 26.32, 26.29, 24.04, 15.01 ppm.

HRMS (ESI$^-$, m/z, [M-H]$^-$) calculated for $C_{34}H_{61}O_{13}$: 677.4112. Found: 677.4105.

5.19.5 (2*R*,3*R*)-4-Oxo-4-(((2*R*,3*R*,4*R*,5*R*)-2,3,4,5,6-pentahydroxyhexyl)oxy)-2,3-bis(tetradecanoyloxy)butanoic acid (60a)

10 g (0.055 mol) of *D*-mannitol was reacted with 6.1 g (0.011 mol) of *O*-*O'*-di-tetradecanoyl tartaric acid anhydride (**10**) according to the reaction procedure described above for **53a** to afford **60a** in a yield of 5.9 g (73%).

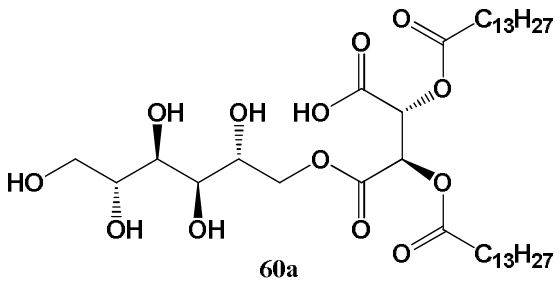

60a

^{1}H NMR (600 MHz, acetone-d$_6$) δ = 5.76 (dd, *J* = 6.2, 3.0 Hz, 2H), 4.51 (dd, *J* = 11.2, 2.7 Hz, 1H), 4.26 (dd, *J* = 11.2, 6.4 Hz, 1H), 3.98 – 3.88 (m, 1H), 3.85 (d, *J* = 7.2 Hz, 1H), 3.83 – 3.76 (m, 2H), 3.76 – 3.65 (m, 2H), 2.52 – 2.30 (m, 4H), 1.65 (m, 4H), 1.35 (m, 40H), 0.89 (t, *J* = 6.9 Hz, 6H) ppm.

^{13}C NMR (151 MHz, acetone-d$_6$) δ = 173.64, 173.51, 168.33, 167.65, 73.90, 72.47, 72.24, 72.20, 71.95, 71.35, 69.78, 65.67, 35.05, 35.03, 33.37, 30.96, 30.93, 30.89, 30.44, 30.42, 30.12, 26.31, 26.28, 24.03, 15.01 ppm.

HRMS (ESI$^-$, m/z, [M-H]$^-$) calculated for $C_{38}H_{69}O_{13}$: 733.4738. Found: 733.4734.

5.19.6 (2*R*,3*R*)-4-Oxo-2,3-bis(palmitoyloxy)-4-(((2*R*,3*R*,4*R*,5*R*)-2,3,4,5,6-pentahydroxyhexyl)oxy)butanoic acid (61a)

10 g (0.055 mol) of *D*-mannitol was reacted with 6.7 g (0.011 mol) of *O*-*O'*-di-palmitoyl tartaric acid anhydride (**11)** according to the reaction procedure described above for **53a** to afford **61a** in a yield of 5.9 g (73%).

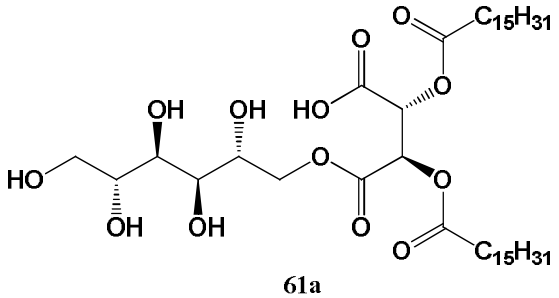

61a

^{1}H NMR (600 MHz, acetone-d_6) δ = 5.88 (s), 4.58 (dd, *J* = 11.4, 2.9 Hz, 1H), 4.26 (dd, *J* = 11.4, 6.4 Hz, 1H), 3.98 –3.65 (m, 6H), 2.52 – 2.30 (m, 4H), 1.65 (m, 4H), 1.35 (m, 48H), 0.89 (t, *J* = 6.8 Hz, 6H) ppm.

^{13}C NMR (151 MHz, acetone-d_6) δ = 174.09, 173.97, 170.46, 167.88, 73.29, 72.21, 71.84, 71.71, 71.40, 71.28, 71.15, 64.62, 34.76, 32.94, 30.05, 25.86, 23.58, 20.58, 19.41, 14.44 ppm.

HRMS (ESI$^-$, m/z, [M-H]$^-$) calculated for $C_{42}H_{77}O_{13}$: 789.5364. Found: 789.5363.

List of abbreviations

α	*alpha*
abs.	absolute
aer.	*aerogenosa*
APG	Alkylpolyglycoside
Asp. niger	*Aspergillus niger*
β	*Beta*
Bn	Benzyl
C-LMWG	Carbohydrate based low molecular weight gelator
Ca. albicans	*Candida albicans*
CMC	Critical micellar concentration
COSY	Coupled Spectroscopy
d	Doublet
Da	Dalton
dd	Doublet of doublets
DEPT	Distortionless Enhancement by Polarization Transfer
d	day
DSC	Differential scanning calorimetry
DIN	Deutsches Institut für Normung
DME	1,2-Dimethoxyethane
DMF	*N*,*N*-Dimethylformamide
DMA	*N*,*N*-Dimethylacetamide

ESI	Electrospray ionization
EU	European Union
E. coli	*Echerichia coli*
LCMS	Liquid Chromatography–Mass Spectrometry
MGC	Minimum gelation concentration
γ	Surface tension (mN/m)
γ_{CMC}	Surface tension at critical micelle concentration (CMC)
t	triplet
TLC	Thin layer chromatography
T_g	Thermal stability of gel
h	hour
Hz	Herz
HRMS	High-resolution mass spectrometry
LB-agar	Lysogeny broth-agar
LMWG	Low molecular weight gelator
m	Multiplet
Max.	Maximum
MES	Methyl ester sulfonates
Mio	Million
M. luteus	*Mikrococcus luteus*
NMR	Nuclear magnetic resonance
SEM	Scanning electron microscopy
OEM	Optical electron microscopy

O/W	Oil in water emulsion
p	*para*
PEG	Polyethylene glycol
TEM	Transmission electron microscopy
ppm	Parts per million
Ps.	*Pseudomonas*
R_f	Retention factor
rt	Room temperature
S. aureus	*Staphylococcus aureus*
SDS	Sodium Dodecyl Sulfate
t	Triplet
TEA-Salt	Triethanolamine salt
THF	Tetrahydrofuran
W	Watt

References

[1] D. Peters, N. Holst, B. Herrmann, S. Lulies and H. Stolte; Nachwachsende Rohstoffe in der Industrie, 3 Aufl., Fachagentur Nachwachsende Rohstoffe e.V., Gülzow, 2010, 12-25.

[2] F. W. Lichtenthaler and S. Mondel, *Pure Appl. Chem.*, 1997, **69**, 1853–1866.

[3] F. W. Lichtenthaler, *Acc. Chem. Res.*, 2002, **35**, 728–737.

4 P. T. Anastas and J. C. Warner, *Green chemistry. Theory and practice*, Oxford University Press, Oxford [England] ; Toronto, 2000.

[5] C. Okkerse and H. van Bekkum, *Green Chem.*, 1999, **1**, 107–114.

[6] C. Okkerse and H. van Bekkum, *Green Chem.*, 1999, **1**, 107–114.

[7] J. M. Pestman, *Carbohydrate-derived surfactants containing an N-acylated amine functionality. Fundamental aspects and practical applications*, Rijksuniversiteit Groningen, [Groningen], 1998.

[8] P. T. Anastas and J. C. Warner, *Green chemistry. Theory and practice*, Oxford University Press, Oxford [England] ; Toronto, 2000.

[9] F. W. Lichtenthaler, *Acc. Chem. Res.*, 2002, **35**, 728–737.

[10] E. M. Rubin, *Nature*, 2008, **454**, 841–845.

[11] F. W. Lichtenthaler and S. Mondel, *Pure Appl. Chem.*, 1997, **69**, 1853–1866.

[12] J. M. Pestman, *Carbohydrate-derived surfactants containing an N-acylated amine functionality. Fundamental aspects and practical applications*, Rijksuniversiteit Groningen, [Groningen], 1998.

[13] J. Nowicki, A. Sokołowski and D. Reksa, *J. Surfact. Deterg.*, 2011, **14**, 179–184.

[14] M. K. Matsson, Adsorption of polyhydroxyl based surfactants, Chemical Science and Engineering, KTH, Stockholm, 2005.

[15] U. Olsson and H. Wennerström, *Advances in Colloid and Interface Science*, 1994, **49**, 113–146.

[16] M. Anderson *and* G. Karlstrom, *J. Phys. Chem*. 1985, **89**, 4957.

[17] M. T. Madigan and T. D. Brock, *Brock biology of microorganisms*, Pearson/Benjamin Cummings, San Francisco, CA, 12th edn., 2009.

[18] L.-L. Uppgård, *Nonionic surfactants a multivariate study*, Umeå university, Umeå, 2002.

[19] T. F. Tadros, *Applied surfactants. Principles and applications*, Wiley-VCH, Weinheim, 2005.

[20] R. C. Dart, *Medical toxicology*, Lippincott, Williams & Wilkins, Philadelphia, 3rd edn., 2004.

[21] C. Altieri, A. Bevilacqua, D. Cardillo and M. Sinigaglia, *Int. J. Food Sci. Tech.*, 2009, **44**, 359-366.

[22] A. Corma, S. Iborra, S. Miquel and J. Primo, *J. Catal.*, 1998, **173**, 315-321.

[23] S. Wongsakul, P. Prasertsan, U. T. Bornscheuer and A. H-Kittikun, *Eur. J. Lipid Sci. Technol.*, 2003, **105**, 68-73.

[24] T. Blatt, S. Jaspers, U. Schönrock, U. Koop, Y. Wöhrmann, T. Raschke, C. Mummert, I. Kruse, T. Küper, G.and M. Muhr, German Patent, 2008, WO2008101693 A2.

[25] S. Y. Mhaskar, R. B. N. Prasad and G. Lakshminarayana, *J. Am. Oil Chem. Soc.*, 1990, **67**, 1015-1019.

[26] R. Valivety, P. Jauregi, I. Gill and E. Vulfson, *J. Am. Oil Chem. Soc.*, 1997, **74**, 879-886.

[27] P. Clapés and M. P. Infante, *Biocat. Biotrans.*, 2002, **20**, 215-233.

[28] K. Hill and O. Rhode, *Fett/Lipid*, 1999, **101**, 25-33.

[29] J. A. Arcos, M. Bernabe and C. Otero, *Biotechnol. Bioeng.*, 1998, **57**, 505-509.

[30] P. Nobmann, A. Smith, J. Dunne, G. henehan and P. Bourke; *Int. J. Food Microbiol.*, 2009, **128**, 440-445.

[31] M. Kjellin and I. Johansson, *Surfactants from renewable resources*, Wiley, Chichester, U.K, 2010.

[32] T. Harada, N. Nishikito, Y. Moroi and R. Matuura, *Bull. Chem. Soc. Jpn.*, 1981, **54**, 2592-2597.

[33] C. Frank, H. Frielinghaus, J. Allgaier and H. Prast; *Langmuir*, 2007, **23(12)**, 6526-6535.

[34] K. Suga, T. Miyashige, T. Takada, S. Watanabe and M. Moriyama, *Aust. J. Chem.*, 1968, **21**, 2333-2339.

[35] G. T. Battaglini, J. L. Larson-Zobus and T. G. Baker, *J. Am. Oil Chem. Soc*., 1986, **63**, 1073-1077.

[36] R. Ihizane, Neuartige Gemini Tenside - Synthesen und Tensideigenschaften. Stoffliche Nutzung nachwachsende Rohstoffe, Suedwestdeutscher Verlag fuer Hochschulschriften, Saarbrücken, 2011.

[37] K. Schmid, A. Syldath, M. Neuss, D. Kischkel, T. Krohnen and H. Pawelczyk, 1997, EP 19940906150

[38] B. Farby, Tenside, *Chemie in unser Zeit*, **1991**, 25, 214-222.

[39] F. M. Menger and C. A. Littau, *J. Am. Chem. Soc.*, 1991, **113**, 1451–1452.

[40] M. J. Rosen and D. J. Tracy, *J. Surf. Det.*, 1998, **1**, 547.

[41] F. M. Menger and C.A. Littau, *J. Am. Chem. Soc.*, 1993, **115**, 10083-10090.

[42] R. Zana and J. Xia, Gemini Surfactants: Synthesis, Interfacial and Solution-Phase Behavior, and Applications, (Eds.) Marcel Dekker, New York, 2003, 331.

[43] B. S. Sekhon, *Resonance*, 2004, **9**, 42-49.

[44] L. A. Estroff and A. D. Hamilton, *Chem. Rev.*, 2004, **104**, 1201–1218.

[45] F. Fages, Low molecular mass gelators, Springer, Berlin; Heidelberg; New York, NY, op. 2005.

[46] (a) P. Terech and R. G. Weiss, *Chem. Rev*., 1997, **97**, 3133–3159; (b) J. H. Van Esch and B. L. Feringa, *Angew. Chem., Int. Ed*., 2000, **112**, 2351–2354.

[47] G. D. Rees and B. H. Robinson, *Adv. Mater*., 1993, **5**, 608–619.

[48] G. Haering and P. L. Luisi, *J. Phys. Chem.*, 1986, **90**, 5892–5895.

[49] J. H. Jung, S. Shinkai and T. Shimizu, *Chem. Eur. J.* 2002, **8(12)**, 2684–2690 and references therein.

[50] K. Y. Lee and D. J. Mooney, *Chem. Rev*., 2001, **101 (7)**, 1869–1880.

[51] P. K. Vemula, J. Li and G. John, *J. Am. Chem. Soc*, 2006, **128**, 8932–8938.

[52] (a) Van K. J. C Bommel, M. C. A. Stuart and Van Esch B. L. Feringa, *J. Org. Biomol. Chem.*, 2005, **3**, 2917–2920.

[53] D. Khatua, R. Maiti and J. Dey, *Chem. Commun.*, 2006, 4903.

[54] B. Simmons, S. Li, V. T. John, G. L. McPherson, C. Taylor, D. K. Schwartz and K. Maskos, *Nano Lett.*, 2002, **2**, 1037–1042.

[55] J. F. Miravet and B. Escuder, *Org. Lett.*, 2005, **7**, 4791–4794.

[56] M. George and G. R. Weiss, *Acc. Chem. Res.*, 2006, **39 (8)**, 489–497 and references therein.

[57] (a) X. Y. Liu, *Top. Curr. Chem*., 2005, **256**, 1–37; (b) R. Wang, C. Geiger, L. Chen, B. Swanson and D. G. Whitten, *J. Am. Chem. Soc*., 2000, **122**, 2399; (c) K. Sakurai, Y. Jeong, K. Koumoto, A. Friggeri, O. Gronwald, K. Sakurai, S. Okamoto, K. Inoue and S. Shinkai, *Langmuir*, 2003, **19**, 8211.

[58] N. Zweep, *Control of structure and function of organogels through self-assembly*, s.n.]; University Library Groningen] [Host], [S.l, [Groningen, 2006.

[59] K. Dusek, Responsive Gels: Volume Transitions (Adv. Polym. Sci. series), 1993, 109–110, Springer-Verlag, New York.

[60] (a) R. Daganli, *Chem. & Eng. News*, 1997, **23**, 26; (b) C. M. Dorski, F. J Doyle and N. A. Peppas, *Polym. Mater. Sci. Eng. Proc.*, 1997, **76**, 281.

[61] B. Boury, R. J. P. Corriu, Le V. Strat, P. Delord and M. Nobili, *Angew. Chem., Int. Ed.*, 1999, **38**, 3172–3175.

[62] (a) J. Israelchivili, *Intermolecular and Surface Forces*, 2nd ed.; Academic Press: New York, 1991; (b) L. J. M. Gaspar and G. Baskar, *J. Mater. Chem.*, 2005, **15**, 5144; (c) D. Khatua, R. Maiti and J. Dey, *Chem. Commun.*, 2006, 4903; (d) S. Roy, A. Dasgupta and P. K. Das, *Langmuir*, 2007, **23**, 11769-11776.

[63] R. G. Weiss and P. Terech, Molecular Gels. Materials with Self-Assembled Fibrillar Networks, Springer, Dordrecht, 2006.

[64] Y. Lin and R. G. Weiss, *Macromolecules*, 1987, **20**, 414.

[65] D. J. Abdallah and R. G. Weiss, *Langmuir*, 2000, **16**, 352–355.

[66] P. *J.* Flory, *Faraday Discuss*., 1974, 7, 57.

[67] R. Wang, C. Geiger, L. Chen, B. Swanson and D. G. Whitten, *J. Am. Chem. Soc*., 2000, **122**, 2399.

[68] H. Fenniri, P. Mathivanan, K. L. Vidale, D. M. Sherman, K. Hallenga, K. V. Wood and J. G. Stowell, *J. Am. Chem. Soc*., 2001, **123**, 3854.

[69] J. N. Israelachvili, *Intermolecular and Surface Forces*, 2nd ed.; Academic Press: New York, 1991.

[70] G. C. Maity, *Journal of Physical Sciences*, 2007, **11**, 156-171.

[71] (a) M. T. Reetz, A. Zonta and J. Simpelkamp, *Angew. Chem., Int. Ed. Engl*., 1995, **34**, 301-303; (b) Y. Yasuda, Y. Takebe, M. Fukumoto, H. Inada and Y. Shirota, *Adv. Mater*., 1996, **8**, 740–741; (c) W. Gu, L. Lu, G. B. Chapman and R. G. Weiss, *Chem. Commun*., 1997, 543–544; (d) R. J. H. Hafkamp, B. P. A. Kokke, I. M. Danke, H. P. M. Geurts, A. E. Rowan, M. C. Feiters and R. J. M. Nolte, *Chem. Commun.*, 1997, 545–546; (e) R. Yoshida, T. Takahashi, T. Yamaguchi and H. Ichijo *J. Am. Chem. Soc*., 1996, **118**, 5134–5135; (f) C. Shi, Z. Huang, S. Kilic, J. Xu, R. M. Enick, E. J. Beckman, A. J. Carr, R. E. Melendez and A. D. Hamilton, *Science*, 1999, **286**, 1540– 1543; (g) U. Maitra, V. K. Potluri, N. M. Sangeetha, P. Babu, and A. R. Raju, *Tetrahedron: Asymmetry*, **2000**, 12, 477–480.

[72] Van J. Esch, F. Schoonbeek, De M. Loos, E.M. Veen, R.M. Kellogg and B.L. Feringa, Supramolecular Science: where it is and where it is going 1999, Nato ASI Series C: Mathematical and Physical Science, Vol. 527, 233-259, Kluwer, Deventer.

[73] T. Brotin, R. Untermöhlen, Fages, H. Bouas-Laurent and J-P. Desvergne, *J. Chem. Soc., Chem. Commun*., 1991, 416–418.

[74] K. Hanabusa, M. Yamada, M. Kimura and H. Shirai, *Angew. Chem., Int. Ed.*, 1996, **35**, 1949-1951.

[75] P.W. Atkins, Physical Chemistry 5th ed., 1994, Oxford University Press, Oxford. ISBN 0-19-855730-2.

[76] R. F. G. Visintin, R. Lapasin, E. Vignati, P. D'Antona and T. P. Lockhart, *Langmuir*, 2005, **21**, 6240-6249.

[77] M. L. N. Yvonne, Semicarbazide Organogels Containing Inorganic Nanoparticles New Supramer Hybrid Systems; University Library Aachen, Aachen, 2009.

[78] N. Kimizuka, M. Shimizu, S. Fujikawa, K. Fujimura, M. Sano and T. Kunitake *Chem. Lett.*, 1998, 967-968.

[79] P. K. Vemula, U. Aslam, V. Ajay Mallia and G. John, *Chem. Mater.*, 2007, **19**, 138–140.

[80] D. Khatua, R. Maiti and J. Dey, *Chem. Commun*., 2006, 4903.

[81] L. J. M. Gaspar and G. Baskar, *J. Mater. Chem.*, 2005, **15**, 5144.

[82] S. Roy, A. Dasgupta and P. K. Das, *Langmuir*, 2007, **23**, 11769–11776.

[83] N. Yan, G. He, H. Zhang, L. Ding and Y. Fang, *Langmuir*, 2010, **26**, 5909–5917.

[84] L. A. Estroff and A. D. Hamilton, *Chem. Rev*., 2004, **104**, 1201-1218.

[85] S. Cheuk, Glucose and Glucosamine Derivatives as Novel Low Molecular Weight Gelators, 2008.

[86] T. Kunitake, Y. Okahata, M. Shimomura, S. Yasunami and K. Takarabe, *J. Am. Chem. Soc*., 1981, **103**, 5401-5413.

[87] L. Frkanec, M. Jokíc, J. Makarevic, K. Wolsperger and M. Zinic, *J. Am. Chem. Soc*., 2002, **124**, 9716-9717.

[88] M. Suzuki, M. Yumoto, M. Kimura, H. Shirai and K. Hanabusa, *Chem. Commun*., 2002, 884-885.

[89] U. Maitra, S. Mukhopadhyay, A. Sarkar, P. Rao and S. S. Indi, *Angew. Chem., Int. Ed. Engl*., 2001, **40**, 2281-2283.

[90] T. Nakashima and N. Kimizuka, *Adv. Mater*., 2002, **14**, 1113-1116.

[91] (a) J. Makarevic, M. Jokic, B. Peric, V. Tomisic, B. Kojic-Prodic and M. Zinic, *Chem. Eur. J*., 2001, **7**, 3328-3341; (b) R. Iwaura, K. Yoshida, M. Masuda, M. Ohnishi-Kameyama, M. Yoshida and T. Shimizu, *Angew. Chem., Int. Ed. Engl.*, 2003, **42**, 1009-1012; (c) T. Shimizu and M. Masuda, *J. Am. Chem. Soc.*, 1997, **119**, 2812-2818; (d) M. Kogiso, T. Hanada, K. Yase and T. Shimizu, *Chem. Commun*., 1998, **17**, 1791-1792; (e) M. Kogiso, S. Ohnishi, K. Yase, M. Masuda and T. Shimizu, *Langmuir*, 1998, **14**, 4978-4986; (f) M. Suzuki, M. Yumoto, M. Kimura, H. Shirai and K. Hanabusa, *Chem. Eur. J*., 2003, **9**, 348-53.

[92] P. K. Vemula, J. Li and G. John, *J. Am. Chem. Soc*., 2006, **128**, 8932–8938.

[93] J. H. Fuhrhop, S. Svenson, C. Boettcher, E. Roessler and H. M. Vieth, *J. Am. Chem. Soc*., 1990, **112**, 4307–4312.

[94] J. H. Jung, S. Shinkai and T. Shimizu, *Chem. Eur. J*., 2002, **8(12)**, 2684–2690 and references therein.

[95] G. John, G. Zhu, J. Li and J. S. Dordick, *Angew. Chem. Int. Ed.*, 2006, **45**, 4772–4775.

[96] K. Lange and M. P. Schneider, German Patent, 2006**,** DE 102006014732 A1.

[97] M. Elsayed, Bergische Universität Wuppertal, Diploma work 2001.

[98] R. Ihizane, Bergische Universität Wuppertal, Diploma work 2006.

[99] K. K. Maiti, W. S. Lee, T. Takeuchi, C. Watkins, M. Fretz, D.-C. Kim, S. Futaki, A. Jones, K.-T. Kim and S.-K. Chung, *Angew. Chem. Int. Ed.*, 2007, **46**, 5880–5884.

[100] M. Goličnik, L. F. Olguin, G. Feng, N. J. Baxter, J. P. Waltho, N. H. Williams and F. Hollfelder, *J. Am. Chem. Soc.*, 2009, **131**, 1575–1588.

[101] K. Katsuraya, Y. Imoto, K. Okuyama, K. Hashimoto, H. Takei, R. Aono and K. Hatanaka, *Carbohydr. Lett.*, 2001, **4**, 131–136.

[102] A. Sakakura, K. Kawajiri, T. Ohkubo, Y. Kosugi and K. Ishihara, *J. Am. Chem. Soc*., 2007, **129**, 14775–14779.

[103] T. C. Owen and D. J. Austin, *J. Org. Chem*., 1993, **58**, 756–758.

[104] I. Redmann, M. Pina, B. Guyot, P. Blaise, M. Farines and J. Graille, *Carbohydrate Research*, **1997**, 300, 103 108 and references therein.

[105] F. M. Menger and K. L. Caran, *J. Am. Chem. Soc*., 2000, **122**, 11679–11691.

[106] D. Dasgupta, S. Malik, A. Thierry, J. M. Guenet and A. K. Nandi, *Macromolecules*, 2006, **39**, 6110–6114; (b) G. Palui, A. Garai, J. Nanda, A. K. Nandi and A. Banerjee, *J. Phys. Chem. B*, 2010, **114**, 1249–1256; (c) A. Pérez, J. L. Serrano, T. Sierra, A. Ballesteros, D. de Saá and J. Barluenga, *J. Am. Chem. Soc.*, 2011, **133**, 8110–8113; (d) N. Laurent, D. Lafont, F. Dumoulin, P. Boullanger, G. Mackenzie, P. H. J. Kouwer and J. W. Goodby,

J. Am. Chem. Soc., 2003, **125**, 15499–15506; (e) D. K. Rout, S. K. Pulapura and R. A. Gross, *Macromolecules*, 1993, **26**, 6007–6010; (f) H. Binder, A. Anikin, G. Lantzsch and G. Klose, *J. Phys. Chem. B*, 1999, **103**, 461–471.

[107] (a) L. A. Estroff and A. D. Hamilton, *Chem. Rev.*, 2004, **104**, 1201–1218. (b) S. Debnath, A. Shome, S. Dutta and P. K. Das, *Chem. Eur. J.*, 2008, **14**, 6870–6881.

[108] P. Kumar Vemula, U. Aslam, V. Ajay Mallia and G. John, *Chem. Mater.*, 2007, **19**, 138–140.

[109] G. John, J. H. Jung, M. Masuda and T. Shimizu, *Langmuir*, 2004, **20**, 2060–2065.

[110] G. John, M. Mason, P. M. Ajayan and J. S. Dordick, *J. Am. Chem. Soc.*, 2004, **126**, 15012–15013. (b) K. Tomioka, T. Sumiyoshi, S. Narui, Y. Nagaoka, A. Iida, Y. Miwa, T. Taga, M. Nakano and T. Handa, *J. Am. Chem. Soc.*, 2001, **123**, 11817–11818.

[111] G. John, J. H. Jung, M. Masuda and T. Shimizu, *Langmuir*, 2004, **20**, 2060–2065.

[112] H. Kobayashi, A. Friggeri, K. Koumoto, M. Amaike, S. Shinkai and D. N. Reinhoudt, *Org. Lett.*, 2002, **4**, 1423–1426.

[113] L. Frkanec, M. Jokić, J. Makarević, K. Wolsperger and M. Žinić, *J. Am. Chem. Soc.*, 2002, **124**, 9716–9717 and references therein.

[114] J. H. Jung, S. Shinkai and T. Shimizu, *Chem. Eur. J.*, 2002, **8(12)**, 2684-2690 and references therein.

[115] J. H. Jung, J. A. Rim, W. S. Han, S. J. Lee, Y. J. Lee, E. J. Cho, J. S. Kim, Q. Ji and T. Shimizu, *Org. Biomol. Chem.*, 2006, **4**, 2033–2038.

[116] J. H. Jung, G. John, K. Yoshida and T. Shimizu, *J. Am. Chem. Soc.*, 2002, **124**, 10674–10675.

[117] J. H. Jung, J. A. Rim, W. S. Han, S. J. Lee, Y. J. Lee, E. J. Cho, J. S. Kim, Q. Ji and T. Shimizu, *Org. Biomol. Chem.*, 2006, **4**, 2033–2038.

[118] J. Cui, Y. Zheng, Z. Shen and X. Wan, *Langmuir*, 2010, **26**, 15508–15515.

[119] N. Yan, G. He, H. Zhang, L. Ding and Y. Fang, *Langmuir*, 2010, **26**, 5909–5917.

[120] S. Soultani, S. Ognier, J.-M. Engasser and M. Ghoul, *Colloids and Surfaces A: Physicochemical and Engineering Aspects*, 2003, **227**, 35–44.

[121] (a) R. L. Grant and D. Acosta, *Fundam. Appl. Toxicol.*, 1996, **33**, 71–82; (b) J. H. Baert,. and R. J. Veys, *Journal of Oral Pathology & Medicine*, 1997, **26(4)**, 181–186.

[122] P. L. Du Nouy, *The Journal of General Physiology*, 1919, **1**, 521–524.

[123] Z. Xie and Y. Feng, *J. Surfact. Deterg.*, **2010**, 13, 51–57.

[124] A. Sakakura, K. Kawajiri, T. Ohkubo, Y. Kosugi and K. Ishihara, *J. Am. Chem. Soc.*, 2007, **129**, 14775–14779.

[125] D. F. Ewing, J. W. Goodby, J. A. Haley, S. M. Kelly, P. Letellier and G. Mackenzie, *TLCT*, 1997, **23**, 759–769.

[126] F. Dardoize, *Tetrahedron*, 1989, **45**, 7783–7794.

[127] T. Plat and R. J. Linhardt, *J. Surfact. Deterg.*, 2001, **4**, 415–421.

[128] S. Matsumura, Y. Kawamura, S. Yoshikawa, K. Kawada and T. Uchibori, *J. Am. Oil Chem. Soc.*, 1993, **70**, 17–22.

[129] M. A. M. Alho, N. B. D'Accorso and I. M. E. Thiel, *Journal of Heterocyclic Chemistry*, 1996, **33**, 1339–1343.

[130] G. Carrea, S. Riva, F. Secundo and B. Danieli, *J. Chem. Soc., Perkin Trans. 1*, 1989, 1057.

[131] S. Ritthitham, R. Wimmer, A. Stensballe and L. H. Pedersen, *Journal of Chromatography A*, 2009, **1216**, 4963–4967.

[132] I. Pérez-Victoria, A. Zafra and J. C. Morales, *Carbohydrate Research*, 2007, **342**, 236–242.

[133] D. B. Sarney, M. J. Barnard, D. A. MacManus and E. N. Vulfson, *J. Am. Oil Chem. Soc*., 1996, **73**, 1481–1487.

[134] N. Anoune, M. Nouiri, Y. Berrah, J.-Y. Gauvrit and P. Lanteri, *J. Surfact. Deterg.*, 2002, **5**, 45–53.

[135] Z. Xie and Y. Feng, *J. Surfact. Deterg.*, 2010, **13**, 51–57.

[136] B. Lakhrissi, L. Lakhrissi, M. Massoui, E. M. Essassi, F. Comelles, J. Esquena, C. Solans and C. Rodríguez-Abreu, *J. Surfact. Deterg*., 2010, **13**, 329–338.

[137] Z. Xie and Y. Feng, *J. Surfact. Deterg.*, 2010, **13**, 51–57.

[138] B. M. Folmer, K. Holmberg, E. G. Klingskog and K. Bergström, *J. Surfact. Deterg*., 2001, **4**, 175–183.

[139] B. Lakhrissi, L. Lakhrissi, M. Massoui, E. M. Essassi, F. Comelles, J. Esquena, C. Solans and C. Rodríguez-Abreu, *J. Surfact. Deterg*., 2010, **13**, 329–338.

[140] R. L. Grant and D. Acosta, *Fundam. Appl. Toxicol*., 1996, **33**, 71–82. (b) J. H., Baert and R. J. Veys, *Journal of Oral Pathology & Medicine*, 1997, **26(4)**, 181–186.

[141] M. Marciello, C. Mateo and J. M. Guisan, *Colloids and Surfaces B: Biointerfaces*, 2011, **84**, 556–560.

[142] (a) Y. Nihro, H. Miyataka, T. Sudo, H. Matsumoto and T. Sathoh, *J. Med. Chem*., 1991, **34**, 2152–2157; (b) R. H. Bisby and A. W. Parker, *J. Am. Chem. Soc*., 1995, **117**, 5664–5670.

[143] S. K. Karmee, *Appl. Microbiol. Biotechnol.*, 2009. **81**. 1013-1022.

[144] Lo P. Nostro, R. Ramsch, E. Fratini, M. Lagi, F. Ridi, E. Carretti, M. Ambrosi, B. W. Ninham and P. Baglioni, *J. Phys. Chem. B*, 2007, **111**, 11714-11721.

[145] S. Nandi, H.-J. Altenbach, B. Jakob, K. Lange, R. Ihizane and M. P. Schneider, *Org. Lett*., 2011, **13**, 1980–1983.

[146] F. M. Menger and K. L. Caran, *J. Am. Chem. Soc*., 2000, **122**, 11679–11691.

[147] G. John, M. Mason, P. M. Ajayan and J. S. Dordick, *J. Am. Chem. Soc*., 2004, **126**, 15012−15013.

[148] Y. Miwa, T. Taga, M. Nakano and T. Handa, *J. Am. Chem. Soc*., 2001, **123**, 11817–11818.

[149] http://www.aocs.org/Membership/FreeCover.cfm?itemnumber=1076

[150] (a) M. S. Blois, *Nature*, 1958, 1199–1200; (b) R. Giorgi, L. P. Nostro and P. Baglioni, *J. Am. Chem. Soc.*, 2006**, 128**, 7209–7214; (c) S. M. M. Asker, G. M. Mahmoud and S. G. Ibrahim, *J. Appl. Sci. Res.*, 2007, **3(10)**, 1170–1177; (d) P. Molyneux, *Songklanakarin, J. Sci. Technol*., 2004, **26(2)**, 211–219; (e) I. Yamamoto, A. Tai, Y. Fujinami, K. Sasaki and S. Okazaki, *J. Med. Chem.*, 2002, **45**, 462–468; (f) Y. Fujinami, A. Tai and I. Yamamoto, *Chem. Pharm. Bull*., 2001, **49**, 642–644; (g) K. Kate, S. Terao, N. Shimamoto and M. Hirata, *J. Med. Chem.*, 1998, **31**, 793–798.

[151] The intersections of each curve in Figure 61 are different because the concentration of DPPH radical have been taken approximately 60-100 µM and the exact concentration has been calculated based on Lambert- Beers Law.

[152] Lo P. Nostro, G. Capuzzi, A. Romani and N. Mulinacci, *Langmuir*, 2000, **16**, 1744–1750.

[153] A. Akbarzadeh, D. Zare, A. Farhangi, M. R. Mehrabi, D. Norouzian, S. Tangestani, M. Moghadam and N. Bararpour, *American J. of Applied Sciences*, 2009, **6**, 691–695 and references therein.

[154] M. Potara, D. Maniu and S. Astilean, *Nanotechnology*, 2009, **20**, 315602 and references therein.

[155] M. Iosin, P. Baldeck and S. Astilean, *J Nanopart. Res*., 2010, **12**, 2843–2849 and references therein.

[156] Semicarbazide organogels containing inorganic nanoparticles. New supramer particle hybrid systems, RWTH Aachen; 01 Fakultät für Mathematik, Informatik und Naturwissenschaften. Lehrstuhl für Textilchemie und Makromolekulare Chemie [154610], 2009.

[157] P. K. Vemula and G. John, *Chem. Commun.*, 2006, 2218.

[158] (a) K. L. Kelly, E. Coronado, L. L. Zhao and G. C. Schatz, *J. Phys. Chem. B*, 2003, **107**, 668–677; (b) C. F. Bohren and D. R. Huffman, Absorption and Scattering of Light by Small Particles, Wiley, New York, 1983, 287–380, and references therein; (c) U. Kreibig and M. Vollmer, Optical Properties of Metal Clusters, Springer, Berlin, 1995, 14–123, and references therein. (d) G. Mie, *Ann. Phys.*, 1908, **25**, 377–445.

[159] T. Huang and X.-H. N. Xu, *J. Mater. Chem.*, 2010, **20**, 9867.

[160] A. Kumar, P. K. Vemula, P. M. Ajayan and G. John, *Nat. Mater.*, 2008, **7**, 236–241.

[161] http://www.scientificamerican.com/article.cfm?id=silver-coating-fights-microbes

[162] X. Li, J. J. Lenhart and H. W. Walker, *Langmuir*, 2010, **26**, 16690–16698.

[163] F. M. Menger and K. L. Caran, *J. Am. Chem. Soc.*, 2000, **122**, 11679–11691.

[164] G. John, J. H. Jung, M. Masuda and T. Shimizu, *Langmuir*, 2004, **20**, 2060–2065.

[165] P. Kumar Vemula, U. Aslam, V. Ajay Mallia and G. John, *Chem. Mater.*, 2007, **19**, 138–140.

[166] G. John, J. H. Jung, M. Masuda and T. Shimizu, *Langmuir*, 2004, **20**, 2060–2065.

[167] (a) R. L. Grant and D. Acosta, *Fundam. Appl. Toxicol.*, 1996, **33**, 71–82; (b) J. H. Baert and R. J. Veys, Journal of Oral Pathology & Medicine, 1997, **26(4)**, 181–186.

[168] P. L. Du Nouy, *The Journal of General Physiology*, 1919, **1**, 521–524.

[169] Z. Xie and Y. Feng, *J. Surfact. Deterg.*, 2010, **13**, 51–57.

[170] A. Abe, K. Asakura and S. Osanai, *J. Surfact. Deterg.*, 2004, 7, 297–303.

[171] H.-J. Altenbach, R. Ihizane, B. Jakob, K. Lange, M. Schneider, Z. Yilmaz and S. Nandi, *J. Surfact. Deterg.*, 2010, **13**, 399–407 and references therein.

[172] W. C. Griffin, *J. Soc. Cosmet. Chem.*, 1954, **5**, 249−256.

[173] W. C. Griffin, *J. Soc. Cosmet. Chem.*, 1949, **1**, 311−326.

[174] J. Bentham, J. A Coates, D. L Connell, 1981**,** DE 3118527 A1.

[175] P. L. Du Nouy, *The Journal of General Physiology*, 1919, **1**, 521–524.

[176] K. Baczko and D. Plusquellec, *Tetrahedron*, 1991, **47**, 3817–3828.

[177] I. Redmann, M. Pina, B. Guyot, P. Blaise, M. Farines and J. Graille, *Carbohydrate Research*, 1997, **300**, 103–108 and references therein.

[178] M. A. M. Alho, N. B. D'Accorso and I. M. E. Thiel, *Journal of Heterocyclic Chemistry*, 1996, **33**, 1339–1343.